UNIVERSITA' DEGLI STUDI DI PALERMO

FACOLTA' DI INGEGNERIA

Dipartimento di Ingegneria Chimica, Gestionale, Meccanica e Informatica

PhD Thesis:

Sheet Stamping Processes Design: Optimization Methodologies for Robust and Environmental Conscious Decisions.

PhD in Production Engineering, Cycle XXIII, Years 2009-2011

(Dottorato in Ingegneria della Produzione, Ciclo 23, Triennio 2009-2011)

SSD: ***ING-IND 16***

PhD Candidate:
LAURA MARRETTA

Tutor:
Prof. **ROSA DI LORENZO**

PhD Coordinator:
Prof. **LIVAN FRATINI**

INDEX

INTRODUCTION

Sheet stamping processes have an extremely wide application, from automotive manufacturing to daily life products; thus they have been appealing both industry and academic researchers. Nowadays, zero defect products, fulfilling all the specifications that might be required, are imperative. Time and costs have to be minimized at the same time, by reducing part rejection rate and reworking operations as well.

Quality maximization is then one of the main issues in sheet stamping processes design, drawing plenty of efforts in developing effective methodologies for successful forming operations. In manufacturing process design, the main objective becomes therefore to find the best process set up to produce parts as close as possible to the nominal values. This is commonly meant as optimization process and it is carried out by properly calibrating the control parameters that significantly relate to the onset of any product defect. Therefore, optimization problems are conveniently modeled as a set of independent variables $X = [x_1, x_2, \dots, x_n]$ to be tuned, and one or more objectives $f_i(X)$ to get optimized by those.

As of the past 20 years, many research works have been focused on improving stamping tool systems and technologies to fulfill geometric requirements, beside properly tuning restraining forces and inducing suitable stress distributions over the blank thickness. Thus, control variables might be the blank holder force, either time and space dependent, drawbead forces and location, tool geometry, blank design, etc.

The objectives have been all the dominant defects affecting sheet stamping operations, like excessive localized thinning and fracture, which directly relate to part performances and safety, both flange and side walls wrinkling, which influence the shape quality, and uncompensated springback, often leading to assembly problems as well.

Forming processes are highly nonlinear problems, quite sensitive to several factors, making difficult to predict the system response, even by a good process expertise. Therefore, a wholly experiments based optimization procedure would result unaffordable in most of the cases. But nowadays Finite Elements (FE) simulation has become an acknowledged tool to powerfully evaluate any forming process with an acceptable accuracy. Then for instance, Gantar et al. (2005a) used the Finite Element Method (FEM) to evaluate not only the size of technological windows but also to increase the stability of

production processes. Of course, the more accurate the numerical simulation is, the lower the discrepancy between predicted and experimental results turns out to be. Thus, in the last years, several investigations on the effectiveness of numerical models have been developed comparing numerical predictions with experimental evidences as well, taking into account both the effects of process parameters and numerical ones (Li et al (2002)). Xu et al. (2004) analyzed the effect of using a fully explicit scheme, the number integration points, the blank sheet element size and the punch velocity on a U-bending process proposed as benchmark in the Numisheet'93 Conference. Guidelines for the number of integration points through the thickness required are reported by Wagoner et al. (2007).

The reliability of any FE simulation strongly relies on the material hardening behavior as well, thus some authors compared the results obtained by using different hardening rules, namely isotropic, kinematic and combined isotropic-nonlinear kinematic, for different materials (Banu et al. (2006), Taherizadeh et al. (2009)). The shape of the yield surface is also critical in modeling the material behavior. Four different yield functions (von Mises, Hill's 48, Barlat's three parameters 89 and Barlat's 96) were investigated by Wagoner (2004): simulations by using Barlat's 96 yield function showed a remarkable agreement with experiments. Several material models were also analyzed by Laurent et al. (2009), all considering isotropic and kinematic hardening combined with several plasticity criteria for an AA5754-0 aluminum alloy.

Sometimes FE approaches require large computational efforts and CPU time to calculate the value of any optimization function, often constrained by engineering tolerances, to check both feasibility and optimality. Each FE simulation is moreover a direct problem to be solved, therefore any modification to the design setting would imply further experimental and numerical simulations and the time needed to optimize the entire forming process would prohibitively rise. Eventually, even though they still represent high fidelity models, they turn out to be computationally very intensive.

Statistical techniques referred as Design of Experiments (DoE) (Myers and Montgomery (2002)) have been extensively integrated to FE simulation to provide the designer with efficient sampling techniques that properly space out all the runs within the design space. In (Browne and Hillery (2003)), DoE is used in investigating the influence of tool geometry and some process parameters on a deep drawing process, likewise in (Liu et al. (2002)) an orthogonal design is integrated to FE analysis for a draw bending problem.

Even by using efficient sampling methods, the task to simulate each point and then to check the feasibility and the optimality of the corresponding process setting might be still prohibitive in the industrial practice as too time consuming. Additionally, DoE might help to come close or even to find the optimal process calibration, but typically such approach would leave out a large amount of possible design combinations as limited just to the explored solutions, and no information on what is in between could be drawn. Therefore, there would be no sureness of optimality but mostly reliance on the process expertise.

Surrogate model based methods have been developed over direct optimization strategies to successfully design forming processes, overcoming all the mentioned shortcomings. Surrogate models are metamodels or emulators either for predicting or evaluating the multivariate input/output behavior of any process investigated function, while being computationally lighter to carry out than all the direct problems that would be required for the same optimization purpose.

The most popular surrogate models applied to forming processes are Artificial Neural Networks (ANN) (Zhang et al. (2000)), that reproduce the process behavior by a proper training data set, Support Vector Machines (SVM) (Vapnik (1995)), Radial Basis Functions (RBF) (Powell (1987)), Multivariate Adaptive Regression Splines (MARS) (Friedman (1991)), Smoothing Splines (Lancaster and Salkauskas (1986)), Response Surface Methodology (RSM) (Myers and Montgomery (2002)) and Kriging (Sacks et al. (1989), Koehler and Owen (1996)), often integrated to Genetic Algorithms (GA), that provide a mathematical model of any objective as a function of all the used independent variables. Often, only a fraction of the DoE is required by using such models, which makes those really attractive to further reduce the computational effort.

Piotr et al. (2005) used surrogate models to design the initial blank of a Renault Twingo dashpot cup. Artificial Neural Networks were utilized by Kazan et al. (2009) for a wipe-bending process; likewise Liew et al. (2004) integrated ANN to an evolutionary algorithm to reduce springback for hemispherical cup drawing. Some authors integrated RSM to FE simulation in order to find out both process and material parameters for springback minimization (Naceur et al. (2006) and (2008)). Jakumeit et al. (2005) tested both kriging and RSM models on sheet forming applications for thinning, wrinkling and springback minimization by a time dependent blank holder history. Furthermore, Hu et al. (2008) also used a kriging based strategy in the high nonlinear optimization of a vehicle's outer flank

forming.

Especially when there is shallow knowledge of the process, it is not obvious which surrogate model will be most accurate. In the technical literature, the accuracy of such surrogate models has been investigated (Jin et al. (2000), Lebaal et al. (2011), Rijpkema et al. (2001)), addressing process designers towards more suitable choices.

Therefore, the integration between FE simulations and surrogate models is the most efficient strategy to successfully optimize forming processes, as a deeper knowledge of the process is achieved while limiting the computational efforts.

Moreover, sheet stamping processes are often multiobjective optimization problems, as featuring clashing performances: it is well known, for instance, that to minimize the occurrence of wrinkles generally means to induce an excessive localized thinning.

From a mathematical perspective, no actual optimum exists when conflicting goals are accounted for, while a set of compromise solutions referred as Pareto front are instead available. Even though an actual optimization is not feasible, the significant advantage for industrial applications is the availability of a plurality of still good solutions to accomplish any engineering constraint as well.

Therefore, multiobjective optimization (MOO) techniques have been developed. Some authors used MO genetics algorithm (Wei et al. (2008) and (2009)) to design sheet stamping processes, even integrated to finite element analysis (FEA) (Wei et al. (2007)). An attempt of simultaneous control of springback and thinning distribution utilizing MOGA was in fact developed by Wei et al. (2009). In particular, in Wei et al. (2008) MOGA are used to design an auto-body stamping process to minimize fracture danger, wrinkling, stretching and thickness variation, while Wei et al. (2007) focused on the optimal design of forming operations by integrating finite element analysis (FEA) and multi-objective genetic algorithm (MOGA).

Other authors efficiently utilized surrogate response surface models to optimize multiple objective functions, thus the design of a deep drawing operation on aluminum parts is reported by Zang and Shivpuri (2009). Liu et al. (2008) developed an iterated sequential approximation method, to minimize wrinkling and fracture risk for a shoe plate of a car front floor. The optimal design of varying frictional constraints to reduce wrinkling and thinning is instead described by Shivpuri and Zang (2008). A multi-objective approach for sheet stamping design by changing the initial blank shape together with the blank holder

action is by Ingarao et al. (2009a) and (2009b).

In fact, the more complicated the optimization problem is, like with multiple objectives and engineering constraints, the more convenient the integrated use of FE simulation and metamodeling technique turns out to be.

The above mentioned optimization strategies are any way referred as deterministic. But the presence of variability during manufacturing processes, and in particular sheet stamping processes, significantly affects the quality and introduces an undesired uncertainty into the process design. In fact, even if forming process is optimally designed, the part could have significant variations in dimensions and properties due to uncontrollable factors, sometimes evolving up to the onset of part defects.

Majeske and Hammett (2002) report variations within the same batch over the 21% of the nominal geometry, pointing part variability as a crucial issue in automobile manufacturing. An accurate study of variation in sheet stamping processes for automobile manufacturing is reported by the analysis project team of the Auto/Steel Partnership Program (2000). The Auto/Steel Partnership (A/SP), which is an international association including DaimlerChrysler, Ford, General Motors and eleven North American sheet steel producers, has in fact focused on such a critical issue in auto making, highlighting the necessity to account for variability in sheet forming: on average, more than the 30% of the part dimensions in some of the companies member resulted outside the tolerance.

The more sensitive the process responses are to any variation of such uncontrollable factors, the less robust the process is, inducing higher risk of failure. Typically, process robustness is considered to be good if the scatter of the process results around the nominal values is not higher than 1% (de Souza and Rolfe (2008)). According to Taguchi, there are two categories of parameters: control variables, that can be adjusted on purpose, and uncontrollable parameters generating noises, i.e. variations. As there is no chance to calibrate those noises, the possibility still is to choose control settings where the process robustness turns out to be higher.

Noises influencing sheet stamping processes are typically related to tool geometry, blank dimensions, friction conditions and indeed to material properties scattering (de Souza and Rolfe (2008), Gantar and Kuzman (2002)).

The variability range of both material properties and lubricating conditions is documented by Simões et al. (2003) within the European project INETFORSMEP. Moreover, Cao and

Kinsey (2001) report a variation of the strength coefficient as high as 20%, while the friction coefficient might even vary by 65%. On the other hand, Karthik et al. (2002) found that the strain hardening coefficient can have coil-to-coil variation even up to 14%.

Therefore, an extensive research has been done on the effect of variability in sheet forming. Some authors, for instance, analyzed the effect on springback of the noise variation (Chen and Koc (2007), de Souza and Rolfe (2008), Jansson et al. (2008)), even at different control of the restraining forces.

Thus, in Chapter 1 an overview of the state of art on the investigation of variability in sheet stamping processes and the analysis of the effects of such variability on the process results is reported, supported by a case study.

The sensitivity of sheet stamping processes even to slight variations of such variables makes in fact mandatory to account for the process robustness. To neglect any noise influence might affect the final performances and make the process design inexorably fail: part rejection rate would become unacceptable and time and costs unviable. In fact, as it is stressed in the report by the Auto/Steel Partnership Program (2000), component dimensions that deviate from their design nominal cannot always be predictably adjusted to the desired nominal without excessive rework costs. Moreover, such rework may correct one particular deviation, but adversely affect correlated points on the same part.

The challenge is eventually to obtain parts complying with all the specifications and robust at the same time to the sources of variation. Therefore, robustness and reliability are strongly connected in sheet stamping optimization, as the capability of the process design to keep successful the level of its performances against the variation of the surrounding conditions.

As a matter of fact, together with the rising of the demand of high quality stamped part, more efforts have become focusing on evaluating and improving processes robustness. Since traditional optimization methods (i.e. deterministic ones) are not able to deal with process variations, stochastic approaches to control variability have been developed lately, becoming one of the major issues in manufacturing processes design. In fact, while control variables can be assumed certain, noises have generally a probabilistic behavior to model the scatter of possible occurrences around their expected values.

As it is highlighted by Zhang and Shivpuri (2009), extensive research has been done in exploring the deterministic effect of each design variable on the part quality, but very little

on the impact of process uncertainties and their interaction with process design in influencing part variability.

Like for deterministic approaches, FE simulation has been massively used also for robust strategies, while experiments are typically used just for validation purposes. Moreover, the infinite number of designs and process possibilities make it nearly impossible to accumulate sufficient historical knowledge for a designer to accurately assign tolerances that consistently meet future process capability (Auto/Steel Partnership Program (2000)). Therefore, due to the complexity of this type of problems and the high number of runs that generally are required to make reliable estimations for stochastic optimizations, computer experiments are commonly combined with statistical techniques for robust design, able to reduce or to manage such a heavy computational effort. In fact, as it is pointed out by Kleiber et al. (2002), to use an approximation of the real model is necessary to assess and control the process robustness. Therefore, either surrogate models properly integrated to techniques for stochastic analysis or more strictly probabilistic approaches have been applied to sheet forming optimization. Then, for instance, response surface based approaches are in the technical literature for stamping robust design, often combined with Monte Carlo Simulation (MCS) methods (Zhang and Shivpuri (2009)). Beside those, other approaches based on the Dual Response Surface method (Sun et al. (2009)) have been used as well. As it was previously pointed out, wide investigations for robust design relate to multiobjective problems. In Chapter 2, the robust approaches mostly used for multiobjective sheet forming design are described and case studies are also reported to give a better understanding of the influence of the uncertainty on such processes. Comparisons of different approaches were also carried out.

Beside the optimization of sheet stamping processes aimed at a zero defect quality, another crucial objective has been recently raised for industrial applications: the increasing concern over environmental friendly processes and products has been addressing lately the interest of the scientific community towards new methods and technologies for more environmental friendly solutions in any industrial field. In fact, the consumptions of energy and raw material by industry have been massively growing, critically using up and threatening to drain the resources still available in nature. Therefore, the traditional unselective use of resources and technologies, neglecting any consideration of the environmental burden related to industrial processes and products, results in a myopic

strategy over the necessity of more sustainable practices. The concept of *sustainable development* is defined by the United Nation's Brundtland Commission, as "*meeting the needs of the present without compromising the ability of future generations to meet their own needs*" (Brundtland Commission (1987), Joshi et al. (2006)), highlighting the necessity of a more responsible use of resources. Over time, many of the problems related to the overuse of natural resources and pollution from human activities have been identified: ozone depletion, global warming, acidification, and eutrophication, among others. Corrective actions may involve changes in the types and ways materials and energy are used for manufacturing, use, and disposal of products.

In Figure 1 the worldwide contributions by sector is reported by the International Energy Agency (2011), enhancing the relevance of the contribution of the industrial sector to the worldwide greenhouse gases emissions.

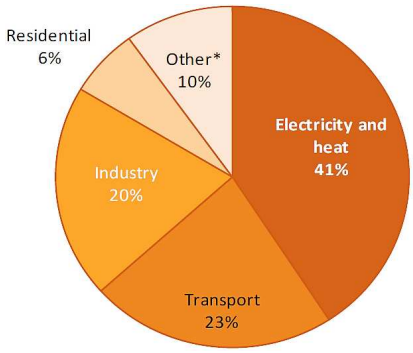

Figure 1: Worldwide greenhouse gases emissions by sector in 2009 (International Energy Agency (2011)).

Within industry, Gutowski (2004) identified in particular commonly agreed environmental concerns and related linkages to manufacturing processes, which are listed in Table 1.

Environmental Concerns	Linkage to Manufacturing Processes
1. Global climate change	Greenhouse gas (GHG) emissions from direct and indirect energy use, land fill gases, etc.
2. Human organism damage	Emission of toxins, carcinogens, etc. including use of heavy metals, acids, solvents, coal burning…
3. Water availability and quality	Water usage and discharges e.g. cooling and cleaning use in particular
4. Depletion of fossil fuel resources	Electricity and direct fossil fuel usage e.g. power and heating requirements, reducing agents
5. Loss of biodiversity	Land use, water usage, acid deposition, thermal pollution
6. Stratospheric ozone depletion	Emissions of CFCs, HCFCs, halons, nitrous oxides e.g. cooling requirements, refrigerants, cleaning methods, use of fluorine compounds
7. Land use patterns	Land appropriated for mining, growing of bio-materials, manufacturing, waste disposal
8. Depletion of non-fossil fuel resources	Materials usage and waste
9. Acid disposition	Sulfur and NO_x emissions from smelting and fossil fuels, acid leaching and cleaning

Table 1: Environmental concerns and linkages to manufacturing processes (Gutowski (2004)).

In (Gutowski (2004)) the message that many of the environmental problems from manufacturing are directly related to materials usage including energetic aspects is carried. Additionally, other factors raise the need of sustainability: the price of raw materials is increasing and environmental laws state both penalties and incentives, addressing new industrial policies for companies, whose customers, increasingly sensitive to environmental issues and climate change, have started appreciating sustainable strategies from them. Therefore, efficiency in energy use and new energy fonts have become a crucial concern in the industrial production (Herrmann and Thiede (2009)) and new requirements for manufacturing practices accounting for sustainability have been stated and managed differently by countries (Kaebernick et al. (2003), Kaebernick and Kara (2006)). Accordingly, a growing interest towards sustainable methods and solutions for manufacturing led many researches even to establish some milestones on crucial aspects of competitive sustainable manufacturing: manufacturing processes must be designed and developed with the aim to reduce, eliminate or recycle wastes, to avoid any hazard condition to human health or environment, with the goal to save energy and materials by eventually using more appropriate sources of energy and materials as well (Jovane et al. (2008), Veleva et al. (2001)).

Environmental friendly strategies may be performed through the entire life cycle of any product and process, for instance by selecting less impactful materials, by minimizing wastes and scraps, by reducing the requirements of energy or just smartly using it. Even end-of-life strategies might be performed. These all are included in the 6R concept, whose framework implies six possible leverages towards more sustainable products to apply throughout their life cycle: to Recover, to Reuse, to Recycle, to Redesign, to Reduce, and to Remanufacture. In this way, different design elements are associated with the life-cycle of a product and multi-life cycles can be associated with a single product (Joshi et al. (2006)).

As the interest of industry and academia towards sustainability has been growing and more and more attempts have been done for such purpose, the International Standards Organization (ISO) initiated a global standardization process for Life Cycle Assessment (LCA) that is a technique to assess environmental impacts associated with all the stages of a product's life from-cradle-to-grave (i.e. from raw material extraction through materials processing, manufacture, distribution, use, repair and maintenance, and disposal or

recycling) (ISO (2006a) and (2006b)). Four standards were developed for life cycle assessment and its main phases are issued in the ISO 14000 series of standards for Environmental Management, which provide minimum requirements of the performance of any life cycle assessment and define a standard framework for LCA as shown in Figure 2.

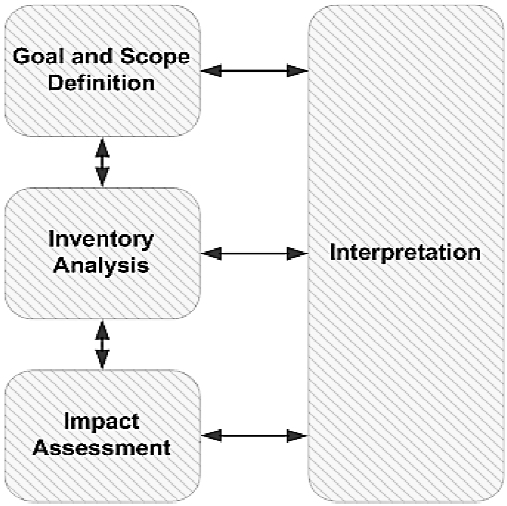

Figure 2: LCA framework from the ISO 14000 standards.

In fact, many LCA methodologies are available in the technical literature, like CML 1996, CML 2001, Eco-Indicator 95, Eco-Indicator 99, EDIP 1997, Impact 2002, TRACI, among others, which account for several categories of impact and often use different techniques to quantify either intermediate or global impact on the environment. On the contrary, the ISO 14001 standard harmonizes the general use of any LCA methodology and increases the reliability of the results. Following, the main steps of the LCA framework according to the ISO standards are summarized:

Goal and scope definition: the objective of the LCA application is defined, together with the boundaries of the product/process system as both temporal and technological scope. The assessment parameters to consider and the functional unit, which quantitatively defines the reference flows in the LCA analysis, are specified as well.

Life Cycle Inventory (LCI): the inventory analysis collects the input and output data flows within the boundaries of the product/process system, according to the defined functional unit.

Life Cycle Impact Assessment (LCIA): the purpose of such phase is to calculate the potential impact by categories, by using the data collected during the inventory step. Several LCIA methodologies are available to convert data from the inventory into

environmental impact by using proper characterization factors and different results and conclusions might be drawn by using different techniques.

Life Cycle Impact Interpretation: this is the final stage, when information from the LCI and LCIA stages are evaluated in order to address changes and improvements, to compare products and processes or to contrast the obtained results with a specific target.

Nowadays, Life Cycle Assessment (LCA) methodology and Design for Environment (DFE) procedures are widely investigated in many research labs all over the world (Hauschild et al. (2005)) and are massively used by industry. Figure 3 shows how companies mainly use LCA from the results of a survey by Baumann (1996): LCA methodologies are massively used for product analysis and design. Applications to process optimization, meant as improvement of the environmental performances, are significant as well.

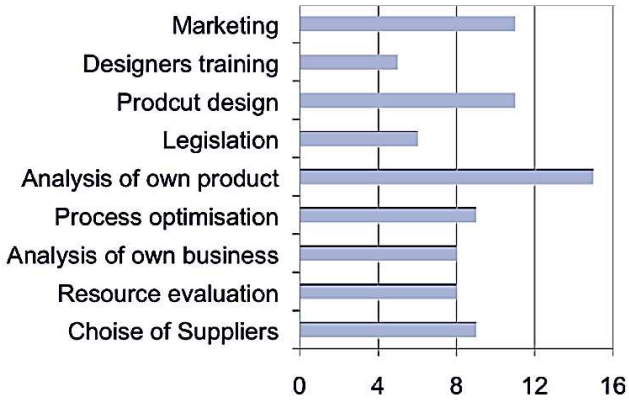

Figure 3: Use of LCA by industry (Baumann (1996).

As it was observed by Ingarao et al. (2011a), generally the attempt to improve manufacturing processes from a sustainability standpoint is quite complex: the topic of making more sustainable such processes means to find out either new technologies or solutions, which result more environment-friendly than the existing ones. Obviously, the development of proper models able to account for all the aspects to be considered and to quantify such improvements is required. Materials, energy, wastes, lubricants use, tooling systems are some of the input/output flows to take into account for a given manufacturing process. While a number of quantitative models of machining processes have been done, there is a significant lack of knowledge on metal forming and in particular sheet stamping, still needing a proper modelling of the factors to account for, in order to first evaluate and then suggest possible directions of improvement. In fact, there is a widely documented

state of art for machining applications (Gutowski (2004), Gutowski et al. (2006), Pusavec et al. (2010a) and (2010b), Vijayaraghavan and Dornfeld (2010)) emphasizing the possibility to precisely model all the machining processes sustainability factors; the estimation of the environmental burden of forming technologies is instead really complicated as particularly process-dependent. In fact, if two forming technologies are contrasted in terms of environmental performances, there are usually really peculiar features strictly depending on the process in terms of tooling system and operative parameters, among others.

Therefore, there are many LCA applications to formed components, especially in the automotive field, but really few attempts to assess and to model, even qualitatively, forming processes. A sort of holistic vision aimed at providing with basic guidelines to identify possible solutions through the life cycle of formed parts is given by Ingarao et al. (2011a). Gantar et al. (2005b) identified two main aspects to reduce the environmental burden of sheet stamping processes: material efficiency (i.e. die design, optimization of the initial blank shape, etc.), with consideration of the scrap rate, and lubrication together with the cleaning process. Some studies on the tribological aspects have been presented by Bay et al. (2005) and Wang (2004): the authors investigated environmental friendly lubrication technologies, emphasizing the importance of dry manufacturing or manufacturing with environmental benign lubricants, by analyzing the energy saving at decreasing of the friction coefficient.

Jeswiet and Kara (2008) applied a framework to model and calculate the deformation energy required by an upsetting process by using the FE analysis. In particular, they converted such energy requirements into greenhouse gas emissions depending on the power grid location. The objective of the work was to develop a method connecting the electrical energy used in manufacturing directly to the carbon emissions created in using the electrical energy. The proposed model referred as Carbon Emission Signature method (CES^{TM}) allowed quantifying the emissions and actually it could be applied both to forming and machining operations. Nava et al. (2010) improved such modeling including also “non-energy factors” like lubrication. A further development in sustainability modeling of metal forming processes is given by Rahimifard et al. (2010). These authors developed a comprehensive model accounting for direct energy requirements for products manufacturing (i.e. process energy and auxiliary energy required by supporting activities)

and indirect energy related to overhead activities, like lighting or heating. More recent studies have compared conventional deep drawing processes with single point incremental forming technology (SPIF) by ecological aspects (Anghinelli et al. (2011), Ingarao et al. (2011b), Petek et al. (2007)).

Therefore, a poor knowledge on sustainable forming operations and in particular on green solutions for sheet stamping processes has been developed over the years. Nevertheless, it is well known that sheet stamping operations are massively spread to manufacture a wide range of products, opening a great potential towards greener manufacturing processes. As a matter of fact, the 90% of the components of a common passenger car are manufactured by sheet stamping operations and over the 19% of the carbon emissions broken down by sector are from transportation, with a strong contribution from light duty vehicles. Figure 4, 5 and 6 detail such considerations.

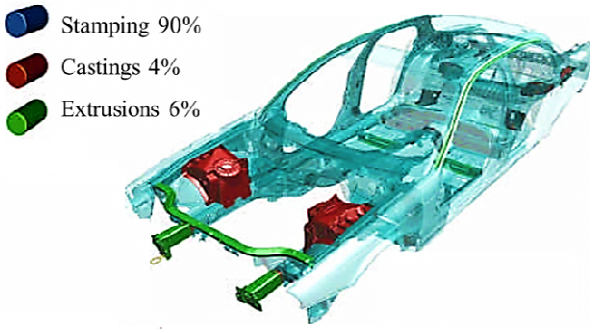

Figure 4: Manufacturing processes in a common passenger car (White (2006)).

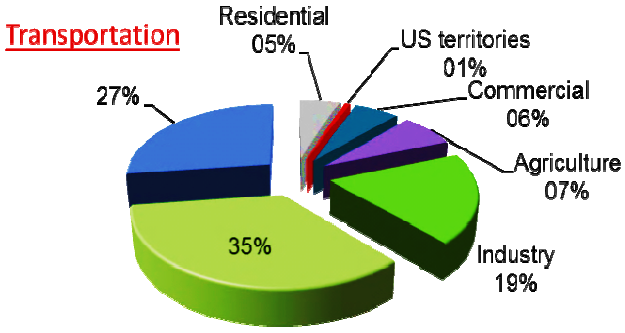

Figure 5: USA carbon emissions by economic sector in 2011 (adapted from EPA (2011)).

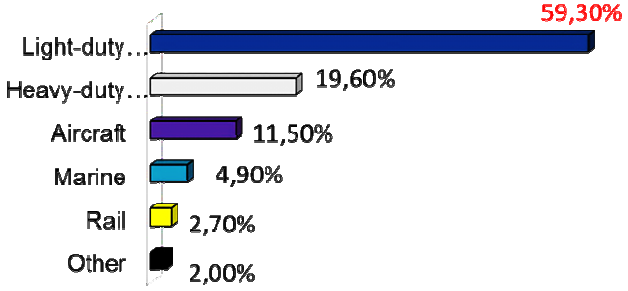

Figure 6: USA carbon emissions by transportation mode (adapted from EPA (2011)).

From the carbon emissions breakdown by life cycle phase, approximately just the 4% comes from the manufacturing phase (Geyger (2007)), as it shown in Figure 7.

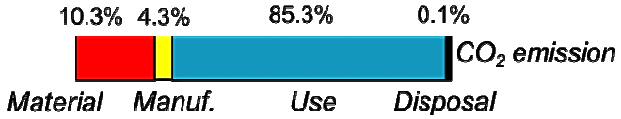

Figure 7: Carbon emissions breakdown by life cycle phase of a passenger car.

Deeper details of the type of emissions to air and to water are given in Figure 8, comparing the impacts respectively from utilization, fuel production and car manufacturing for a Volkswagen Golf A4 (Schweimer and Levin (2002)). Again, the use phase is the most impactful one as carbon emissions (CO_2) are concerned.

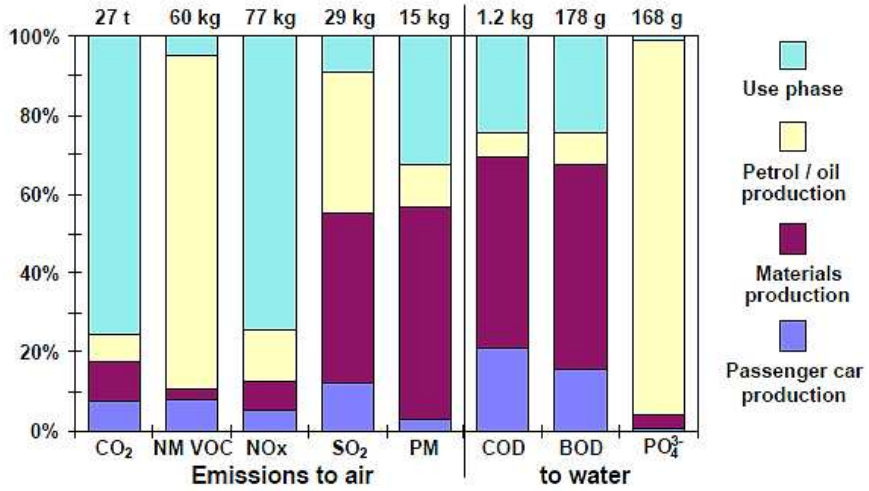

Figure 8: Emissions to air and to water of a Volkswagen Golf A4 (Schweimer and Levin (2002)).

Additionally, the stamping operations themselves are even less impactful among the manufacturing chain given a deeper look at the primary energy requirements (which obviously imply carbon emissions) for instance of a Volkswagen Golf (Volkswagen AG and Florin (1995)): the contribution of the sheet stamping is less than 1% of the total energy per car as it can be observed in Figure 9.

Nevertheless, the potential of sheet stamping operations to significantly reduce the environmental impact from transportation is crucial: in fact, they might play a sort of leverage effect, triggering a quite positive externality onto the whole vehicle life cycle.

As a matter of fact, the use of lightweight materials and technologies might enable a more efficient material use and a remarkable reduction of the vehicle weight, allowing less fuel consumptions and accordingly carbon emissions to air, as it will be discussed in Chapter 3.

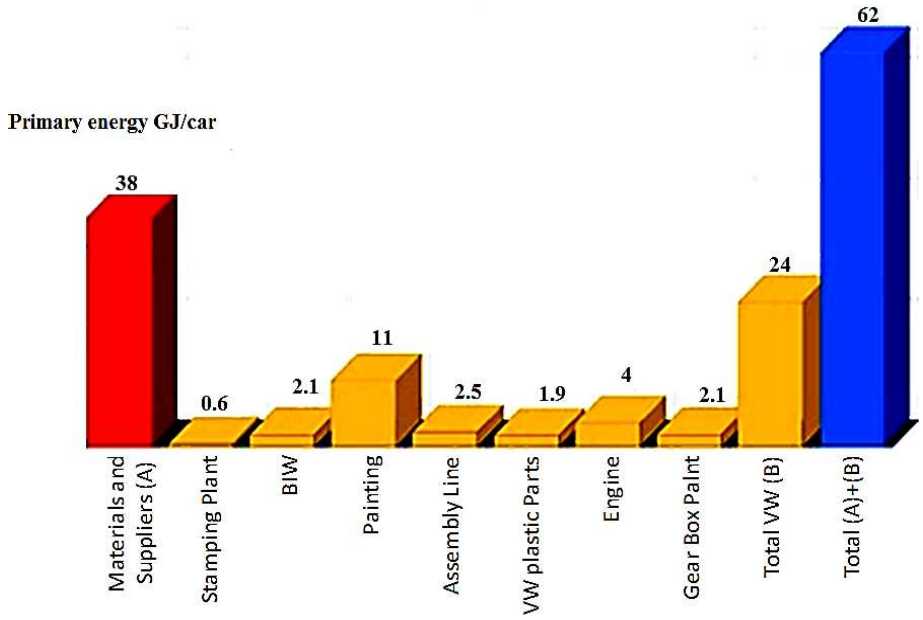

Figure 9: Details of the primary energy requirements to manufacture a VW Golf (Volkswagen AG and Florin H. (1995)).

A 6% to 8% fuel saving can be in fact realized every 10% reduction in weight by substituting steel with light alloys: 9g of CO_2/km can potentially be saved per 100kg (www.wordautosteeel.com).

Even more, the application of tailored blanks may allow further material savings where typically higher strength is required. As an example, weight reduction up to 13% can be reached by the combination of unequal sheet thicknesses and alloys (Cherubini et al. (2008), www.eaa.net).

Additionally, non-conventional stamping technologies such as hydro-forming, superplastic forming, incremental forming and hot stamping enable better load and stress distributions: more uniform material deformations are reached and 40% to 50% thinner blanks can be used over traditional methods (Neugebauer et al. (2006)).

More sustainable vehicle life cycle begin with process design and material selection, key factors for environmental friendly production. The process set up should then account for the global impact on the environment and incorporate such awareness within the design choices. Frameworks and evaluation procedures that address sustainable production are therefore strongly required.

An overview of sustainable strategies for sheet stamping processes and products is given in Chapter 3. Useful considerations and discussions about those have been done in

collaboration with General Motors R&D (Warren, MI), by visiting also the stamping plants at Lansing and Flint.

Environmental aspects of industrial activity are being ranked alongside technical and financial issues as well. Cost and production goals have to be accomplished while at the same time exercising greater responsibility for the environment.

The most of the time in fact, more sustainable choices imply higher costs to afford or even tougher operations to carry out though. Thus, often the most sustainable solution is not the less pricy or the easiest from a technical standpoint. For instance, despite having great potential as fuel saving, lightweight materials raise serious formability problems and imply higher costs to afford. Decision making frameworks able to account for environmental, technical and economic issues have to be developed, in order to address viable and feasible sustainable choices.

Additionally, as it was earlier discussed, life cycle assessment follows the rules of ISO 14040 according to which different characterization procedures have been developed to aggregate the inventory data by categories of impact and derive impact indicators.

But this assessment strongly depends on the goal and scope definition, and contradictory conclusions may be even drawn. The definition of the boundaries of the analysis therefore results in complex and sometimes unreliable comparisons among different companies, especially with respect to fixed targets.

Therefore, comprehensive and structured approaches enabling consistent decisions and metrics of improvements are worth developing by integrating evaluation of environmental performances with decision making tools comparing different states.

A decision making framework is described in Chapter 3 together with the discussion of some case studies. Such results were in particular obtained during the visiting research program at University of California, Berkeley (USA) at the third year of the PhD course. Moreover, in collaboration with the University of Calabria, Italy, a comparison between traditional sheet stamping operations and incremental forming processes was developed.

In conclusion, the objective of this PhD thesis is to develop methodologies for the optimization of sheet stamping processes both in terms of zero defect quality and environmental conscious decisions.

The imperative need of products strictly complying with all the requirements and technical specifications leads to focus on robust techniques to control the inherent process

variability, especially due to the variation of the material properties, but at the same time the widely spread attention about more sustainable choices in manufacturing operations imposes to extend the focus to a wider concept of quality for sheet stamped parts: zero defect but still environmental friendly products and processes. The perspective is therefore to provide with a comprehensive view of the current issues and methods for sheet stamping processes to develop in future more general approaches able to account for all of them.

Chapter 1

EFFECTS OF VARIABILITY ON SHEET STAMPING PROCESSES AND DESIGN.

Material deformation and the interaction between tooling system and material in sheet stamping processes take place under conditions changing for instance with the increasing of the tool temperature. As long as the parameters influencing the process are specified deterministically, implying perfect repeatability of the process outputs, only a shallow understanding of the real behavior of any process function would be possible.

In the reality, in fact, the parameters influencing sheet stamping processes vary and the necessity of approach to control process variability rise.

The main variability sources of a sheet metal forming process can be summarized into the following main categories (de Souza and Rolfe (2008)):

- **Material**: variability depending on the used workpiece (material properties, surface roughness, thickness, initial geometric characteristics, hardening coefficient, etc.);
- **Tooling**: variability due to changes in the tools geometry for instance by temperature and wear at locations with high contact pressure like die radii and drawbeads;
- **Process**: variability related to process parameters such as blank holder force, punch velocity, that may lead to a significant rise of the tool temperature, etc.;
- **Friction**: the tribological conditions can change with changing of the tool temperature, likewise lubricant concentration can change locally.

While it is possible to better control some parameters kept steadily between two forming operations or batches, like for instance the blank holder force, on the other hand it is difficult to limit the inherent variability for example of the supplied coils of material, as well as of the lubricating conditions throughout the process.

Therefore, investigations of the range of variation of the main sources of variability in sheet stamping processes have been carried out.

Karthik et al. (2002) investigated the scatter in formability of several coils of three different

steel alloys, by using two types of tests at three different laboratories. In order to give an understanding of the amount of variation of some material properties, a summary of their results is reported in Table 1.1 and 1.2, where variations are expressed as standard deviations.

Property	Type 409 RD (27 coils)	Type 409 TD (32 coils)	Type 439 TD (14 coils)
n	2.2	1.8	3.9
K	2.0	1.8	1.6
Elongation	2.9	5.3	2.7
YS	4.3	3.9	3.4
UTS	2.4	2.2	1.5
r-0	12.0	–	5.9
r-45	18.0	–	6.4
r-90	13.0	–	5.5
$\bar{r}$	10.0	–	3.3
Δr	76.7	–	15.7
PHF	1.3	4.1	1.6
Load at failure	1.7	5.0	3.2

Table 1.1: Coil to coil standard deviations of material properties (Karthik et al. (2002)).

Standard deviation (%)	439		409		18Cr–Cb	
	RD	TD	RD	TD	RD	TD
OSU	0.73	2.50	1.03	2.38	0.72	3.05
AK	0.58	2.44	0.71	2.03	0.59	0.30
AM	0.58	2.17	0.71	3.58	1.62	0.74
Average[a]	0.63	2.37	0.82	2.66	0.98	1.36
Lab-to-lab[b]	0.37	1.35	2.20	1.14	1.35	1.81

[a] Average: mean of standard deviations reported by the three laboratories (i.e. average standard deviation at one laboratory).
[b] Lab-to-lab: standard deviation of the three average test values, one at each laboratory.

Table 1.2: Test to test and lab to lab standard deviations by material (Karthik et al. (2002)).

As it can also be drawn by the above results, they came up with the conclusion that coil to coil variations were always greater than test to test or lab to lab ones.

Cao and Kinsey (2001) observed that the material strength coefficient may vary by 20% during a sheet bending operation, the strain hardening coefficient by 16% while the friction conditions even by 65%.

Geometrical features variations have also been investigated. Gantar and Kuzman (2002) and Jaisingh and Narasimhan (2004) reported a stochastic variation of sheet thickness as high as 5% while tool dimensions as die and punch radii vary by less than 1% for a deep drawing

process.

Table 1.3 summarizes the variation of the main noise in sheet stamping processes investigations by de Souza and Rolfe (2010). It can be observed that even though there are several sources of scatter, the most remarkable one comes from material properties variability, followed by friction conditions.

Noise source	Mean	Std. dev.	Min.	Max.	Range (%)	CV Std.dev./Mean (%)
Yield Stress	489.5 MPa	12.6 MPa	467.7 MPa	535.0 MPa	13.7	2.57
Ultimate Tensile Stress	633.0 MPa	14.4 MPa	605.4 MPa	674.6 MPa	10.9	2.27
Initial tickness	1.96 mm	0.01 mm	1.91 mm	1.98 mm	3.57	0.51
Friction Coefficient	0.135	0.0027	0.127	0.143	11.85	2.00

Table 1.3: Variation of the main noises in sheet stamping processes (adapted from de Souza and Rolfe (2010)).

De Souza and Rolfe (2010) characterized the effect of material and process variation on the robustness of springback for a semi-cylindrical channel forming operation of an Advanced High Strength Steel (AHSS), using the package AutoForm^{TM} Sigma v.4.1, which is a FEM commercial code, able to account for uncertainty while performing FE analysis by incrementally introducing each of the noise sources (i.e. material properties variations as first, then blank geometry and process parameter variations). They analyzed the scatter of the effective strain and stress for a critical region of the stamped component and in particular they observed that the greatest spread in the major stress distribution is caused when variation in mechanical properties is introduced. They concluded that variation in process parameters, which primarily influence the magnitude of work in the stamping system, such as the blank holder pressure, friction and blank geometry, affect the strain component of the response window and can be detected by scatter in punch force response from stamping to stamping.

As a matter of fact, material parameters strongly influence formability, that it is also affected by the friction generated through the contact. Hazra et al. (2011) investigated the press formability of AA6111-T4 and AA5754-O, due to changes to overall material properties, tooling surface roughness, with particular emphasis on the effect of tooling temperature in relation to the properties of the lubricant. Material properties were found to have an effect on the formability of both materials while AA5754-O was also found to be affected by the

temperature of the tooling.

Consequently, there is a need to better understand the impact of variability in the stamping process towards a more aware and proper design of stamped parts. In fact, according to Majeske and Hammett (2002), part variability still remains a predominant issue especially in the stamping of complex and thin-walled parts. They analyzed data from several leading automobile manufacturers and reported that within the same batch part to part geometric variation can be as high as 21%. In the report presented by the Auto/Steel Partnership Program (2000), the amount of variations experienced for several automotive components by the car manufactured listed in Figure 1.1 is reported.

Company	Model
GM	Grand Am
NUMMI (Toyota)	Corolla
DamlerChrysler	Neon
Nissan	Altima
Ford	Taurus
Renault	Clio II
Opel	Vectra

(a)

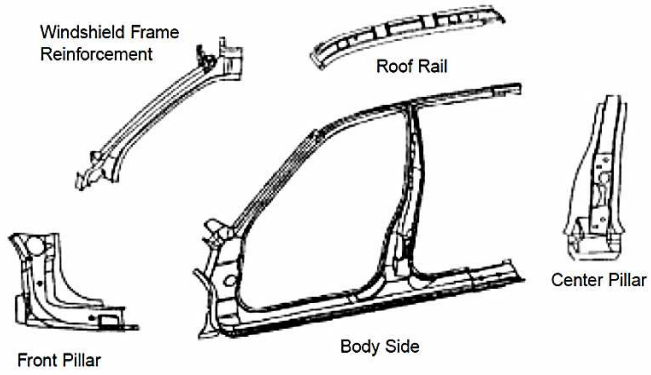

(b)

Figure 1.1: Variations experienced by some automakers (a) and some of the analyzed components (b) (adapted from Auto/Steel Partnership Program (2000)).

Such results, published by the Auto/Steel Partnership Body Systems Analysis Project Team on stamping and assembly variation, highlighted severe scatters for the analyzed components leading to fail the typical tolerances on the geometric requirements. Table 1.4 summarizes the average percentage of dimensional failure of some automotive components.

Company	Body Side Type	Typical tolerance	# cross car clamps in fixture	Average [Mean]	% Dimensions [Mean] >tol (t)
A	Integrated Quarter	+/- 0.7	11	1.10	66%
B	Integrated Quarter	+/- 0.7	14	0.73	39%
C	Two-piece	+/- 1.25	7	0.51	5%
D	Two-piece	+/- 1.0	8	0.88	39%
E	Two-piece	+/- 0.5	22	0.36	14%
F	Two-piece	+/- 0.3	16	0.31	39%
G	Integrated Quarter	+/- 0.5	17	0.37	28%

Table 1.4: Average percentage of failure (adapted from Auto/Steel Partnership Program (2000)).

Many authors used FEM based approaches to investigate the variability effects on sheet

stamping processes, as reasonably time consuming tool if compared to experiments. It has to be pointed out though that a standalone FEM approach, even effective for sensitivity analysis, is not suitable to deal with stochastic behaviors. FEM analysis is in fact traditionally considered a deterministic tool and more complex robust approaches have been applied in the technical literature as better discussed in Chapter 2. In particular, FE analysis and probabilistic Design of Experiments have been used to easily account for the scatter of the noises. In fact, typically the levels of the DoE space out properly through the probability distribution of such variables, whose effect is modeled in this way within the design space. For instance, Chen and Koc (2007) analyzed the influence of material properties and some process parameters on springback, under the noise effect of blank thickness variation. They randomized the levels of a Box-Behnken DoE, according with assigned probability distributions. The relationship between process variables and springback was achieved therefore considering random variability of input levels. Gantar and Kuzman (2002) studied the influence of variability on necking and wrinkling occurrence in a deep drawing of a rectangular box, based on finite element method as well. They, for instance, showed how a variation of strength modulus can produce an increase of fracture danger of about 4%. On the other hand, de Souza et al. (2008) implemented a probabilistic modeling approach, integrating FEM simulations and meta-modeling techniques. They found that material properties such as yield strength and the strain hardening index are important in dimensional stability for springback control. Asgari et al. (2008) used an orthogonal array with two levels for springback prediction of TRansformation Induced Plasticity (TRIP) through an industrial case study. They observed that changes of up to $\pm$10% in Young's modulus and coefficient of friction were found to be insignificant in improving or deteriorating the statistical correlation of springback accuracies.

Following a sensitivity case study is proposed: FE analysis and metamodeling techniques integrated to Monte Carlo Simulation Methods were used in order to better investigate the effect of material variability in a deep drawing operation of an S-shaped U-channel component. Significant scatters of thinning and springback were observed, highlighting the need of robust design approaches able to deal with the influence of stochastic noises in sheet forming.

1.1 Sensitivity analysis of a sheet stamping process: a case study.

The robustness of the design process against the uncertainty due to coil to coil variation of the material parameters was evaluated in a deep drawing process case study. In particular, the main goal was to understand the way thinning and springback are affected by the material inner variability with respect to the expected nominal value. In fact, as the use of Advanced High Strength Steels (AHSS) and lightweight alloys, like aluminum or magnesium, progressively raised, springback control has become a crucial issue. In particular, some studies on springback (Santos and Teixeira (2008), Simões et al. (2003)) have demonstrated that a more pronounced springback occurrence characterizes aluminum alloys with respect to other materials.

Springback occurrence is mainly due to unbalanced residual stress state as forming tools are removed. During loading phase, the internal stresses are completely balanced by external tools action and an inhomogeneous strain distribution through the sheet thickness occurs, since a variable region of the sheet remains elastic. Therefore, as tools are removed, elastic deformation is released up to reach a self-equilibrated residual internal stress, then springback occurs leading to geometrical deviations from the desired final shape.

There have been many attempts in the technical literature to optimize, compensate or at least reduce springback in automotive applications. For instance, Lingbeek et al. (2005) compared two different ways of geometric optimization, the smooth displacement adjustment (SDA) method and the surface controlled over-bending (SCO). On the other hand, since it is very difficult to apply analytical methods to fully three-dimensional parts, FEM based integrated approaches have been increasingly developed to accurately investigate springback phenomenon.

Many authors studied both process set up and numerical parameters influence on springback control. In (Panthi et al. (2007)) the effects of load on springback at the varying of the thickness as well as of the die radius were examined. Other authors have investigated the influence on springback of blank holder force, friction, spatial integration, time integration scheme and constitutive laws (Papeleux and Ponthot (2002)). Several papers assessed how springback prediction capability depends on the utilized numerical approach (Lee and Yang (1998), Meinders et al. (2008)). Generally, explicit method is preferred for forming phase

being faster and more reliable, while implicit one is used for unloading aiming at balancing computational efficiency and prediction accuracy. A coupled explicit - implicit finite element procedure is evaluated by Narasimhan and Lowell (1999) for automotive components. Meanwhile, there are other possible coupled approaches proposed in literature, explicit-explicit, static explicit-static explicit, and even one step methods (Wagoner (2002)).

However, as it was earlier pointed out, the robustness of process results is an even more complex issue to deal with as uncontrollable effects have to be managed.

A better understanding of the cause-effect linkage between thinning and springback variation and noises related to coil to coil variations is provided in the following section.

1.1.1 The investigated process and numerical set-up.

The process chosen to the inner variability investigate of sheet stamping operations was an S-shaped U-bending process, proposed as benchmark in the Numisheet'93 Conference. Figure 1.2 illustrates a sketch of the process with particular focus on the geometrical details of the tooling (a), initial blank shape (b) and final formed part (c). Drawing depth and die fillet radius were, respectively, equal to 15[mm] and 3[mm], clearance between die and punch was equal to 1.5[mm], blank thickness was 1[mm]. In particular, the material investigated in the present study was an aluminum alloy (AA6016).

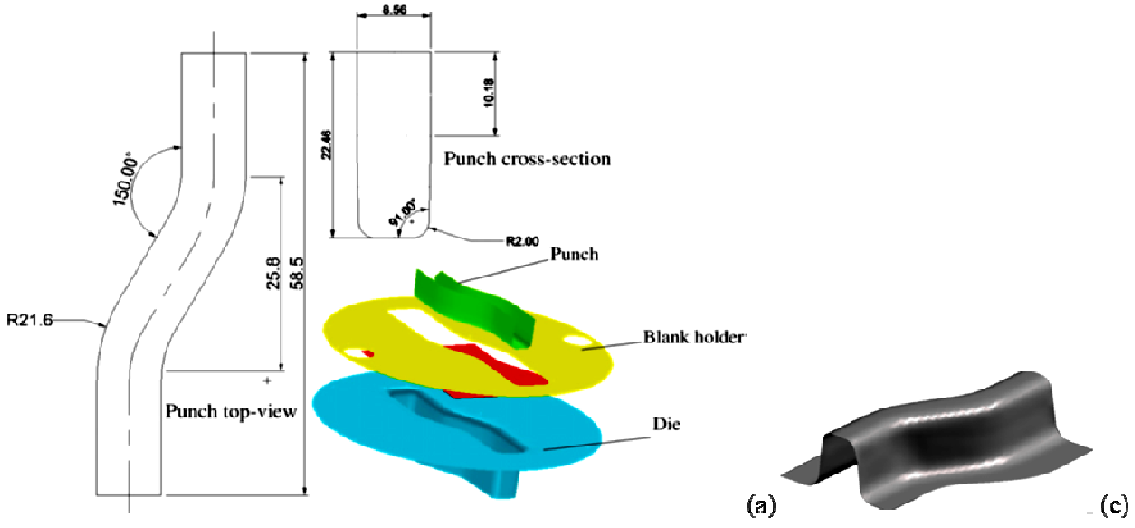

Figure 1.2: Tooling geometry (a), initial blank shape (b) and final formed part (c).

The process mechanics essentially consists of a bending and unbending on the side walls; the

work hardening determined by the deformation process, coupled with the stretching produced by blank holder force action determine the thinning occurrence on the final part. Such phenomenon, if not properly controlled, could excessively increase and also lead to ductile fractures. Moreover, a further drawback of such process is springback phenomenon.

It has to be noticed, that the material properties strongly influence the occurrence of the above mentioned defects, since they affect material formability and its elastic behavior.

The investigated process was numerically simulated using explicit code LS-DYNA and a subsequent springback analysis was carried out with its implicit solver. The punch velocity was artificially increased for the explicit formulation, checking that the kinetic energy was below the 10% of the deformation work in order to avoid any inertia effect.

According with the technical literature (Ingarao et al. (2009b)), the blank sheet was meshed by fully integrated quadrilateral shell elements with 9 integration points along the thickness, while the tool parts are modeled as rigid bodies. In particular, the starting sheet element size is 3mm and a three levels geometric remeshing strategy was applied all over the numerical simulations. The total number of elements at the end of the explicit simulations was higher than 4000; a Coulomb model was considered for frictional actions. In order to take into account material anisotropy, the Barlat-Lian constitutive model with an isotropic work hardening was utilized (Fratini et al. (2008)).

In Figure 1.3 an example of the results of the numerical simulations is shown, in particular, a map of plastic deformation distribution is reported.

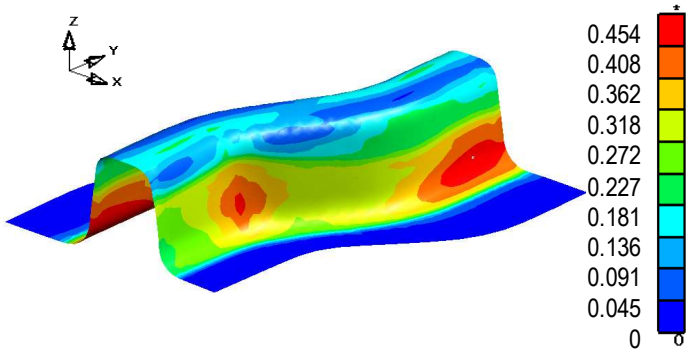

Figure 1.3: Map of plastic deformation distribution from LS-DYNA numerical code.

1.1.2 The proposed methodology.

The functional scheme of the proposed methodology is summarized in Figure 1.4.

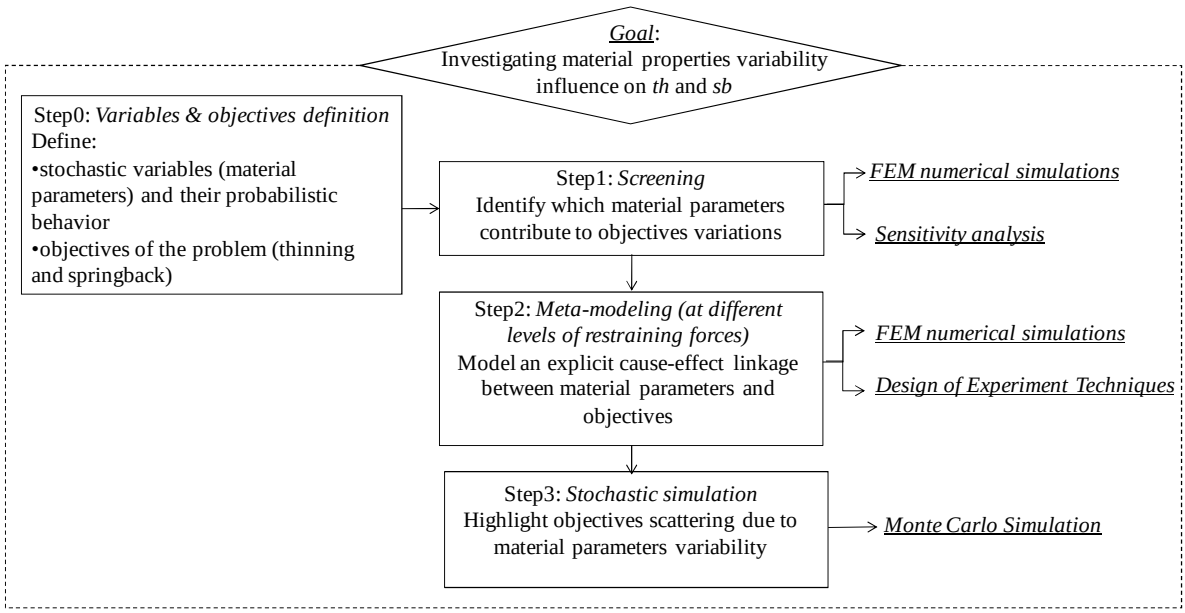

Figure 1.4: Scheme of the proposed methodology.

Step0: Variables and objective definition.

A fundamental step to analyze the stamping process uncertainty is to select the possible sources of variation that could compromise a good process design. Generally, a stamping process design is based on deterministic considerations; actually, if certain process "performances" are desired, it is necessary to investigate which factors produce a scatter of the final results and consequently also the way they determines variations of such results from their expected values. In this way, such case study investigated how some of material parameters may cause process performances variations with focus on springback and thinning results. The maximum thinning percentage (th[%]) was utilized to express process performances related to thinning. Such measure is commonly utilized as fracture risk indicator (Barlat and Lian (1989), Shivpuri and Zhang (2008)) also in industrial environments: actually, for industrially stamped components a range of acceptable thinning levels is generally requested. On the contrary, Forming Limit Diagrams (FLDs), for instance, are not effective in this way. The utilization of FLDs is commonly recognized as a very effective tool to investigate failure. Nevertheless, the state of the art in this research field assesses that FLDs do not perform well if non-linear strain paths are concerned (Wu et al. (2005)). On the other hand, the utilization of forming limit stress diagrams is considered a good tool to represent

fracture limits but such diagrams need to be properly tuned to derive a proper indicator of fracture risk. Such considerations, together with the observation that in an industrial environment a quick and simple fracture danger indicator is necessary, led to the choice of th[%] as objective function. Moreover, the maximum thinning was chosen instead of thinning distribution because the control of wrinkling (which should be evidenced by eventual thickening) is not necessary for the investigated process in consideration of the obtained circumferential stress ranges.

In order to measure springback occurrence and to quantify process performances in this sense, a CAD environment was initially utilized in order to provide a good evaluation of springback. In particular, comparisons between deformed blank after load removing and final stamped part were developed trying to measure different springback indicators. After this analysis, a comparison between deformed blank after load removing and final stamped part was utilized as it proved to be the most straightforward representation. Furthermore, such choice is fully justified by the consideration that this indicator is quite efficient in terms of springback prediction as it allows taking into account both flange relief in Z direction and blank section opening in X direction. LS-DYNA directly provides the chosen springback measure indicated as sb[mm] in the following. In particular, the displacements calculated in normal direction between deformed blank after load removing and final stamped part was utilized. Figure 1.5 reports two maps extracted from the numerical simulations: maximum thinning (th[%]) distribution (a) and springback indicator (sb[mm]) distribution (b).

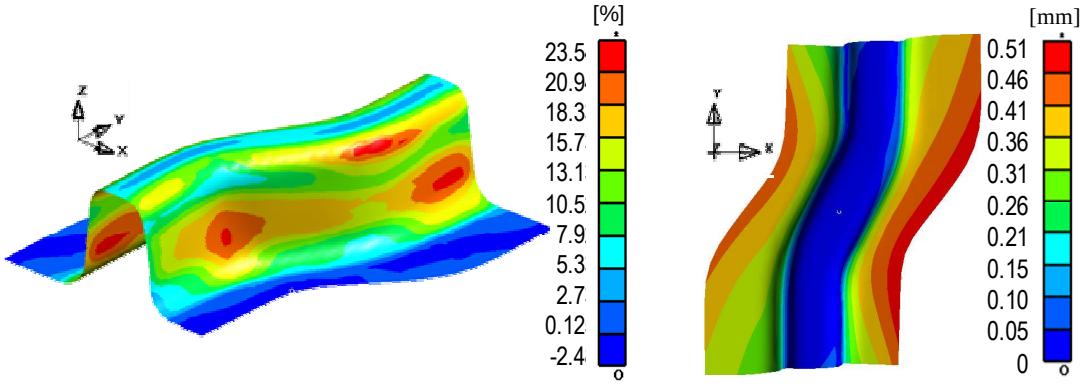

(a) (b)

Figure 1.5: Examples of thinning [%] (a) and springback [mm] (b) distributions.

As material properties are regarded, it is well known that springback phenomenon strongly

depends on the ratio between material flow stress (σ) and Young modulus. Some researchers have also pointed out that most of the metallic materials are characterized by an inelastic recovery behavior after plastic deformation since the elastic modulus decreases with plastic strain (Morestin and Boivin (1996), Zang et al. (2006)). Yu (2009) studied a U-channel stamping process and analyzed the variation and influence of elastic modulus of TRIP steels during plastic deformation: springback effects were more evident taking into account variations in E with the respect to the case with constant Young modulus.

Additionally, according to Verma and Haldar (2007), higher anisotropy gives higher springback. Moreover, normal anisotropy is also an efficient indicator of thinning tendency, which, in turn, also depends on material strength. Many authors investigated the effect of material anisotropy on springback amount. Gomes et al. (2005) analyzed the variability of springback of anisotropic high strength steel, comparing numerical and experimental investigations of a benchmark U-shape stamping process (NUMISHEET'93). Springback variation comparing the results along rolling direction (0°) and along transverse one (90◦) was considerable: springback increases at the increasing of the angle from the rolling direction. The role of anisotropy on the springback occurrence was also assessed by Ragai et al. (2005): they studied stainless steel 410 draw-bend specimens, at the varying of blank holder force and noticed differences on springback at 0°, 45° and 90° from the rolling direction. In particular, such differences were more pronounced for specimens tested at the higher blank holding pressure, where more plastic work occurred, proving that the effect on the process results is different for different restraining forces levels.

Verma and Haldar (2007) developed both FE and analytical models to analyze effect of normal anisotropy, concluding that higher anisotropy gives higher springback, so that springback is least for an isotropic material. They also analyzed by analytical models the effects of sheet thickness and strain hardening exponent observing that both parameters increase implies a springback lowering.

Therefore, basic on the above considerations, the following material properties were taken into account in the analysis here proposed: strength coefficient (C) and strain-hardening exponent (n) (defining the material flow rule in the form $\sigma=C*\varepsilon^n$), anisotropy coefficients (r_0, r_{45}, r_{90}), Young modulus (E).

Once the material variables were defined, it was necessary to define their stochastic variability in order to perform a stochastic analysis. Such variability can be described by a Gaussian (normal) probability distribution with given mean (μ) and standard deviation (σ).

The mean values of each material parameter (stochastic factor) are the ones corresponding to nominal values for the chosen material (see Table 1.5).

	C [MPa]	n	r_0	r_{45}	r_{90}	E [GPa]
Material parameters nominal values	422	0.247	0.684	0.555	0.684	70

Table 1.5: AA6016 nominal parameters i.e. mean values (μ) of the probability distributions

The most suitable values of σ, for each parameter distribution, were chosen on the basis of an accurate literature analysis about proper coefficients of variation.

Actually, the technical literature investigation provided the values of the ratio between standard deviation and mean value (σ/μ) for each chosen factor (de Souza and Rolfe (2008), Karthik et al. (2002), Zang and Shivpuri (2009)). Furthermore, the hypothesis of independent variables was assumed: it means that correlation among parameters is neglected (i.e. the statistic co-variance is null). Table 1.6 summarizes the standard deviation of each selected variable together with the utilized coefficient of variation.

	C [MPa]	n	r_0	r_{45}	r_{90}	E [GPa]
Standard deviation (σ)	27	0.0285	0.0178	0.0300	0.0445	1.6
Coefficient of variation (σ/μ)	6.38%	12%	3%	5%	7%	2.27%

Table 1.6: Standard deviation and utilized coefficient of variation of each selected variable.

In order to focus on the influence of coil to coil variation of material properties, other parameters were fixed within assigned operative windows at the varying of restraining forces (i.e. at the varying of blank holder action). It was assumed that lubricating conditions are fixed with a friction coefficient equal to 0.1. Moreover, the analysis was performed at different levels of blank holder force (BHF), namely 10[kN], 45[kN] and 80[kN] also with aim to represent a significant restraining forces range. Actually, such assumption was justified by the consideration that, in order to evaluate the actual effect of material inner variability on process results "stability", different operative conditions have to be taken into account: in fact, a reliability analysis performed at certain restraining forces level may lead to consider some parameters as not relevant, while, on the contrary, the same parameters may produce a strong

instability for higher restraining forces levels.

Step1: Screening.

This step of the procedure investigated how the uncertainty of th and sb results can be allocated to different sources of variation. The final aim was to screen the set of variables selected to represent material variability. Even if a noise variable has an influence on a given objective from a deterministic point of view, its slight stochastic variation could produce no significant variation on the objective itself. Thus a proper screening technique would be useful. There are many screening techniques in literature whose application is more or less suitable depending on the analyzed problem features (problem dimension, linear or quadratic relationships, absence of variables interactions, and so on). Some common screening techniques are summarized in the following.

Fractional factorial designs.

An artful combination of variables coded values (±1) is used to estimate the main variables and the interactions effects with a limited number of experiments (Myers and Montgomery (2002)). A crucial issue is the sizing of the variables domain, which should be neither too large nor narrow to not compromise the technique capability to determine the relationship between experimental response and variables at multiple levels.

ANOVA

It is a simple statistical method that partitions the observed variance to different variables, comparing the means of several sample groups (Myers and Montgomery (2002)).

Latin hypercube designs

Such technique stratifies the design space into n equal regions within which each variable is present once and at one level.

Such approach provides the possibility to drastically reduce the computational effort. The key question in constructing a Latin hypercube design is how to match the levels according to different criteria, such as orthogonality and space filling (Bingham et al. (2009), Georgiou (2009), Prescott P. (2009), Roshan and Hung (2008)).

Plackett Burman designs

Such approach allows to carry out a few number of experiments (also n+1 with n variables to be analyzed); in Plackett–Burman designs the interactions estimations are confounded with the main variables effects, meaning that the designs is not able to distinguish between certain main effects and certain interactions (Beres and Hawkins (2001), Magallanes and Olivieri (2010)).

Sensitivity analysis technique

A largely used method, simple and effective to be developed, that systematically changes each variable within its domain to determine the effects of such changes, while the others are fixed. Of course, such screening step is requested for each objective function and the final output is a set of control and noise variables, whose effects will be deeply investigated in the subsequent phases.

A sensitivity analysis was carried out trying to answer questions related to the effects relevance of each material parameter on thinning and springback. A typical question may be formulated as follows: it is known that low values of normal anisotropy imply higher thinning tendency, but which of the anisotropic coefficients has the greater influence? The sensitivity analysis was carried out varying just one variable within its stochastic range of variation, while the others were fixed at their own nominal value, Figure 1.6 shows the normal distributions of parameters E (a) and n (b) evidencing their basic points (it has to be noticed that normal distributions are statistically described by probability density curves).

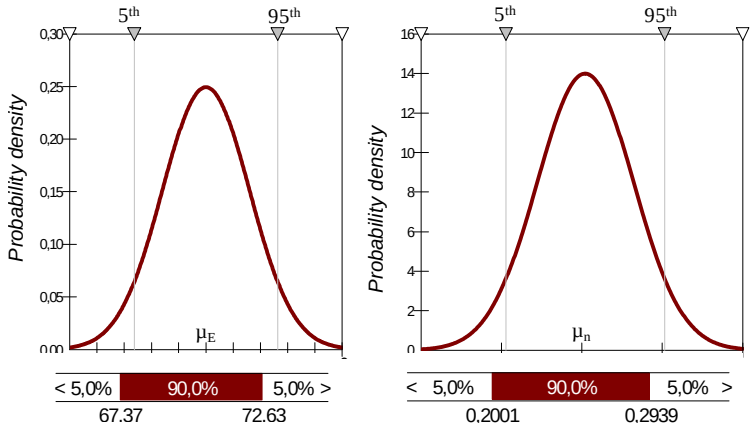

Figure 1.6: Normal distribution of parameters E (a) and n (b).

The sensitivity analysis was performed taking into account three levels for each parameter variation, corresponding respectively with 5th percentile, mean value (nominal), and 95th percentile of its normal distribution. Such choice allows reproducing a large enough perturbation of the chosen parameter to represent its variation influence. Table 1.7 reports the above mentioned levels (5th percentile, mean and 95th percentile) for each material parameter.

	C [MPa]	n	r0	r45	r90	E [GPa]
5th	377.6	0.2001	0.6547	0.5057	0.6108	67.37
μ	422	0.247	0.684	0.555	0.684	70
95th	466.4	0.2939	0.7133	0.6043	0.7572	72.63

Table 1.7: 5th percentile, mean and 95th percentile for each material parameter variation.

The analysis was carried out by numerical simulations at the above mentioned levels of BHF (10[kN], 45[kN] and 80[kN]) for each material factor variation. In particular, at given BHF, FEM simulations were developed at level μ (mean value) and at levels 5th and 95th of each factor. It has to be noticed that level μ for each factor reproduces the deterministic conditions for that factor, i.e. the expected value of that factor with no inner variability effect.

Step2: Meta-modeling.

Once the material parameters were screened, in order to stochastically analyze their influence on objectives (th and sb) it was useful to carry out a meta-modeling step to obtain an analytical link between the parameters and the objectives themselves. Such modeling is preliminary to the actual stochastic investigation and the obtained meta-models are the foundation for the subsequent Monte Carlo method application.

The meta-modeling step was based on Response Surface Method (RSM): in particular, a proper Design of Experiments (DoE) was formulated, namely, a Central Composite Design (CCD) was chosen. The CCD structure for a general case with 3 variables (i.e. x_1, x_2, x_3) is shown in Figure 1.7 (a) and (b) with levels ±1 and ± α highlighted.

Thanks to the utilized DoE, an appropriate number of points was designed to independently estimate first and second order coefficients, as well as paired interactions. Therefore, the corresponding FEM simulations were run and a full quadratic regression model was obtained.

Of course, the above mentioned approach was applied using only the variables which were not screened out from Step1 of the procedure. Moreover, the meta-modeling was repeated for each

above mentioned BHF level. The meta-model development provided a polynomial equation that describes how a specific output depends on a set of input variables.

Runs	x_1	x_2	x_3
1	+1	+1	+1
2	+1	+1	-1
3	+1	-1	+1
4	+1	-1	-1
5	-1	+1	+1
6	-1	+1	-1
7	-1	-1	+1
8	-1	-1	-1
9	+α	0	0
10	-α	0	0
11	0	+α	0
12	0	-α	0
13	0	0	+α
14	0	0	-α
15	0	0	0

(a)

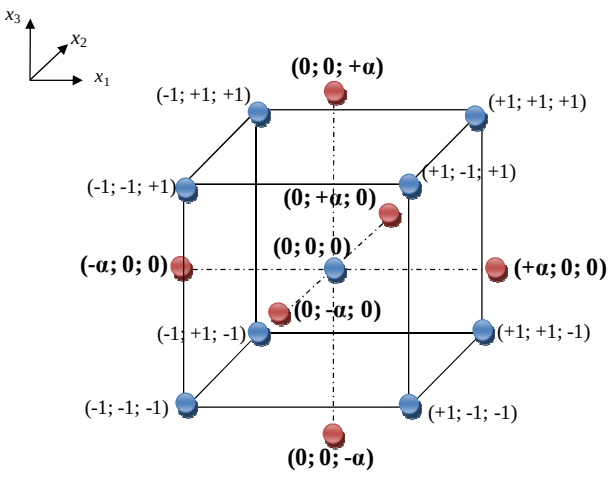

(b)

Figure 1.7: CCD general structure with 3 variables: points configuration (a) and spatial distribution (b).

Nevertheless, such linkage is a deterministic one neglecting all possible probabilistic considerations about the effects of parameters stochastic variations. For this reason, it was advisable to integrate a stochastic interpretation within the utilized DoE: the meta-modeling is functional to the stochastic analysis, thus the domain of variation of the variables included in the meta-model has to replicate the stochastic investigation range. Therefore, the levels ± α of the CCD designed for each parameter correspond with 5^{th} and 95^{th} percentiles of that parameter normal distribution. The approximation meta-model capability was evaluated by two indicators: a correlation coefficient (R-sq adj) and absolute mean difference (e) between numerical results and predicted ones. The former was utilized as meta-model data fitting indicator, the latter as prediction capability one (which evidences the deviation of the predicted results from the actual ones).

Step3: Stochastic simulations.

Thanks to the availability of meta-models linking th and sb to material parameters, it was possible:

- to quantify the parameters variation effects;

- to provide a tool able to understand how the objectives may vary due to a simultaneous perturbation of different uncontrolled parameters.

Actually, the meta-models express the relation between each output and different material factors, thus, they allow analyzing the simultaneous variations of such parameters. At each restraining forces level (i.e. controllable value of BHF), the associated th and sb values are not unique, but they change within a possible range of occurrences. An uncontrollable inner material variability implies that th (and/or sb) does not reach a deterministic value but it may change within different occurrences whose probability distribution has to be identified.

The assessment of process robustness under the effect of uncontrolled parameters variation was carried out by Monte Carlo Simulation Method (MCS) (Haldar and Mahadevan (2000)).

As it is well known, MCS is an efficient technique aimed at evaluating the outputs uncertainty in a perspective of improvement of the process reliability. In fact, even if it isn't possible to control material coil to coil variations, it is however possible to design the stamping process accounting for such noise perturbations. MCS searches problem solution as a statistical parameter belonging to a hypothetical population: the solution is achieved by analyzing sample data from random generations. It calculates a series of possible values of the investigated output by randomly generating different occurrences of each process variables (inputs), extracted from a given probability distribution. The basic concept of MCS technique is the generation a proper number of input occurrences according with defined probability distributions and subsequently the determination of the related outputs values. In particular, Monte Carlo method consists of six main steps (Haldar and Mahadevan (2000)):

1. problem definition in terms of stochastic variables;
2. quantification of each variable statistical properties;
3. generation of sample data for each variable by random extractions from assigned probability distributions;
4. deterministic evaluation of output associated with every sequence of random extractions;
5. extraction of probabilistic distribution for each output;
6. verification of efficiency and accuracy of simulation.

The determined analytic linkage (by meta-modeling) allows to reduce computational effort in

MCS application since it decreases the number of experimental/numerical data which otherwise would have to be run, In the presented application, 5000 Monte Carlo simulations were run for each meta-model (th and sb at various BHF levels),

The application of the MCS steps to this case study consisted then of the following steps:

1. generating a proper number of random input occurrences, i.e. set of material properties parameters, according with probability distributions defined in Step0 of the procedure;
2. calculating the th and sb values by the meta-models for each BHF level obtained in Step2 of the procedure;
3. extracting the corresponding th and sb probabilistic distributions from such calculated objective occurrences (one distribution for each BHF level).

The final results of this Step 3of the procedure are, in other words, the stochastic distributions of th and sb for each level of restraining forces. These distributions will allow explaining the effect of stochastic material parameters variation on the objectives of the process design (i.e. to verify the robustness of the design choices).

1.1.3 Discussion of the results.

The final contribution of the proposed stochastic analysis is to assist the process designers in the stamping process set up taking into account uncertainty on the process stability deriving from material parameters stochastic variability. In this way, the proposed methodology aims at providing a tool able to show and quantify th and sb scattering at the varying of the restraining forces, due to uncontrolled coil to coil material properties variations.

Sensitivity analysis.

As mentioned, the early step of procedure concerns the sensitivity analysis: the numerical simulations were performed making the material parameter vary within their, previously defined, stochastic ranges of variation. The results provided by the FEM simulations performed for the sensitivity analysis in terms of thinning and springback are shown in Table 1.8: the values of th[%] and sb[mm] are reported for each level of variation of each parameter (levels μ, 5^{th} and 95^{th}) respectively at BHF equal to 10[kN], 45[kN] and 80[kN].

	C	n	r0	r45	r90	E	BHF 10 kN th	BHF 10 kN sb	BHF 45 kN th	BHF 45 kN sb	BHF 80 kN th	BHF 80 kN sb
C	**95th**	0	0	0	+	0	9,9	1,12	14,7	0,83	20,0	0,63
	5th	0	0	0	-	0	10,6	0,90	16,5	0,61	39,4	0,38
n	0	**95th**	0	0	0	0	10,5	0,95	16,4	0,67	29,7	0,41
	0	**5th**	0	0	0	0	10,1	1,10	14,9	0,77	20,1	0,60
r0	0	0	**95th**	0	0	0	10,2	1,00	15,5	0,72	25,3	0,49
	0	0	**5th**	0	0	0	10,2	1,00	15,1	0,73	23,9	0,51
r45	0	0	0	**95th**	0	0	10,2	1,01	15,4	0,74	23,5	0,48
	0	0	0	**5th**	0	0	10,2	1,00	15,6	0,73	23,5	0,50
r90	0	0	0	0	**95th**	0	10,2	1,02	15,5	0,74	23,3	0,50
	0	0	0	0	**5th**	0	10,3	0,99	15,5	0,72	31,1	0,46
E	0	0	0	0	0	**95th**	10,3	0,96	15,6	0,68	23,5	0,46
	0	0	0	0	0	**5th**	10,2	1,04	15,5	0,75	23,5	0,51
nominal	**μ**	**μ**	**μ**	**μ**	**μ**	**μ**	10,2	1,00	15,5	0,72	23,5	0,51

Table 1.8: FEM simulation results within the sensitivity analysis

As it can be observed a great scattering of the results is present at the varying of the restraining forces both in terms of thinning and springback. Such result proves that the analysis at different levels of restraining forces is quite necessary. Moreover, the influence of each parameter variation will be deeply analyzed in the following.

It is worth pointing out that the above Table 1.8 reports also the results of thinning and springback in the numerical configuration corresponding to the expected values of material parameter (indicated with nominal values). Such results, for each level of BHF, represent the terms of comparison of all the other configurations analyzed within the sensitivity analysis. Table 1.9 shows th and sb maps, corresponding to such nominal material parameter values (level μ) of each selected material parameter, like a deterministic condition in which no stochastic effect is taken into account.

Starting from the availability of FEM results, it was possible to analyze the variations of th and sb caused by each single material parameter's probabilistic behavior. Therefore, a plot of the outputs variations at the varying of each of the material parameters (and considering the other fixed to their own nominal value) was performed.

Such results are shown in Figure 1.8 for thinning: the scattering from th nominal value (central point in each range of variation of a given material parameter) at each BHF level are reported. Figure 1.8 synthesizes the variation affecting th at 5^{th} and 95^{th} percentile values of each material parameter stochastic distribution (see again Table 1.8).

BHF [kN]	*th* [%]	*sb* [mm]
10	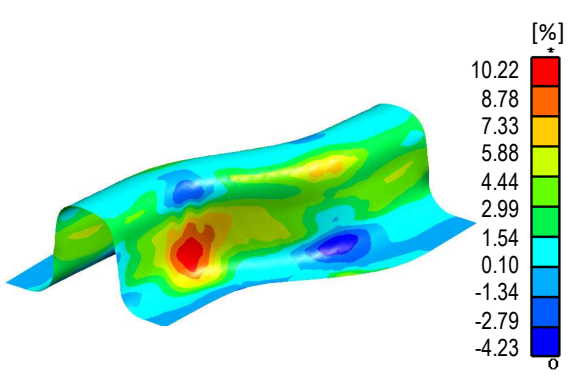	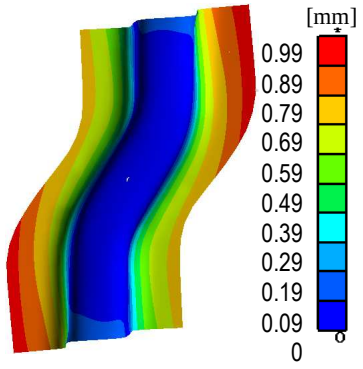
45	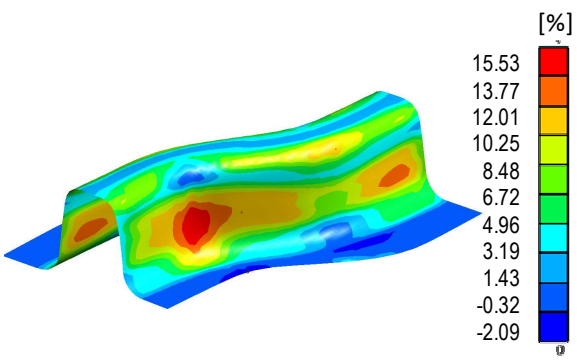	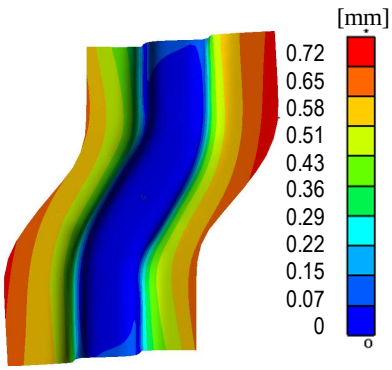
80	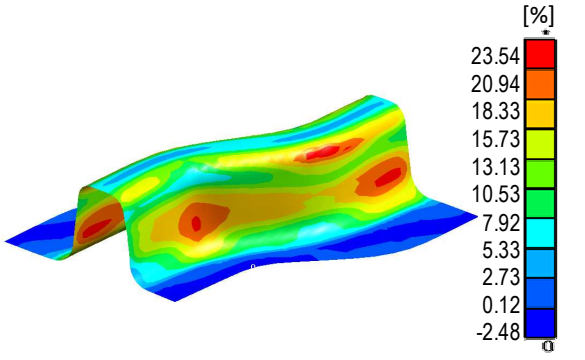	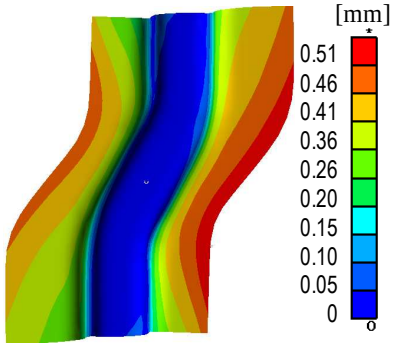

Table 1.9: Maps of th [%] and sb [mm] for nominal material parameter values by BHF level.

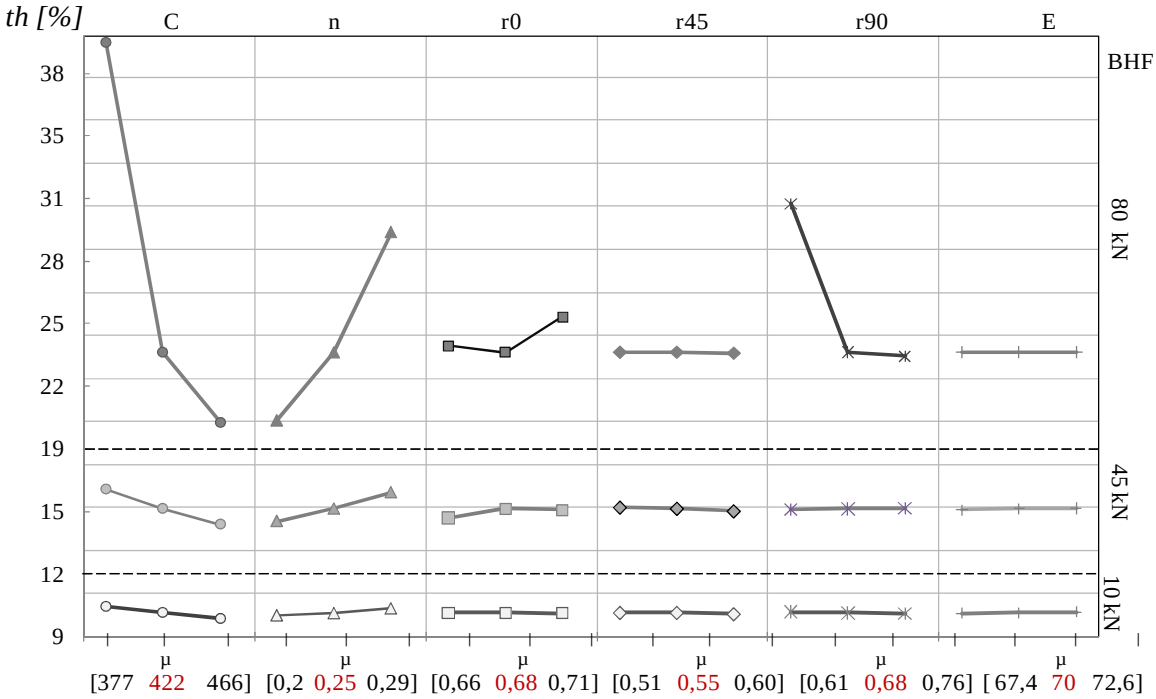

Figure 1.8: Thinning [%] scattering from nominal value at each BHF level.

A more relevant scatter can be noticed when the material flow into the die is more controlled (high BHF). In other words, as more onerous stretching conditions arise, a stochastic change in the material properties could produce a crucial change in the thinning. Such heavy conditions may evolve up to ductile fracture onset in that part regions where a localized thinning is expected (necking occurrence). In particular, for BHF equal to 80kN the strength modulus (C) variation produces very evident scatters of thinning from its nominal value (for instance from th =23.5% to 39.4%). In order to evidence the effects of C variations on final thinning, a draw-in analysis is very useful. Actually, Figure 1.9 compares the different draw-in behaviors associated respectively with C nominal value and its 5^{th} and 95^{th} percentiles.

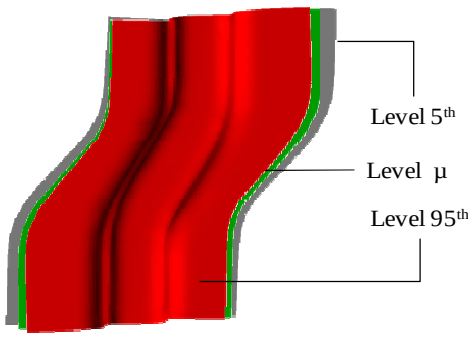

Figure 1.9: Draw-in comparison among nominal and end points of C variation range

As it can be observed draw-in is enhanced as C moves towards higher values thus, a lower stretching is obtained and consequently thinning decreases. As strain hardening exponent variation is concerned, a higher strain-hardening corresponds to higher material capability to accumulate deformations thus, as it is expected, thinning will be higher. This result is evident in Table 1.10 which shows the effect of the strain-hardening exponent on th by BHF level.

BHF [kN]	5th percentile	95th percentile
10	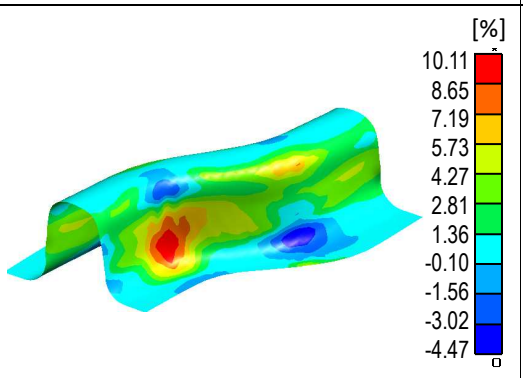	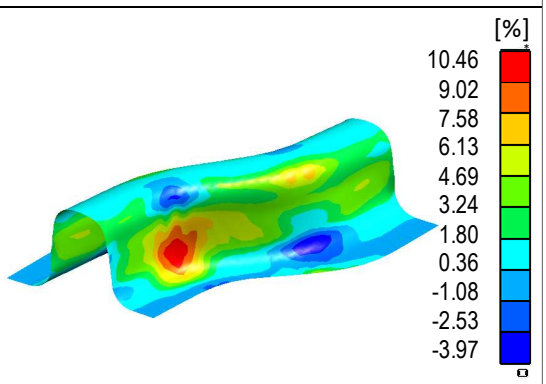
45	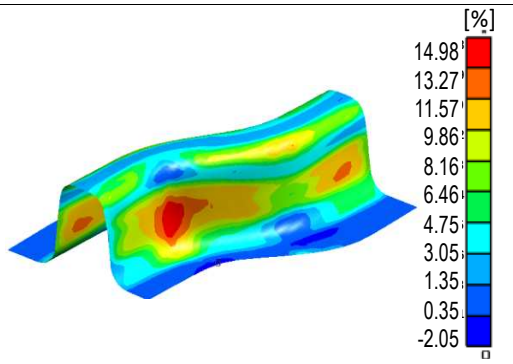	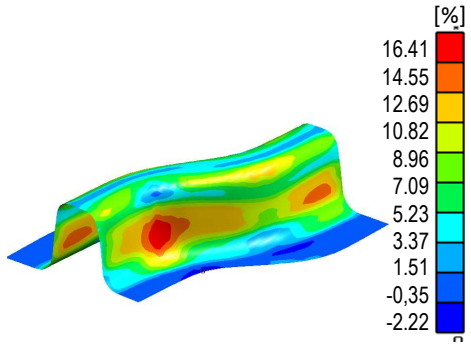
80	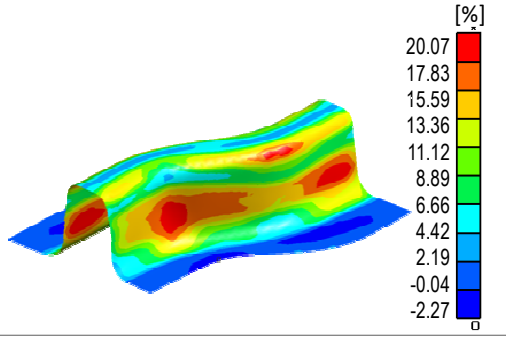	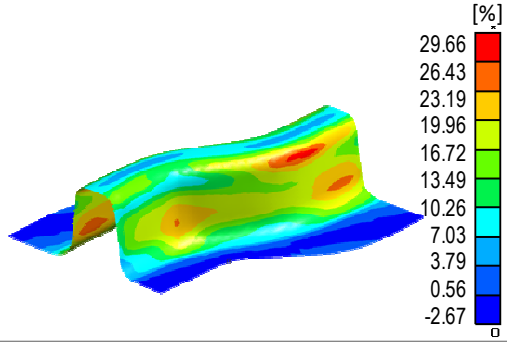

Table 1.10: Effect of the strain-hardening exponent on th at each BHF level.

Interesting evidence concerns the opposite tendency of material behavior corresponding to anisotropy coefficients stochastic variations (see again Figure 1.9).

In particular, the most relevant result concerns the r_{90} coefficient: for high restraining forces action (BHF equal to 80[kN]) the variation of r_{90} towards lower values implies a significantly higher thinning of the part. Such results could be justified according to the results obtained in the technical literature on the influence of anisotropy on sheet metal stamping operations (Barlat et al. (2004)): the r_{90} coefficient lowering produces variation of the yield surface which implies lower material strength; thus, in the analyzed operation, restraining force actions prevail and thinning strongly increases.

As the results in terms of springback are regarded, Figure 1.10 presents the outcomes obtained at the different BHF values for each parameter stochastic variation (of course, the same material parameters perturbations and operative conditions utilized for thinning sensitivity analysis are taken into account).

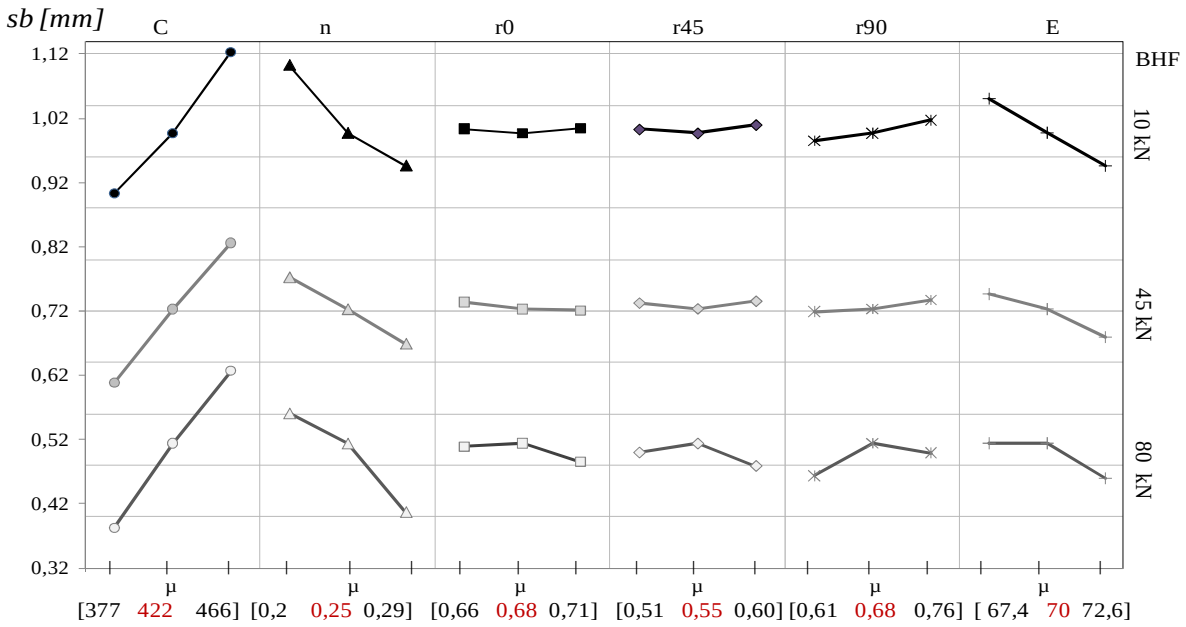

Figure 1.10: sb [mm] scattering from nominal value at different BHF values

It is well known that springback and thinning phenomena have generally conflicting behaviors (evident comparing Figures 1.8 and 1.10): each condition determining springback increase is related to thinning decrease and vice versa. The main differences with th results concern the effects at the three BHF levels: while the effects of material parameters stochastic variations on the th amount become more evident at higher restraining forces levels, as sb is concerned, the scatter of its values is nearly the same.

Another important topic to be stressed concerns the variation of the Young modulus which, as expected, strongly influences sb variation. Table 1.11 shows sb scatter produced by the variation of E from the 5th to 95th percentiles of its stochastic distribution for the three restraining forces levels.

BHF [kN]	5th percentile	95th percentile
10	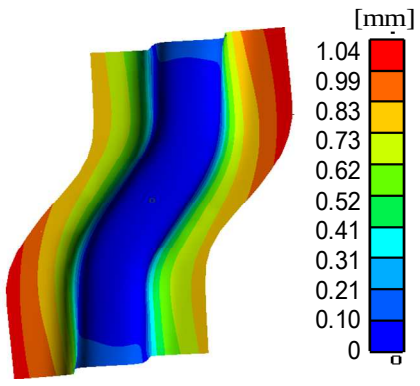	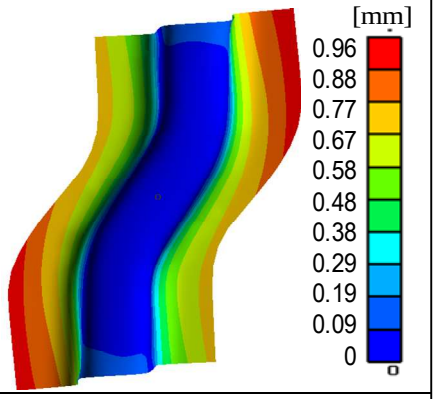
45	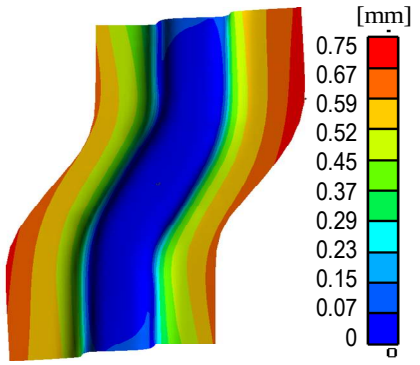	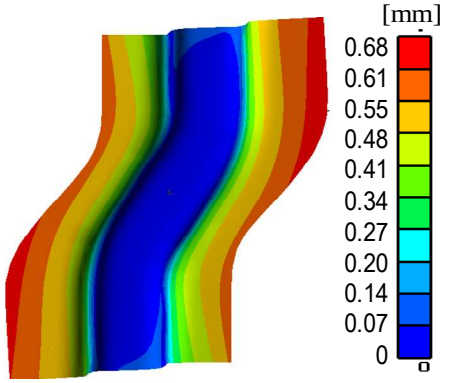
80	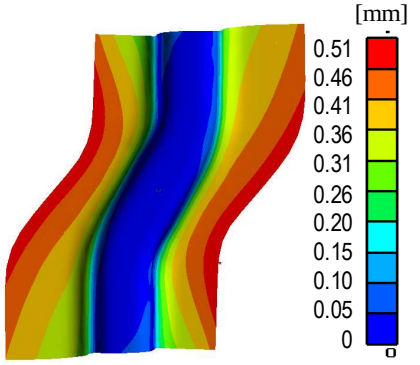	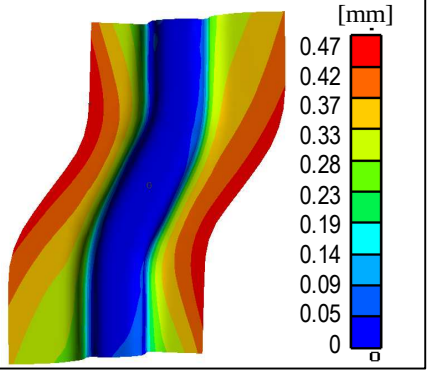

Table 1.11: sb scatter produced by Young modulus variation at the varying of restraining forces.

The above presented results make clear that taking into account parameters variability within process parameters tuning is fundamental to improve process robustness (for instance, through

a significant reduction of parts rejection).

Variable screening.

Based on sensitivity analysis results, variable screening was subsequently carried out in order to reduce computational effort and to fully focus on the most significant stochastic material parameters.

Therefore, it is useful to calculate a proper index able to synthetically quantify the influence of each material parameter on each objective. In particular, the aim was to properly represent the objectives scatter around their nominal value. Thus, the measure should not simply calculate the difference between objective occurrences respectively at 5^{th} and 95^{th} percentiles of the analyzed material parameter variation, but it should efficiently describe the objective scatter both when mean value of the material variables moves toward higher or lower values. Such index should also allow comparing the effects of material parameters at the varying of the restraining forces, which is very useful in terms of identification of the most significant ones on the process robustness.

The chosen index is indicated with Δ [%] and expressed as follows (Gantar and Kuzman (2002)):

$$\Delta[\%] = \frac{\sum_{i=1}^{n}(x_i - \mathrm{M})}{n \cdot \mathrm{M}} * 100 \qquad (1.1)$$

where: M indicates the objective nominal value (i.e. the one corresponding to the generic material parameter mean value μ), x_i is the current objective value (i.e. the value corresponding to 5^{th} and/or 95^{th} percentile of each material parameter distribution); n is the iterative number of occurrences (which is 2 in the analyzed case as the material parameter values can be at 5^{th} or 95^{th} percentile).

Figures 1.11 and 1.12 compare the Δ[%] values for each material parameter at each BHF level respectively for th and sb.

Moreover, Table 1.12 shows the contribution of each stochastic parameter to the scatter of th and sb in order to better explain how the explored instability can be allocated on the different sources of variation.

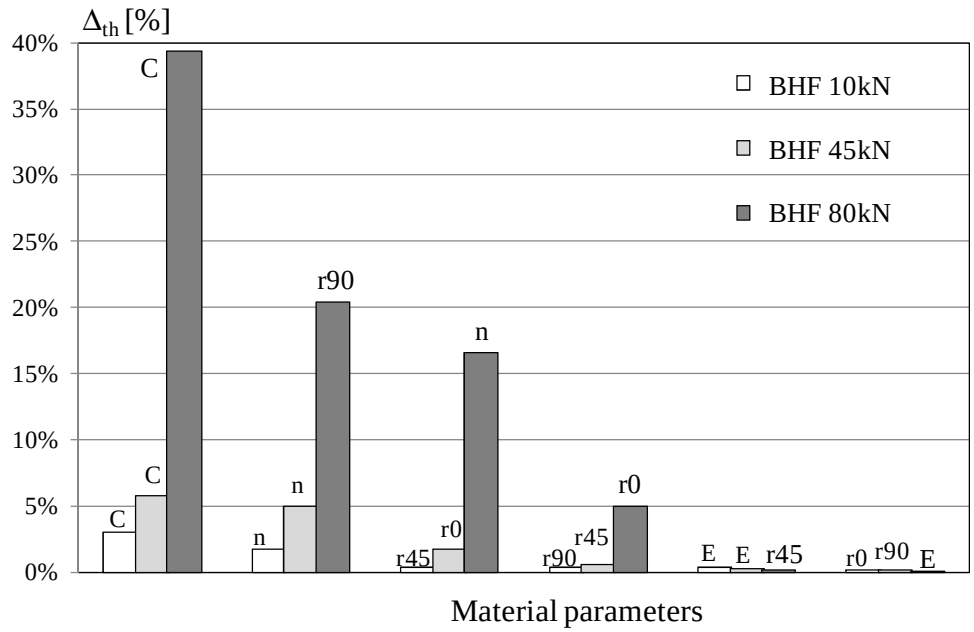

Figure 1.11: Δ[%] values for th at each BHF level.

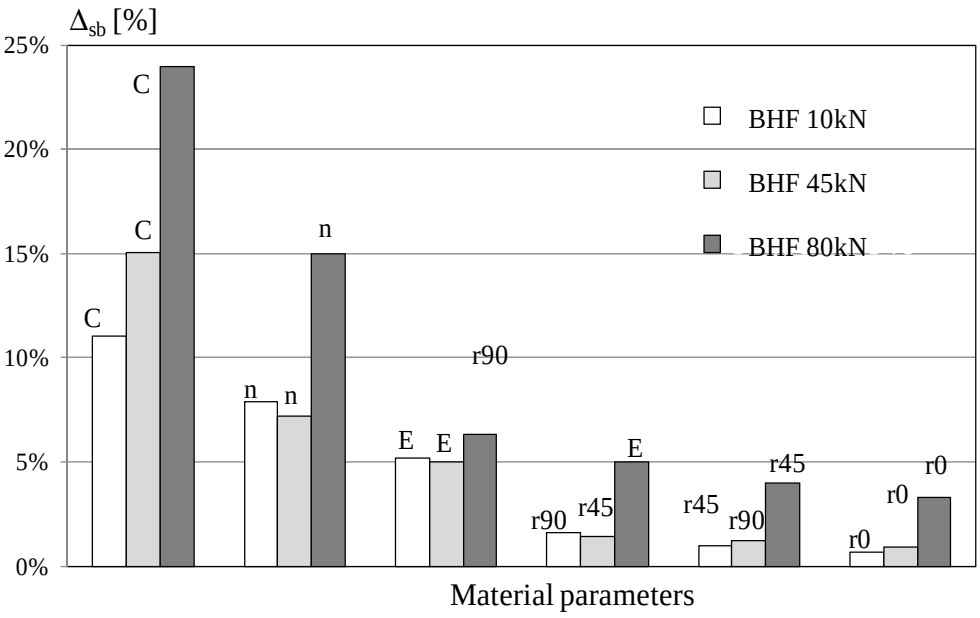

Figure 1.12: Δ[%] values for sb at each BHF level.

BHF [kN]	Thinning	Springback
10	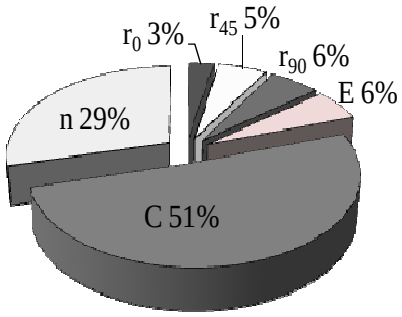	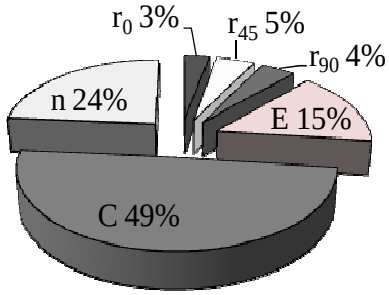
45	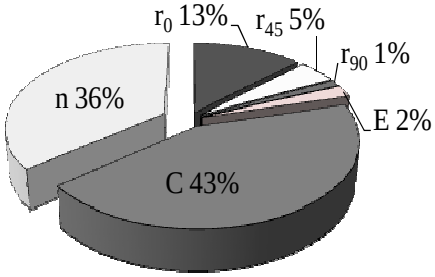	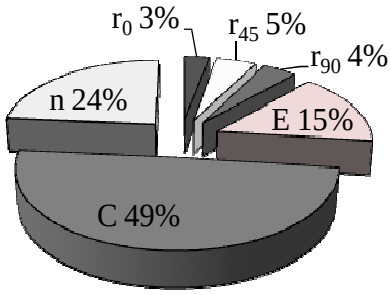
80	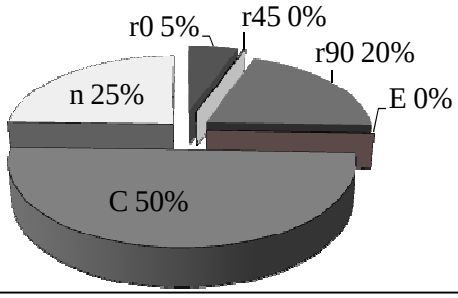	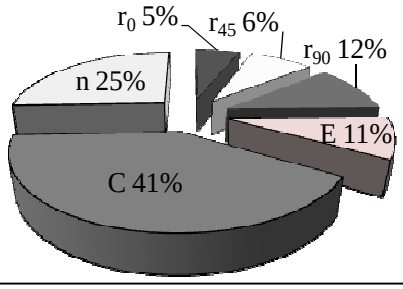

Table 1.12: Contribution of each parameter to th and sb scatter.

The analysis of such results evidences that:

- strength modulus (C) and material hardening exponent (n) are the most significant sources of variation for both objectives, Their contribution to the explored objectives scattering is about 75%;
- as anisotropic coefficients (r_0, r_{45}, r_{90}) are concerned, their stochastic contribution are relevant only in few cases;
- Young modulus (E) has no influence on th variation, as it was expected.

It is worth pointing out that as thinning is regarded, at low restraining forces level (BHF 10[kN]) the effects of material parameters variations can be considered negligible hence no

further stochastic analysis is necessary in this case. On the other hand, even if similar consideration can be made for BHF equal to 45[kN], such case was anyway taken into account in order to explore a wide operative parameter window i.e. in order to be able to model the investigated phenomenon within a reasonable restraining forces range.

Table 1.13 summarizes the screened material parameters for th at the varying of the restraining forces (YES indicates that particular parameter has to be included in the meta-modeling analysis).

BHF [kN]	Material parameters					
	C	n	r_0	r_{45}	r_{90}	E
10	-	-	-	-	-	-
45	YES	YES	-	-	-	-
80	YES	YES	YES	-	YES	-

Table 1.13: Screening final results for th.

As th is concerned, the selection of the parameters was quite simple since straightforward effects were observed. On the contrary, as sb is regarded, a Pareto chart analysis was carried out on Δ[%] to screen the parameters in order to better express the major part of sb variability. The Pareto chart analysis is a statistical technique used to identify a limited number of significant variables by plotting the percentage of cumulated values of a chosen output (Δ[%]). In other words a Pareto chart allows to evidence which factors contribute most to a given output explanation. A threshold of 90% of the sb variability was chosen in the analysis: only material parameters included within such threshold (responsible for such variability) were accounted for in the following steps. Figure 1.13 below shows the Pareto charts by BHF level.

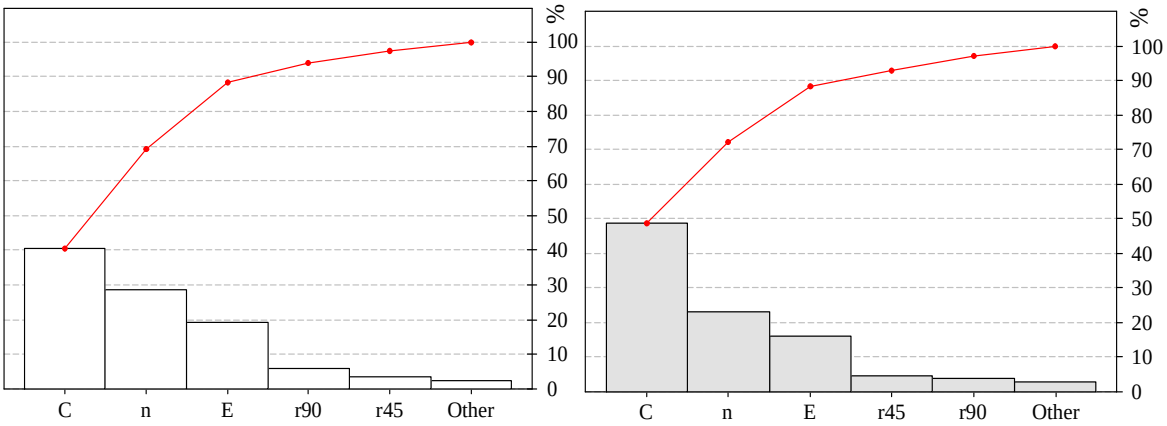

(a) (b)

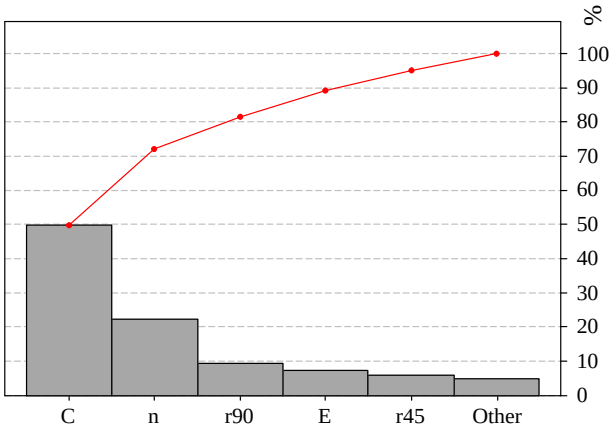

(c)

Figure 1.13: Pareto charts for sb at BHF 10[kN] (a), 45[kN] (b) and 80[kN] (c).

On the basis of the above charts, the following (Table 1.14) material parameters were screened for sb at the varying of the restraining forces.

BHF [kN]	Material parameters					
	C	n	r_0	r_{45}	r_{90}	E
10	YES	YES	-	-	-	YES
45	YES	YES	-	-	-	YES
80	YES	YES	-	-	YES	YES

Table 1.14: Screening final results for sb.

Meta-modeling.

Once the main sources of objectives variation were identified, a meta-modeling step based on RSM concepts was applied. The application of response surface method led to different meta-models for th and sb at the varying of BHF. Table 1.15 summarizes the number of numerical simulations (runs) utilized to build up a given meta-model (related to the number of coefficients to be estimated) together with the approximation capability indexes of each meta-model itself. In particular, the differences between numerical and predicted value of each objective (e_{th}, e_{sb}) and correlation coefficients (R-sq adj) were considered to evaluate the fitting performances of the meta-models.

BHF [kN]	FE runs	th[%]		sb[mm]	
		$R\text{-}sq_{adj}$	e_{th}	$R\text{-}sq_{adj}$	e_{sb}
10	15	-	-	99%	0.03
45	15	99.62%	0.02	87.40%	0.03
80	43	96.90%	1.14	95%	0.08

Table 1.15: Input set, number of simulations and utilized approximation capability indexes.

The above values of R-sq adj coefficients testify that a good data interpolation was obtained, as well a good prediction capability is reached shown by low spreads between numerical and predicted results (e_{th} and e_{sb} values).

Monte Carlo simulation.

The final step of the proposed procedure consists of a set of MCS simulations, in order to quantify the uncertainty of the investigated objectives in terms of dispersion around their nominal values. Actually, the MCS approach leads to a probability distribution of a given objective depending on the stochastic variation of material parameters. As above mentioned, the MCS was properly integrated with the achieved meta-models, providing a time efficient tool to reproduce inner process variability. Table 1.16 shows the main statistical parameters of th and sb probability distributions (namely, standard deviation σ, mean value M, 5th and 95th percentiles) achieved at 10[kN], 45[kN] and 80[kN], under the simultaneous effect of the parameters previously screened. The obtained statistical distributions are represented in Figures 1.14 and 1.15.

BHF[kN]	**10**				**45**				**80**			
	σ	5th	M	95th	σ	5th	M	95th	σ	5th	M	95th
th[%]	-	-	10.22	-	0.69	14.62	15.54	16.87	8.97	19.97	23.54	46.01
sb[mm]	0.27	0.75	1.00	1.58	0.08	0.57	0.72	0.84	0.11	0.28	0.51	0.64

Table 1.16: Statistical parameters of th and sb probability distributions.

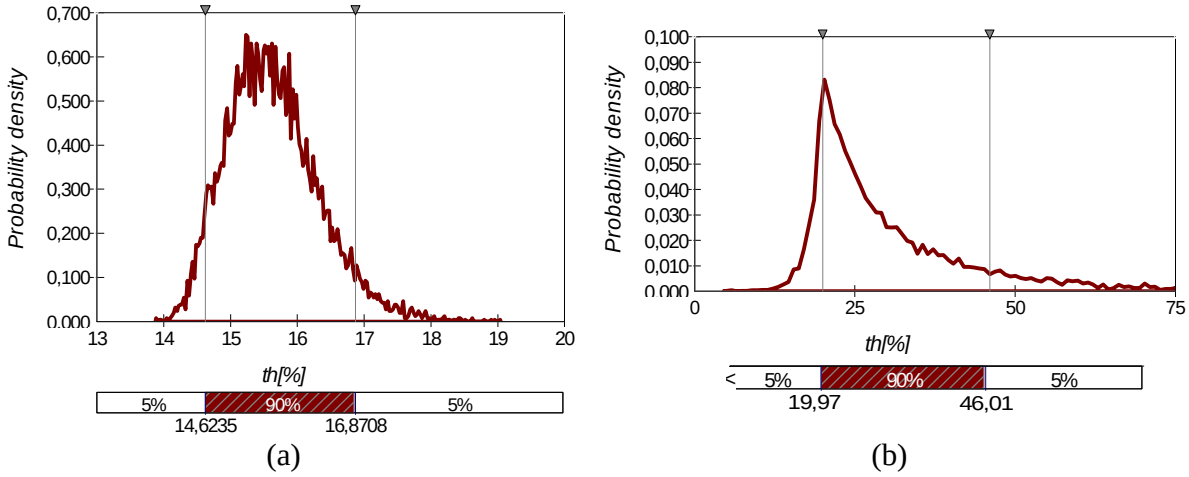

(a) (b)

Figure 1.14: th probability distribution curves at BHF 45[kN] (a) and 80[kN] (b).

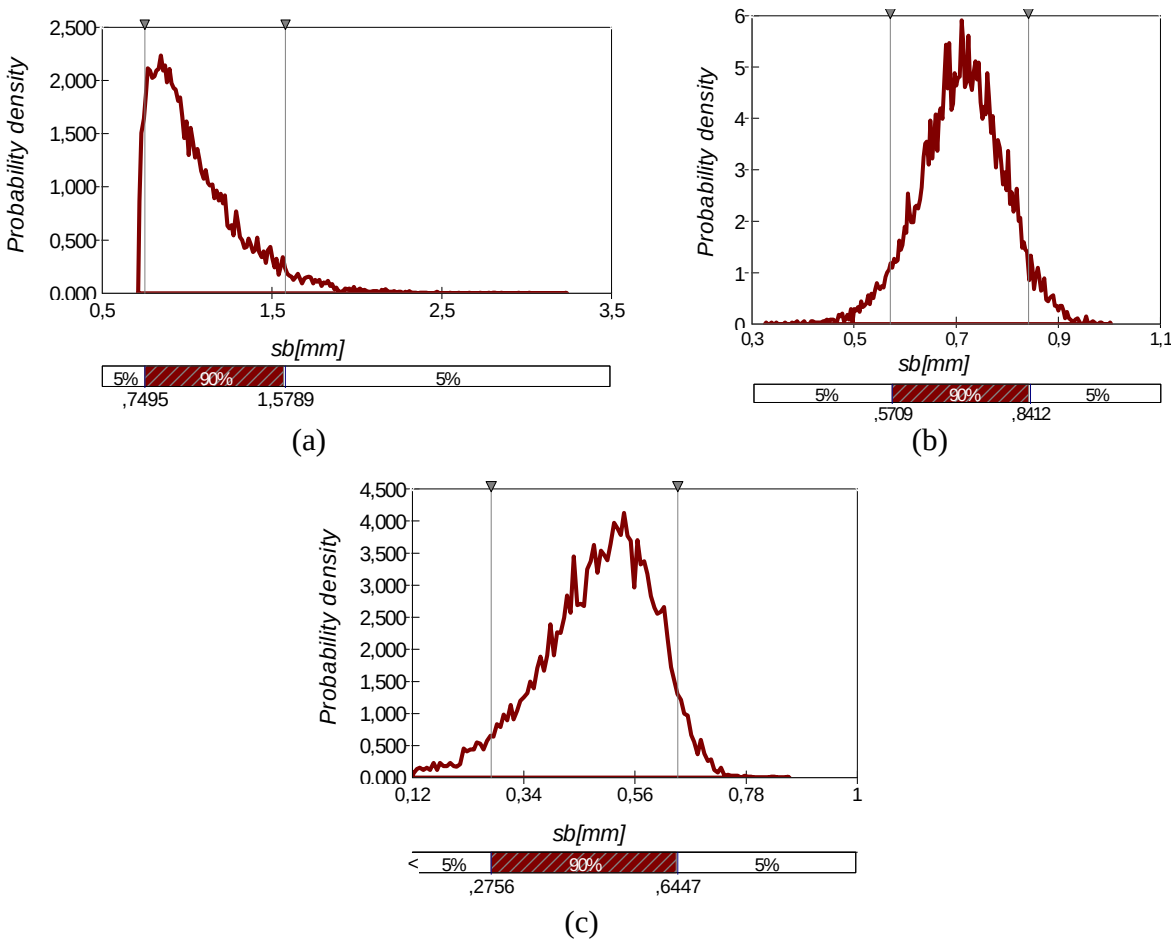

Figure 1.15: sb probability distribution curves at BHF 10[kN] (a), 45[kN] (b) and 80[kN] (c).

It is worth pointing out that from the process designer's point of view, the obtained curves enable to predict what a stochastic material behavior may imply, Actually, each curve represents the probability to reach values of th (or sb) different from the expected ones. The process designer has to be aware that thinning values may worsen (for instance, from the expected value of about 24% up to about 46%, see Figure 1.14 (b)) due to material variability if an high level of restraining forces is utilized (BHF=80kN). Higher springback may arise as well if the level of restraining forces is low (see Figure 1.15 (a)).

To sum up the proposed procedure provides the possibility to quantify and predict with a good approximation the scattering of the selected process performances (thinning and springback).

Moreover, it has to be observed that if a process designer would neglect material stochastic behavior any process design procedure may fail. Therefore, improvement of process

robustness represents a crucial issue. In this way, the proposed procedure is also an effective tool to identify the different scattering to be expected at different restraining forces levels: the analysis of Figure 1.16 shows that sb stochastic distributions present higher or lower spread depending on BHF values.

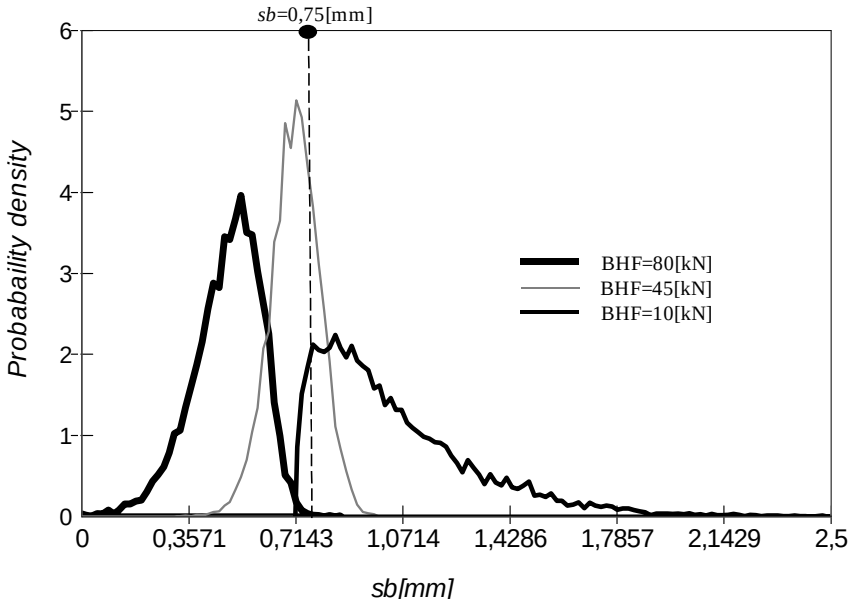

Figure 1.16: Comparison among probability density curves of sb at the varying of BHF.

Moreover, hypothesizing a limit for springback (for instance sb=0.75[mm] in Figure 1.16) it is possible to evaluate which is the probability that the real value of sb is over this threshold: this probability is the area beyond the fixed threshold under the probability curve valid for one of the operative conditions. In Figure 16 the above example is illustrated: at BHF=10[kN] there is an area out of the fixed threshold equal to 95% which becomes respectively 32% and 1% for BHF equal to 45[kN] and 80[kN]. Therefore, the process designer is aware that it could be useful to change the operative conditions (BHF) in order to lessen the risk to exceed a threshold due to material stochastic behavior.

1.1.4 Conclusions.

Sheet metal stamping process robustness improvement is a crucial topic in the design of such operations since the dependency of final results on many uncontrollable factors variability is the main cause of undesired scattering from expected performances. A process design completely based on deterministic considerations could not be much robust. In this study, the

influence of coil to coil material properties variation on thinning and springback phenomena was analyzed. A sensitivity analysis at the varying of restraining forces (i.e. different blank holder actions) was carried out. Subsequently, a stochastic analysis based on Monte Carlo Simulation Method was performed. In particular, the integration between meta-models and MCS technique was applied to perform the stochastic analysis of the chosen objectives. The obtained results showed that material properties influence is not the same at the varying of operative conditions and, in particular, that it is more relevant within working regions characterized by higher restraining force levels, when, for instance, a stochastic coil to coil variation could induce even fracture onset. Therefore, the main advantages of the proposed procedure can be summarized as follows:

- possibility to identify the most relevant material uncertainty sources;
- knowledge of how and how much final process results undergo uncertainty sources influence;
- enhanced robustness and awareness in stamping process design, which may so reduce the consequences of uncertain results.

Moreover, the obtained results may be used in the prospective of a multi-objective optimization approach aimed at accomplishing conflicting objective functions as thinning and springback.

Chapter 2

ROBUST DESIGN OF SHEET STAMPING PROCESSES.

The awareness of the influence of uncontrollable variables on sheet stamping processes leads towards the necessity of developing robust design approaches able to deal with the process variability related to it. It becomes then obvious that a process design based just on a deterministic approach may lack of robustness and lead to fail any specification. In particular, Arvidsson and Gremyr (2008) identified four central principles of robust design: awareness of variation, insensitivity to noise factors, application of various methods and application in all the stages of a design process. These all contribute to the definition of robust design as systematic efforts to achieve insensitivity to noise factors. It means that the narrower the range of scatter around the designed value is for each objective function at a given process setting, the higher the robustness is. Figure 2.1 gives a better understanding of the difference among just optimal solutions, reliable and robust solutions (Sun et al. (2009)): given an objective function to minimize, f(x), such as wrinkling in a sheet stamping process, $x_{(1)}$ would be the optimal solution corresponding to that process setting that minimizes the investigated function. If engineering constraints are also to account for, like excessive thinning, uncontrollable variations (i.e. $\pm\Delta x$) raise the chance to overcome such constraints. Then $x_{(2)}$ would be a more reliable solution, not optimal but the best one for given constraints. If the least possible scatter of the process results is also aimed, $x_{(3)}$ would be the most robust solution as producing the smallest scattering $\Delta f(x)$ while respecting the constraint and assuring pretty good results.

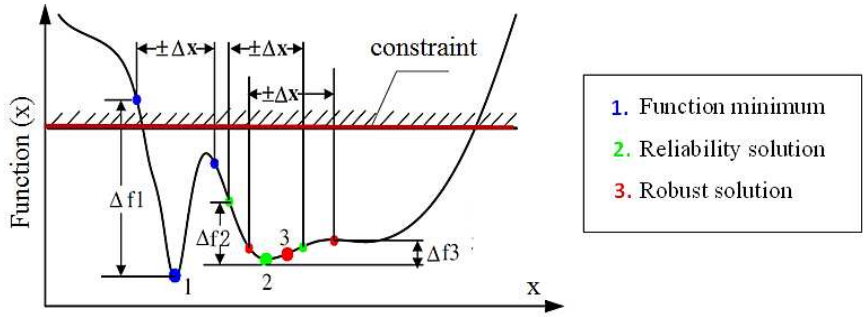

Figure 2.1: Difference among optimal, reliable and robust solutions (adapted from Sun et al. (2009)).

From a design perspective, all the factors that have an influence on the final process results can be categorized by:

- **Controllable variables (x_i)**: process parameters that are reasonably supposed easy to calibrate and to keep at a given level. Typically, control variables have a deterministic behavior as all their outcomes are realistically assumed certain. For instance a deterministic variable is the blank holder force as it can be close looped controlled.
- **Noises (z_j):** uncontrollable or hard to control variables, whose variations and effects were discussed in Chapter 1. Noises are assumed stochastic and their behavior is modeled by probability distributions whose mean (μ) and standard deviations (σ) have to be experimentally determined.

Therefore, to robustly design a process means to look for the control variables settings, which minimize the scatter of the final process results while respecting the engineering constraints, under the effect of any stochastic variation of the noises.

In terms of process optimization, the impact of the noises changes also the design perspective: an univocal correspondence between design variables and resulting process objectives cannot be assumed anymore and the behavior of the objective responses themselves turns out probabilistic because of unpredictable noise occurrences. Then, the design challenge becomes how to reduce the process sensitivity while getting the best performances. Such implications are sketched in Figure 2.2.

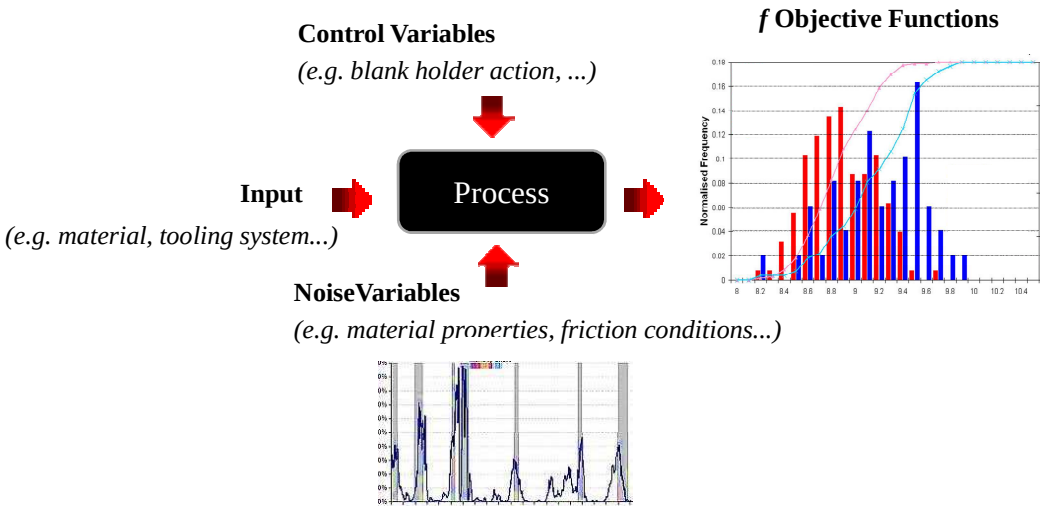

Figure 2.2: Variability effect on the objective function from a design perspective.

Robust approaches have been developed for sheet stamping processes design to effectively bridge the aim of free defect products with the need of robustness in the industry. Multiobjective problems have particularly been considered.

From an accurate analysis of the technical literature, a possible categorization by two main clusters of approaches is here suggested, depending on how they account for the process variability within the process design itself:

- **Hybrid deterministic-stochastic approaches**: the effect of variability sources is evaluated as last optimization step; the process design first investigates the objectives neglecting any stochastic behavior and then evaluates process robustness by probabilistic investigations. Process setting minimizing the effects of the noises is explicitly identified and comparisons among several solutions are possible by robustness.
- **Stochastic approaches**: the process design is carried out under the stochastic perturbations of noise variables. Typically, isolating the stochastic effect of the noises on the investigated objectives is not possible and the final process set up reflects the average effect of the noises while minimizing the deviation induced on the process results.

As earlier remarked, robust design is typically supported by numerical simulations as a standalone implementation of any stochastic procedure might result unaffordable for optimization problems, mainly if multiobjective.

Following an overview of the most common robust design approaches for sheet stamping applications is reported by the above categorization, together with some case studies.

2.1 Hybrid deterministic-stochastic approaches.

Hybrid deterministic-stochastic approaches have been widely applied for sheet stamping optimization aimed to evaluate and control process robustness. From a methodological standpoint, a first deterministic step is typically carried out by neglecting the probabilistic behavior of the noises while still modeling their deterministic effect on the process. It means that the influence of the noises is incorporated at this stage as they would be deterministic variables. Typically this is carried out by using metamodeling techniques such as response surfaces approaches. The knowledge of the magnitude of each noise effect on the process results opens the possibility to carry out further probabilistic investigations by stochastically

perturbing the process. Many authors have proved the efficacy of using Monte Carlo Simulations (MCS) for such purpose. The integration among FEM, metamodeling techniques and MCS through such hybrid approaches has in fact turned out to be a very powerful tool to reduce the computational effort in the process robustness investigation, while reliably estimating the probabilistic behavior of the analyzed objectives. Eventually, an explicit analysis of the robustness of the process can be carried out as the effect of any stochastic variation of the noises on the deterministic response of the process at a given design setting comes up clearly.

A hybrid procedure is provided by Wiebenga et al. (2011). They applied a metamodel based strategy combined with a sequential improvement algorithm to an industrial V-bending process. The robust optimization problem was solved by performing a full factorial design combined with a space filling Latin Hypercube Design (LHD) as DoE; afterwards a metamodel was fitted in the combined control–noise variable space using both RSM and Kriging metamodeling techniques. The computationally expensive non-linear FE simulations are thus replaced by a surrogate model. MCS were run onto the metamodel as stochastic step and the optimization was then carried out by applying a Genetic Algorithm (GA).

Zhang and Shivpuri (2009) applied a hybrid integrated approach to simultaneously optimize thinning and wrinkling in a deep drawing operation. They deterministically computed a polynomial input-output link using RSM, followed by a stochastic step aimed to multi-objective optimization. They formulated a global function as a Quality Index (QI), expressed as the weighted function of the probability of failure of the two objectives and used MCS to calculate it at several process settings. They also performed in (Shivpuri and Zhang (2008)) the robust design of spatially distributed friction still for wrinkling and thinning failure reduction by a FEM based genetic algorithm approach.

Jansonn et al. (2008) used linear and quadratic meta-models in a reliability evaluation of variations in springback and thickness distribution for a U-channel sheet stamping process. They used both D-optimal and Latin Hypercube sampling techniques to metamodel the two objectives with respect to the variability of some noises, material properties and process related, followed by the MCS method.

Another example of hybrid robust design was performed by Tang and Chen (2009) for a cup

drawing process by an adaptive importance sampling. Moreover, they used Support Vector Machine (SVM) as surrogate model followed by MCS again.

Ledoux et al. (2010) proposed a robust procedure for deep drawing processes based on the optimization of a desirability function by GA applied on deterministic parameters only. RSM and MCS method were applied at the three best solutions for robustness evaluations also considering noise variables.

Hou et al. (2009) compared deterministic and RSM/MCS integrated stochastic approaches applied to a deck lid inner panel stamping in DC06 steel sheet under the noise effect of the hardening exponent, yield stress, sheet thickness, friction conditions and anisotropy coefficient.

The optimization procedure proposed by G. Gantar and K. Kuzman (2005c) integrated process metamodeling and simple stochastic optimization by Monte Carlo to reduce instability in a rectangular deep drawing process. An appropriate number of MCS was run for each level of a fixed BHF range, in order to predict percentage of rejected products under effect of design variables variation controlling wrinkling and fracture occurrences. A similar approach was used by Post et al. (2009) for the analysis of variation and transformation in a multistage metal forming process of stainless steels.

Furthermore, Demir et al. (2008) proposed an effective and efficient hybrid design strategy to design sheet-metal die in order to reduce stress and increase fatigue life of sheet-metal die. In such application, FE analysis, approximate models, a numerical optimization algorithm and probabilistic design method by MCS were integrated to create an automated design tool.

Also de Souza and Rolfe (2008) studied stochastic behavior of springback like frequency distribution, starting from a five levels probabilistic full factorial design, complying with assigned probability distributions of the noises. For each DoE run the probability of the inputs occurring is calculated as a multivariate joint distribution and in turn the likelihood of the output was determined. The springback distributions were determined by coupling the input density, with the output springback response it produces. A range of sheet stresses was investigated, simulating different operative windows accounting to highlight robust regions for the springback prediction.

Finally, Buranathiti et al. (2005) used the weighted three-point-based method to approximate

the statistical characteristics (mean and variance) of the margins of failures in both tearing and wrinkling for a wheelhouse stamping process, starting from a deterministic metamodel properly perturbed by MCS as well.

All the above mentioned applications highlight the wide use of metamodeling techniques for robust design and, more in general, for optimization purpose. Obviously, the reliability of any analysis strongly relies on the accuracy of the metamodel as first step of the entire stochastic investigation. Moreover, as a model generally fitting any process doesn't exist, preliminary observations about which metamodel is more suitable to the features of the investigated problem (e.g. dimensions, linearity, etc.) should be initially done.

An evaluation of some of the most used metamodeling techniques for sheet stamping applications is proposed in section 2.1.1. A single objective problem was considered for sake of simplicity to better focus on the comparisons of efficiency and prediction capabilities within a sort of cost-benefits analysis. Afterwards, in section 2.1.2, a case study on the application of a multiobjective framework for robust design of deep drawing processes is described, followed by a further development in section 2.1.3.

2.1.1 Metamodeling based strategies: preliminary considerations for hybrid optimization approaches.

As it was already observed, the use of numerical simulations has strongly reduced costs and times of sheet metal forming design but, due the relevance that such operations have assumed as manufacturing technologies, very complex shapes have to be obtained and therefore designed. This implies that stamping operations have become very complex to design mainly because the increasing number of design variables to account for. Computer aided procedures to design and optimize forming processes have become therefore crucial research topics as the industrial interest in cost and time reduction has been increasing. A standalone numerical simulation approach could make the design too time consuming while meta-modeling techniques enable faster approximations of the investigated phenomena, reducing the simulation time.

Especially if robust optimization problems are dealt with, the integration with metamodeling techniques turns out to be crucial to efficiently solve such problems without losing

effectiveness or accuracy. Therefore, the wide use of such techniques for robustness purposes makes mandatory a preliminary investigation of the above mentioned methodologies.

Nowadays many researchers have been facing such research challenge by using various approaches. Some of them are characterized by iterations of an algorithm (usually gradient based) stopped when convergence is reached. Generally, such algorithms are interfaced with numerical simulations to solve direct problems necessary to calculate the objective function gradients. They may also lead to local minima instead of global ones even though many of these algorithms are very efficient. In fact, a few iterations are required to reach technologically satisfying results (Di Lorenzo et al. (2009a), Di Lorenzo et al. (2010), Fann and Hsiao (2003), Kleinermann and Ponthot (2003), Naceur et al. (2004), Zhao et al. (2004)).

Another approach is based on intelligent techniques; for instance, genetic algorithms are extensively applied (Castro et al. (2004), Schenk and Hillmann (2004)) even though they require a high number of evaluations of the objective function. Some authors presented also some approaches which are based on the possibility to adapt the finite element analysis by some proper adaptive algorithms aimed to optimize some time dependent variables of a given process along the numerical simulations: of course, such approaches imply the possibility to manage the source code of a finite element software (Jansson et al. (2007), Sheng et al. (2004)).

One of the most effective approaches in the last few years is based on response surface methodology whose effectiveness was demonstrated in the past years. The effectiveness of RSM depends both on the definition of the Design of Experiments (DoE) and the accuracy of the function approximation though. Some researchers focused on the application of RSM to sheet metal forming to reduce the number of numerical simulations (Breitkopf et al. (2005)). A very interesting aspect in RSM application is the possibility to determine response surfaces by Moving Least Squares Approximations (MLS) utilizing a moving region of interest (Breitkopf et al. (2005), Oudjene et al. (2009)). MLS are commonly used in mesh free methods as well as in many computational mechanics applications (Breitkopf et al. (1996), Breitkopf et al. (2004)). The MLS approach was also applied to metal forming problems like the optimization of complex stamping operation even for industrial automotive applications (Bahloul et al. (2010), Breitkopf et al. (2005), Breitkopf et al. (2004)). Besides the abovementioned

optimization strategies, Kriging models have been extensively used. Literature widely describes such interpolation strategies (Kleijnen (2009), Martin and Simpson (2004), Sacks et al. (1989), van Beers (2004)), often in comparison with other surrogate models as RSM based ones (Bahloul et al. (2010), Breitkopf et al. (2005), Naucer at el. (2006)). Guinta (1997) presented an investigation of the use of Kriging for the multidisciplinary design optimization of a high speed civil transport aircraft. He explored a five and a ten variable design problem, observing that the Kriging and response surface modeling approaches yield similar results due to the quadratic trend of the responses. Allen et al. (2003) noticed that regression modeling should not be quickly discarded for cases in which the number of runs is comparable to the number of terms in a quadratic polynomial model. The use of Kriging as approximation technique would be in fact justified by highly nonlinear functions to bit fit.

Moreover, Kriging has been used for manufacturing processes applications. For instance, Lebaal et al (2011) used Kriging interpolation with sequential quadratic programming algorithm to find the optimal cutting conditions for dry machining of titanium alloys. Jakumeit et al. (2005) tested both kriging and RSM models on sheet forming applications as well. In particular, they found Kriging to show a faster convergence for thinning, wrinkling and springback minimization of deep drawn S-rail and hat shaped components using a time dependent blank holder history. Del Prete et al. (2008) used a kriging based metamodel to optimize a hydroformed rectangular panel by multiple blank holder forces and fluid pressures curves. Furthermore, Wang et al. (2008) also used a kriging based strategy in the high nonlinear optimization of a vehicle's outer flank forming.

The choice of the proper meta-models is therefore critical: Jin et al. (2000) compared four popular meta-modeling techniques (polynomial regression, multivariate adaptive regression splines, radial basis functions and Kriging) concluding that there is not a unique meta-modeling technique suitable for every problem; actually, the performances depend on sample size and on the non-linearity order of the approximation function.

A contribution on the statistical methodologies for metamodels building when deterministic numerical simulation is utilized is reported by Simpson et al. (2001). In this work a deep review of several techniques, including design of experiments, response surface methodology, Taguchi methods, neural networks, inductive learning and Kriging, is reported. Also,

guidelines able to address the designer towards the correct metamodeling choice to implement are reported.

Then, there are two main topics as far as metamodeling techniques: efficiency and accuracy. The number of numerical simulations can be in fact strongly reduced if a proper optimization approach is implemented and additionally either global or local approximation can be performed to better fit the results, obviously depending on the problem features.

Thus, following the accuracy and effectiveness of widely used meta-modeling techniques for sheet forming applications is tested on the optimization of a T-shaped hydroforming process. In particular, three optimization approaches based on different meta-modeling techniques are implemented: Polynomial Regression approach (PR), Moving Least Squares approximation (MLS) and Kriging method. The results showed that, by exploiting the peculiarities of MLS and Kriging methods, it is possible to reduce the computational effort in sheet metal forming optimization, particularly in comparison with a classical PR approach. Other considerations could be drawn as far as accuracy. Differences were highlighted and quantified with the aim to discuss their suitability as optimization tools for sheet metal forming processes.

2.1.1.1 Discussion of methodologies.

A brief overview of the investigated metamodeling techniques is discussed in the following section, in order to show basic principles and main differences. A better understanding of the results obtained for the analyzed case study will be then possible.

Polynomial Regression approach (PR).

The Polynomial Regression approach (PR) is a widely used metamodeling technique based on the Response Surface Methodology (RSM) that fits a given objective function f(X) through a set of points belonging to the domain of variation of independent variables, X.

As earlier observed, the effectiveness of RSM depends both on the definition of the Design of Experiments (DoE) and on the accuracy of the approximation function. When a Polynomial regression approach is carried out, a proper Design of Experiments is applied to solve a predefined set of direct problems based on a defined variables vector (x_i) within a design domain. Moreover, such domain is often constrained by the technological boundaries of the investigated problem.

A Central Composite Design (CCD) is widely used as DoE, as fulfilling all the orthogonality criteria and assuring a quite accurate estimation of both linear and quadratic effects. Other DoE, as Latin Hypercube Design (LHD) have been also extensively used as significantly reducing the number of runs. Despite being useful for high dimension problem, besides orthogonality other criteria can be preferred as the space filling one.

The results of the above mentioned direct problems are then used to approximate the response function of a chosen objective ($f(x_i)$) by a classical least squares approach of a proper approximation order.

For quadratic polynomial case, the analytic linkage is described by equation (2.1):

$$f(X) = \beta_0 + \sum_{j=1}^{k} \beta_j \, x_j + \sum_{j=1}^{k} \beta_{jj} \, x_j^2 + \sum_{i=1}^{k-1} \sum_{j=1+1}^{k} \beta_{ij} \, x_i x_j + \varepsilon \qquad (2.1)$$

where ε is the approximation error and linear, quadratic and interaction effects are included. In matrix form, equation (2.1) becomes:

$$f(X) = X\beta + \varepsilon \qquad (2.2)$$

The least square error method is traditionally the basis of the described fitting technique, where the square error is formulated by equation (2.3):

$$\varepsilon^T \varepsilon = {}^1\!/_2 \, (f(X) - X\beta)^T \, (f(X) - X\beta) \qquad (2.3)$$

The variables effects described by the unknown coefficients β_j are determined minimizing equation (2.3) with respect to β. This leads to the resolution of a linear system of equations and it is found that:

$$\beta = (X^T X)^{-1} (X \, f(X)) \qquad (2.4)$$

Once β is computed, the approximated function *f(X)* is entirely defined inside the variable domain. The metamodeling technique above described is generally categorized as global, since the whole design domain is contemporarily accounted for to approximate the process behavior. A sequential quadratic programming procedure might be applied though to search the objective optimum by iterating the procedure within a progressively updated DoE. Of course, the number of runs significantly rises.

Moving Least Squares approximation (MLS).

A very interesting aspect in RSM application regards the possibility to build response surfaces

basing on Moving Least Squares Approximations (MLS) by utilizing a moving region of interest (Breitkopf et al. (2005), Oudjene et al. (2009)). MLS are commonly used in mesh free methods as well as in many computational mechanics applications (Belytschko et al. (1996), Breitkopf et al. (2004), Rassineux et al. (2003)). The MLS approach was also utilized in metal forming problems such as complex stamping operation even for industrial automotive applications (Breitkopf et al. (2005), Naceur et al. (2006)).

The MLS approximation is generally considered a quite good local approximation method; this means that the MLS approach better approximates the region closer to the one chosen as reference through k iterations. In particular, it is more utilized with irregular data grids to get better approximation flexibility (Breitkopf et al. (2004), Breitkopf et al. (2005)).

Starting from a proper DoE, each iteration of advanced response surface methodologies based on the MLS technique can be detailed as follows:

1. the fitting function f(x) can be defined through a basis function *p* and proper vector of coefficients *a* according to the following polynomial expression (2.5):

$$\tilde{f}(x) = p^T(x)a(x) \tag{2.5}$$

2. the basis function p(x) can be defined as consisting of linear and quadratic monomials:

$$p(x) = \left[1 \quad x_1 \quad x_2 \quad \dots \quad x_n \quad x_1x_2 \quad \dots \quad x_ix_{i+1} \quad \dots \quad \frac{x_1^2}{2} \quad \dots \quad \frac{x_n^2}{2} \quad \right]^T \tag{2.6}$$

   where $x_1 \dots x_n$ are the component of the vector *x*;

3. the coefficients *a(x)* can be obtained by minimizing the error *J(a)* between experimental and approximated values of the objective function at each iteration k and it can be expressed as:

$$J(a) = \sum_{i=1}^{N} w(\|x_i - x\|)(p^T(x_i - x)a - f(x_i))^2 \tag{2.7}$$

   with N indicating the number of experiments/simulations belonging to the defined DoE; *w* is a weight function defined in the interval [0;1] and allowing a local approximation. Namely, *w* is equal to *0* out of a defined region of interest of the current optimum, while 1 means an exact correspondence between the optimum at the iteration k and the one at k-1. Several weighting functions are available in the technical literature (Oudjene et al. (2007)).

$$w(x-x_I)=\begin{cases} \left.\left\{e^{\left[\frac{\|x-x_I\|}{\alpha d}\right]^2}-e^{-\frac{1}{\alpha^2}}\right\}\right/\left[1-e^{-\frac{1}{\alpha^2}}\right] & se\ \|x-x_I\|\le d \\ 0 & otherwise \end{cases} \tag{2.8}$$

where α is a shape parameter of the weighting function and *d* is the radius of the region of interest around the current optimum. A possible formulation of *d* with a progressive radius reduction might be the following:

$$d_k=\begin{cases} d_{\min} & se\ d_k\left|\left(\frac{k}{k+1}\right)^2-1\right|\le d_{min} \\ d_k\left|\left(\frac{k}{k+1}\right)^2-1\right| & otherwise \end{cases} \tag{2.9}$$

where d_{min} is a given minimum distance;

4. minimizing the error *J(a)* provides at each iteration k:

$$a(x)=A^{-1}Bf \tag{2.10}$$

where:

$$A=PWP^T \qquad B=PW$$

$$P=[\dots p(x_i-x)\dots]\ ,\ W=\begin{bmatrix} w(x_1-x) & & 0 \\ & \ddots & \\ 0 & & w(x_n-x) \end{bmatrix} \tag{2.11}$$

Therefore a general application of the MLS can be summarized as follows:

1. identify of a starting point P_0, within a defined Design of Experiments;
2. approximate of the fitting function by estimating the above coefficient through the error minimization; a new point $P_0^{\,i}$ is found and that is the current optimum at the iteration k;
3. if $P_0^{\,i+1}$ is out of the region of interest of $P_0^{\,i}$, or in general if the distance $\left\|P_0^{i+1}-P_{0i}\right\|\ge 10-4$, go back to the step 1;
4. stop when the distance $\left\|P_0^{i+1}-P_0^{i}\right\|$ between the current optimum and the previous one is negligible.

A sketch of the region of interest iteratively changing in the Moving Least Square Approach is shown in Figure 2.3.

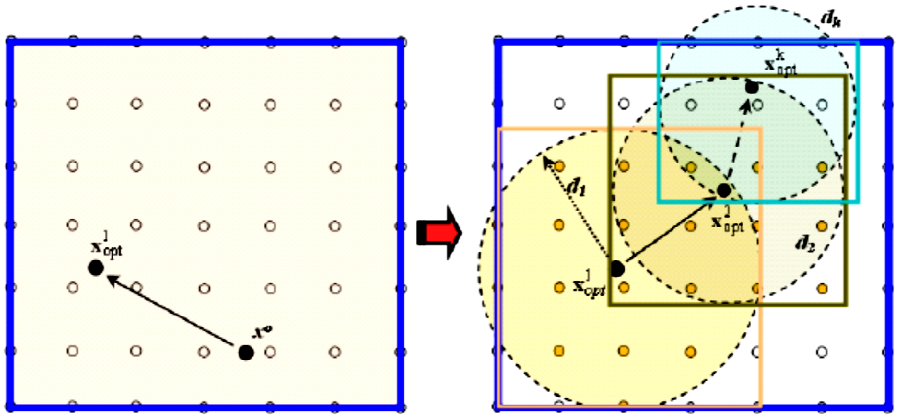

Figure 2.3: Moving DoE with a progressive radius reduction (Oudjene et al. (2007)).

For a sheet forming approximation problem, an example of application of the MLS metamodeling strategy might be performed as follows:

1. minimization of the polynomial regression function to find the minimum (indicated as M_1 at the first iteration);
2. implementation of MLS based approximations by considering M_1as reference point.
3. minimization of the objective function and selection of the best value (minimum M_2).
4. implementation of MLS based approximations by considering M_2 as reference point.
5. iteration of the procedure by zooming in the region of interest until no significant improvement is obtained.

It is worth pointing out that such procedure implies that only the current optimal points (M_k) are progressively added to the starting DoE, implying a very few number of points and only where it is really appropriate. In fact, additional points are only in the optimum region. Then, the domain, where the current optimum is, has to be zoomed in at each iteration.

In the end, the use of an MLS based approach allows zooming in the approximation region around a certain reference point: instead of iterating the metamodel by zooming in the interest region and implementing a new DoE, it is possible to locally approximate the objective function if the MLS approximation is applied.

Kriging.

While the metamodeling techniques above described are categorized as approximation techniques, Kriging (Sacks et al. (1989)), also referred to as DACE (Design and Analysis of

Computer Experiments), is instead an interpolation strategy as exactly fitting all the investigated points within the Design of Experiments.

A kriging metamodel consists of a sum of many local carrier functions, differently modelled (e.g. Gauss function, Exponential, Linear, …) and one global function, which might be a polynomial as in RSM or simply a constant, depending on the order of the polynomial function itself. Such model can be expressed as follows in equation (2.12):

(2.12)

where y(x) is the unknown function of interest to be fit, f(x) is a known polynomial function of x, and Z(x) is the realisation of a normally distributed Gaussian random process with mean zero, variance σ^2, and non-zero covariance. In particular, f(x) is similar to the polynomial model in a response surface and provides a 'global' model of the design space; as observed, in many cases, f(x) is simply taken to be a constant term. While f(x) globally approximates the design space, Z(x) creates localized deviations or carriers, whose definition is crucial in the interpolation of the sampled data points.

The covariance matrix of Z(x) is given by equation (2.13):

(2.13)

where R(θ, ,) is the correlation model with parameters θ between any two of the sample points and , while σ^2 is the process variance.

The correlation function R is specified by the user. A common R function is expressed by equation (2.14):

(2.14)

Other correlation functions are available as showed in Table 2.1, where :

Name	$\mathcal{R}_j(\theta, d_j)$	
EXP	$\exp(-\theta_j \lvert d_j \rvert)$	
EXPG	$\exp(-\theta_j \lvert d_j \rvert^{\theta_{n+1}}),$	$0 < \theta_{n+1} \leq 2$
GAUSS	$\exp(-\theta_j d_j^2)$	
LIN	$\max\{0,\ 1-\theta_j \lvert d_j \rvert\}$	
SPHERICAL	$1 - 1.5\xi_j + 0.5\xi_j^3,$	$\xi_j = \min\{1,\ \theta_j \lvert d_j \rvert\}$
CUBIC	$1 - 3\xi_j^2 + 2\xi_j^3,$	$\xi_j = \min\{1,\ \theta_j \lvert d_j \rvert\}$
SPLINE	$\varsigma(\xi_j),\ (2.24)$	$\xi_j = \theta_j \lvert d_j \rvert$

Table 2.1: Correlation functions (Lophaven et al. (2002)).

According to Lophaven et al. (2002), the correlation functions in Table 2.1 can be separated into two groups by their behaviour near the origin: parabolic behaviour function (Gauss, Cubic and Spline), and linear behaviour functions (Exp, Lin and Spherical).

The choice of correlation function should depend on the features of the function to optimize or the physical process to model, but in general it is possible to assume correlation functions with parabolic behaviour, which means Gaussian, Cubic or Spline functions, when the investigated phenomenon is continuously differentiable. On the contrary, physical phenomena usually show a linear behaviour near the origin, and Exp, Expg, Lin or Spherical would usually perform better. Moreover, for large distances the correlation is 0 according to the Linear, Cubic, Spherical and Spline functions, while it is asymptotically 0 when applying the other functions. Some of the choices are illustrated in Figure 2.4: it has to be observed that in all cases the correlation decreases with $|d_i|$ and a larger value for θ leads to a faster decrease.

The width of the local carrier functions can be in fact tailored to fit the most likely interpolation model by properly setting the theta parameter (θ), even differently for each design variables. Often the phenomenon is in fact anisotropic: different correlations are identified in different directions, i.e. the shape of the correlation function differs between different directions. This is accounted for in the functions in Table 2.1, as different parameters θ in the n dimensions can be set. In general, the higher θ, the smaller the width of the local carrier. Therefore, by changing θ, a different level of interpretation of the investigated process, whose behaviour has to be fit, can be chosen: higher θ makes the process investigation quite local, while smaller θ more global. It appears evident that metamodeling by Kriging methods is not a straightforward technique: a preliminary analysis of the model parameters to be set has to be carried out, strongly reducing time efficiency while increasing the computational effort. Different results would be obtained in fact by changing the polynomial order and the θ parameter as it will be later discussed.

In the following section, a case study is analyzed, where the above three metamodeling techniques were applied to a hydroforming process. In particular, beside the traditional implementation of such methods, a sequential Kriging approach was developed on the basis of the MLS procedure: formerly a polynomial regression allowed identifying the optimum area, and a local Kriging interpolation follows in such design region.

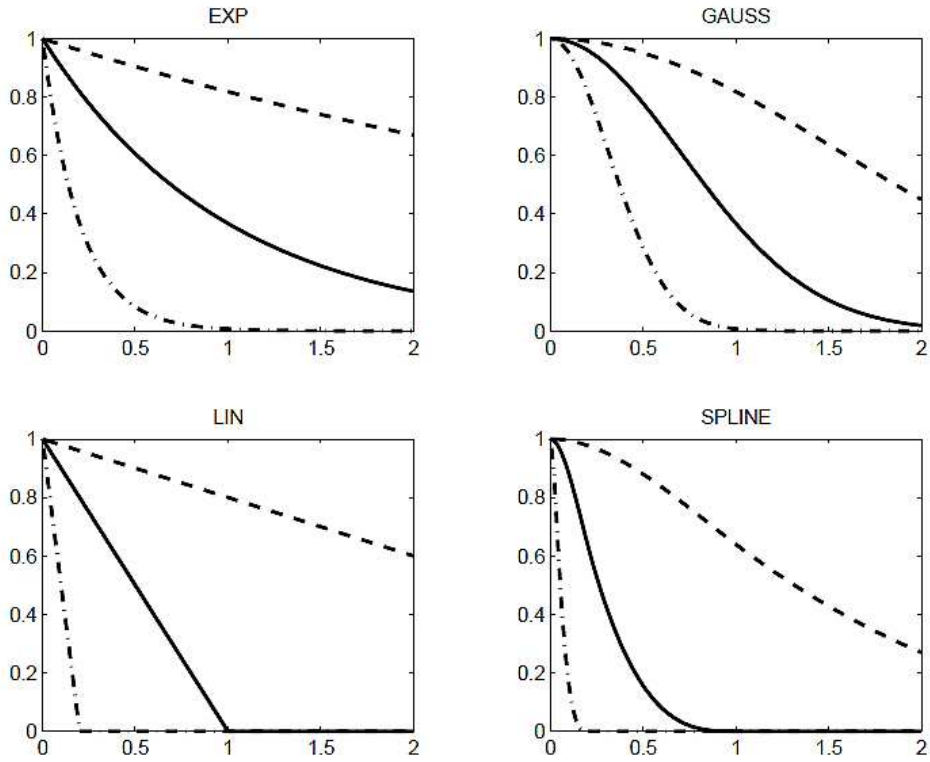

Figure 2.4: Correlation functions for 0 . Dashed, full and dash-dotted line: = 0.2, 1, 5 (Lophaven et al. (2002)).

2.1.1.2 Case study: investigation of the accuracy of surrogate models typically used for sheet stamping design.

In the last years, tube hydroforming processes have been significantly developed both with regards to the knowledge of process mechanics and parameters, and to issues concerning their industrial applicability. Of course, a central concern in the design of tube hydroforming processes is the calibration of both material feeding history and internal pressure path during the process, whose calibration strongly influences the prevention of bursting or buckling.

In this case study, a T-shaped tube hydroforming operation is taken into account in order to implement the proposed optimization procedures. The tube material is an aluminum AA 6060-T6 alloy with the following experimental flow rule: $\sigma=370\varepsilon^{0.11}$MPa.

Two design variables were chosen and indicated as PR_1 and s_1 in Figure 2.5 (a), whose calibration defines the internal pressure path. PR_2 value was fixed. PR_1 indicates the pressure during the early phase of the process, while s_1 is the punch stroke at the beginning of the

calibration phase. The tool die is also showed in Figure 2.5 (b).

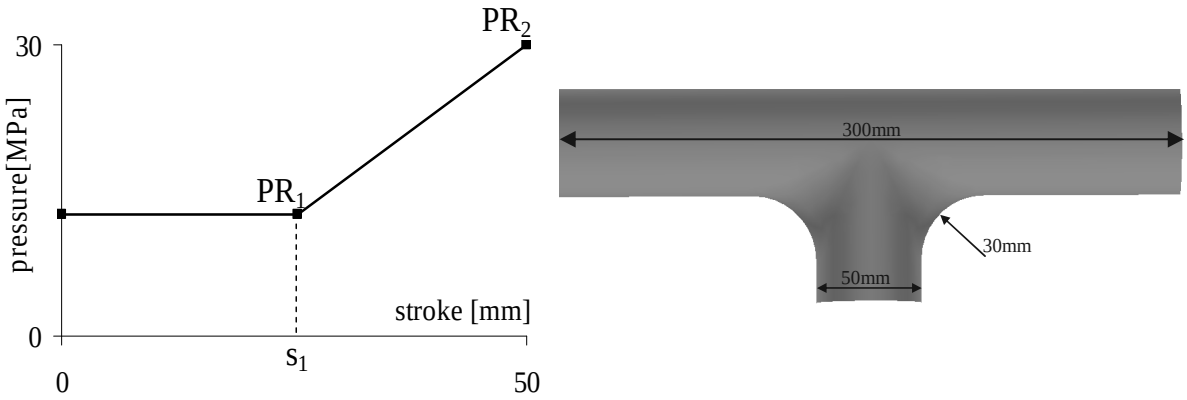

(a) (b)

Figure 2.5: Design variables (a) and T-shaped die (b).

As observed, sheet forming design problems are generally multiobjective. Nevertheless, the will to investigate the effectiveness of different metamodeling techniques and to better understand the differences beside their individual capabilities, leads to investigate a mono-objective problem for sake of simplicity, also supported by the possibility to formulate the objective function to be by the following expression (2.15):

$$f(x) = \Delta t\% + K\frac{(h_{desired} - h_{reached})}{h_{desired}} \tag{2.15}$$

where Δt% is the difference between the maximum and the minimum thickness through the hydroformed sheet; $h_{desired}$ and $h_{reached}$ are, respectively, the desired and the obtained bulge heights. K is a weight which was chosen on the basis of a preliminary numerical procedure which provided a good calibration of the two terms of the objective function. It is worth pointing out that the first term of the function is a very effective synthesis both of thinning and thickening of the tube walls. Thus, Δt% controls both fracture risk (excessive thinning) and buckling occurrence (excessive thickening). On the other hand, the second term relates to the aim to reach a bulge height as high as possible. The use of the above described case study and objective function was driven by two main considerations: the design problem is well known from previous investigation, thus the position of the global optimum within the variables domain is known; moreover, the investigated objective function is characterized by a strong

non-linear trend. Such considerations make the chosen case study quite suitable to apply different optimization approaches and to compare the results they come up with.

2.1.1.2.1 Discussion of the results.

All the investigated optimization strategies were tested on two different designs of experiments, in particular a Central Composite Design and a Latin Hypercube designed by the maxmin criterion. In fact, the technical literature addresses different designs of experiments depending on the utilized metamodeling method. The main results of the comparison here developed will be discussed in the following paragraphs.

Results of the CCD based approaches.

The starting Design of Experiment is a Central Composite Design with 9 points. In particular the pressure PR1 varies in the range [5;18] MPa while s1 [0;50] mm.

In particular, as far as the first two metamodeling techniques, PR and MLS, 23 runs were carried out in LS-DYNA environment for the regression approach as a sequential PR strategy was implemented to get a quite good approximation level, while just 10 runs were required by the proposed MLS approach (i.e. starting DoE points plus just one further optimum point P^i).

An R-Sq(adj) equal to 99.1% was also obtained for the polynomial regression.

As far as the Kriging based approach, as already mentioned, it needs to be set up by properly calibrating the carrier functions: a sensitivity analysis was therefore carried out by varying θ and the polynomial order of the deterministic function.

Four test points were also picked within the design space and relate to ±1/5 levels of the coded units, to better assess the fitness of the corresponding Kriging model set up. In order to explore a wide range of θ, three quite different values were chosen.

Moreover, the average and the maximum deviations (i.e. respectively $e_{average}$ and $e_{maximum}$) between predicted and simulated results were calculated on four test points to compare the fitness of the corresponding Kriging metamodels. The capability to identify the right optimum region was also investigated.

The results of the above mentioned sensitivity analyses are showed in Figures 2.6, 2.7, 2.8 by θ and polynomial order (i.e. *Poly*).

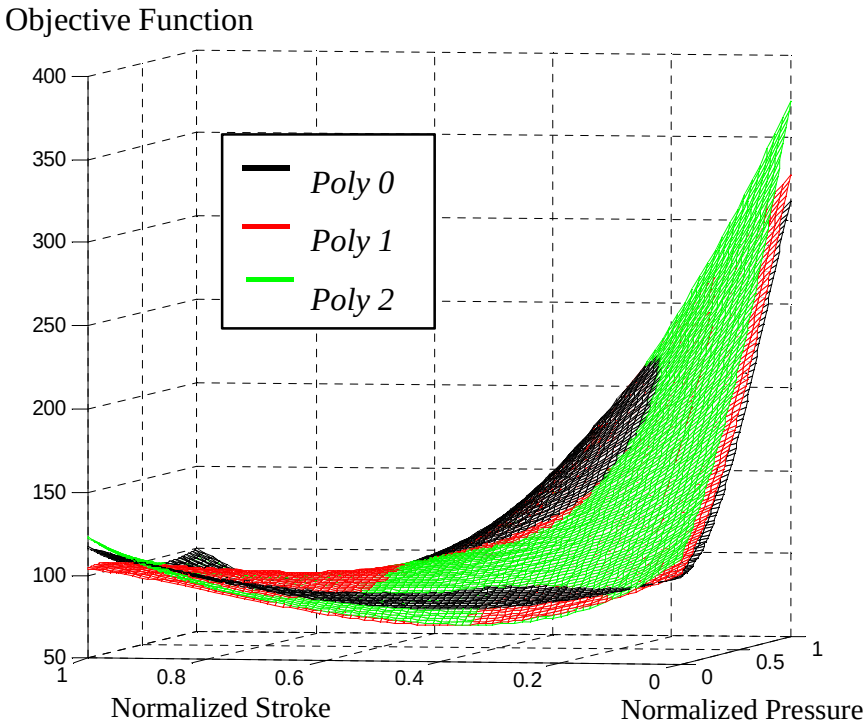

Polynomial Order	$e_{average}$	e_{max}
0	9.2	16.4
1	17.4	37.5
2	15.9	34.6

normalized

Optimum	***S1***	***PR1***
72.40	1	0.76

Figure 2.6: Kriging metamodels with θ = 0.1 and errors.

The Kriging model featuring the best prediction capability on the simulated points and able to rightly identify the optimum region was then implemented.

In particular, the best fitting parameters were the one performing a more global prediction model, i.e. θ = 0.1 and poly 0.

Such Kriging model was initially contrasted to the regression based one: the corresponding surfaces are pictured in Figure 2.9.

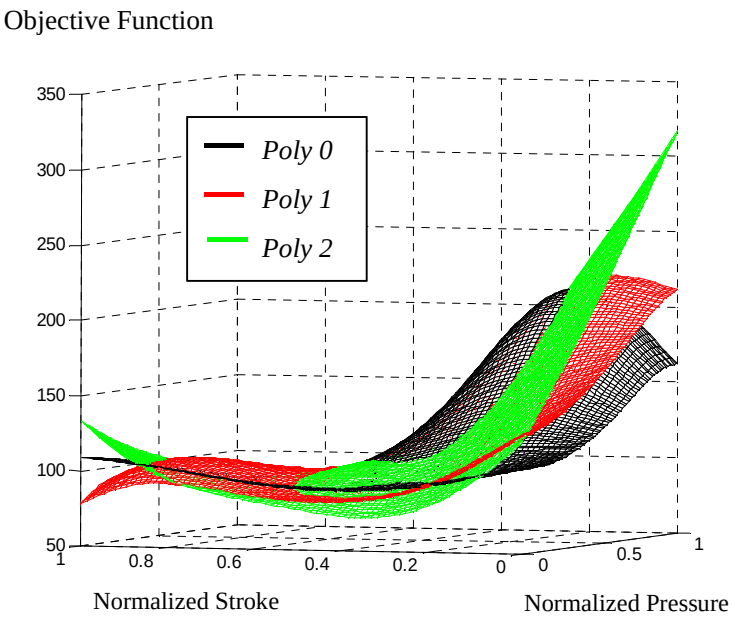

Polynomial Order	$e_{average}$	e_{max}
0	13.5	26.9
1	19.9	48.6
2	14.4	37.5

normalized

Optimum	S1	PR1
72.89	0.95	0.73

Figure 2.7: Kriging metamodels with θ = 1 and errors.

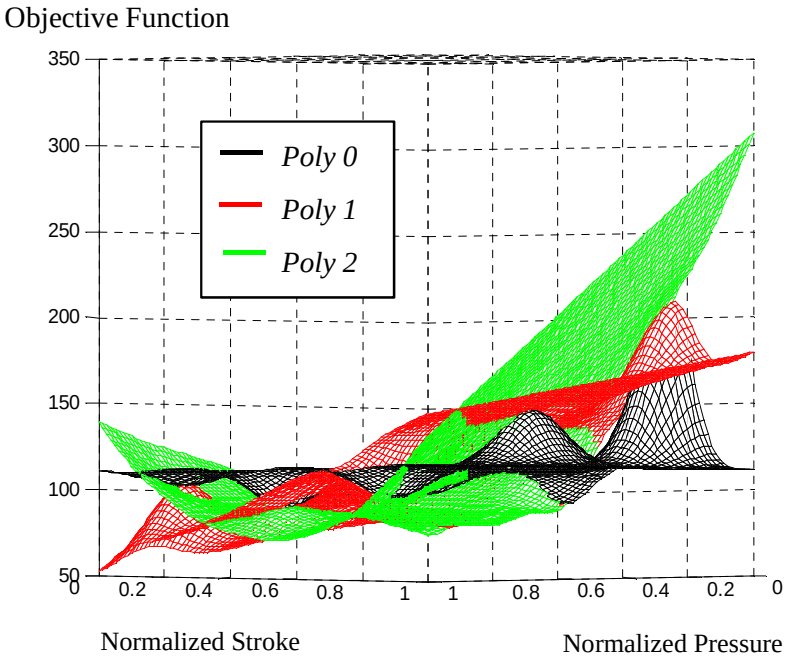

Polynomial Order	$e_{average}$	e_{max}
0	15.3	21.3
1	22.1	44.3
2	14.5	41.5

normalized

Optimum	S1	PR1
82.25	1	0.89

Figure 2.8: Kriging metamodels with θ = 10 and errors.

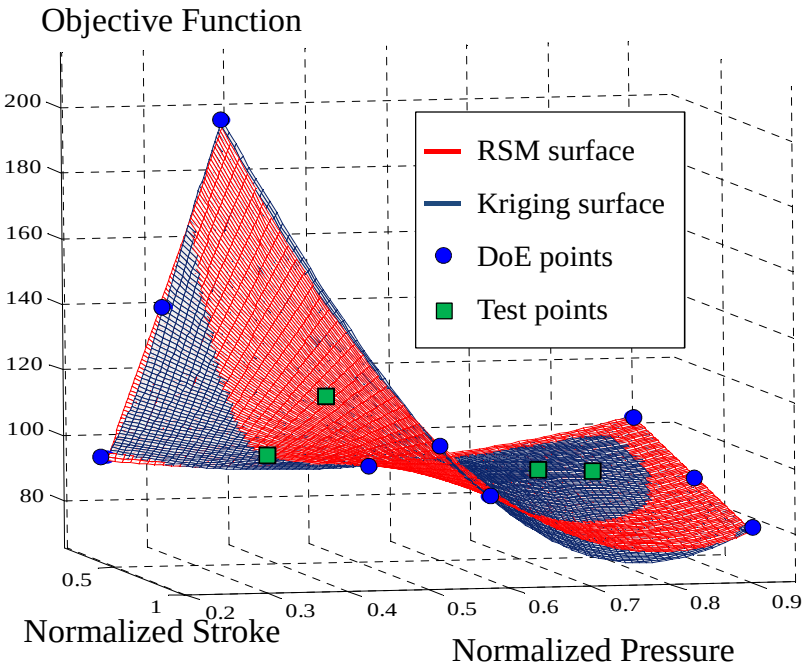

Figure 2.9: Comparison of PR and Kriging surfaces.

Even though Kriging surface exactly interpolates all the design points while regression surface generally misfits them by passing through, no remarkable differences can be observed in the case study. Even more, Kriging has globally a worse prediction capability on the test points, assessed by calculating the average error between simulated and predicted results, and identifies not the right minimum points, even close. Therefore, there is no value added in using Kriging as metamodeling technique since it results more time consuming and features higher computational costs, while PR results to be a quite effective tool to approximate the behavior of the investigated phenomena. According to Ingarao et al. (2010), the optimum point found by polynomial regression, M_1, was added into the first Design of Experiment with the aim to investigate how better the interpolation approach might perform if a more local fitting is computed. Therefore, a sort of sequential Kriging was implemented on the basis of the MLS principles. As a matter of fact, such sequential procedure comes close to the proposed MLS approach. By minimizing the Kriging function, in fact, a quite optimal design is identified, as it can be drawn by comparing the surfaces of Kriging and MLS approaches. A worse estimation of real optimum value (i.e. red point in Figure 2.10) is calculated by Kriging though. In the end, sequential Kriging is still a quite effective optimization strategy but MLS

approach allows a faster and even more accurate estimation of the optimum area.

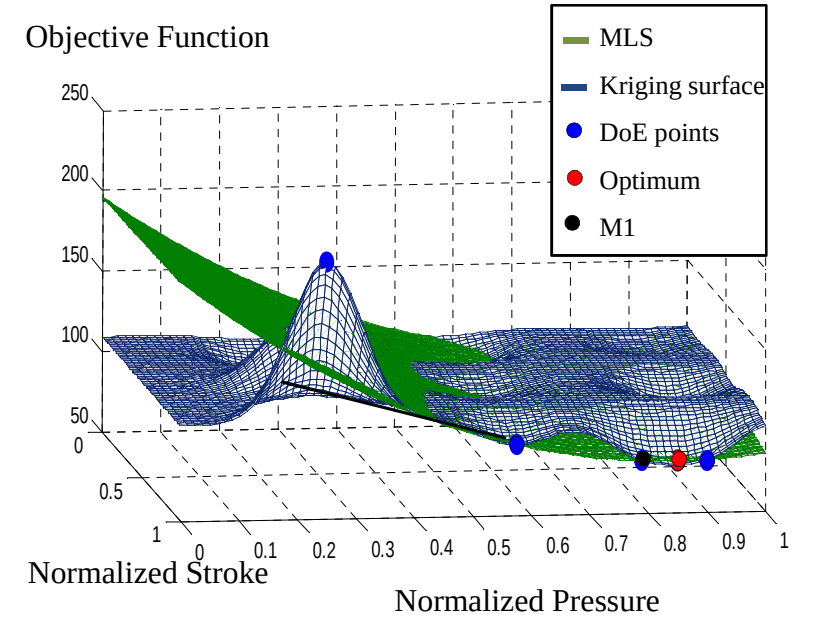

(a)

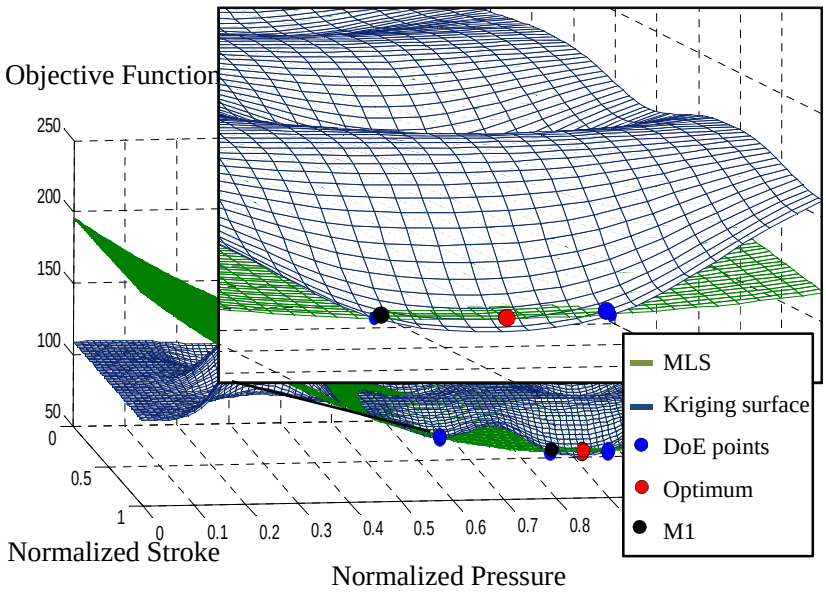

(b)

Figure 2.10: MLS and Kriging local surfaces (a) and optimum area by the two local metamodels (b).

In conclusion, as the first analyzed DoE is concerned, PR performs quite better than Kriging if compared on a global scale. Even though the optimum so found by PR (M_1) do not match

exactly the real one (i.e. red point in Figure 2.10), know on the basis of the process knowledge, it actually comes close. If a more local investigation is carried out by adding the optimum point first identified by the PR itself, results even closer to the real optimum are possible.
But in the end, even though Kriging improve its prediction capability, the MLS approach turns out to be the best one.

Results of LHD based approaches.

MLS and Kriging approaches were both applied again to a Latin Hypercube Design. In fact, according to the technical literature, such design of experiments is more suitable for Kriging implementation than traditional full orthogonal designs (Jack (2009)).
Thus, it might be possible to contrast these approaches by a fairer comparison basis. Of course, a sensitvity analysis of θ and polynomial order was done for the Latin Hypercube design as well. In particular, also in this case θ was set equal to 0.1 while Poly = 0 on the basis of the same criteria above discussed. In the end, while MLS quickly identifies the optimum design, a global Kriging approach doesn't even find where the optimum region is.
Then, sequential Kriging was implemented by adding the optimum point computed by polynomial regression on LHD design (i.e. M_1). Figure 2.11 shows MLS and sequential Kriging surfaces for the local approximation of the area sourronding M_1. Even though a further point was added in the optimum design area, local Kriging misfits again the computation of the optimum.
Eventually, more points should be added in such area to address Kriging towards better estimations, while just 10 simulations were run for the MLS approach. There is again no value added in using sequential Kriging when compared with the proposed MLS optimization approach.
As it is also evident from Figure 2.11, PR doesn't perform well on a LH design as it was actually expected. In fact, orthogonal designs are more generally suitable for such techniques over other criteria (Myers and Montgomery (2002)). As matter of fact, M_1 is quite farther from the real optimum than it was in the former CCD design.

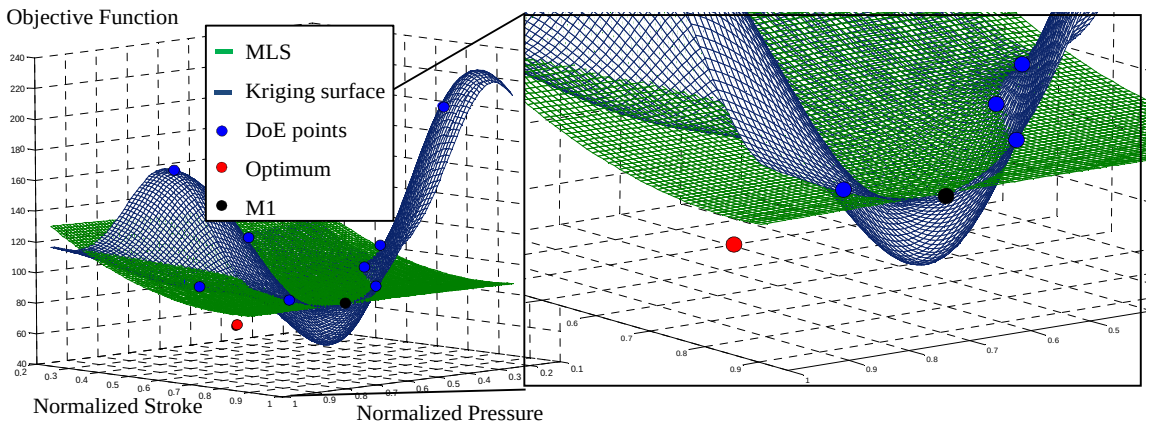

Figure 2.11: comparison between MLS and sequential Kriging surfaces.

To sum up, Response Surface Models, Kriging approaches and MLS strategies were applied to a sheet stamping hydroforming process by two different Designs of Experiments. The results are summarized in Table 2.2.

Optimization technique	***D.o.E.***	***Optimum convergence***	***#Numerical simulations***	***Implementation complexity***
P. R.	CCD	YES	23	Easy
MLS	CCD	YES	10	Easy
Seq. Kriging	CCD	YES	10	Difficult
Seq. Kriging	LHD	NO	10	Difficult
MLS	LHD	YES	10	Easy

Table 2.2: Summary of the results

2.1.1.2.2 Final remarks.

Polynomial regression models are very easy to implement but they usually requires many more numerical simulations than others optimization methods if an iterative procedure is implemented. They may also be preferred when working on a global scale, e.g. for identifying promising regions in design space for optimal designs. In general, PR may be less suitable to capture detailed local functional behavior while Kriging may be more adequate, as all the simulated training data are exactly fitted: no significant differences were observed though. Moreover, Kriging models usually need to be properly set up to get reliable estimations, raising time and computational efforts. On the other hand, a sequential Kriging based strategy was tested on the basis of the proposed MLS approach, which resulted really effective since faster and more accurate than others optimization strategies.

By adding further points close by the optimum region, Kriging's prediction capability was improved but it resulted however worse than MLS's.

There was no value added in the end in using Kriging based approach for the investigated hydroforming application as less straightforward to implement, less effective and in some cases even less reliable in the identification of the optimum.

A more general consideration has also to be made: if two or more objectives have to be accomplished, local approximations, even more accurate in single objective problems, might be meaningless in multiobjective problems. In fact, as it often happens for conflicting objective functions, the optimum region in the design space of one of those functions is quite far from the optimum region of the other ones. Therefore, from a Pareto optimality perspective, a local knowledge, which is indeed very good in some area of the design space for one objective, might imply on the other hand a lack of information where other objective functions perform instead well. In this case, more global approaches are recommended.

2.1.2 Case study 1: multiobjective robust design of a deep drawing process.

In the following case study, a hybrid framework for robust design is applied to a sheet stamping process. In particular, the developed tool is able to evaluate and to deal with the scatter of the final part quality due to the inner variability of such operations. The analyzed process is a S-shaped U-channel stamping operation carried out on a lightweight aluminum alloy of automotive interest. A multi-objective optimization problem integrating finite element (FEM) numerical simulation, Response Surface Methodology (RSM) and Monte Carlo Simulation (MCS) method within a hybrid procedure was in particular implemented.

The design procedure results able to foresee the potential direction along which a Pareto solution may scatter due to the effects of the noise factors, while being able to fully account for the variability effects and to provide with an accurate understanding of the possible perturbations on the objective functions. A comparison with a traditional deterministic approach is reported to highlight differences and capabilities of such hybrid approach.

Following the investigated process and the problem modeling are described, along with the details of the implemented hybrid approach. The obtained results and conclusive considerations are reported afterwards.

2.1.2.1 Problem modeling.

On the basis of the results obtained from the sensitivity analysis discussed in section 1.1, the same S-shaped U-channel case study was used to investigate the hybrid robust procedure here proposed. The material properties have been previously showed in Table 1.5. Similarly, the details of the numerical simulation implemented by the commercial code LS-DYNA refer to section 1.1 as well.

Both excessive thinning risk and springback effects were taken into account as objective functions to be minimized. The maximum thinning percentage, th[%], was utilized to express fracture risk again. Similarly, the total displacement, i.e. the displacements calculated in normal direction between deformed blank after load removing and final stamped part was utilized as springback indicator.

As the design variables are concerned, since the stamping processes are driven by the restraining forces, the blank holder forces were controlled. In particular, a constant blank holder force (BHF) was taken into account as design variable due to the simplicity of the stamped part. A single design variable was chosen as aiming at investigating a simplified model to test the proposed optimization procedure. BHF can be reasonably considered a deterministic variable easy to control and any possible variation of it is then neglected. Initial blank and tool geometric properties are supposed fixed. As the chosen noise factors are concerned, two factors were considered: the strain hardening coefficient (n) and the friction coefficient (μ) at the interface between the blank and respectively the die and the binder.

2.1.2.2 The proposed optimization methodology.

As mentioned, two approaches were implemented and compared in this case study in order to provide a better understanding of the application and capability of the hybrid robust approach. In particular, a fully deterministic approach, traditionally disregarding any stochastic effect or variability consideration, and a hybrid one, as robust design framework for sheet stamping processes, were developed.

2.1.2.2.1 Fully deterministic model.

In the fully deterministic model, process variability due to noise factors was completely neglected and therefore only the BHF influence was considered. In this way, μ and n were

kept at their nominal value. In particular, μ was assumed equal to 0.109, while n 0.247. A scheme of the deterministic procedure is shown in Figure 2.12.

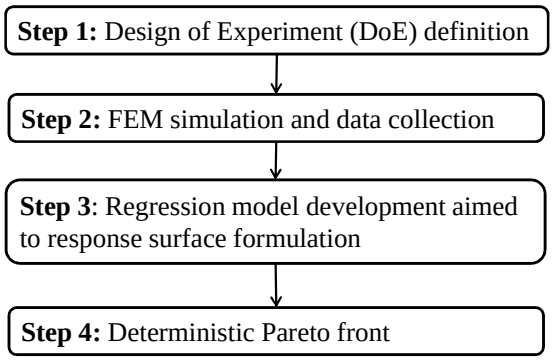

Figure 2.12: Sketch of the deterministic procedure.

Step 1: Design of Experiment (DoE) definition.

Since one single input parameter was selected, DoE consisted of 8 equidistant points in a given BHF range. In order to explore a significant restraining forces range, which still avoids excessive thinning conditions and enables investigating an industrially reasonable domain, BHF values from 10kN to 80kN were chosen.

Step 2: FEM simulation and data collection.

A numerical simulation for each DoE point was run and th and sb results were collected. Table 2.3 shows the DoE details and the outputs of the FEM simulation.

DoE points	*BHF [kN]*	*th [%]*	*sb[mm]*
1	10	10.22	0.99
2	20	12.01	0.96
3	30	13.44	0.85
4	40	14.75	0.77
5	50	16.34	0.70
6	60	18.10	0.67
7	70	19.90	0.58
8	80	23.54	0.51

Table 2.3: DoE points and simulation outputs.

Figure 2.13 and 2.14 illustrate respectively the sb maps obtained from simulations of DoE points 1 and 8 reported from Table 2.3. Section AA' was chosen since it is the one, which better illustrated the springback deflection between deformed blank after load removing and

the desired final part. A relevant difference in terms of springback occurrence is due to the quite different conditions of restraining forces in the two analyzed conditions. Moreover, a difference as high as 13% on th is noticed.

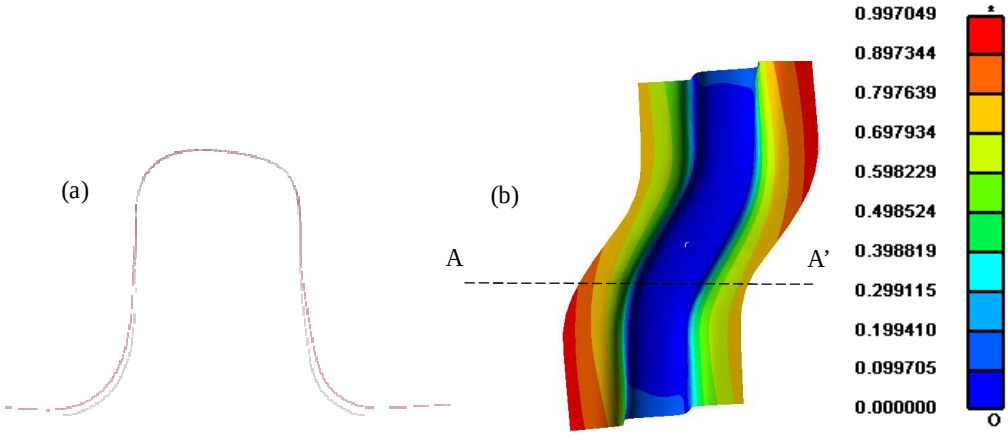

Figure 2.13: Section AA' (a) and sb map (b) for BHF 10 [kN].

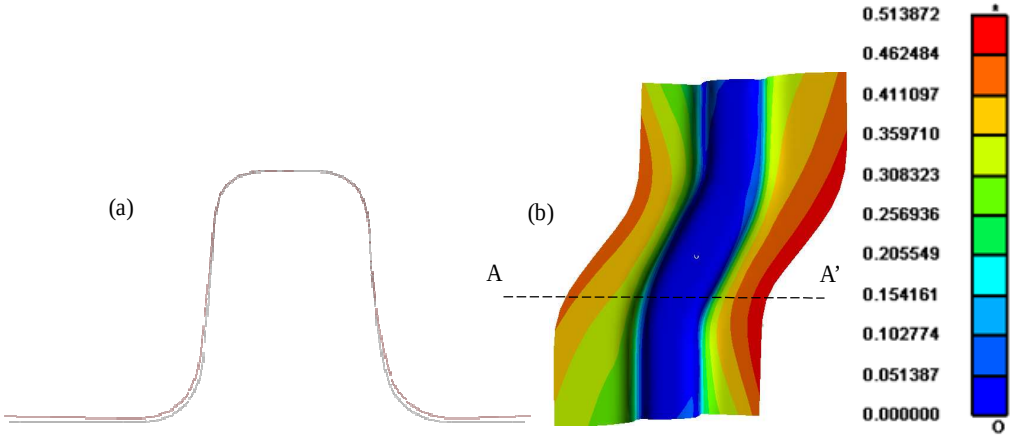

Figure 2.14: Section AA' (a) and sb map (b) for BHF 80 [kN].

Step 3: Regression model development aimed at response surface formulation.

A second order regression model was developed within MINITAB environment to analytically formulate a response surface (y) for each objective function. In particular, a stepwise regression was developed by progressively eliminating the less statistically significant terms to optimize the correlation index R-Sq(adj), which provides a measure of the approximation capability of the model. The results are summarized in Table 2.4: values of R-Sq(adj) higher than 98% were reached confirming a good data approximation.

DoE points	*th [%]*	*th predicted [%]*	*sb [mm]*	*sb predicted [mm]*
1	10.22	10.62	0.99	1.01179
2	12.01	11.73	0.96	0.93282
3	13.44	13.07	0.85	0.85666
4	14.75	14.61	0.77	0.78333
5	16.34	16.38	0.70	0.71282
6	18.10	18.36	0.67	0.64513
7	19.90	20.55	0.58	0.58026
8	23.54	22.97	0.51	0.51821
$y_{th} = 9.7175 + 0.07924 * BHF + 0.00108 * BHF^2$			R-Sq(adj)	98.70%
$y_{sb} = 1.09359 - 0.0083 * BHF + 1.4E-05 * BHF^2$			R-Sq(adj)	98.60%

Table 2.4: Response surface equations and indexes of approximation capability.

Figure 2.15 shows the fitting curves evidencing the conflicting trend of the two goals (th and sb are reported as normalized values, in order to properly compare them). Both fitting curves present a monotonous behavior at increase of restraining forces: decreasing for springback and increasing for thinning.

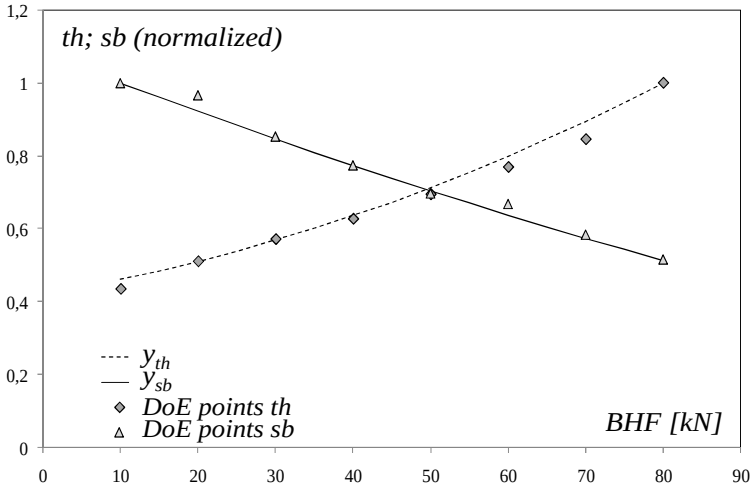

Figure 2.15: Fitting curves.

Step 4: Deterministic Pareto front.

Once the two objective functions were analytically formulated, it was necessary to identify compromise solutions minimizing simultaneously th and sb. Therefore, a Pareto front was constructed. A Pareto optimal solution is a solution which guarantees that no improvement of one objective function can be made without worsening any other goal (Deb (2001)). The corresponding Pareto front is then an effective tool providing with a quite good set of feasible

solutions that compromise all the objectives to be accomplished inside the design domain. Several techniques are available in literature to reach Pareto solutions: Summing Weighted Scores Method, ε-Constraint, Genetic Algorithm (GA), Multi Objectives Particle Swarm Optimization Method (MOPSO), Normal Boundary Intersection method (Das and Dennis (1997)), the physical programming (Messac and Mattson (2002)) and so on. Das and Dennis (1997) showed that, when Summing Weighted Scores Method is applied an even spread of the weights does not necessary result in an even distribution of the points in the Pareto set. Moreover, the spread of the points strongly depends on the relative scaling of the objectives. They also observed that the main drawbacks of Summing Weighted Scores Method enhance with the increasing of the number of the objectives to be managed and different approaches are proposed to overcome the aforementioned drawbacks, such as the Normal Boundary Intersection (NBI) method or, according to Messac and Mattson (2002), the physical programming (PP) one. The effectiveness of each technique depends on investigated problem features as dimension or non linear functions behavior. Here, due to the presence of just one design variable and to the conflicting objective functions behaviors, the Pareto front results of prompt determination without using any multi-objective methods. In fact, every th-sb couple, which corresponds to a specific BHF value, is a Pareto solution: for given operative conditions, i.e. for given BHF, no solution exists that allows a lower springback at fixed thinning value. Figure 2.16 shows the deterministic Pareto front.

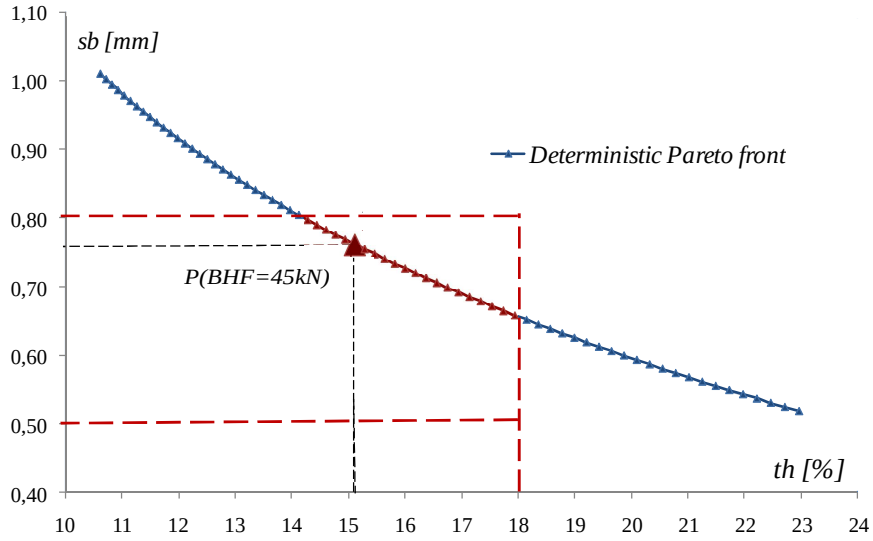

Figure 2.16: Pareto front for the deterministic model.

As expected, the maximum thinning increases as springback decreases in the stamped part. As it is well known, the Pareto front is a very useful design tool as it provides with all the possible compromise solutions and predicting the best possible value of a given objective once the other one is fixed.

It has to be noticed that the proposed procedure also allows determining the most suitable BHF value to be chosen if a particular configuration of th-sb is desired.

If a th of about 15% (point P in Figure 2.16) is desired, a BHF of 45kN has to be calibrated and the best possible value of sb to be expected is 0.76mm.

On the other hand, if a boundary in terms of one of the objective functions is given (for example, 18% of maximum tolerable thinning), there is the possibility to choose among several BHF values according to the will to obtain certain values of the other objective.

For instance, if sb has to be from 0.50mm to 0.8mm in Figure 2.16 all the points belonging to the red part of the Pareto curve are possible solutions, thus a BHF ranging from 35kN to 75kN could be chosen.

2.1.2.2.2 Hybrid model for robust design.

Given the deterministic analysis above, a different perspective is here investigated: how do the effects of the noises affect the final Pareto solutions? And therefore, how does considering variability within the design tool change the choices of the process designer?

The focus of a robust procedure becomes to provide with an effective tool able to enhance the awareness on the influence of the noises on the final results of the objective functions, to identify robust operative windows limiting such effects, and to plainly show how any Pareto solutions, which deterministically fulfills all the process specifications, might turn out to be on the contrary less robust or even reliable.

Specifically, the application of the hybrid approach to the investigated case study should here explore the scatter of th and sb due to μ and n effects at different controllable levels of BHF.

Figure 2.17 illustrates the hybrid optimization strategy, whose steps 1 and 2 are deterministic while the Step 3 is stochastic. More details are in the following.

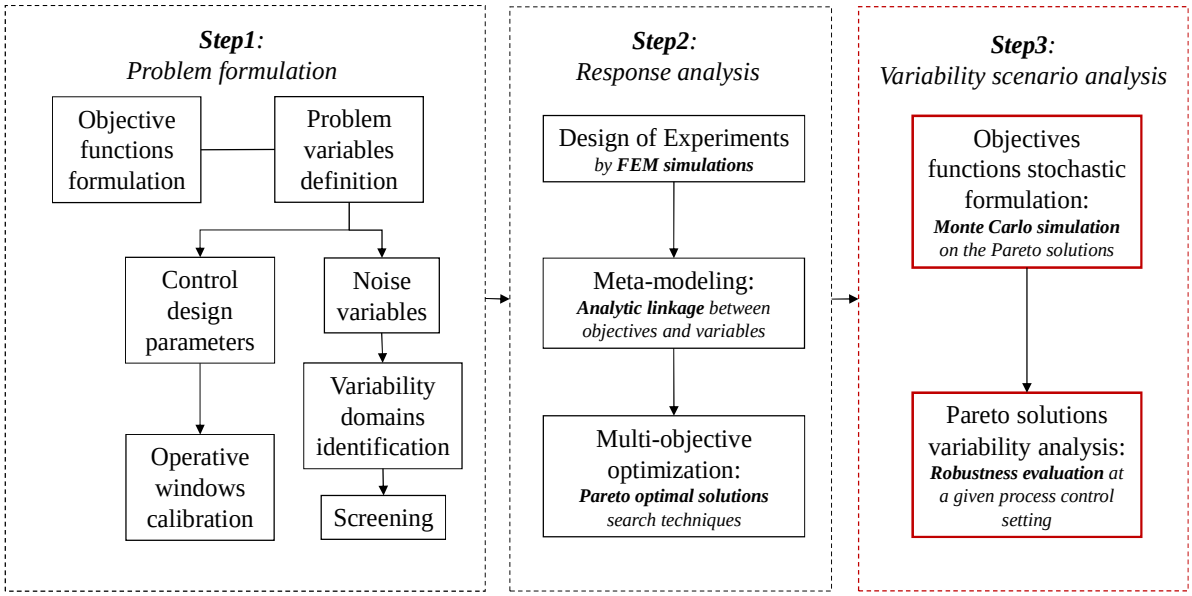

Figure 2.17: Hybrid optimization strategy.

Step 1: Problem formulation.

In this early phase the investigated process should be modeled in terms of performances to be optimized (i.e. objective functions) and variables influencing such performances, whose identification is widely based on the process designer expertise. In order to develop any stochastic model, a preliminary difference between design variables and noise factors has to be performed: as earlier mentioned, a single design variable was chosen, and namely the BHF constant in time and space, while the noise factors are the strain hardening coefficient (n) and the friction coefficient (μ).

Moreover, it is necessary to properly identify a feasible operative window, where all the following investigation will be carried out.

The control design parameters have to be varied within a domain ensuring the process feasibility. As earlier discussed, in order to explore a significant and industrially reasonable restraining forces range, a BHF domain from 10kN to 80kN were here chosen.

As noise variables are regarded, a variability domain within which each variable may occur has to be identified. As such variables are assumed to have a stochastic behavior, a first step concerns therefore the probability distribution to use for each one. The most effective way would be a campaign of experimental investigations to properly describe the stochastic

behavior of the noises, otherwise data from the technical literature can be utilized. Obviously, only the most influent variables should be accounted for.

Table 2.5 lists the noises variables here investigated, whose statistical parameters are from the analysis of the technical literature. The standard deviation for factor μ was taken from (Zang and Shivpuri (2008)), while a coil to coil variation was considered for factor n, since such choice seemed the most proper for the investigated case study in order to provide an industrially applicable tool.

Variables	Distribution	Mean	Standard Deviation
μ	Normal	0.109	0.01
n	Normal	0.247	0.0285

Table 2.5: Noise factors statistical parameters.

Thanks to the Central Limit Theorem it is possible to hypothesize that they are distributed according to a normal distribution. Moreover, it has to be observed that the mean values are the same ones utilized in the deterministic approach.

Step 2: Response analysis.

The response analysis step is a propaedeutic phase to the quantification of the stochastic effects of the noise variables on the objective functions. In this sense, the analysis should be formerly carried out from a deterministic point of view, aiming to optimize the investigated process by the control parameters calibration.

Therefore, a preliminary metamodel on the basis of a proper Design of Experiments is needed in order to build up an analytical linkage between each selected objective and all the related variables, both control and noises. A polynomial regression based on the Response Surface Methodology (RSM) was here used.

Although such technique neglects any stochastic behavior, the metamodeling step is fundamental as a preliminary tool for the variability investigation since it allows drastically reducing the computational effort. Therefore, the choice of the levels of each variable within the DoE domain have to take into account the actual range of variation of each stochastic variable. A Central Composite Design (CCD) with 15 points was in particular carried out. Table 2.6 reports the CCD levels of each variable: in particular the BHF levels are the ones utilized in the deterministic approach, while, since μ and n are noises, their variations have to

reflect assigned probability distributions. In particular, ±α levels of the noise variables respectively correspond to the 5th and 95th percentiles of their probability distributions.

	- α	*- 1*	*0*	*+ 1*	*+ α*
BHF	10	24.19	45	65.81	80
μ	0.093	0.099	0.109	0.119	0.125
n	0.2	0.219	0.247	0.29	0.294

Table 2.6: CCD levels.

The presence of unreasonable thinning conditions within the CCD points was also verified. Table 2.7 reports the FEM simulation results together with the response surface equations (y) and indexes of the approximation capability of each metamodel.

Points	*th [%]*	*th predicted [%]*	*sb [mm]*	*sb predicted [mm]*
1	11.986	11.80	0.94	0.93541
2	17.425	17.81	0.66	0.66186
3	12.704	12.57	0.87	0.87381
4	19.431	19.90	0.56	0.56618
5	12.798	12.48	0.87	0.86575
6	19.164	19.64	0.60	0.59220
7	13.484	13.24	0.78	0.78989
8	21.646	21.73	0.48	0.48226
9	10.224	10.81	0.997	0.99881
10	23.536	22.76	0.514	0.51010
11	14.508	14.35	0.792	0.80517
12	16.671	16.75	0.672	0.66398
13	14.958	14.76	0.76	0.75691
14	16.416	16.34	0.67	0.67549
15	15.535	15.55	0.742	0.73458
				R-Sq(adj)
y_{th} = 9.917- 0.194*BHF+0.001*BHF^2+ +1.665*BHF*μ+0.373*BHF*n				98.7%
y_{sb}=0.7864-0.0037*BHF+1.623E-05*BHF^2+4.35*n-8.35*n^2-0.043*BHF*μ-10.024*μ*n				99.7%

Table 2.7: Regression model results for CCD points.

A second order interpolation is able to explain with a good approximation the investigated phenomena, actually, R-Sq(adj) of about 99% were obtained.

Given a metamodels of each objective function, the multiobjective optimization problem can be easily formulated as follows:

$$\begin{aligned} &\textit{Minimize/maximize} && F(X) = (f_1(X_1), f_2(X_3), f_3(X_3) \dots f_j(X_j)) && j=1, 2 \dots m \\ &\textit{Subjected to} && x_{i,\,low} \leq x_{i} \leq x_{i,\,upper} && i=1, 2 \dots n \\ & && g_k(x_i) \leq 0 && k=1,2 \dots p \end{aligned}$$

where X_j is the vector consisting of the control parameters x_i (n is the total number of control parameters); f_j, indicates each objective (m is the total number of objective functions) and $g_k(x_i)$ is the k^{th} constraint function (p is the total number of constraints).

Since the noise variables cannot be calibrated by the designer, each Pareto solution consists of a control parameters setting over which the noise stochastic effect will be subsequently evaluated. Therefore, the Pareto front is the one showed in Figure 2.16 from the deterministic approach.

Step 3: Variability scenario analysis.

In order to analyze the influence of the noise variability on the design choices, a proper number of Monte Carlo Simulations (MCS) was run.

As far as the developed hybrid methodology, it is here important to stress the need of integrating metamodeling and MCS. In fact, it was earlier observed how the MCS method calculates a series of possible values of any investigated objectives by generating different occurrences of all the noise variables (random sequences) from a given probability distribution, to derive at the end a probability distribution of each analyzed objective.

From a different point of view, the MCS technique is simply a numeric integral method and its effectiveness increases with the problem dimension. Starting from the canonic form (2.16), it is possible to express the canonic integral form in probabilistic terms as followed:

$$I = \int_a^b f(x)dx \quad \rightarrow \quad I = \int_a^b f(x)\frac{p(x)}{p(X)}d(x) \tag{2.16}$$

where f(x) is a generic function defined in the [a, b] interval and p(x) is a generic probability density function of a random variable X. If it is considered a further random variable G defined as f(x)/p(x), from the expected value definition ($\overline{G}$), the following expression is derived:

$$\bar{G} = \int_a^b \left. f(x) \right/ p(x) \; p(x)d(x) = I \tag{2.17}$$

From the above expressions, the computation of the integral I can be usefully conducted to

equation (2.18):

$$\bar{} \tag{2.18}$$

where g is a generic occurrence of the random variable G. Therefore, the integral solution becomes a problem statistically solvable by proper sample investigation.

The number of random sequences to be generated in order to assure the convergence of the method to the real phenomenon behavior (or, at least, in order to evaluate the main statistical parameters such as mean and variance of the distribution), makes the integration with the metamodeling step unavoidable: a standalone implementation of Monte Carlo method, in fact, would imply a too large problem dimension. In this way, an integration between MCS and RSM allows drastically reducing the computational effort and, even though the noise levels cannot be calibrated, it is however necessary to incorporate them into a metamodel (Ledoux et al. (2010)). Figure 2.18 reports a simplified scheme of the above mentioned integration between MCS and RSM for a generic Pareto solution, with reference to one of the objective functions.

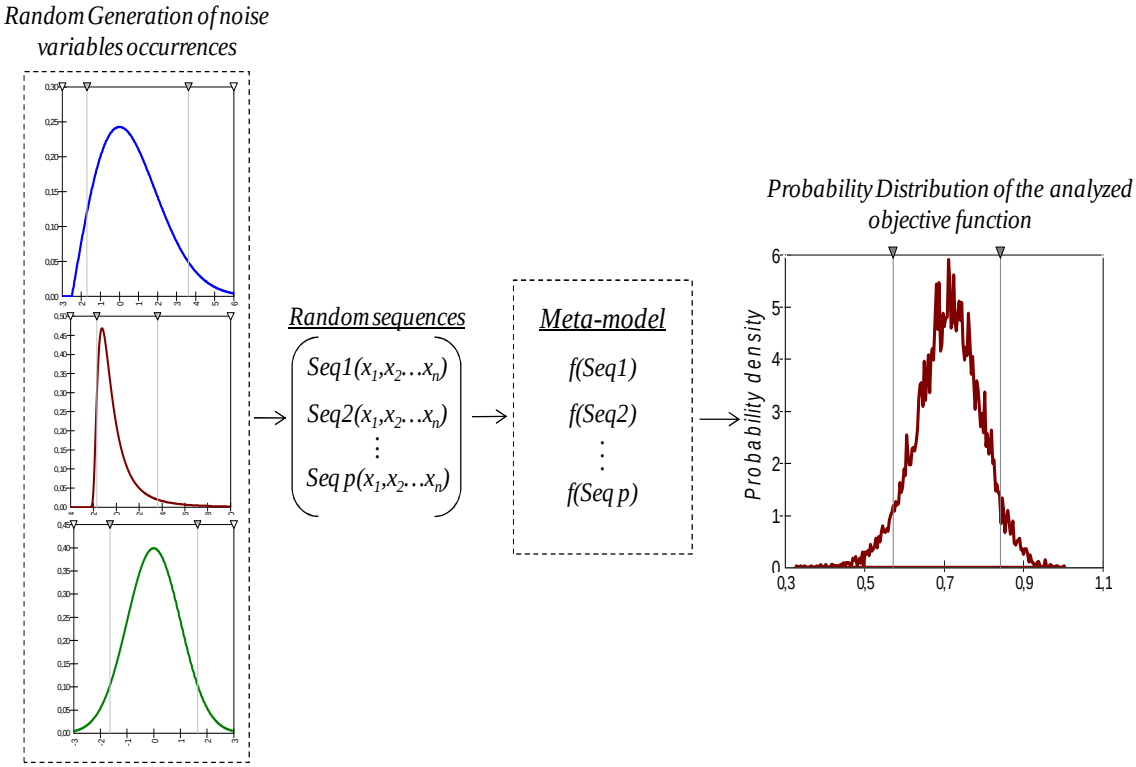

Figure 2.18: MCS and RSM integration scheme for each objective of a generic Pareto solution.

To sum up, for each Pareto solution, a proper number of noise variables sequences is generated and the corresponding objectives values calculated by the earlier obtained metamodels. In this way, according to the Monte Carlo simulation principles, each objective probability distribution is build up with respect to a certain process design setting.

Therefore, for the investigated case study, random sequences of μ and n were generated from their probability distributions.

The availability of the analytical linkages (y_{th} and y_{sb}) between input variables and objective functions makes possible to calculate the values of th and sb corresponding to the generated random sequences. Thus, 35 different levels of BHF were analyzed (with a step of 2 kN to explore the range 10kN to 80kN) and outputs probability distributions for each level were obtained by MCS. Thus, at given BHF level, the corresponding outputs values are not unique, but they change within a possible range of occurrences with different probabilities.

A sensitivity analysis was performed in order to identify the appropriate number of Monte Carlo simulations required to converge and at the end 1300 Monte Carlo simulations were run for each objective at each BFH level (i.e. 1300 runs x 2 objectives x 35 BHF levels).

Figure 2.19 shows for instance the probability distribution of thinning obtained at BHF=10kN, with a mean value equal to 10.82% and the standard deviation as high as 0.198.

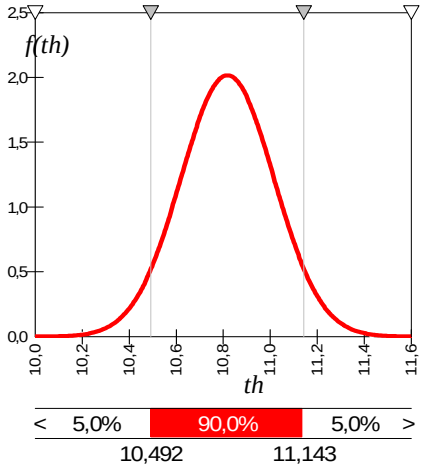

Figure 2.19: th density probability distribution by MCS when BHF is equal to 10kN.

At a given action of blank-holder, simultaneous variations of noise factors imply that th is not always the expected one but it changes within a possible occurrences range whose probability distribution is the one represented in Figure 2.19. Of course, the same considerations can be

made for sb. It has to be noticed, that the knowledge of a probability distribution for each output, allows obtaining all the statistical parameters characterizing these distributions.

By the th and sb probability distributions determined by MCS for each BHF level, Figure 2.20 shows the stochastic Pareto curve built just on the mean values. It is important to point out that the deterministic front and the stochastic one (mean values) are nearly overlapped. But the real occurrences of th and sb may vary somehow "around" the stochastic Pareto front for mean values because of μ and n variations.

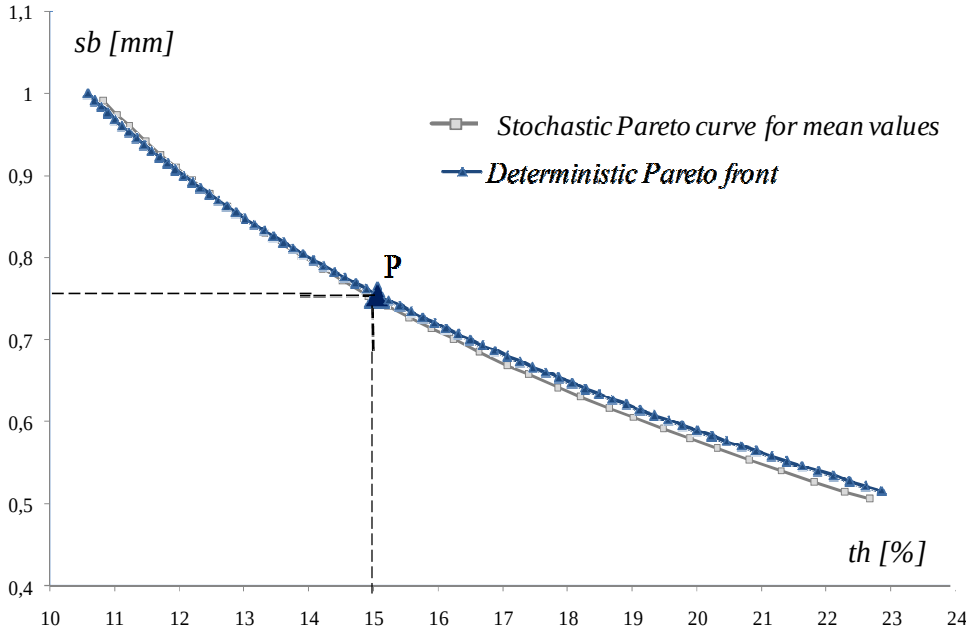

Figure 2.20: Pareto front by mean values.

The main advantage of a multiobjective problem formulation is the possibility to obtain a set of different design solutions which are equivalent in terms of Pareto optimality.

All these solutions are optimal ones from a deterministic point of view, but if a stochastic scenario is considered such Pareto optimality might not be valid anymore.

Therefore, the availability of the probability distributions of the objectives allows evaluating which values of such functions might be obtained when the noise variables vary within their stochastic domains (of course for given control parameters configuration, i.e. Pareto solution).

As last step, a variability analysis of the Pareto solutions is to perform. A detailed description of its application and results follows in the next section.

2.1.2.2.3 Discussion of the results: variability analysis of the Pareto solutions.

The basic idea of a Pareto analysis is the following: once a desired level of one of the output (i.e. th) is fixed, which is the expected best possible value of the other output (i.e. sb)? If a stochastic environment is considered, the will to investigate the effects of the noise factors leads to the need to take into account process sensitivity and to get a more aware view of outputs variation ranges. Moreover, if one of the outputs (i.e. th) changes undergoing the effect of noise factors, which is the expected variation of the other output (i.e. sb) due to the same effect? In other words, starting from a point of the Pareto stochastic front, the effects of μ and n variations would imply, for instance, that th moves towards lower or higher values; under such hypothesis, where springback values would move?

It becomes then really helpful to identify the direction along which the final objective functions scatter due to noise effects and to quantify the probability of such possible changes. Figure 2.21 illustrates how that is possible by the procedure developed to determine the couples of th and sb on the basis of the knowledge of the variations of μ and n.

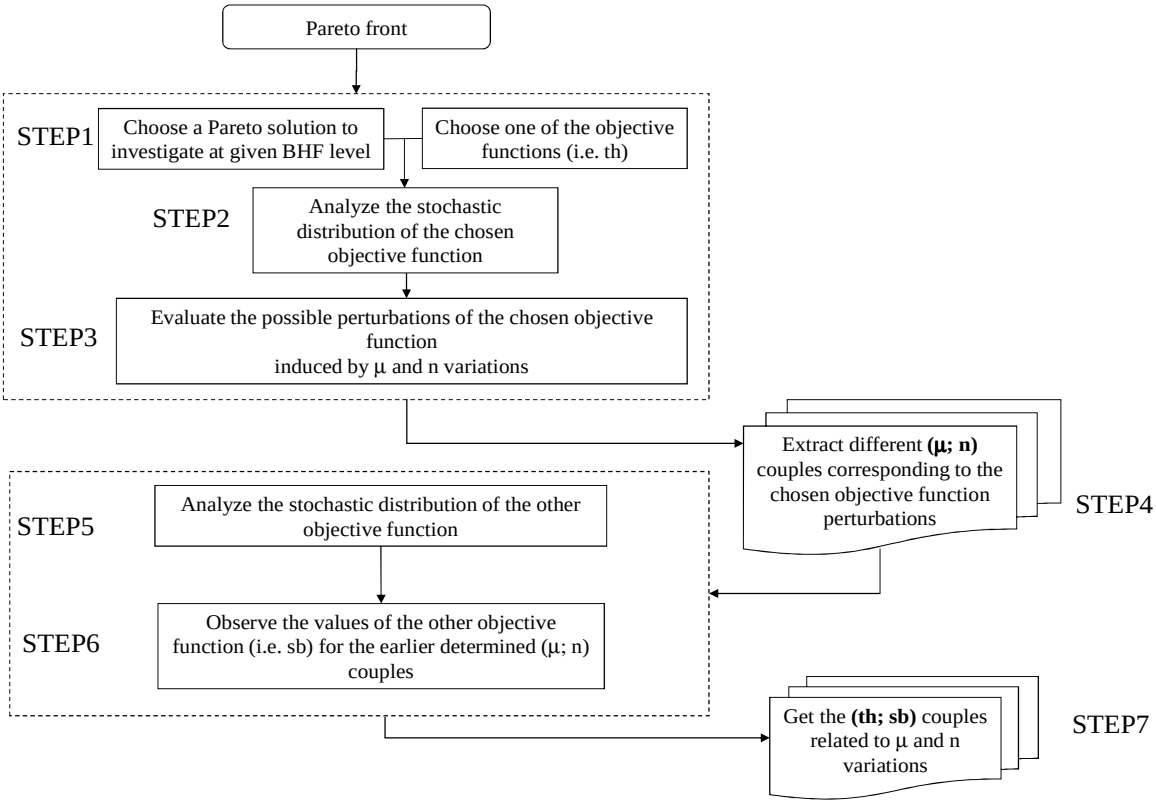

Figure 2.21: Workflow procedure of the Pareto solutions variability analysis.

Figure 2.22 clarifies the single steps of the procedure: taking the point A from the Pareto front, it corresponds to a BHF level as high as 49kN, where th is equal to 16% and sb 0.7mm. For such BHF level, the variations of μ and n imply that th (for example) has a certain probability distribution. From this distribution different percentiles (th occurrences) can be extracted, and a different couple of μ and n would correspond to each occurrence.

It is important to point out that in this case study this couple of noises is unique due to the convexity of th response function.

For each couple of μ and n, the corresponding sb value (for the same BHF level) can be determined. Thus, points such as A_1 A_2 and A_3 (or A'_1, A'_2, A'_3) can be identified. Namely, the distance between the points A_2 and A'_2 is the one which corresponds to 90% of the probability distribution, as well, the distance A_1-A'_1 corresponds to almost the whole distribution while A_3-A'_3 corresponds to about 70% probability.

Figure 2.22 illustrates the six considered perturbations of the Pareto solution A. Moreover, the th and sb distributions with the 5^{th} (A_2) and 95^{th} (A'_2) percentiles are highlighted.

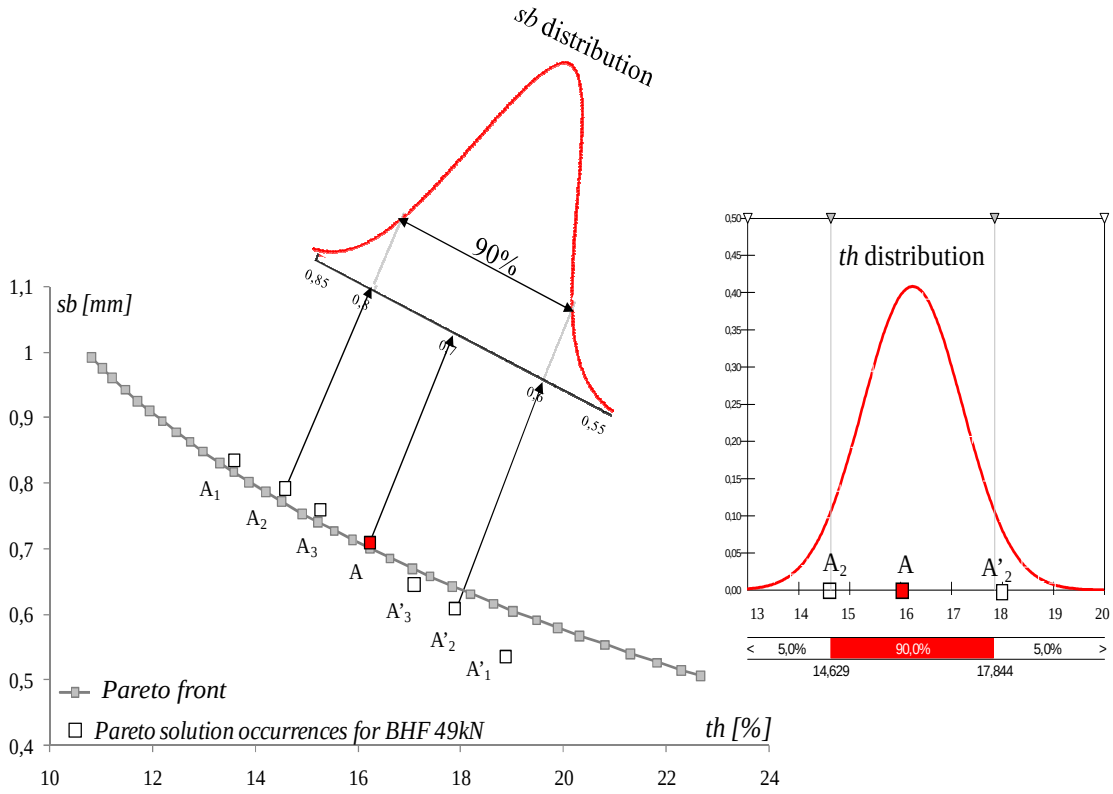

Figure 2.22: Application of the workflow procedure for BHF= 49kN (point A).

As it can be observed, significant differences are obtained on thinning and springback values at the same level of BHF moving from the point A_1 towards the point A'_1. In Table 2.8 the numerical simulation results respectively related to the point A, A_2, A'_2, are reported and a difference of 3% can be noticed in th. As far as the springback amount, the difference between A_2 and A'_2 reaches almost 0.2mm. Such considerations emphasize the stochastic approach relevance in sheet metal forming process design.

Point	*th*	*sb*
A μ=0,109 n=0,247	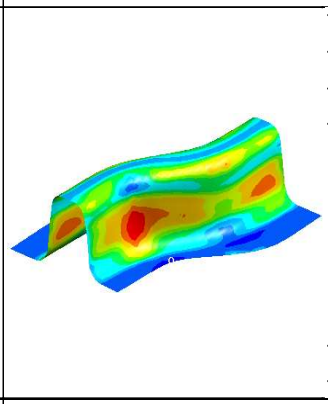	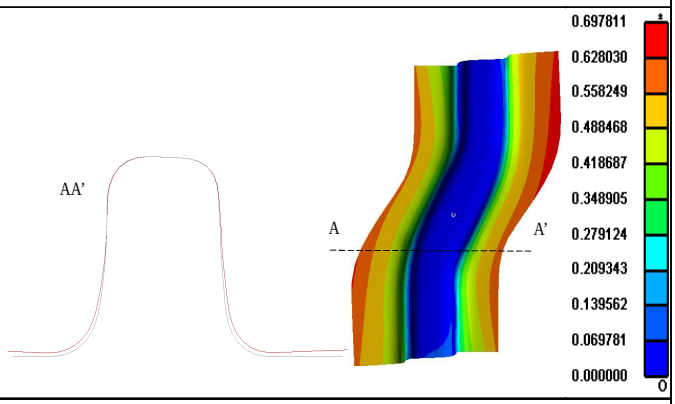
A_2 μ=0,092 n=0,230	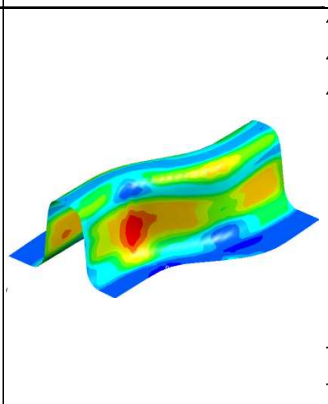	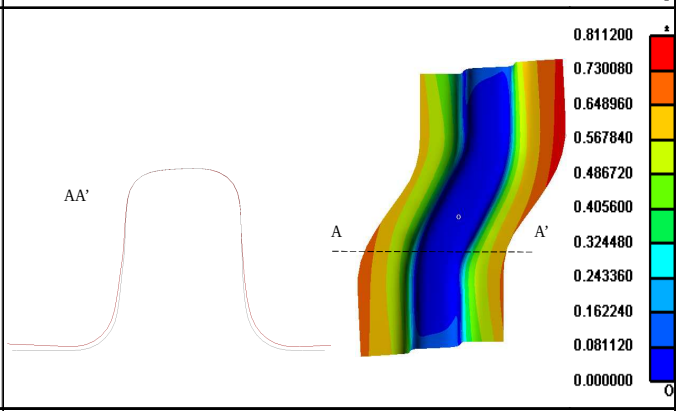
A'_2 μ=0,121 n=0,277	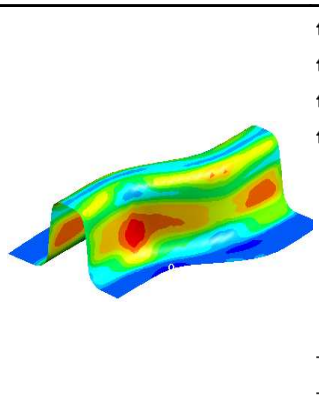	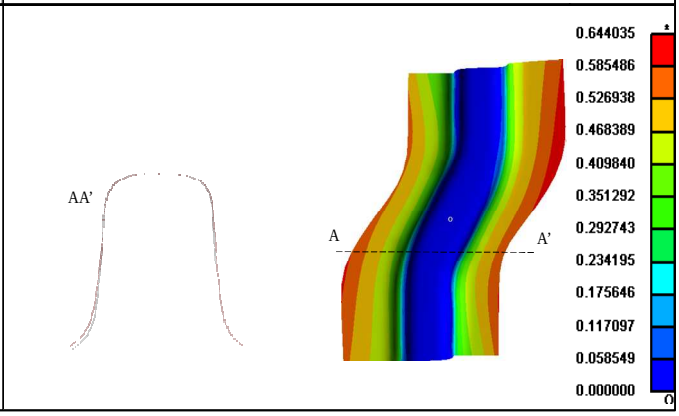

Table 2.8: th and sb maps for points A, A_2 and A'_2.

Of course, the procedure can be iterated for each point of the front (see Figure 2.23 corresponding to the application of the procedure for BHF= 10kN and BHF=80kN).

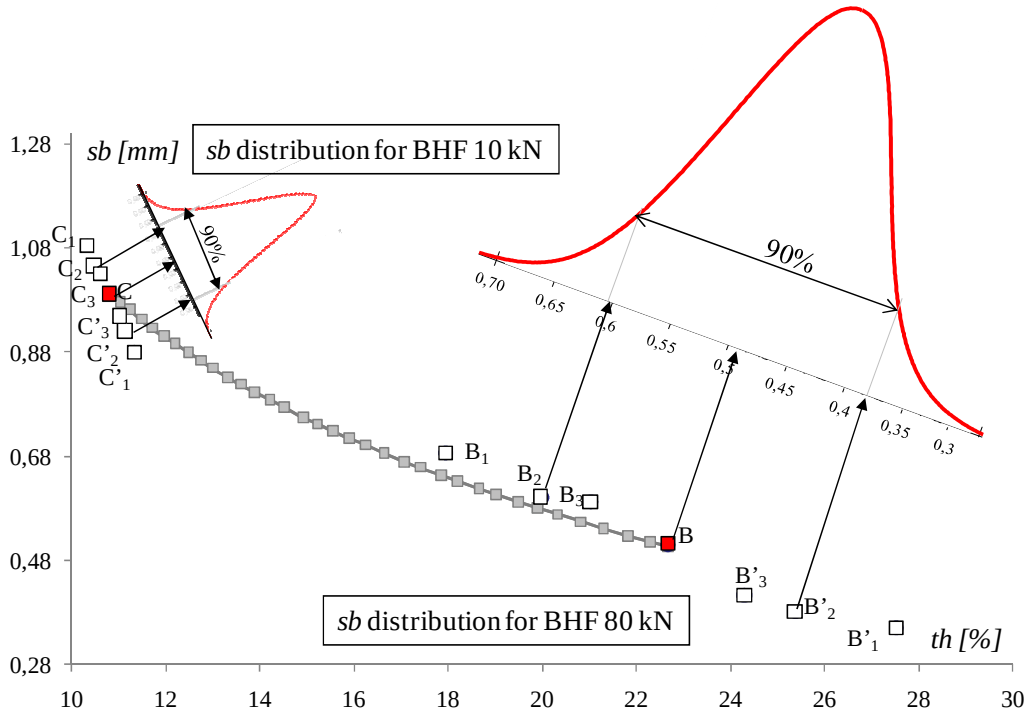

Table 2.23: Application of the workflow procedure for BHF 80kN (point B) and 10kN (point C).

In this study, the 90% of th distribution was considered suitable to analyze the process variability. It means taking into account the 5th and 95th percentiles of the th distribution as boundary points. Iterating the procedure for each of the 35 BHF levels, it is possible to determine the same "lower and upper bounds" (above indicated respectively as $A_2 - A'_2$, $B_2 - B'_2$, $C_2 - C'_2$) for all these levels. Thus, it is possible to build up a sort of variability range. Such range is identified by two different curves (obtained at the varying of BHF levels) which interpolate the lower and upper bounds of the positions assumed by each Pareto front points (Figure 2.24). The variability range is a very powerful tool to visualize th and sb occurrences under the effects of noise factors for all BHF levels.

As it can be observed in Figure 2.24, some numerical simulations were carried out related to different values of BHF, randomizing μ and n within their whole variation interval (test points in the Figure) and the corresponding points are all included within the variability range.

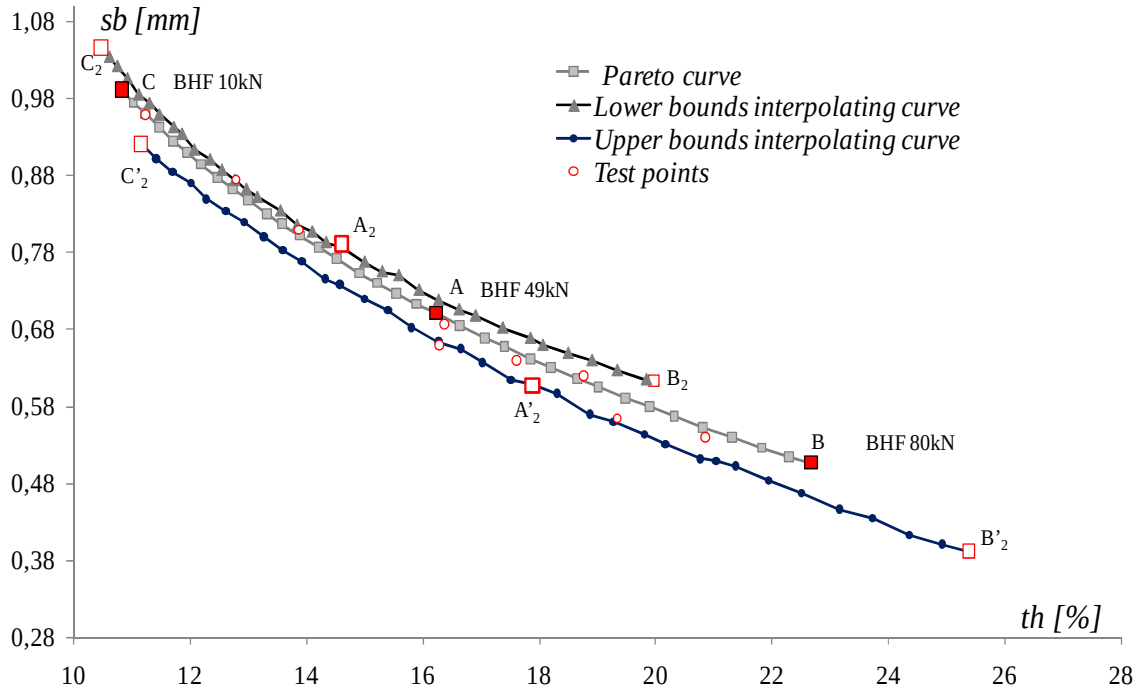

Figure 2.24: Variability range and test points.

Analyzing the variability range, it is possible to notice that at a fixed level of BHF, the influence of μ and n variations on th and sb couples imply a scatter along a known direction: for instance, if the process designer calibrates the blank holder action equal to 80kN, the expected result is the one corresponding to the point B (th= 22.68%; sb= 0.51mm); the effect of μ and n variations may lead for instance to the point B'_2, where th is equal to 25.38% and correspondingly sb 0.39. Such prediction capability is verified in the entire range of operative conditions (BHF domain).

Figure 2.25 shows the directions of scatter for five different Pareto points. Points indicated as D and E in Figure 2.25 correspond to BHF values respectively equal to 25kN and 60kN. As it can be observed, for the five selected Pareto points known directions along which all the possible occurrences lay can be identified. It is evident that the variation range is much wider moving towards higher BHF values, highlighting a loss of robustness due to a more evident effect of the noise factors in the region where the restraining forces act more significantly on the process mechanics. Moreover, standard deviation of objective functions probability distributions is rather higher as the restraining forces rise (in fact, the segment B_2-B'_2 is quite

larger than C_2-C'_2). The variability affecting a Pareto solution may be quite relevant, as it is clear by analyzing again the differences among points A, A_2, and A'_2 (see again Table 2.8). To sum up, the developed hybrid framework is able to predict, for each Pareto solution, the potential direction of scatter and, in particular, the maximum range of variation (segment between the corresponding lower and upper bounds).

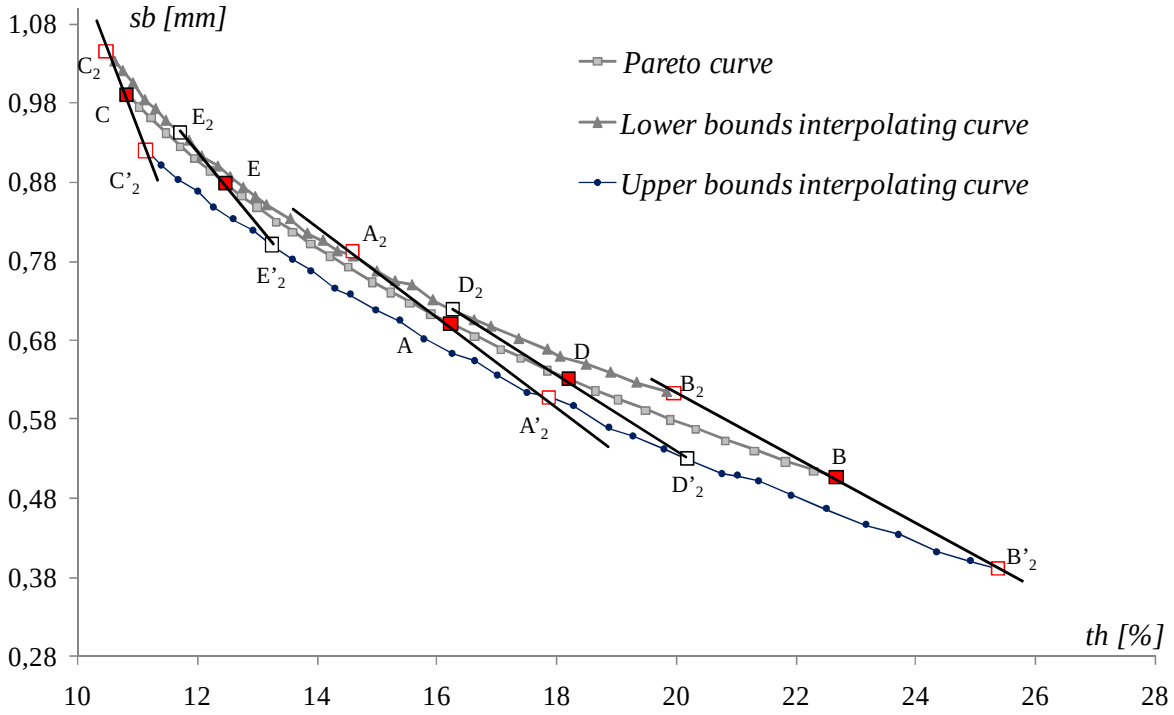

Figure 2.25: Pareto points scatter directions.

A further step of the proposed design approach is related to the possibility to determine the probability level related to each points belonging to the abovementioned direction of scatter. That means that for each potential occurrence it is possible to argue what the probability to have conditions different from the expected ones (expressed as th and sb amount) is.

An example is given in Figure 2.26 where one hundred of the potential occurrences for the point A are reported at the varying of noises. As it can be observed, all the observed points lay on the scatter direction. If the process designer would choose the Pareto solution corresponding to the above mentioned point A (BHF=49kN, th=16% , sb= 0.7mm), he would be aware that the obtained stamped part might differ from the desired one. In particular, the point A may move to A_4 which means that th would be as high as 17.5% (and correspondingly

sb would improve towards the value of 0.63mm). Such occurrence identifies an area under the th probability distribution curve equal to 11% (to the right of the point A_4).

Such consideration might be explained as follows: the expected value of thinning is the one identified by the point A, but there is a probability of 11% that the actual amount of th is worse than the one identified by point A_4 (i.e. over 17.5%). Thus, if the process designer has to manage a tolerance on the maximum thinning up to 17.5%, he would know that such tolerance would be respected with a probability as high as 88%.

Similarly, taking into account the point A_5, it can be noticed that it corresponds to better an amount of th with respect to the point A, but it corresponds to worse conditions as far as sb. The point A_5 relates in fact to a probability of 16% in the sb probability distribution (left side of A_5). In others words, if a designer has a tolerance on the springback too, which cannot exceed the amount of 0.75mm, the tool shows that such threshold might be respected with a probability of 84%.

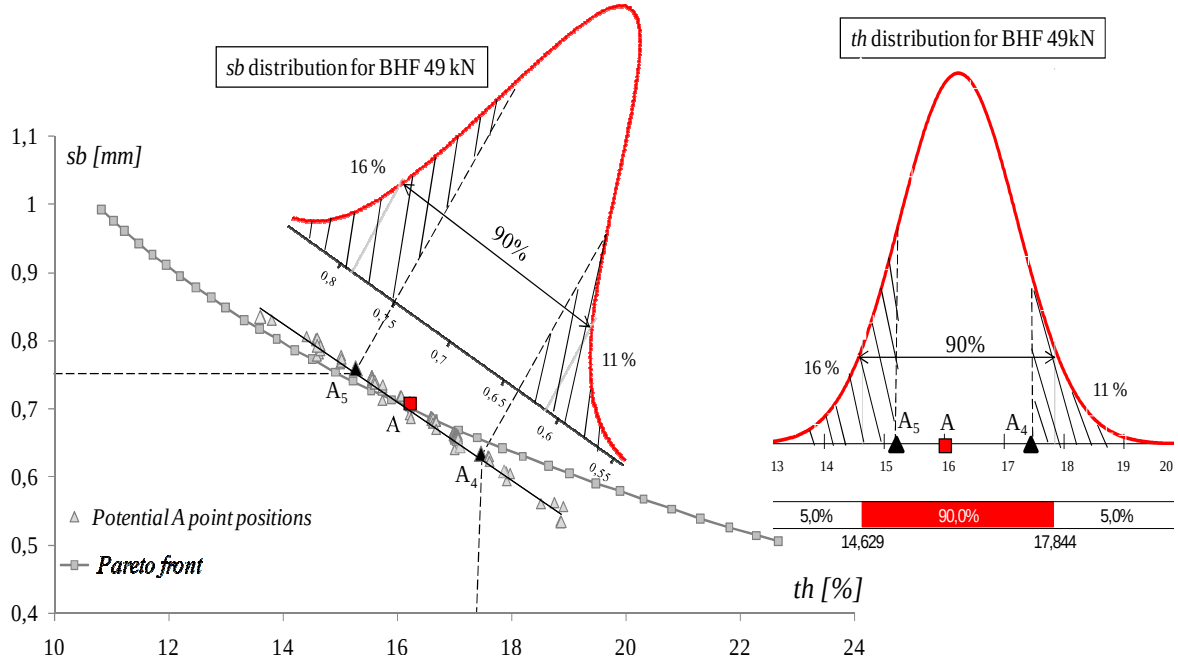

Figure 2.26: Example of application of the hybrid tool.

In this way, the proposed hybrid tool is able to account for the variability effects of the noises onto the final process results, while providing with an accurate overview of all the possible perturbations of the analyzed objective functions.

2.1.2.2.4 Final remarks.

The hybrid approach proposed above described integrates FEM analysis, Response Surface Methodology and Monte Carlo method in order to deal with variability in a sheet stamping process. Control and minimization of springback distortions together with excessive thinning conditions were the main goals of the earlier discussed multiobjective problem.

In fact, as the stretching conditions increase, springback would be reduced, while the thinning tendency would unavoidably rise. Thus, the restraining forces have to be calibrated by tuning the blank holder action, in order to achieve a good balance between springback and thinning minimization. A Pareto approach is then useful in an industrial environment since the availability of a cluster of several compromise solutions results really attractive.

Thus, the variability of some factors was taken into account in order to estimate its influence on springback and thinning in an S-shaped U-channel stamping operation. The BHF was considered as design variable while two noise factors were chosen: lubricating conditions (by the friction coefficient μ) and strain-hardening index (n).

A design methodology able to consider all the most important and innovative issues in sheet metal stamping design was hence developed: an aluminum alloy typical of automotive applications was used; the relevant topic of springback amount was selected as one of the objective functions to be controlled; an integration between multi-objective optimization techniques and robust approaches was presented. The former result was a sort of variability range where the Pareto solutions expressed as couple of th and sb would fall if the perturbations due to noise factors are accounted for.

Moreover, thanks to the proposed hybrid tool, a deeper understanding of the effects of unavoidable noise variables on the investigated stamping process is possible.

In particular, in the investigated case study, the hybrid tool enables to identify the direction along which an expected Pareto solution may scatter because of the variability of the noises.

In other words the design tool has the potential of a Pareto front combined with the possibility to predict the probability related to the failure of given tolerances on the objectives of interest.

Further development of such hybrid approach follows in section 2.1.3.

2.1.3 Case study 2: multiobjective robust design with many noise variables.

A further investigation of the effects of variability on sheet stamping processes was carried out. In fact, the case study described in section 2.1.2 provides indeed with a quite good understanding of the application of the hybrid robust procedure to sheet stamping processes, but still considers a few number of noise effects. Then, a higher number of noise variables was handled in order to test the applicability of such hybrid approach to the same sheet stamping process earlier discussed, but with a more complex variability scenario where five noises are more realistically accounted for. Nor a variability range of the Pareto front, neither a scatter direction of any Pareto solution can be straightforwardly identified anymore, as the variations of many noises all together raises the complexity of further stochastic investigations.

In the following case study, the application of the proposed hybrid approach leads in fact to the representation of the scatter of a generic Pareto solution as a cloud of points, being all induced by the stochastic occurrences of the noises. The hybrid method still enables though to evaluate and to effectively compare solutions by the robustness of the results and the fulfillment of the specifications on the process objectives, being a still effective robust tool for sheet stamping applications. By using the same scheme shown in Figure 2.17 for the hybrid procedure, the details of the case study are described in the following paragraphs.

Step 1: Problem formulation.

The blank holder force (BHF) to be calibrated in a range spacing from 10[kN] to 80[kN] was still chosen as control parameter, constant in time and space again. According to the sensitivity analysis developed in section 1.1 for this process, the main sources of variation that actually produce scatters of the objective functions are listed in Table 2.9: only the material properties variations from coil to coil were considered while the initial blank, lubricating conditions and tool geometric properties were supposed fixed and their stochastic effects neglected.

	C [MPa]	n	r_0	r_{90}	E [GPa]
Mean Value (μ)	422	0.247	0.684	0.684	70
Standard deviation (σ)	27	0.028	0.018	0.044	1.60
5^{th}	377,6	0.200	0.655	0.611	67.37
95^{th}	466.4	0.294	0.713	0.757	72.63

Table 2.9: Mean value (μ), standard deviation (σ), 5^{th} and 95^{th} percentiles of noise variables.

Step 2: Response analysis.

As earlier discussed, both control and noise variables have to be accounted for in the meta-modeling step. A CCD was utilized to investigate both linear and quadratic effects with a proper number of points with respect to screened variables. In particular, 27 numerical simulations were needed for both th and sb objectives. The design space reflects both the probability distribution of the noises, as done before, and the variation domain of the control variable. A stepwise regression was developed within MINITAB environment by using R-Sq(adj) as approximation capability indicator. The prediction capability of the obtained meta-models was also evaluated by comparing the absolute error between the predicted and the simulated data. Table 2.10 summarizes the equations coefficients both for th and sb, R-Sq(adj) values and the mean value of the absolute errors (e). As it can be noticed, R-Sq(adj) is higher than 90% confirming a good data approximation.

th		***sb***	
PREDICTOR	**COEFF**	**PREDICTOR**	**COEFF**
Constant	-161	**Constant**	1.07616
BHF	0.1759	**BHF**	-0.009315
C	0.00123	**C**	0.0001299
n	-0.09	**n**	0.0228
r_0	497.4	**E**	0.0003657
BHF*C	-0.0004722	**BHF*n**	0.001576
BHF*n	0.3803	**BHF* r_{90}**	0.000635
BHF^2	0.0010622	**C*n**	-0.01079
r_0^2	-362.1	**C* r_{90}**	0.00642
r_{90}^2	-0.144	**n*E**	0.0432
		r_{90}*E	-0.03292
		BHF^2	0.00002008
$e_{th[\%]}$	**0.2**	**$e_{sb[mm]}$**	**0.04**
R-Sq(adj)	**98.40%**	**R-Sq(adj)**	**90.90%**

Table 2.10: Equations coefficients and R-Sq(adj) values.

Figure 2.27 shows the response surfaces as functions of BHF and C for th (a) and sb (b). Furthermore, a plot of normalized th and sb values with respect to the above mentioned variables is reported in Figure 2.27 (c) stressing their conflicting behavior again.

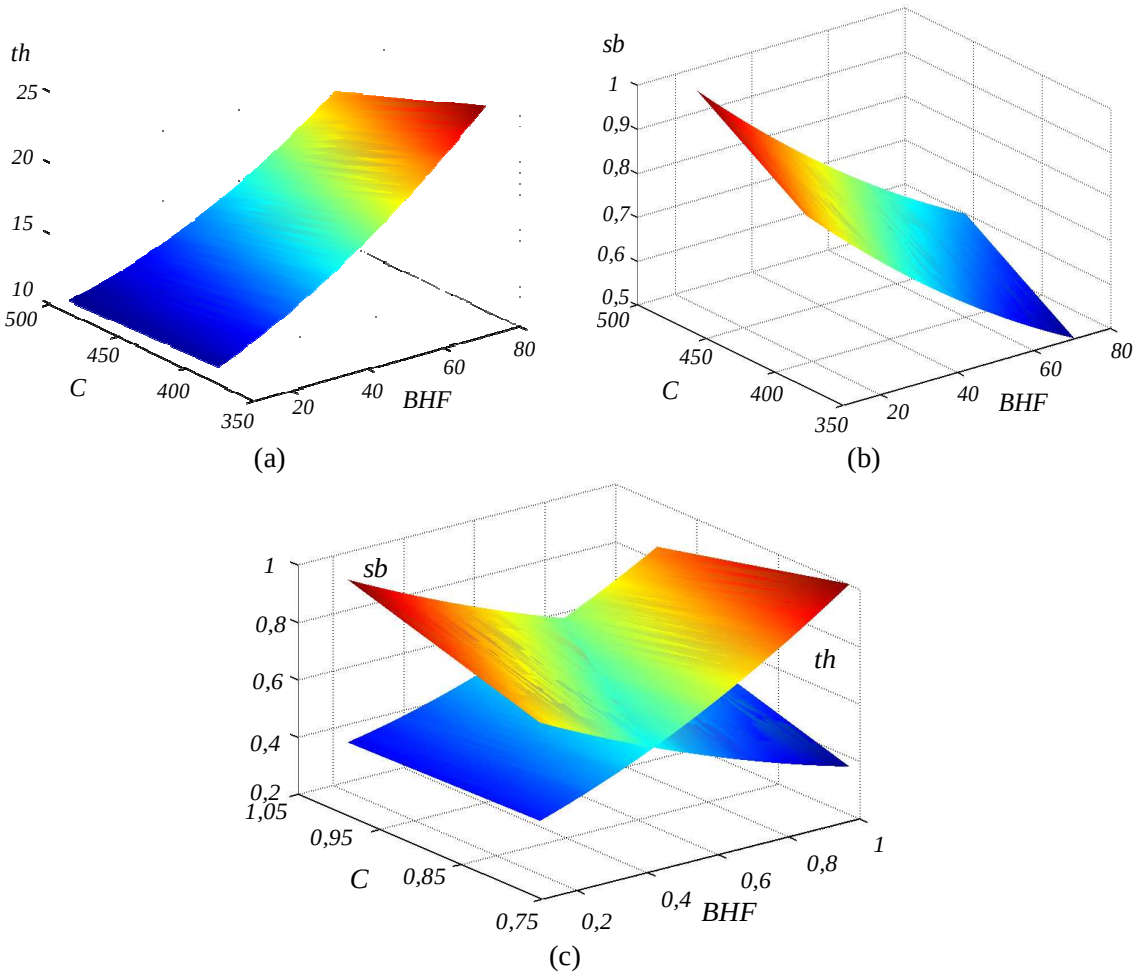

Figure 2.27: Response surfaces as functions of BHF and C, respectively for th (a) and sb (b); surfaces plot of normalized th and sb values (c).

The Pareto solutions were of course searched only on BHF which is the only controllable design parameter in this case study. It has to be noticed that here the BHF domain was investigated with reference to a more restricted range of values with respect to the whole domain width as the investigation was oriented to an operative window more realistic in terms of industrial applicability, thus avoiding extreme process conditions (less reasonable in real applications). Thus, the investigated window varies from BHF=27.5kN to BHF=62.5kN (i.e. ±1 levels of the CCD). Figure 2.28 shows the obtained Pareto front.

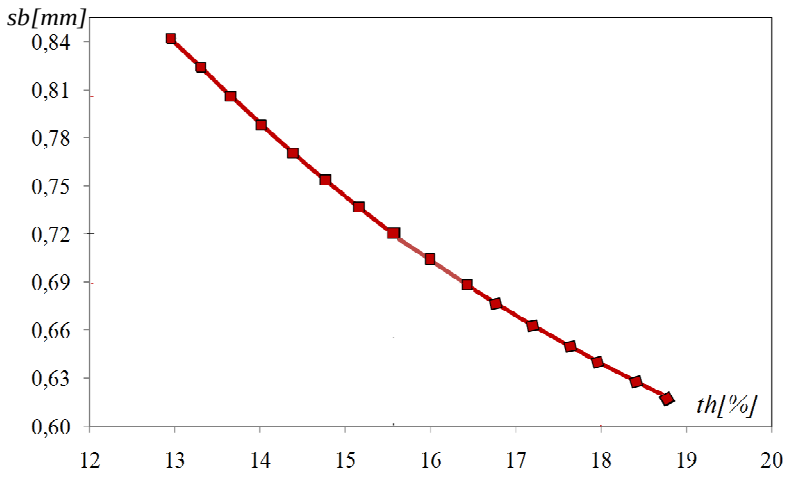

Figure 2.28: Deterministic Pareto front.

Step 3: Variability scenario analysis.

In the case study here analyzed, 1500 random sequences of noise variables were generated from the probability distributions previously defined by using the MCS method. The results of MCS at BHF 45kN expressed as th-sb couples of occurrences at all the generated inputs sequences of noises are plotted in Figure 2.29: a wide scattering of the corresponding Pareto solution can be observed with respect to the deterministic front.

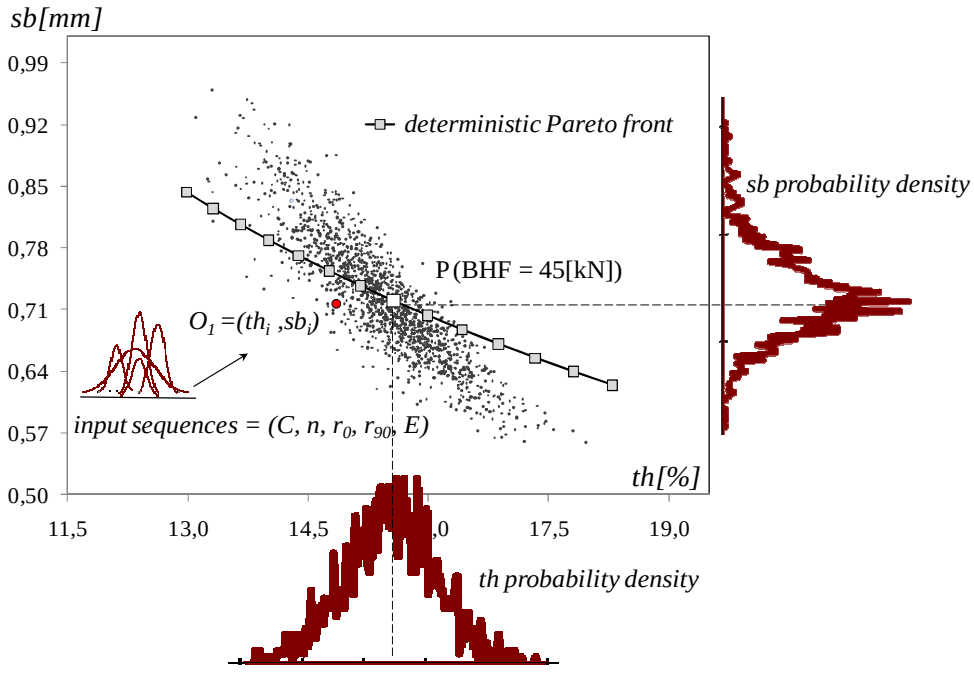

Figure 2.29: Plot of the MCS results at BHF 45kN.

As it turns out clearly from Figure 2.29, the higher number of noises, whose variations is concurrently dealt with, significantly raises the complexity of any stochastic evaluation and makes meaningless the attempt to represent a variability range that combines the occurrences of the two objectives with respect to all the noises. In fact, while in the case study discussed in section 2.1.2, it was possible to straightforwardly identify the couple of noises that univocally produces a given objective occurrence (i.e. 5^{th}), and then to extract exactly the corresponding amount of the second function (i.e. 95^{th}), a wider variability analysis, as here carried out, does not allow it. It means that at a given BHF level there is a number of values of one of the objective function that corresponds to a specific occurrence of the other one.

Nevertheless, robustness evaluations and comparisons, even with respect to any engineering constraint, are still possible by using the proposed hybrid approach.

Table 2.11 shows the th and sb maps for the point P in Figure 2.29. Moreover these maps are compared with the ones obtained for the point O_1 in the same figure. Such point is shown as example of possible stochastic variations of a generic Pareto point, which corresponds to a generic occurrence of th and sb caused by the random generation of the inputs sequences.

	th	*sb*
P	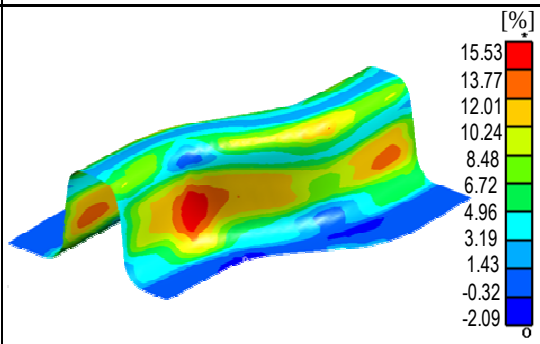	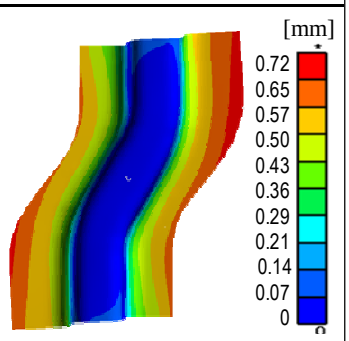
O_1	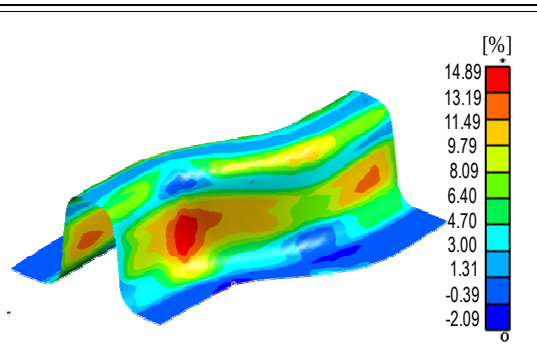	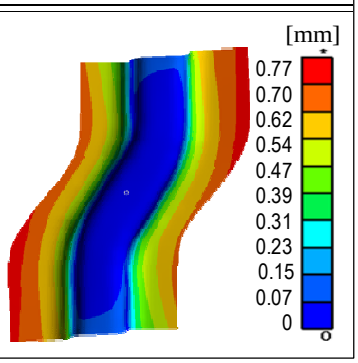

Table 2.11: th and sb maps of the points P and O_1.

The RSM-MCS integration is still low time consuming, also for the design of even larger industrial parts. In fact the run time of one MC simulation was about 1 minute. The time consuming step is instead the metamodeling that determines the total number of direct problems (numerical simulation or experiments). Alternative DoE configurations may be utilized in order to reduce the computational effort without excessive loss of accuracy of the response surfaces.

Step 3: Variability scenario analysis.

The availability of the probability distributions of the investigated objectives turns out to be very useful as it is possible to analyze several variability scenarios of objectives occurrences. Figure 2.30 shows the details of th and sb probability distributions at BHF 45kN (i.e. the point P in Figure 2.29).

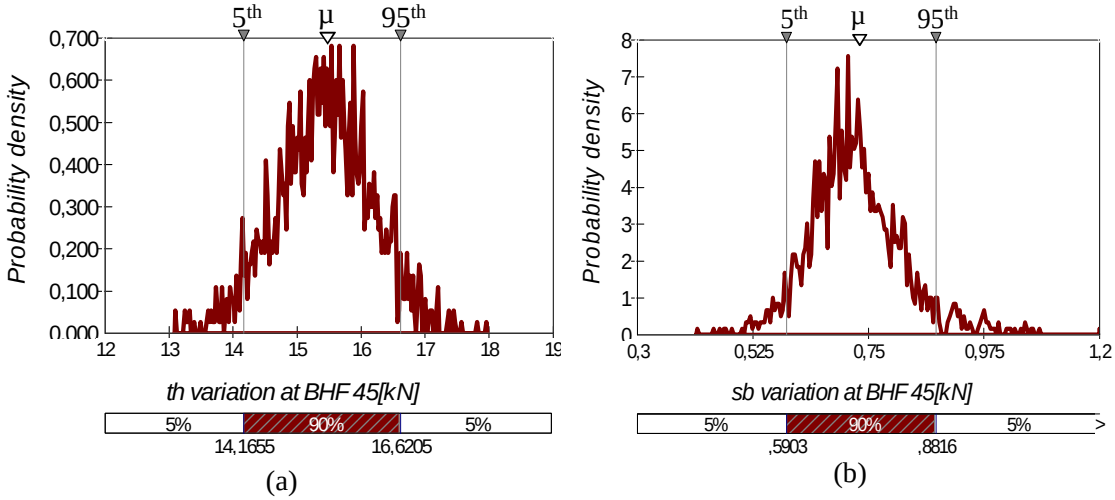

Figure 2.30: th (a) and sb (b) probability density distributions at BHF 45kN (point P).

If the BHF is equal to 45kN, the expected th value from the deterministic Pareto front is 15.5%. Nevertheless, noise factors variations from the 5th to the 95th percentile of their probability distributions may cause variations of th (or sb) which can reach totally different values (th may be as high as 14% or 17% for instance). An example of the variations which may affect springback is illustrated in Figure 2.31, which illustrates the differences between sb at the 5th and 95th percentiles of the sb distribution at a generic section AA' in Figure 2.31 (b).

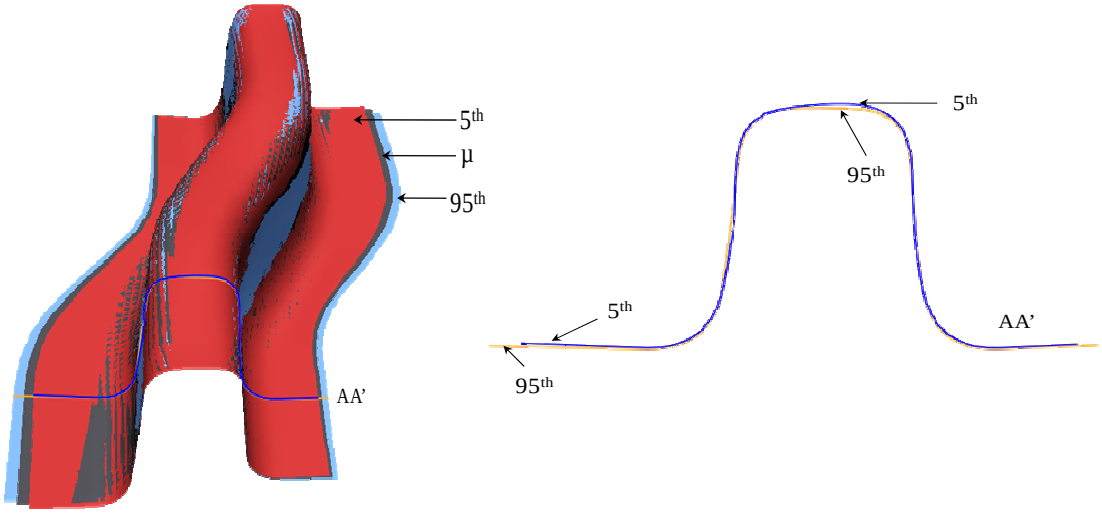

(a) (b)

Figure 2.31: Final shapes after unloading (BHF=45kN) at μ, 5th and 95th percentiles of sb distribution (a) and comparison between the 5th and the 95th percentiles at the section AA' (b).

As it earlier mentioned, there are two main drivers that the designer may use minimizing the effects of the noise: robustness and reliability. Therefore, robustness and reliability indexes able to efficiently describe such design criteria to be accomplished were formulated. It has to be remarked that reliability is evaluated in terms of respect of given boundaries on the objectives. The analytic formulation of computed robustness (I_{RO}) and reliability (I_{RE}) indexes, both to be maximized, are reported in the following equations:

$$I_{RO} = N \Big/ \sqrt{\sum_{i=1}^{N} \sum_{j=1}^{m} (x_{ij} - X_j)^2} \tag{2.19}$$

$$I_{RE} = \sqrt{\sum_{i=1}^{N} w_i * p_i \Big/ N} \; * 100 \tag{2.20}$$

where:

- m is the number of analyzed objectives functions;
- x_{ij} is the current (i) occurrence of the j_{th} objective;
- X_j is the deterministic expected value (on Pareto front) of the objective j;
- N is the total number of MCS runs (i.e. total number of occurrences including the ones of all the objectives)
- w_i is a binary variable that is equal to 1 if both objectives boundaries are respected, 0 otherwise;

- p_i is the probability of occurrence of the particular inputs sequence associated to the i_{th} objective occurrence. Such probability is obtained by the product of each noise variables probability (no variables correlation is assumed).

The higher each index, the better the analyzed solution. In particular, the robustness index (I_{RO}) measures the inverse of the scatter of a Pareto solution due to the variability of the noises, regardless of the associated probabilities (i.e. dispersion of cloud of points around the investigated Pareto solution); the reliability index (I_R) measures the number of occurrences within the boundaries, properly weighted by the probability of happening (i.e. frequency number of success). The proposed formulation can be easily adapted to other optimization problems constrained by lower bounds, upper bounds or tolerance ranges.

Figure 2.32 gives a better understanding of the above mentioned indexes:

- robustness is represented by the dispersion of points around expected point P;
- reliability with respect to two hypothesized boundaries is highlighted by the "points out" in the figure (which, of course, have to be properly weighted by the associated input probability values).

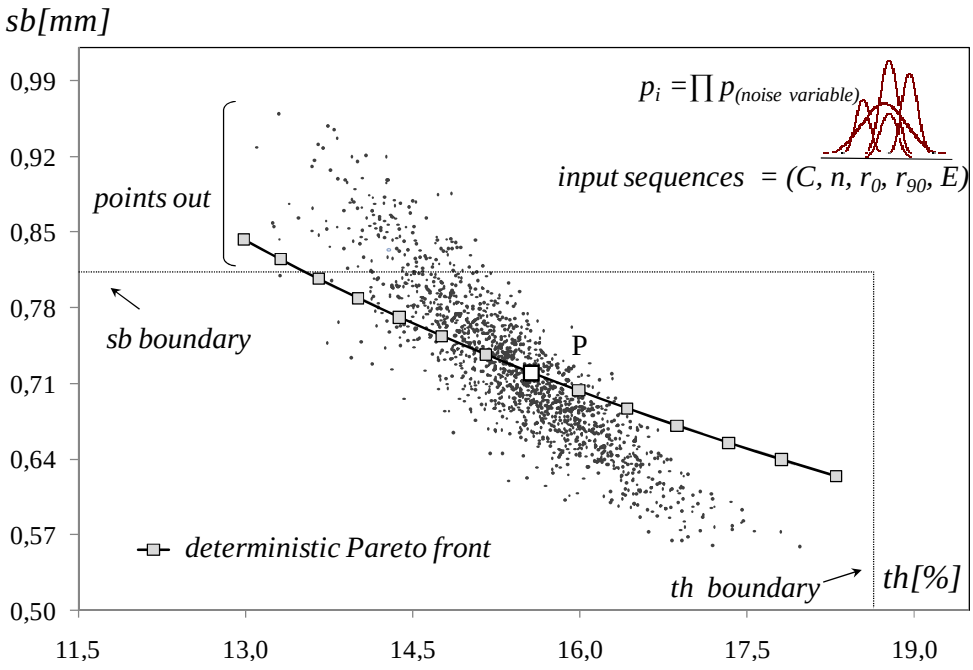

Figure 2.32: Illustration of the robustness and reliability indexes.

Possible scenarios were analyzed in order to stress the potential of the proposed methodology.

In Figure 2.33 three different solutions are highlighted respectively at BHF 35kN (point P_1), 45kN (point P) and 55kN (point P_2). P_1, P and P_2 are surrounded by a cloud of points being all the possible occurrences induced by the variability of the material properties here considered. Such cloud of points is a quick and effective representation of the robustness of the three solutions. Three different scenarios in terms of reliability are outlined as well: in the scenarios respectively indicated by the boundaries B_1 and B_2, the hypothesis is that both th and sb are upper limited; the scenario related to the boundaries B_3 assumes instead that sb is upper limited while tolerance range is given for the maximum thinning.

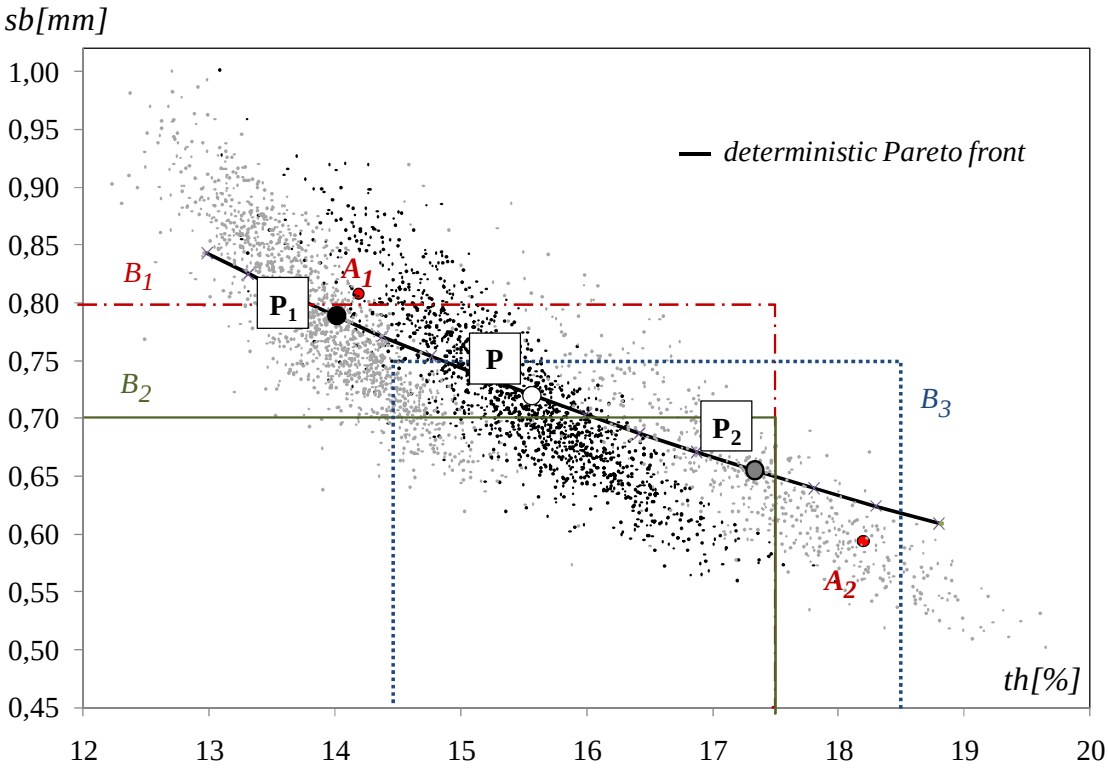

Figure 2.33: Plot of MCS results at BHF 35kN, 45kN and 55kN

The scenario with boundaries B_1 assumes that th has to be lower than 17.5% while sb lower than 0.8mm. Thus, as far as for instance the point P_1, stochastic effects may cause that the real occurrence becomes the point A_1: this means that such setting of the control variable is not reliable since it would fail B_1.

The defined indexes effectively evaluate the robustness and reliability associated to the analyzed solutions and scenarios. Table 2.12 reports the robustness (I_{RO}) and the reliability

(I_{RE}) indexes for the analyzed Pareto solutions in all the three variability scenarios.

Pareto solution	BHF [kN]	X_h [%]	X_{sb} [mm]	I_{RO}	I_{RE} under B_1	I_{RE} under B_2	I_{RE} under B_3
P_1	35	13.8	0.79	2.11	1.59 %	0.16%	0.30%
P	45	15.4	0.72	1.65	2.83%	1.10%	2.13%
P_2	55	17.2	0.66	0.02	1.10%	0.72%	3.02%

Table 2.12: Robustness (I_{RO}) and reliability (I_{RE}) indexes for the analyzed Pareto solutions under different boundaries.

It is worth pointing out that the value of the reliability indexes for each given point/scenario has to be read not only in consideration of the number of occurrences failing the boundaries but also of the assessment of the probability of failure.

From the above results, the most robust solution is P_1, which corresponds to a BHF level of 35kN. Actually, such conclusion agrees with the results in section 2.1.2.2.3; in fact, as the blank holder action BHF increases, a lower robustness is observed which is surely due to the more significant effects of the noise variables at higher levels of restraining forces.

As reliability is analyzed, the most reliable solution would respect the boundaries that were fixed for the investigated scenarios.

Obviously, upper and lower limits directly influence the probability of failure. Moreover, the comparison between the points A_1 and A_2, which are respectively stochastic occurrences of the points P_1 and P_2, helps to introduce a central consideration: in the scenario B_3 occurrence A_1 is out of the boundaries (i.e. it is a not reliable occurrence), while the occurrence A_2 respects the boundaries (i.e. it is a reliable occurrence).

On the other hand, A_1 is indeed more robust than A_2. This comparison is used to give an example of how robustness and reliability do not necessary address towards the choice of the same solution. Table 2.13 reports the th and sb maps of the points A_1 and A_2.

The indexes here formulated would result even more helpful if many objectives functions have to be optimized or many control parameters are accounted for.

In fact, in such cases more complex shapes of the Pareto front might be obtained and synthetic measures enabling quick and effective comparisons of alternative Pareto solutions are definitely even more worth using.

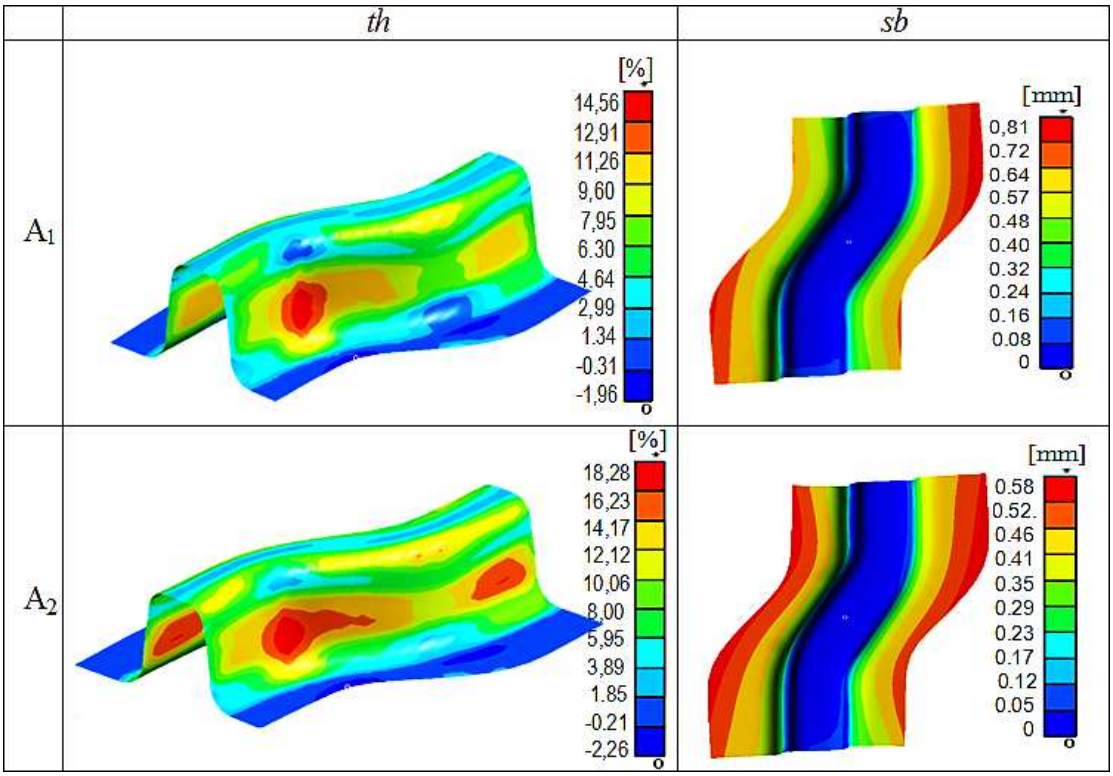

Table 2.13: Maps of *th* and *sb* for points A_1 and A_2.

2.1.4 Summary and conclusions.

The difficulties of a good process design because of the inherent process variability raises the need of robust tools able to address the process designer towards more aware choices. In fact, even if the effects of the stochastic noises influencing the process cannot be controlled directly, it is still possible minimizing such influence by a proper calibration of the process control parameters. It means that robust operative windows have to be identified in order to reduce any variation of the investigated objective functions.

In particular, a hybrid tool efficiently integrating meta-modeling technique and Monte Carlo Simulations was formulated for a multi-objective optimization problem. As applied to a pretty simple case study (in section 2.1.2), such hybrid approach enabled the identification of a sort of variability range along with a direction of scatter for the objective functions, providing the process designer with a very effective tool addressing a more aware settings of the process control parameters. In the industrial environment, quite complex problems with a higher number of noises have to be solved and boundaries on the given objectives are often to be

respected. Therefore, the process designer should be also able to handle more noise variations at the same time and to quantify the risk to overcome such boundaries. The developed hybrid procedure was then applied to a further case study in relation to a wider range of noise variation. In particular, even though a straightforward identification of a variability range is not possible anymore, the applied hybrid approach still proved to be able to analyze a more complex range of problems where the noises variations influence the expected objectives values for given control calibration and, on the basis of such investigation, to compare several design Pareto alternatives. Robustness and reliability indexes formulations were thus provided, in order to identify the most robust settings of the control variables or, on the other hand, the most reliable ones.

In the end, the hybrid methodology here described highlights the weaknesses of a process design only based on deterministic considerations, emphasizing also the necessity of robust design approaches. The discussed hybrid tool provides then the possibility to overcome the limits of a traditional design approach, allowing an indirect control of the undesired effects of variability, making explicit at the same time the stochastic effect of the noises.

2.2 Stochastic approaches.

Beside hybrid approaches, other approaches that can be more strictly referred to as stochastic have been also applied for sheet stamping applications. In fact within such approaches, the stochastic variation of the noises is considered from the beginning of the optimization procedure so that all the following steps account for the inherent process variability. The probabilistic investigation is performed through the all process optimization, not just on possible solutions, whose robustness is eventually to evaluate.

Several stochastic techniques have been proposed in the technical literature. Here are some examples of stochastic approaches for robust optimization of sheet stamping processes.

Some authors have used the Dual Response Surface Methodology (DRSM): within such approach both mean and standard deviation are separately metamodeled for each objective by fixing the control variables and varying at the same time all the noises in a proper DoE. Then, for each objective the problem is formulated as minimization of a global function combining both the mean behavior and the standard deviation.

Yeniay et al. (2006) utilized a DRSM based approach to quantify variability in weight and sizing analysis for an automotive application. Shaibu and Cho (2009) analytically studied the prediction capability of such approach depending on the polynomial order

Moreover, Sun et al. (2009) proposed using of DRSM as robust design tool for multiobjective problems. They minimized fracture and wrinkling in the stamping of an automotive inner panel controlling drawbead design under the stochastic effects of material properties and lubricant variations. A variation of the DRSM by using a genetic algorithm with arithmetic crossover, in contrast to the one-solution-at-a-time approach of most optimization algorithms, was applied by Onur et al. (2008). Li et al. (2006) applied DRSM to eliminate the effects of uncertainties in design of deep drawing of a square cup used as benchmark at the NUMISHEET'93 to minimize the thickness variation, subject to the condition of no wrinkle and no rupture. They identified the tool geometry and the blank holding force as control variables, while material properties as noises. Sun et al. (2009) proposed a multiobjective robust optimization method for drawbead design in sheet metal forming by using DRSM and the particle swarm optimization (PSO) method. PSO is then an adaptive algorithm based on a social psychological metaphor: a population of individuals (referred to as particles) adapts by returning stochastically toward previously successful regions. According to PSO theory, two main parameters are defined for each solution, called position and velocity, whose computations converge to a fitness function as in Genetic Algorithm, but unlike GA, the PSO has no evolution operators such as crossover and mutation. Then, the potential solutions move through the problem space by following the current optimized particles.

Besides DRSM, other stochastic methods have been applied. Kleiber et al. (2002) and Rojek et al. (2004) proposed an Adaptive Monte Carlo Method (AMC) for a deep drawing of an aluminum square cup with six noises related to material and process variations. In the crude MC approach the sample of the variables is typically generated from the joint probability density function, afterwards the probability to fail a given criterion is computed. The AMC method consists of seeking out the design point during sampling by 'moving' the sampling density based on the information from the previous samples. They used the distance from the Forming Limit Diagram (FLD) as criterion of failure as leading to the necking type failure with high or low probability. To improve the computational efficiency of such reliability

analysis they carried out what they called FORM approach, employing the concept of response surface. In (Li B. et al (2006)) a multi-objective optimization based on the Taguchi method is proposed of a tube hydroforming process. According to Taguchi's theory, an outer array of the noises, run at each level of an inner array of the control variables, should simulate the random environment in which the process would function. A signal-to-noise (S/N) ratio, defined by the mean square deviation for the process results, is used to measure the quality deviating from the nominal value. The S/N ratio becomes therefore a straightforward objective function to be minimized incorporating the effect of noises.

It has to be mentioned a wide family of approaches using kriging as robust design tool for a wide range of applications besides sheet stamping processes. Already used in optimization problems, Kriging have emerged in uncertainty propagation (Romero et al. (2004)) and reliability (Bichon et al. (2008), Kaymaz (2005)), studies, as also featured by a local index of uncertainty on the prediction. Lee et al. (2005) proposed a global robust optimization approach using Kriging models with a simulated annealing algorithm. A robust optimization method based on a Kriging model is proposed by Lee (2010) to define the probability of the design success. Echard et al. (2011) also proposed an active learning iterative approach based on Monte Carlo Simulation and Kriging method, as its stochastic nature enables to define a learning function to select among the MC points the best next point to evaluate.

In the following section, an application of the DRSM is described for a sheet stamping process. Afterwards, a comparison between the hybrid approach in section 2.2.1 and a stochastic framework based on the DRSM is discussed.

2.2.1 Case study 1: stochastic framework based on the Dual Response Surface Methodology (DRS).

2.2.1.1 Problem formulation.

The investigated process is the same S-shaped deep drawing operation described in the section 1.1.1. Similarly, the friction coefficient μ and the strain hardening exponent were used as noise variables (see Table 2.5). Any correlation between the noise variables was neglected, beside any statistic covariance as well. Maximum thinning and springback are still the objective function to minimize. The blank holder action is also calibrated from 10kN to 80kN.

2.2.1.2 Discussion of the methodology.

The present approach integrates the Dual Response Surface (DRS) methodology with a Multi-Objective Optimization (MOO) approach in order to obtain a Pareto front which includes the noises stochastic effects on the investigated objectives. In fact, while the hybrid approach initially carries out a deterministic optimization followed by a stochastic investigation, the present approach takes into account the influence of variability from the beginning, searching for non-dominated solutions taking into account such undesired effect. A different perspective has to be used: instead of analyzing the effect of variability on the computed Pareto front, a calibration of the process design tool under the stochastic perturbations of noises variables (i.e. incorporating stochastic effects) is carried out. A sketch of the DRS based approach is shown in Figure 2.34.

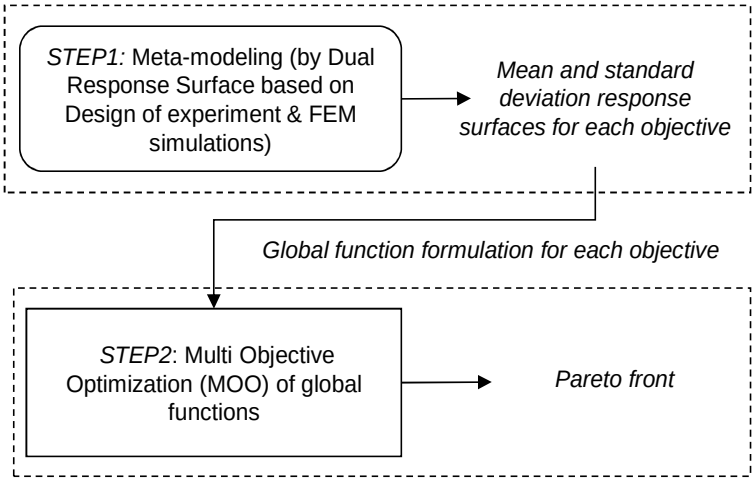

Figure 2.34: DRS approach.

Step 1: Metamodeling.

The effect of the noise variables is taken into account since the beginning, which implies that the calibration of the process parameters is carried out accounting for the variability of the noises. Within this approach, the Dual Response Surface methodology (DRSM) is applied.
While the traditional meta-models generally account just for the mean responses of a function f(x) in dependence on the input variables, while standard deviation is assumed to be small and constant. But, if noises effects have to be studied, a metamodel built from the mean values may not be effective and optimization results can be misleading without further stochastic

considerations. On the contrary, the DRSM (Sun et al. (2009)) models a response surface of both the mean (μ) and standard deviation (σ) for each objective by fixing the control variables ($X=[x_1, x_{2,..,} x_n]$) and varying at the same time all the noises (z_j): the objective responses result from the average effect of the noises, properly modeled by the standard deviation they produce. This implies that the analytic dependence on the noise variables is not explicit but nevertheless considered in the responses computation.

A global function is formulated as the weighted sum of mean and standard deviation. In particular, weighting leads the optimization problem to the minimization either of the mean or the standard deviation. This may be a multi-objective problem itself, as long as mean and standard deviation may have a different trend for the same objective function. Then, generally, a global function is formulated for each objective. One possible expression is taken from (Sun et al. (2009)) as follows:

$$F(\mathbf{X}) = \lambda * f(\mathbf{X})^2_{\mu} + (1-\lambda) * f(\mathbf{X})^2_{\sigma} \quad (2.21)$$

where λ is a weight varying in [0;1] to emphasize either the mean or the standard deviation. Each F(X) becomes a new objective function to be minimized. Accounting for all the objectives at the same times, the optimization problem will be traditionally formulated as there are two conventional objective functions. Similarly, the problem might be formulated as minimization of the mean behavior constrained by the standard deviation, traditionally used as robustness indicator, instead of formulating a global function.

In these terms, DRSM based approaches are considered stochastic methods as incorporating the effect of the noises variation. To model each objective as function of the control setting under the effect of the noises, a proper DoE able to reproduce the effects of noises variations on the selected objectives has to be chosen. Therefore response surfaces of th% and sb were metamodeled for the investigated case study, when μ and n stochastically vary. Namely, a cross product array based on the previously mentioned variables domain was utilized as DoE (Sun et al. (2009)): for each level of the control parameter (outer array) a further plan (inner array) designed on the noise variables (μ and n) has to be developed. In this way, each point (BHF level) results properly replicated enabling to estimate the mean and standard deviation values for given control parameter condition. The arrangement of the developed cross product

array is shown in Table 2.14.

			inner array				
			0.100	0.110	0.126	**μ**	
	Points	**BHF**	0.300	0.187	0.257	**n**	
	1	10	y_{11}	y_{12}	y_{13}	*mean (1)*	*stand. deviation (1)*
	2	27.5					
outer array	3	45	⋮	⋮	⋮	⋮	⋮
	4	62.5					
	5	80	y_{51}	y_{52}	y_{53}	*mean (5)*	*stand. deviation (5)*

Table 2.14: Cross product array.

The inner array follows the Latin Hypercube Design (LHD). In particular, a cascade optimization criterion formerly based on the maximin optimization criterion followed by the correlation one was developed in a MATLAB environment. The developed algorithm iteratively performs a LHD according to maximin criterion, in order to guarantee a suitable space filling, subsequently evaluated in terms of orthogonality. The more effective compromise plan in terms of both criteria is chosen. A sensitivity analysis aimed to identify a suitable number of iterations was also carried out. It has to be observed that different LHD configurations were compared with the utilized one according to the will to explore a representative range of simultaneous effects of the noise variables. Figure 2.35 reports the evaluated LHD configurations, while Table 2.15 shows a couple of maps of thinning and springback for two points belonging to the DoE.

Also in this case, a step wise approximation model was utilized and the regression coefficients were calculated based on least square error minimization method, obtaining R-Sq (adj) values always higher than 98%. The equations obtained respectively for means and standard deviations are reported for th% and sb in the following.

$$f_{th\%,\,mean} = 6.68 + 0.45*BHF - 0.01*BHF^2 + 0.000093*BHF^3 \quad (2.22)$$

$$f_{th\%,\,stand\,dev} = -0.5745 + 0.1106*BHF - 0.00325*BHF^2 + 0.000033*BHF^3 \quad (2.23)$$

$$f_{sb,\,mean} = 1.08 - 0.01*BHF - 0.000025*BHF^2 \quad (2.24)$$

$$f_{sb,\,stand\,dev} = 0.07 + 0.0012*BHF - 0.00004*BHF^2 + 0.00000046*BHF^3 \quad (2.25)$$

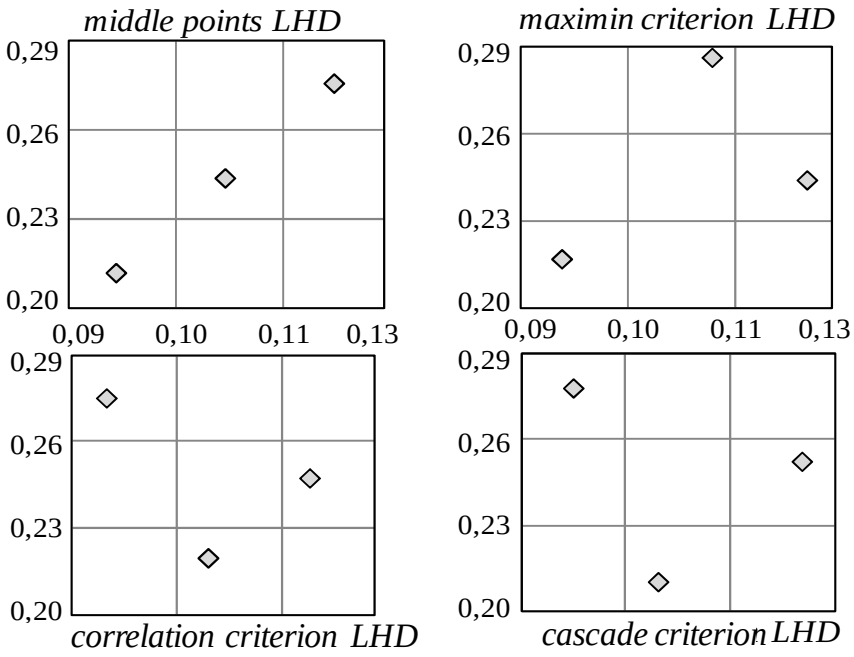

Figure 2.35: Comparison among several LHD configurations.

Point	
$P_{5,1}$ BHF=80kN μ=0.1 n=0.3	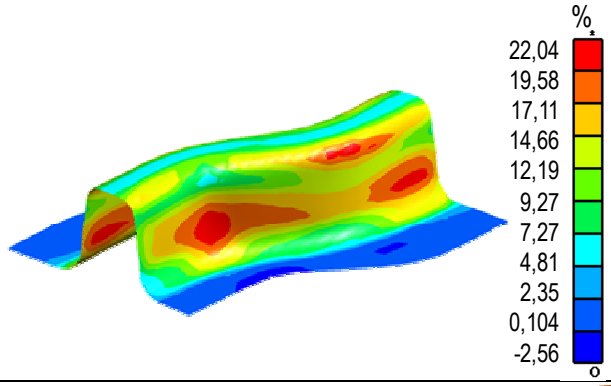
$P_{1,2}$ BHF=10kN μ=0.11 n=0.187	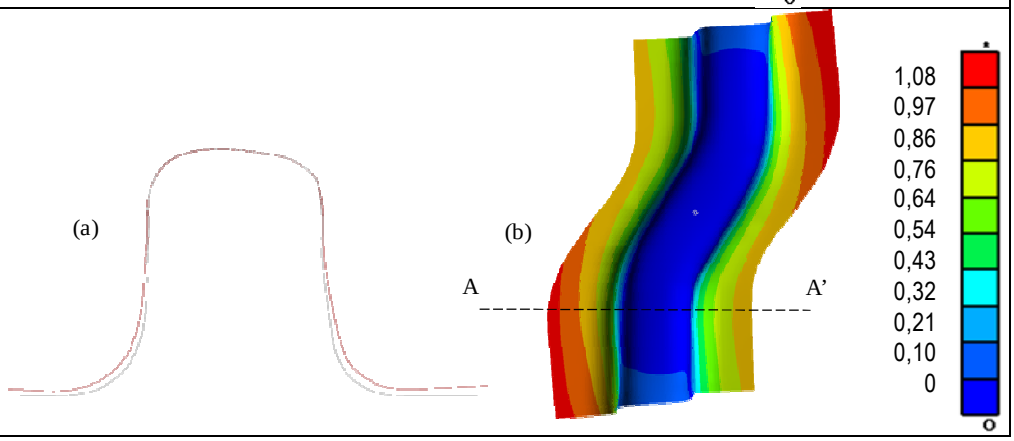

Table 2.15: Maps of thinning and springback for two points of the DoE.

As it can be observed in Figure 2.36 below, the plots of mean values respectively for th% and sb are deeply conflicting. In fact, according to the previous approach results, at increasing of BHF th% mean increases while sb mean decreases.

On the contrary, both standard deviations grow at higher restraining force levels, confirming that a more significant influence of the noise variables is observed if more severe stretching conditions are considered. Such results agree with previous investigations on the effects of material properties variability on both th% and sb. As well lubricating conditions represented by μ are surely more influent at heavier stretching conditions.

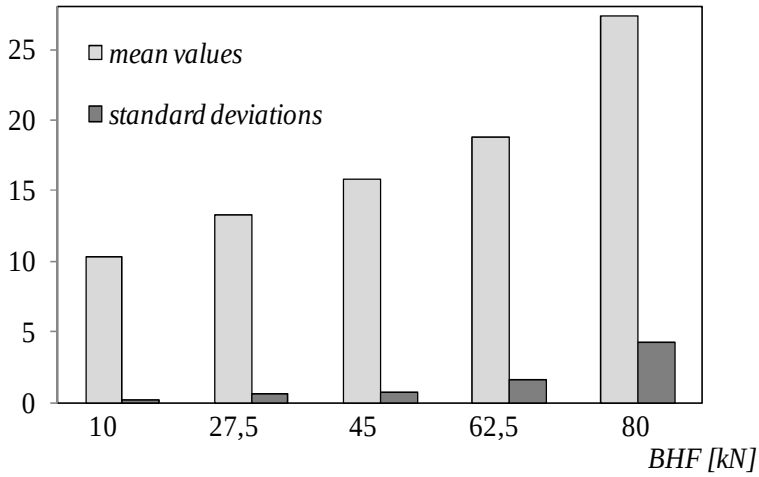

(a)

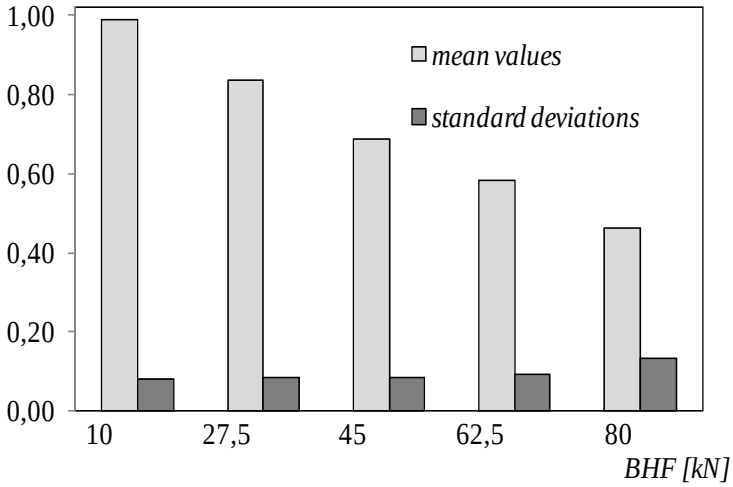

(b)

Figure 2.36: Means and standard deviations histograms respectively for th% (a) and sb (b).

Using DRSM as robust design tool for a generic problem implies the minimization of the standard deviation function subjected to the mean as constraint. In fact, the standard deviation is often used to measure objectives variability in order to evaluate robustness. By the way, the plot of mean values versus standard deviations for th% and sb may be useful. As it can be observed in Figure 2.37, the minimum both for mean and standard deviation is not the same if th% or sb mm function is considered. Therefore, a multiobjective formulation is needed.

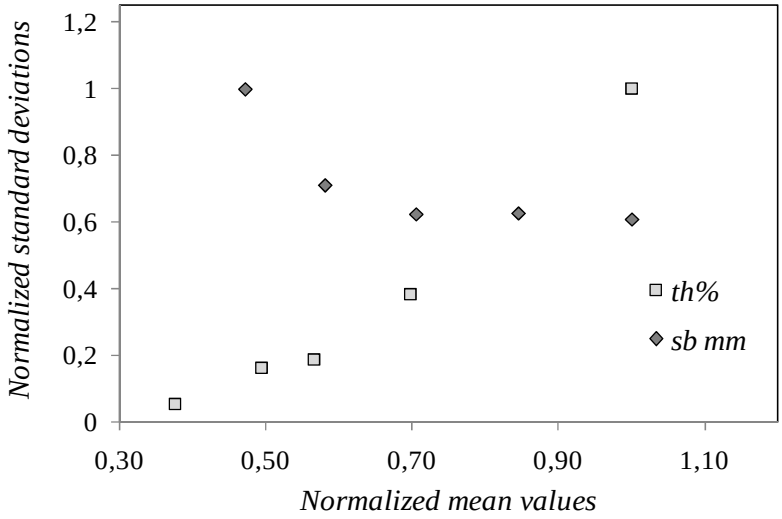

Figure 2.37: Plot of normalized mean values versus standard deviations for th% and sb functions.

According to Sun et al. (2009), the global formulation expressed by equation (2.21) was used for each selected objective. Thus, each F(X) becomes the new objective function to be minimized. Figure 2.38 shows $F_{th\%}$ and F_{sb} behaviors at the varying of λ.

Step 2: Multi-objective optimization.

The Pareto front was determined under the stochastic effect of the noises: instead of analyzing the variability effect on the Pareto front, the process setting is figured out facing the stochastic perturbations of the noises. Then, the multi-objective problem was formulated as:

Minimize $F(X)_{wr} = \lambda * f^2_{wr,\mu} + (1-\lambda) * f^2_{wr,\sigma}$

Subjected to $F(X)_{th} = \lambda * f^2_{th,\mu} + (1-\lambda) * f^2_{th,\sigma}$ *with* $X_{lower\ bound} \leq X \leq X_{upper\ bound}$

Using DRS as robust design tool for a generic problem implies the minimization of the standard deviation function subjected to the mean as constraint.

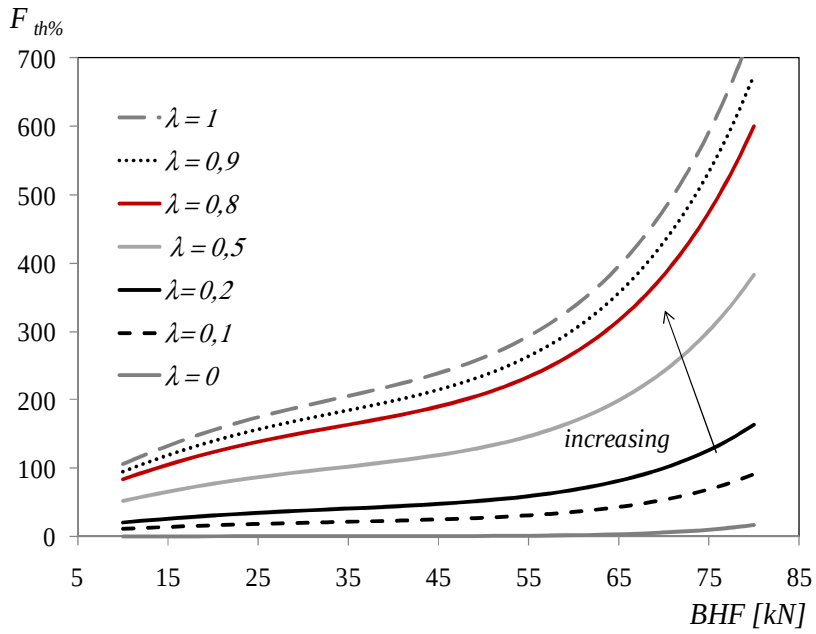

(a)

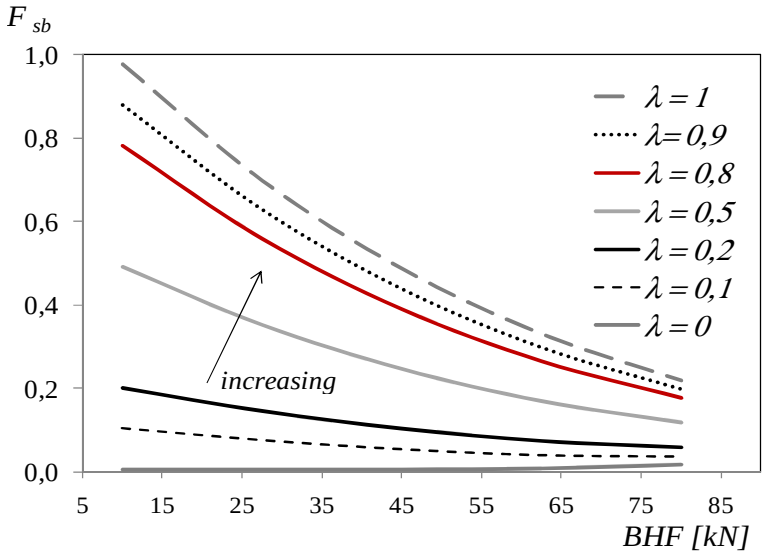

(b)

Figure 2.38: $F_{th\%}$ (a) and F_{sb} (b) behaviors at the varying of λ.

Then, the Pareto front is obtained by a MOO: as a consequence, the prediction capability of the model results from a compensation effect of the noises influence. The ε-constraint optimization method was utilized in a MATLAB environment for the investigated case study: the global function for th% was considered the primary objective, while springback was

utilized as constraint. It is possible to verify that the same Pareto solutions would be reached if the two functions are exchanged. Moreover, a sensitivity analysis at the varying of λ was developed in order to evaluate how the Pareto front changes if mean and standard deviation are differently weighted. Figure 2.39 shows the Pareto fronts obtained for several λ values ($F_{th\%}$ and F_{sb} are of course normalized).

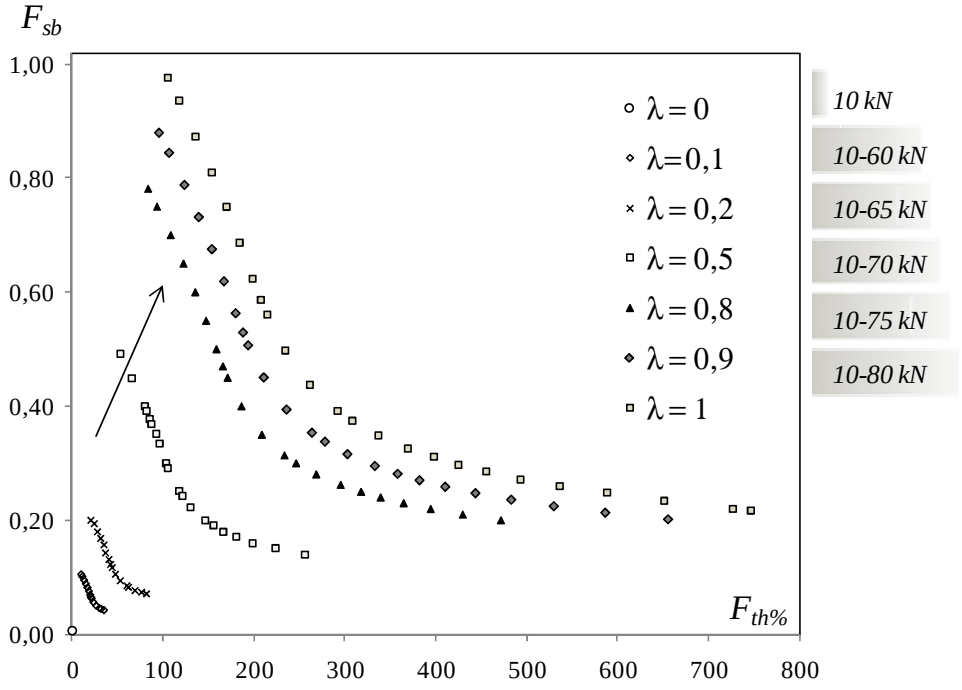

Figure 2.39: Pareto fronts at the varying of λ.

2.2.1.3 Discussion of the results.

The use of DRSM as a robust optimization tool allows a direct determination of the Pareto solutions for the investigated process taking into account since the early optimization steps the inherent process variability: both mean and standard deviation have to be contemporarily minimized. Therefore, the most robust choice in terms of variability effect reduction typically does not correspond to the most effective solution in terms of stamping performances optimization. Thus, a different weight could be assigned complementarily to mean and standard deviation functions (by weight λ). As it can be observed in Figure 2.36, despite of the conflicting behavior of the th% and sb functions, their standard deviations trends anyway agree at the varying of the BHF levels. In fact, at higher restraining force levels the noise

effects of μ and n were more evident both on th% and sb perturbations. In other words, the conflicting behavior of the two objectives results mitigated from the process robustness optimization point of view. By the way, as it can be noticed in Figure 2.39, the λ decreasing (i.e. higher weight to standard deviation) implies that the Pareto front moves towards lower values of both $F_{th\%}$ and F_{sb} for the investigated case study. This means that if standard deviation is emphasized (decreasing λ), an improvement of the Pareto optimality of the new front results. As a matter of fact it implies for λ=0 that the optimum exists and corresponds to 10kN. Moreover, another interesting consideration may be derived from Figure 2.40: as it can be observed, as λ decreases (which mean that standard deviation has a growing role) the number of Pareto solutions decreases if the mean value of the objective functions is considered. In other words, the designer has to choose among a smaller number of optimal solutions. Therefore, the range of operative conditions to be used in order to optimize the investigated process depends on λ choice.

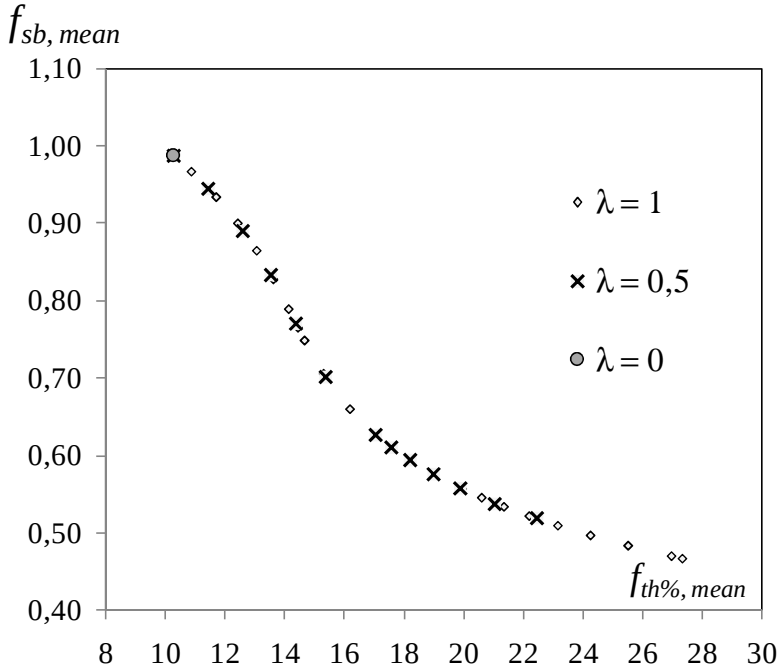

Figure 2.40: Pareto fronts for mean values at λ decreasing.

2.2.1.4 Final remarks.

The DRSM allows directly determining robust Pareto solutions properly weighting process

robustness optimization with respect to performances optimization. In fact, the effect induced by the noises on the process results are implicitly included in the metamodeling step and so accounted for. No further investigation is required but a straightforward computation of the Pareto solutions is possible once the two global objective functions were formulated.

Depending on how crucial limiting the effect of noises is for the process designer, such tool provides the possibility to weigh differently mean and standard deviation, better accomplishing any needs but introducing at the same time a level of arbitrariness into the process design. According to that, a different set of Pareto solutions is in fact obtained.

Therefore, even though such stochastic method might be labeled as quite flexible, choices that will influence all the downstream steps have to be made at the beginning of the optimization procedure. Moreover, despite being a straightforward tool as the assessment of the Pareto solutions is concerned, an actual robustness evaluation is not explicit neither the effects of the noises possible to separately focus.

2.3 Comparison between the two approaches.

Hybrid approach and stochastic strategy for the robust optimization of sheet stamping processes have been discussed so far, also providing with case studies and examples of application of the abovementioned design tool.

In order to better understand the differences between those two approaches and to figure out which one might be more appropriate to use for sheet forming applications, a comparison of the hybrid and the stochastic approaches follows in section 2.3.1.

The first case study just discusses the comparison of the results between the application in section 2.1.2 (i.e. the S-shaped deep drawing processes with one control and two noise variables) and the DRSM applied in the previous section 2.2.1 to the same stamping operation. Afterwards a further investigation is discussed for an IFU Hishida part, where wrinkling and excessive thinning are instead analyzed.

2.3.1 Case study 1.

To sum up, the analyzed stochastic approaches belong to two different categories of robust design tool:

- the former, i.e. the hybrid deterministic-stochastic one, optimizes the process early

neglecting the noises variations and then probabilistically analyzing the perturbations that such variations induce onto the Pareto solutions.

The noise variables effects on both objectives functions can be highlighted and the probability of occurrence of any variability scenarios is studied by MCS. A variability range can be depicted in some cases with a few noises, showing the potential scattering that both objectives functions undergo for fixed operative conditions.

However, even for wider problems, the tool allows the process designer to be aware about the risk of process failure, guiding towards more robust choices;

- the latter, i.e. the DRSM based tool, allows direct identification of the Pareto solutions already accounting for the effect of variability, since the early steps of the optimization. It is a standalone design tool that provides the process designer with a range of solutions not to additionally analyze. Such approach implies a calibration of the tool under the stochastic perturbations of noise variables.

  Nevertheless, such results strongly depend on the choice of λ, regardless of the probability of occurrences of the variations of the noises. In addition, since a response linkage between the investigated goals and the process variables is developed under the scatter produced by the noise variables, the final prediction capabilities result from an average behavior and isolating noises stochastic effects is not possible.

As a consequence, the Pareto front obtained by the latter approach is an average approximation of the previous mentioned variability range.

Figure 2.41 compares the Pareto front for the mean values at λ equal to 0.5 with the variability range obtained by the hybrid RSM-MCS integration. As it can be observed, the Pareto front from the stochastic approach is in the variability range drawn by the hybrid approach. Its capability of prediction is so furthermore proved. Similarly, if lower values of λ are considered, more robust choices may result at lower BHF levels, where also the approach 1 highlights higher process robustness.

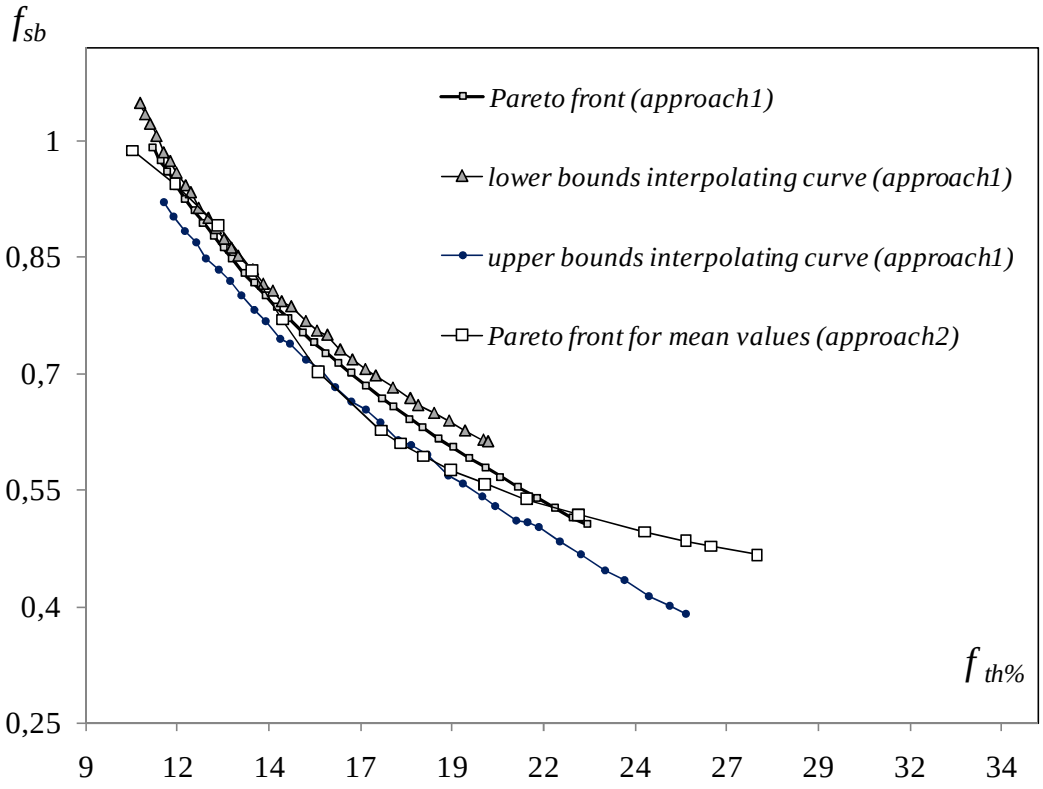

Figure 2.41: Comparison between the analyzed stochastic tool results.

Two main remarks arise by comparing the analyzed approaches:

1. as process robustness evaluation is concerned, the stochastic DRSM based approach results a quite restrained tool as it overestimates the standard deviation of each objective functions. Actually, unlike the MCS method that allows generating a number of occurrences enabling to predict the mean and the standard deviation of a function, the DRSM assesses somehow the variability on the basis of the points of the inner array. Therefore, unless to increase significantly the number of runs, totally losing time efficiency, a lower accuracy in measuring such statistical parameters is unavoidable.
   Additionally, if boundaries (constraints) on the investigated objectives are also to be respected, the stochastic approach might suggest lower BHF operative levels. Figure 2.42 shows an example of the application of the two approaches when boundaries are considered (namely 22% as maximum th% and 0.65mm as maximum sb): the hybrid approach would identify a BHF range 60kN to 75kN, while the DRSM approach a range

from 50kN to 70KN;

2. as risk of failure is concerned, if the same boundaries are considered, the process designer may choice any point on the red Pareto front, like the point Q from the DRSM approach (i.e. approach 2). It corresponds to a BHF equal to 60kN, th% equal to 17.5% and sb as high as 0.6mm, all respecting the given boundaries.

   Nevertheless, if the effects of the noises are analyzed at the same BHF levels, such choice cannot be considered reliable. Actually, from the hybrid approach (i.e. approach 1), if the point P (i.e. BHF=60kN) is considered, any stochastic variation would imply the failure of the sb boundary. In fact, the point P may scatter from the point P_1 to the point P'_1.

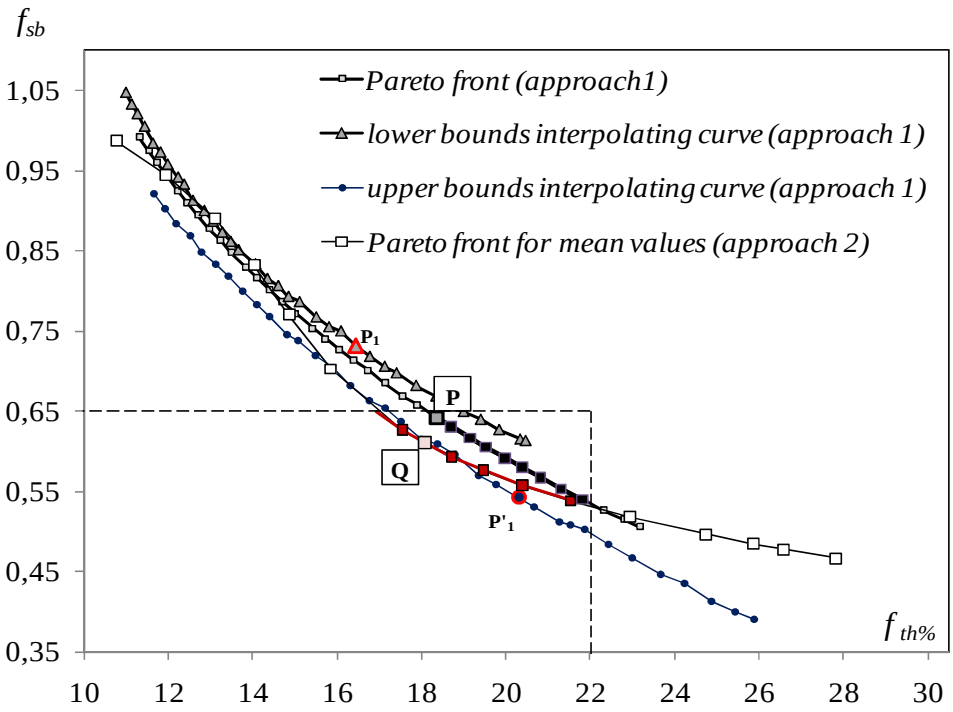

Figure 2.42: Example of application of the analyzed stochastic tool.

2.3.2 Case study 2.

In this study, the stamping of the IFU Hishida part, used also as a benchmark in the NUMISHEET conferences, was designed to validate and compare the two approaches above discussed. The level of the restraining forces was calibrated by the blank holder force, with the aim to minimize both thinning and wrinkling occurrences. Coil to coil variation of the material

properties is accounted for.

2.3.2.1 Hybrid deterministic-stochastic approach application.

Step 1: Problem formulation.

The above mentioned approaches were both validated on the stamping process of the IFU (University of Stuttgart) Hishida part showed in Figure 2.43 (a). The FEM numerical code LS-DYNA was used to investigate the process. A sketch of FEM model is reported in Figure 2.43 (b).

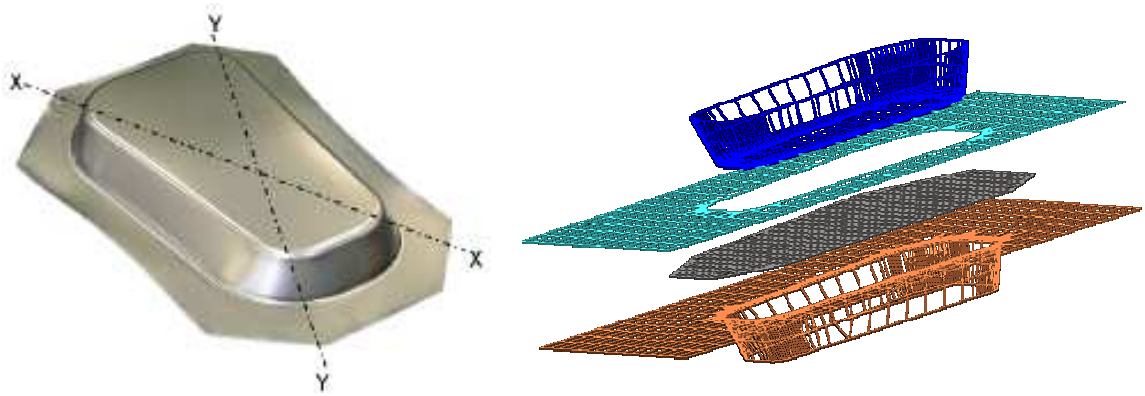

(a) (b)

Figure 2.43: IFU Hishida part (a) and sketch of the tooling (b).

Punch velocity was artificially increased and kinetic energy checked to assure it below the 10% of the deformation work, in order to avoid any inertia effect. The starting sheet element size was 3mm and a three levels geometric remeshing strategy was applied. A friction coefficient of 0.1 was utilized at blank interface and a Coulomb model was used. In order to take into account the material anisotropy, the Barlat Lian constitutive model was implemented (Barlat and Lian (1989)). The material is an AA6111-T4 whose main properties are listed in Table 2.16. Moreover, the sheet thickness is 1mm and the drawing depth 75mm.

C [MPa]	n	r_0	r_{45}	r_{90}
530	0.27	0.65	0.59	0.57

Table 2.16: Material properties of A6111-T4.

The initial blank shape is reported in Figure 2.44 (a) along with the geometrical details of the utilized tools (b) (Palaniswamy et al. (2004)). As preliminary step of both the applied

methodologies, problem formulation and modeling are required. Since a multi-objective problem is investigated, all the objective functions have to be clearly formulated and the process variables.

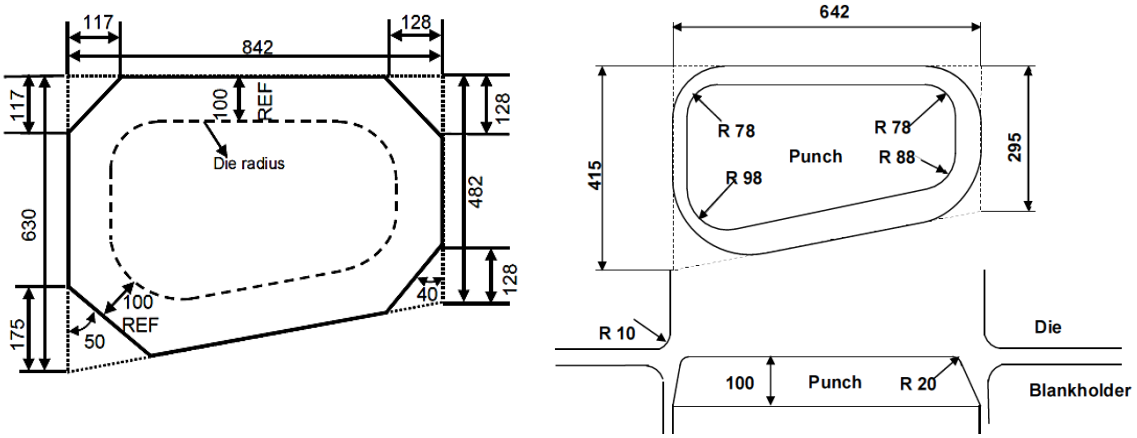

(a) (b)

Figure 2.44: Geometrical details of the initial blank (a) and tooling (b) (dimensions in mm).

Two mains drawbacks were highlighted by the analysis of the investigated stamping process and both fracture and wrinkling occurrences were investigated. The thinning distribution was detected and, in particular, the maximum thinning (th%) used as objective response. Geometrical criteria were instead used to detect the wrinkling occurrence, for both side and corner wrinkling investigation (Palaniswamy et al. (2004), Zang and Shivpuri (2009)). Beside those, the ratio between the two principal strains has been used as wrinkling indicator. Chen and Liao (2002) used such method to predict sidewall wrinkling in tapered rectangular cups and stepped rectangular cups, while Sheng and Shivpuri (2004) to predict the variable blank holder force for a Hishida part as well. Also Di Lorenzo et al. (2009b) used such ratio to detect the wrinkling occurrence for a rectangular deep drawn box. In this study, the ratio β between the minor and the major strains (absolute value of $\varepsilon_{min}/\varepsilon_{max}$) was used as objective function: referring to the material Forming Limit Diagram (FLD), the wrinkling occurrence is more relevant for low major strain values coupled with high compressive minor strains. Then, the greater is such ratio the higher is the possibility of wrinkling to occur. The trimming operation of the flange area was simulated after drawing and the wrinkling calculated in each of the eight different sides (S) and corners (C) in Figure 2.45 (a): according to the abovementioned

criterion, the ten most critical strain points were detected under the wrinkling zone of FLD and β_i calculated. For each zone, the wrinkling was estimated as arithmetic mean of β_i. Then, the maximum average value was kept as wrinkling response. Figure 2.45 (b) shows the FLD from LS-DYNA model.

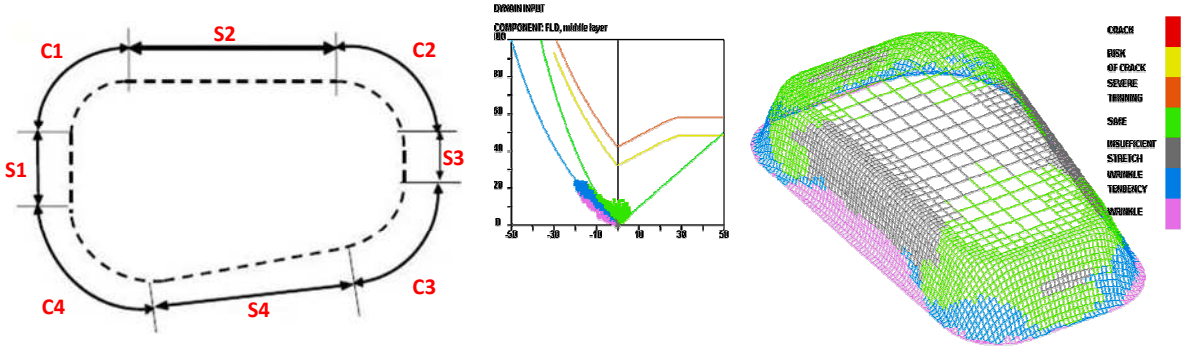

(a) (b)

Figure 2.45: Detected wrinkling zone (a) and FLD from LS-DYNA numerical model (b).

Blank holder force (BHF), constant in time and space, is chosen as control variable, allowing a proper calibration of the restraining force levels in the process. By running a preliminary set of numerical simulations within different ranges of restraining condition, an initial estimation of 650kN was used to start the process investigation. A sensitivity analysis was preliminary carried out in order to screen the significant noises whose variation affects the process results. As each noise is assumed stochastic, the range from the 5^{th} to the 95^{th} percentile of the related density function was explored as representing the 90% of the possible stochastic occurrences. Table 2.17 summarizes the main statistical parameters of the screened noises. A Gaussian distribution was assumed for each noise and no correlation was considered among them.

	5^{th}	μ	95^{th}	σ
C	485.7	**530**	574.3	**26.92**
n	0.2223	**0.27**	0.3177	**0.029**
$\mathbf{r_{90}}$	0.4976	**0.57**	0.6424	**0.044**

Table 2.17: Statistical parameters of the screened noises.

Step 2: Response analysis.

An analytical equation of the dependence of the objectives on all the variables was first deterministically modeled by RSM. Once the cause-effect linkage in known, it is possible to

analyze at the end how each objective changes at given control setting when a stochastic variation occurs. A Central Composite Design (CCD) with 25 runs was performed by FEM numerical simulations. In particular, the design levels explored the previous mentioned variation domain: $\pm\alpha$ levels correspond respectively to 5^{th} and 95^{th} percentiles of each noise variable distribution, while to 300kN and 1000kN for the BHF. R-Sq(adj) indicator was utilized to detect the approximation capability of the model. Then, only the statistically significant terms were kept by a stepwise regression using MINITAB software. In order to test the prediction capability of the obtained functions, further runs were spaced out within the design of experiments and the results compared with the predicted values: a quite accurate estimation resulted. The equation obtained for both the investigated objectives (f_{th} and f_{wr}) were, then, minimized. Figure 2.46 shows the trend of both the objectives as function of BHF (i.e. the control variable), while the noises are fixed at their nominal value.

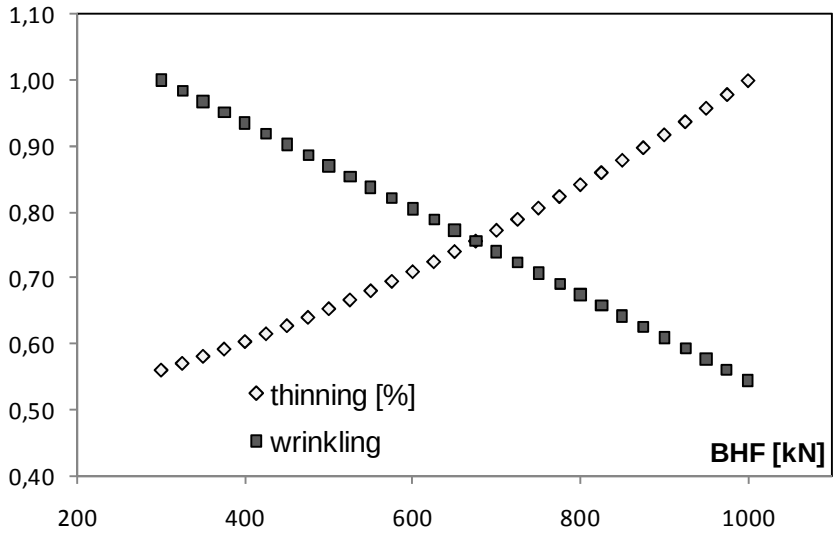

Figure 2.46: Objectives trend as function of BHF.

Given the analytic model of each objective, the Pareto front can be easily determined. In this study, ε-constraint approach was used in Matlab environment: the noises were fixed at the nominal value, and the compromise solutions determined only at the varying of BHF. Figure 2.47 shows the determined Pareto front. If no noise effect could be assumed, the Pareto front itself may provide the best alternative in terms of process performances given any constraints. From this step the question becomes how the variation of the noises affects the designer choices and how any Pareto solution may scatter because of that. For the maximum thinning

indicated in Figure 2.47, would the point A still be the best compromise? Or may the noise effect enhance the risk of failure? Informed choices have to be made.

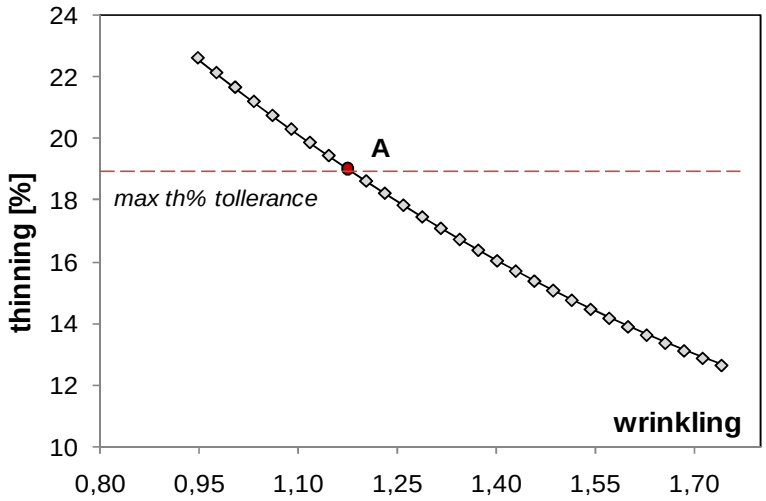

Figure 2.47: Deterministic Pareto front.

Step3: Variability scenario analysis.

Fixed a Pareto solution, e.g. point A in Figure 2.47, a proper number of noises occurrences were randomly generated given their probability distributions. Then, the objectives responses were calculated by the determined meta-models and the related probability distributions fitted by MCS. If the variability is accounted for, the design prospective changes: there is not a one-to-one correspondence between process setting and objective response, but a probabilistic range of responses because of the stochastic behavior of the material properties. In the case study, 1200 Monte Carlo simulations were run for each objective.

Figure 2.48 shows the probability distributions of thinning and wrinkling at the point A (which corresponds to BHF equal to 800kN). Significant differences are obtained on thinning and wrinkling values at the same level of BHF, remarking the necessity of a robust design tool for the sheet stamping process. Known the probability distribution of each objective at given process setting, the probability to get e.g. a thinning amount over the one required can be easily calculated. Then for the point A in Figure 2.47 the probability to get a maximum thinning over the fixed boundary is 55%. As such a remarkable effect shows up, the designer choice just based on deterministic considerations (point A) may fail the requirements: because of the noises, a thinning higher than the imposed one may result.

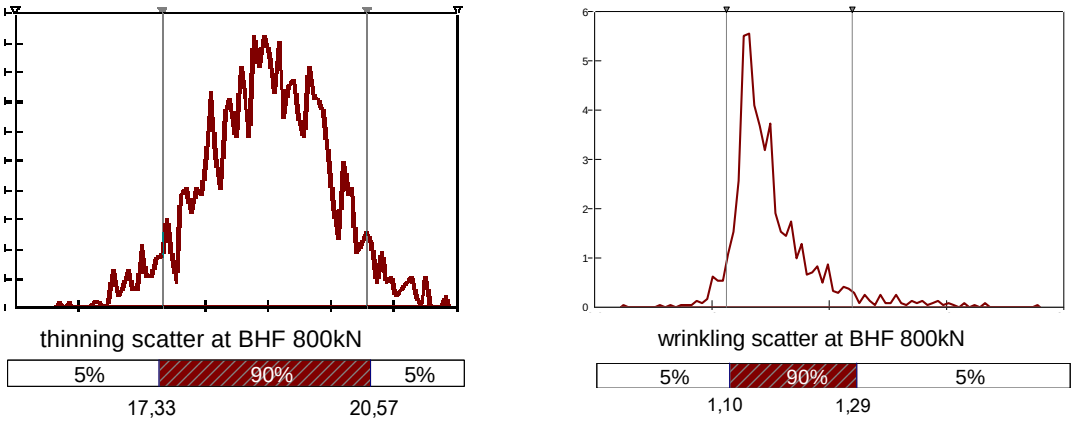

(a) (b)

Figure 2.48: Probability distributions of thinning (a) and wrinkling (b) at BHF 800kN.

Figure 2.49 shows the noise induced scatter of both objectives at 800kN (cloud of point around the point A).

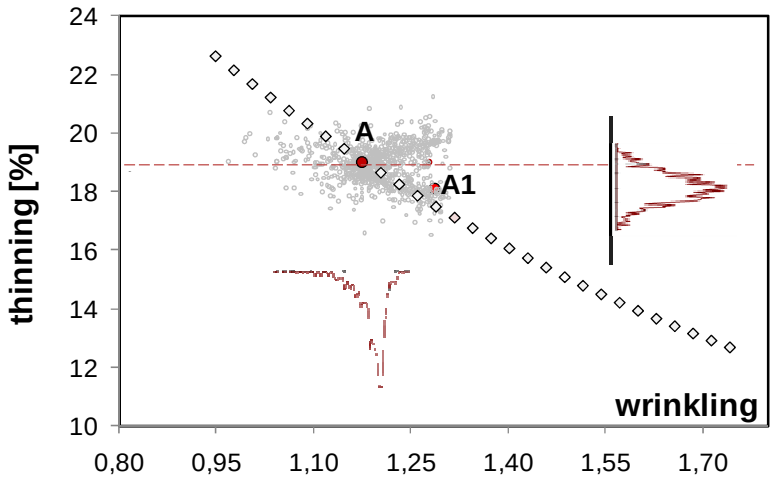

Figure 2.49: Noise induced scatter of the analyzed objectives at given control settings.

Figure 2.50 compares the thinning and wrinkling distributions at point A with one of the stochastic occurrences under the effect of the noises (point A_1 in Figure 2.49). As it is evident, such variability can be handled only by identifying a robust design space, i.e. a control setting that effects small scatters of the objectives, under the noises effect. In particular, an informed decision can be robustness driven or risk driven. In the first case, it becomes necessary to evaluate how sensitive to the noises effect an analyzed solution is, or, similarly, how spread out the cloud of points around the Pareto solution is. In the second case, how high the risk not to fulfill the requirements is, or, similarly, how frequently the requirements may be failed.

Therefore, the robustness (I_{RO}) and risk (I_R) indexes earlier defined were used.

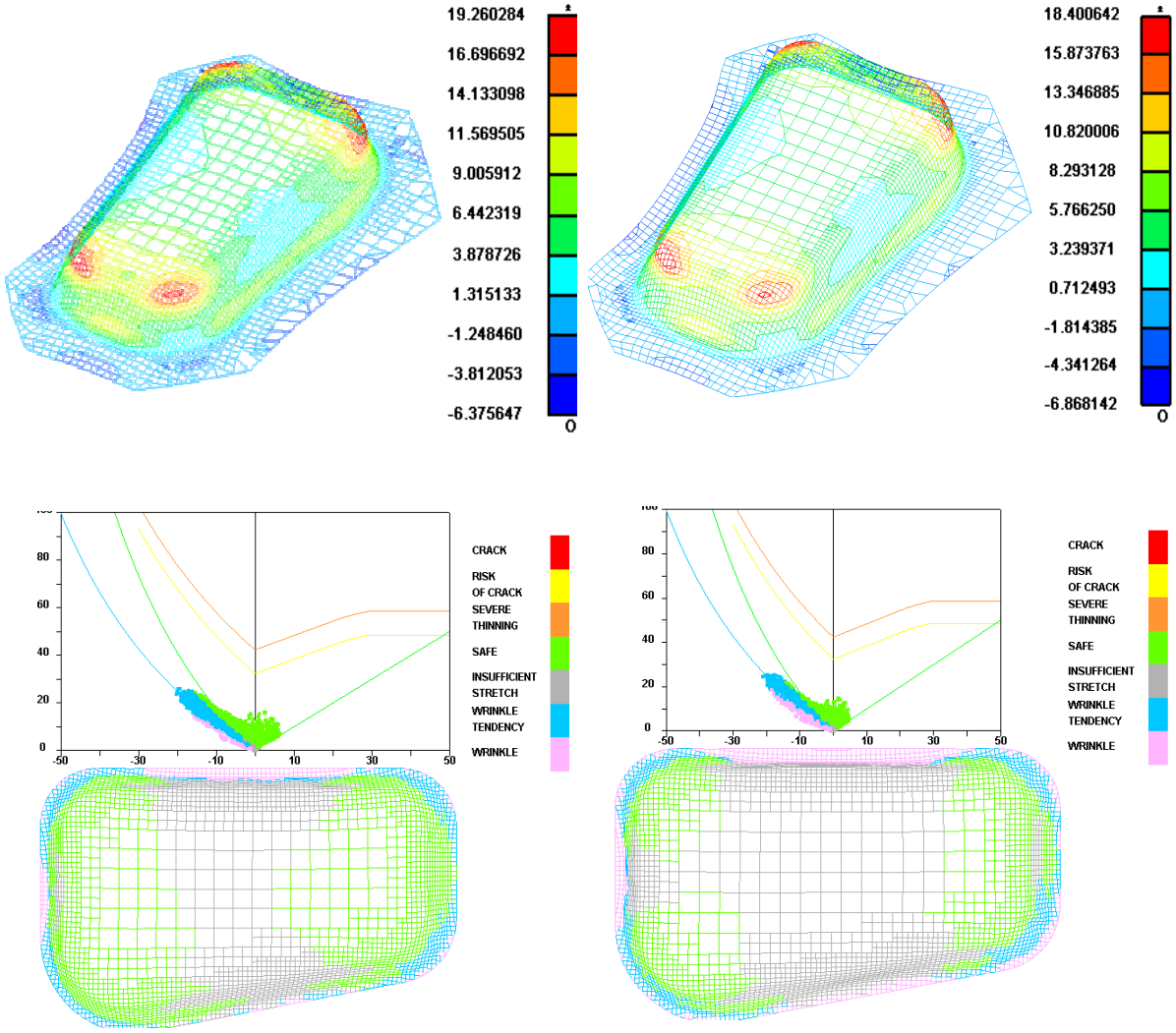

(a) (b)

Figure 2.50: Thinning and wrinkling distributions at BHF 800kN (nominal condition of point A) (a) and under the variation of the noises (point A1) (b).

In Figure 2.51 (a) two different solutions are highlighted, respectively, at BHF 800kN (point A) and 675kN (point B). As it can be observed, B solution fulfills the thinning requirement (19% as upper bound), while presenting a higher robustness than A: B has higher I_{RO} and I_R indexes than A. Moreover, such indexes can be calculated through the whole range of operative (BHF) conditions and the procedure can be iterated at each point of the Pareto front.

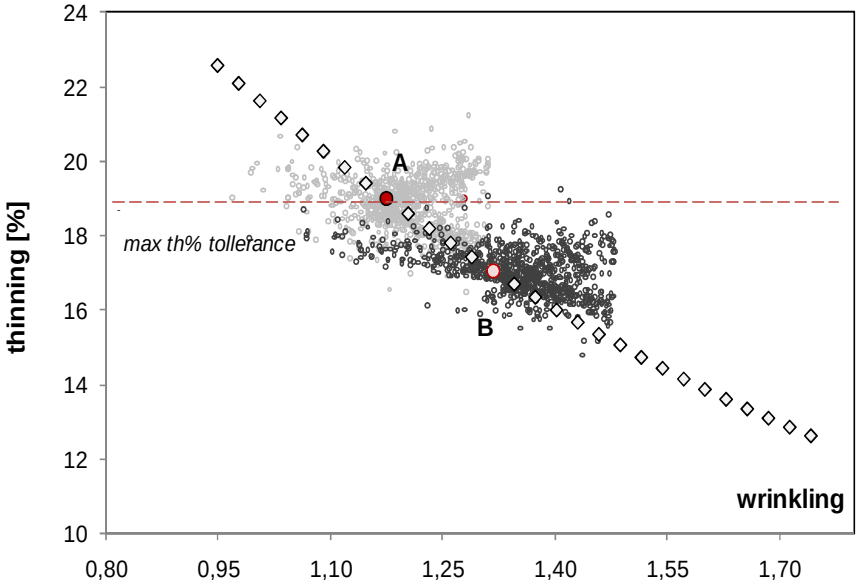

	I_{RO}	I_R
Point A	0.99	0.48
Point B	1.57	0.95

(a) (b)

Figure 2.51: Noise induced scatter at BHF 675kN and 800kN (a) and I_{RO} and I_R (b).

2.3.2.2 DRS based stochastic approach.

Step1: Metamodeling.

The Dual Response Surface Methodology (DRSM) was used to meta-model the objective functions when the material properties stochastically vary.

The cross product array detailed in Table 2.18 was employed: for each level of BHF (outer array) a further DoE (inner array) of the noise variables has to be designed.

In particular, 8 levels of BHF were chosen inside the outer array (i.e. BHF increased of 100kN from 300kN up to 1000kN). At each point of the outer array (i.e. BHF level) an inner array of 2^3 points was designed (3 noise variables of 2 levels).

In Table 2.18 only half inner array is shown for sake of simplicity (in fact the remainder points are easily determined by symmetry). In this way, each run of the outer array (BHF level) results properly replicated, enabling to estimate the mean and standard deviation values for given control setting (i.e. at each point of the outer array on the basis of the inner replicates). 64 simulations were run in total (i.e. 8 outer levels times 8 inner points).

			C	n	r_{90}			
			485.7	0.22	0.49			
			485.7	0.32	0.64		***inner array***	
			574.3	0.22	0.64			
	Points	**BHF**	574.3	0.32	0.49			
	1	300	y_{11}	y_{12}	… y_{18}		*mean (1)*	*stand. dev. (1)*
outer array	⋮	⋮	⋮	⋮	⋮		⋮	⋮
	8	1000	y_{81}	y_{82}	… y_{88}		*mean (8)*	*stand. dev. (8)*

Table 2.18: Cross product array.

Also in this case, a stepwise approximation model was utilized and the regression coefficients were calculated based on least square error minimization method, obtaining R-Sq (adj) values always higher than 98%. The plot of mean and the standard deviation functions for each objective ($f_{th\%,\mu}$; $f_{th\%,\sigma}$; $f_{wr,\mu}$; $f_{wr,\sigma}$), shown in Figure 2.52, highlights a still conflicting behaviors of thinning and wrinkling as BHF is differently set, while a quite similar behavior can be observed for given objective as mean and standard deviation is regarded. This means that, while the general problem formulation is still a multi-objective one, there is no need to formulate a global function F(X) in this case study: for each objective, the minimum mean value is reached at the same control setting that minimizes the standard deviation as well. From a process standpoint, it means that the higher the process control (i.e. BHF level), the higher the standard deviation of the thinning. Then even fractures may occur when noise variations occur at severe stretching conditions, where in fact the gradient of the standard deviation function arises. On the other hand, the higher the control of the process, the lower the amount and the scatter of the wrinkling.

Step 2: Multi-objective optimization.

The Pareto front is stochastically determined under the effect of the noises. In fact, instead of analyzing the effect of variability on the Pareto front, the process setting is figured out facing the stochastic perturbations of the noises. The ε-constraint optimization method was again employed in MATLAB environment to minimize both the mean functions at several process settings. The results are shown in Figure 2.53.

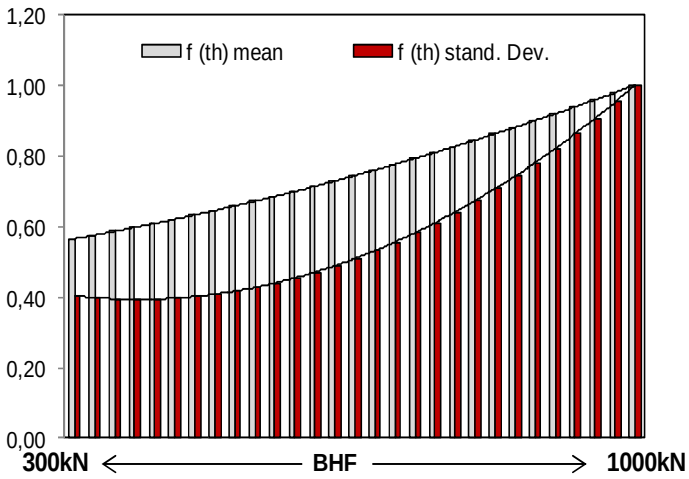

(a)

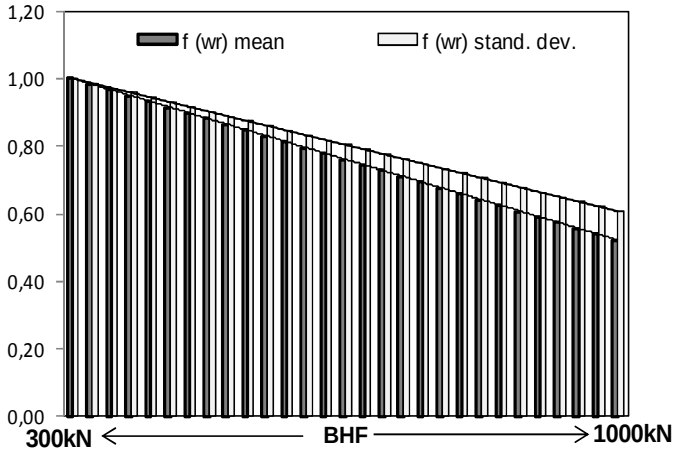

(b)

Figure 2.52: Plot of the mean and standard deviation functions of thinning (a) and wrinkling (b).

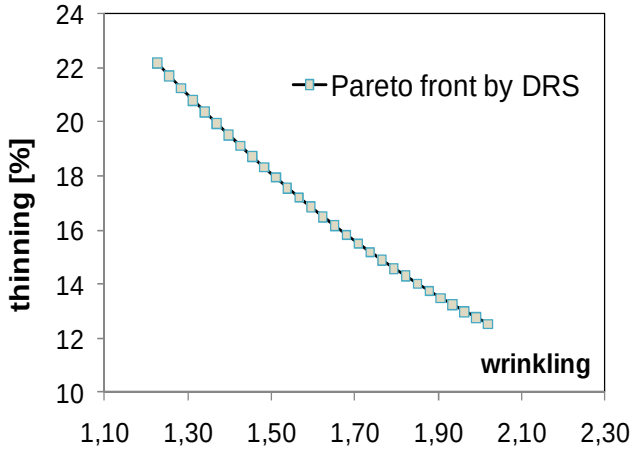

Figure 2.53: Pareto front by the DRS based approach.

2.3.2.3 Comparison between the analyzed approaches.

Figure 2.54 summarizes the results of the two approaches. The hybrid deterministic-stochastic approach allows making explicit the noise effects on the objective functions: the availability of objectives probability distributions by MCS allows figuring out the range of scatter of any objective at given process setting when the noise effect is considered. Assuming at most 19% of thinning, the designer may choose to set the process at point B against at A, respecting the thinning boundary with a reasonable probability. On the other hand, the DRS based approach provides a straightforward Pareto front that can be easily used as a deterministic tool while including the process variability inside. The question become how using an approach over the other one may change or even affect the designer's choices. In fact, without any explicit knowledge of the effect of the noises, i.e. by using the DRS as design tool, the designer may choose even the point A' as Pareto solution, which corresponds to the same process setting (BHF 800kN) incurring in a quite high probability to fail the process requirements. Moreover, if a maximum wrinkling requirement of 1.5 is constrained, the latter approach may cut off most of the Pareto solutions, resulting really conservative. In fact, the Pareto front by the DSR based approach results as an average approximation of the objective responses under the effect of the noises, over concerning the objective scatter. On the contrary, the hybrid deterministic-stochastic approach enhances the awareness of the designer about possible objective scatter, addressing more informed choices.

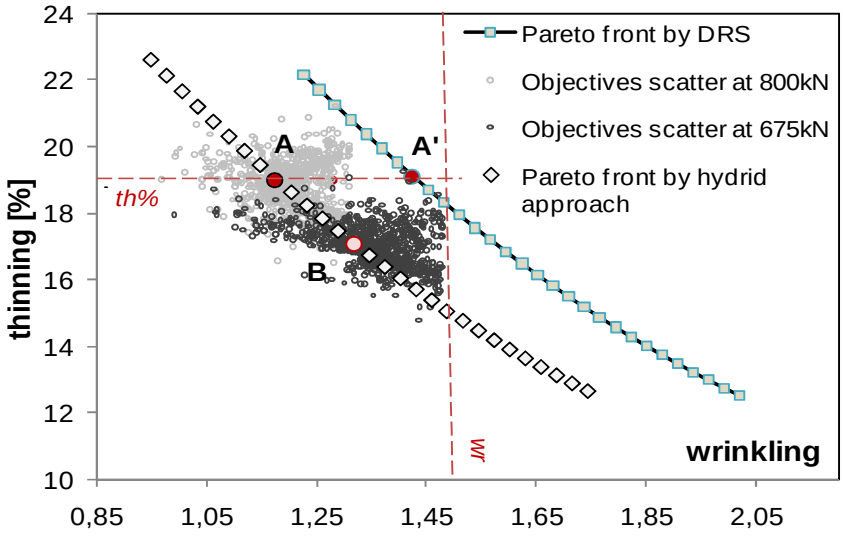

Figure 2.54: Pareto fronts and interpretation of the results.

2.4 Summary and conclusions.

Optimization of sheet stamping operations is typically a multiobjective problem as conflicting performances have to be accomplished. The main traditionally known advantages of the Pareto front are:

- the availability of several compromise solutions accomplishing all the objectives functions, instead of just one;
- the knowledge of the best possible value of a given objective at a desired level of the another one

According to the definition of Pareto optimality, all these solutions are optimal ones from a deterministic standpoint, but if the stochastic effect of some noise variables is accounted for, such optimality might fail and tools able to handle such variability become crucial.

Handling the process variability is in fact an imperative action in the industrial environment if costs, time and part rejection are to be reduced. Robust approaches able to deal with the effect of variability in the process are definitely worth developing: even if it is not possible to control the inner process variability, it is still possible in fact handling such variability by process setting minimizing such effects. Two different robust approaches were in particular applied to the optimization of the some sheet stamping operations. The former was a hybrid deterministic-stochastic one, which early neglects the effects of the noises and then probabilistically analyzes the noise induced scatter on the Pareto solutions. By integrating FEM simulation, RSM and MCS methods, the noise effects on both objectives can be highlighted and the related probabilities analyzed with respect to specific product requirements. In this way, the tool allows to enhance the awareness of the process designer about the risk of failure, addressing more robust choices. The latter was a DRSM based tool, which directly determined Pareto solutions under the effect of the noise variability. It is a standalone design tool that provides a range of results ready to use. Since the objective functions are modeled under the scatter produced by the noises, the final prediction capability results from a sort of average behavior, as noise effects cannot be isolated. Such results hide the objectives scatter though, driving potential failing decisions and strongly depend on λ choice.

As it was discussed in the introduction, beside robust optimization methodologies aimed at a zero defect quality, the efforts of the scientific community and industry have been focusing on tools for environmental conscious decisions as well. The concept of quality and robustness of solutions for sheet stamping processes has been naturally extended to new important objectives related to efforts to improve such processes also by enhancing their environmental performances. Therefore, beside zero defect parts, environmental friendly products and processes have to be pursued as well. A wide overview of possible sustainable strategies for sheet stamping processes is given in Chapter 3, together with a comprehensive decision making framework for environmental conscious decisions while considering both the economic viability and the technical feasibility of such processes. Case studies are also discussed.

Chapter 3

ENVIRONMENTAL CONSCIOUS DECISIONS IN SHEET STAMPING APPLICATIONS.

Recently, environmental considerations in manufacturing have become increasingly important as many industries seek to develop sustainable solutions for industrial applications. The US Department of Commerce defines sustainable manufacturing as *"the creation of manufacturing products that use materials and processes that minimize negative environmental impacts, conserve energy and natural resources, are safe for employees, communities, and consumers and are economically sound"* (www.trade.gov). Then, according to Dornfeld (2011), green manufacturing can be defined as a first step towards sustainability.

As efforts to enhance the environmental performances of manufacturing processes have become imperative both for industry and scientific community, the attention of the research has been naturally extended to developing green solutions and evaluation methods for sheet stamping applications. In particular, a strong interest towards low environmental impact solutions and technologies has arisen in the automotive industry (McAuley (2003), Sutherland and Gunter (2004)). In particular, as it was earlier discussed, the automotive sector plays a crucial role for the reduction of the global carbon emissions as transportation, especially light duty vehicles, contribute significantly to their increase. Transportation, in fact, represents 27% of the global US emissions by economic sector, where the specific contribution from light duty vehicles is as high as 59% among all the transportation modes (EPA (2011)). Similarly, road transportation contributes about one-fifth of the Europe's total emissions of carbon dioxide (CO_2) (http://ec.europa.eu). Moreover, as it was shown by Figure 7 in the introduction, the use phase has the greatest impact throughout a typical vehicle life cycle (Geyger (2007)).

Considerations and discussions on sustainability in sheet stamping operations have been done in collaboration with General Motors R&D at the third year of the PhD program at the University of California, Berkeley (USA).

Therefore, a sort of *Google Earth view* through the manufacturing chain in the automotive

sector was initially done in order to analyze what it has been already done and what it can be done in future, by zooming in from a low level to a progressively higher level of detail (like the known software Google Earth). The goal was to break down the manufacturing chain of a common passenger car to better focus on the opportunities of improvement towards more sustainable sheet stamping processes. Figure 3.1 below shows the *Google Earth view* of the manufacturing chain of a passenger car.

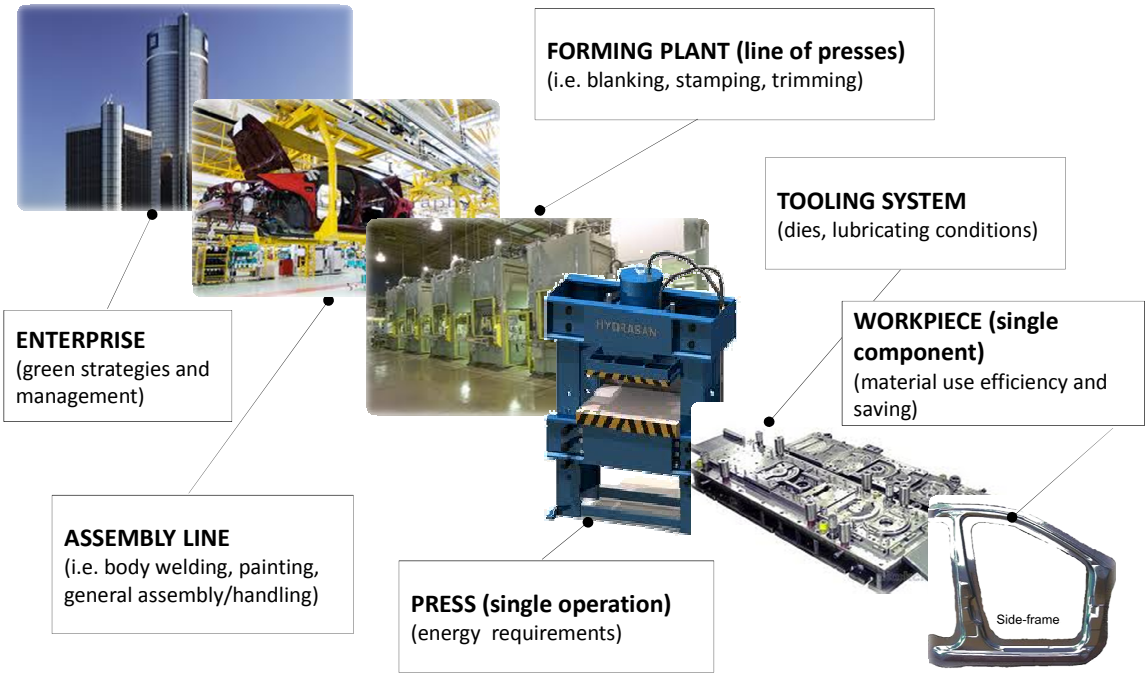

Figure 3.1: Google Earth view of the manufacturing chain of a passenger car.

Only the body in white (BIW) was taken into account with attention just on the sheet stamping processes; therefore, manufacturing of engines, gear or other mechanical components was not included in the analysis. Six main levels were so identified:

Enterprise level: the main strategies that some automakers started adopting will be briefly discussed without looking at any specific process. Efforts to use alternative power sources, to implement green supply chain management and to improve efficiency in production arose from a benchmark analysis. For instance, Ford's Dagenham Diesel Center in UK is the first plant powered by wind (Ford (2009)). Moreover, Toyota's Tsutsumi plant uses one of the largest photovoltaic power generation systems worldwide (Toyota Motor Corporation (2008a)).

As it can be observed in Figure 9 in the introduction, energy related to material supply

contributes critically through the entire manufacturing chain, thus a Green Supply Chain Management (GSCM) has become one of the most spread practice in the industrial environment. The definition of GSCM is still not completely clear though. In the technical literature there are several definitions and examples (Geffen and Rothenberg (2000), Koplin et al. (2007), Simpson et al. (2007), Zhu et al. (2007)), mainly as strategies aimed at green purchases, management of the relations with the suppliers, integrated supply chain and closer cooperation by joined actions. For instance, Ford, Volkswagen and Toyota have required to their suppliers to obtain the ISO 14001 certification.

Another recognized strategy at enterprise level is from Toyota: by the Just In Time (JIT) philosophy, which is meant as "… making only what is needed, when it is needed, and in the amount needed" (www.toyota-global.com), it is possible to eliminate waste, inconsistencies and unreasonable requirements, resulting in a more efficient production. Even quite old, JIT can be reconsidered in terms of sustainability towards a more efficient production.

Assembly line: the assembly line consists mostly of painting and welding operations. In particular, painting operations are the most impactful ones as far as the Volatile Organic Compounds (VOC), which are considered one of the causes of the photochemical smog. Therefore, the main effort has been focused on the reduction of such emissions by using environmental friendly solvents, efficient filters and recovery or reuse systems able to convert emissions to green energy. Toyota and Mazda have developed an Aqua-Tech system where traditional solvents are substituted for water based ones, so enabling a VOC reduction as high as 60% (Mazda Sustainability Report (2010), Toyota Motors Corporation (2008a)). On the other hand, it has also to be observed that more time and energy are required to dry water. Toyota has adopted an intelligent filter system containing microorganisms as well (Toyota Motors Corporation (2008b)): the system gathers the VOC emissions; the microorganisms absorb and digest the VOC emissions, to convert them to water vapor and carbon dioxide. The bio filter is expected to reduce VOC emissions by 65% and carbon emissions by 1000 tons a year.

Another smart solution comes from Ford's plants, where the VOC emissions are recovered and reused as fuel to power fuel cells, getting a sort of self-sustaining system (Ford (2009)). From 15% to 75% of VOCs are reduced, together with 88% of carbon emissions.

As far as the welding operations, conventional processes are characterized by fumes and

the need of material treatments pre and post welding. Joining techniques by forming (e.g. clinching, self-piercing riveting, die less hydroforming, etc.) are therefore noteworthy in these terms. They also have been widely appreciated and used by some automakers like Audi, GM and Lotus. Typical applications fields are fuel tanks and airbag cases.

Solid state welding processes are moreover at the state of art as more sustainable welding technologies. Among these, Friction Stir Welding (FSW) and Linear Friction Welding (LFW) feature a number of potential advantages over conventional fusion-welding processes, which can be summarized as follows (Smith et al.):

1. no fume (i.e. less emissions to air);
2. no spatter of the molten materials (i.e. less wastes);
3. reduced need of cleaning the part (i.e. reduced need of chemical cleaning agents);
4. less welding defects, which reduces reworking and scraps;
5. higher welding speeds.

Forming plant: this level includes the line of presses and all the tooling systems that are generally used to obtain the final stamped components. A typical routing consists of a preliminary blanking operation to get the initial blank shape, followed by series of stamping operations, like bulging, coining, deep drawing and one or more trimming operations to remove the exceeding material. The main strategies at this level are therefore aimed at developing net shape and more flexible processes (such as hydroforming and superplastic forming) able to get complex geometries without performing multistep operations and with less finishing processes.

In particular, the use of tailored blanks (TB) has been proved to be a really efficient strategy to reduce the number of steps through the manufacturing chain. TBs, which will be better discussed later, are blanks with variable thickness, alloys or material grades whose application can shorten the manufacturing chain with remarkable environmental advantages, as showed in Figure 3.2 below.

According to the report on the tailored blanks value from www.arcelormittal.com/fce/repository/Tailored_Blanks/Catalogue-Chapter1.pdf, the conventional stamping process of an automotive component like the front door panel in Figure 3.2 usually requires to stamp and to subsequent assemble two different parts, an inner panel and a hinge reinforcement.

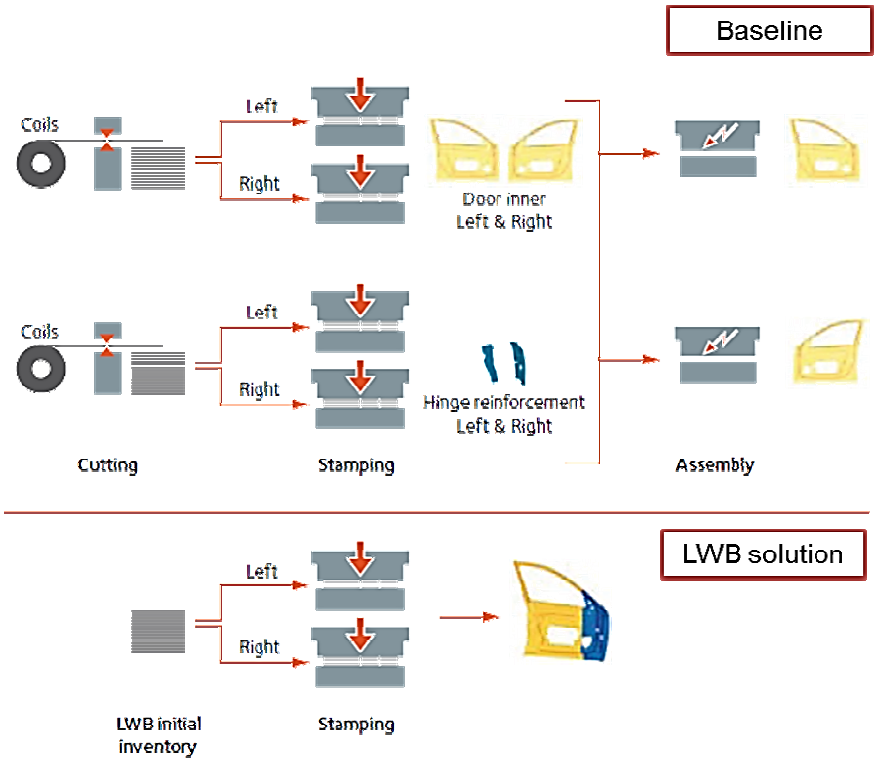

Figure 3.2: Possible process shortening by TBs (adapted from www.arcelormittal.com/fce/repository/Tailored_Blanks/Catalogue-Chapter1.pdf).

Thus, the two components have to be stamped first and then joined for instance by spot welding techniques. Usually sealing is required as well in between of the two blanks, to improve the corrosion resistance. If TWBs are applied instead, the reinforcement could be left out: two blanking operations would be skipped, two stamping and two assembly operations saved. Table 3.1 summarized the considerations above.

** Including left and right assemblies*

Operation Type	***#Parts***		**Δ**
	Baseline	**TWBs**	
Blanking	2	-	2
Stamping	4	2	2
Assembly	2	-	2
Δ Total	**-**	**2**	

Table 3.1: Number of process operations saved by TWBs.

Moreover, less process steps imply lower energy consumptions, together with fewer parts to be handled. Fewer deviations from dimensional tolerances would be also obtained, reducing finishing and re-working operations as well. No overlap from spot welding improves the corrosion resistance and no sealing joint would be required anymore in

between of the two sheets.

Press: this level refers to the single stamping operation at press, with considerations mainly about energy, press efficiency and stamping technologies. Chee et al. (2011) analyzed the energy consumptions through the entire press cycle, breaking down the total energy required to stamp a component. Moreover, Kellens et al. (2011) performed an environmental analysis of an air bending process. In general, no other attempts either to model or to analyze energy requirements strictly focused on sheet stamping operations are in the technical literature. Avram and Xirouchakis (2011) evaluated the use phase energy requirements of an end milling operation. Dahmus J. and Gutowski T. (2006) also carried out an environmental analysis of a machining process. Diaz et al. (2010a) identified sustainable strategies for machine tool design and operations. They also carried out an environmental analysis of a milling machine tool (Diaz et al. (2010b)). Gutowski et al. (2006) proposed models for quantitative evaluations of the relation between electrical energy used in manufacturing and the carbon emissions created in using such energy, but mainly focused on machining processes as well. The development of a prediction system for the environmental burden of a milling operation was carried out by Narita et al. (2006). Also, Munoz and Sheng (1995) developed an analytical approach for determining the environmental impact of machining processes. Pusavec et al. (2010a) and (2010b) and Vijayaraghavan and Dornfeld (2010) also emphasized the possibility to precisely model all the machining processes sustainability factors. Rajemi et al. (2010) made important conclusions on the selection of optimum turning conditions based on minimum energy considerations.

Kellens et al. (2012a) proposed a life cycle analysis (LCA) oriented methodology for systematic inventory analysis of the use phase of manufacturing unit processes and also analyzed some case studies on machine tools use phase (Kellens et al. (2012b)). In particular, the methodology was developed within the framework of the CO_2PE! collaborative research program, whose goal is to provide with a LCA methodology for manufacturing processes together with a database for a broad range of manufacturing unit processes which can be used by LCA-experts and process/product designers to analyze the environmental burden of manufacturing unit processes alongside production chains.

The estimation of the environmental burden of forming technologies is really complicated though, as particularly process-dependent. In general, both the stamping technologies (e.g.

hydroforming, incremental forming, etc.) and the process temperature have a strong influence on the total energy requirements. Therefore, it is possible to state that if hot stamping processes are performed to enhance the formability of the used materials, an increase of the energy consumed should be considered at the same time. An overview of non-conventional stamping technologies for more sustainable processes is given in section 3.1.2. A comparison of two stamping processes, namely deep drawing and incremental forming, is instead discussed in section 3.1.2.1.

Tooling systems: dies and lubricating conditions will be discussed at this level, as obviously they influence the environmental impact from manufacturing. Die less or single tool technologies, like hydroforming and superplastic forming, enable lower wear of the dies, material saving as no or just one die is used, together with lower use of lubricant by smoother plastic deformations.

As far as lubricants, there are several studies on the use of environmental friendly lubricants for sheet stamping processes. Among those, boric acid dry films (Rao and Xie (2006)) seem to be one of the most efficient, due to the balance between green and friction performances. The Environmental Protection Agency and the Clean Water Act classify the boric acid as benign. Moreover, it is a solid lubricant, with a high load carrying capacity and low steady state coefficient, mainly due to the weak interactions and easy sliding among the lamellae layers (Lovell et al. (2006)). Figure 3.3 compares the boric acid with other widely used stamping lubricants for a given process by drawing forces.

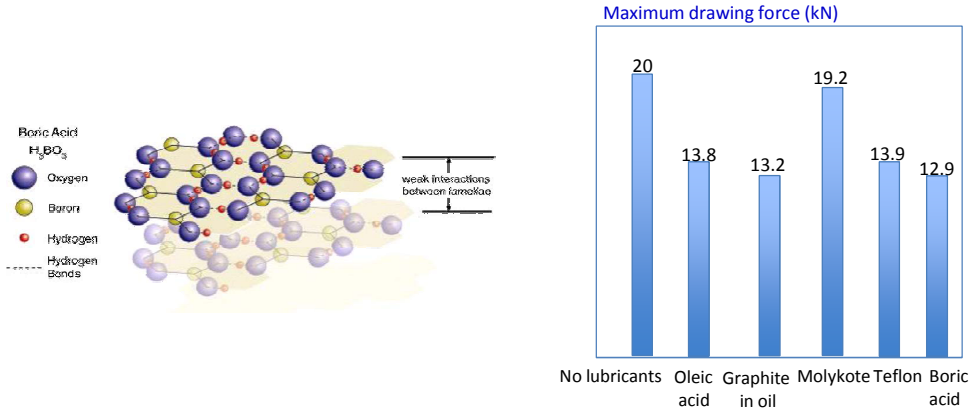

(a) (b)

Figure 3.3: Acid boric microstructure (Lovell et al. (2006)) (a) and comparison with common lubricants for sheet stamping (adapted from Rao and Xie (2006)) (b).

Workpiece: sustainable strategies at workpiece level essentially concern efficiency in

selection and use of materials for sheet stamping operations. Issues regarding the energy requirements for primary processing and shaping, the possibility to save, to recycle or to reuse materials, together with the potential to leverage positive externality on the entire product life cycle will be accounted for, within a comprehensive view of sustainability options. The use of Light Weight Materials (LWMs), such as aluminum, magnesium and titanium alloys, has become a really effective strategy in the automotive sector to reduce the total weight of the vehicles, saving material in manufacturing of the single components. Weight reduction implies, in fact, fuel saving and, accordingly, lower carbon emissions. Figure 3.4 shows the most common automotive materials and their relative use over the years (White (2006)), highlighting a significant percentage of ferrous materials and in particular steel in a common vehicle.

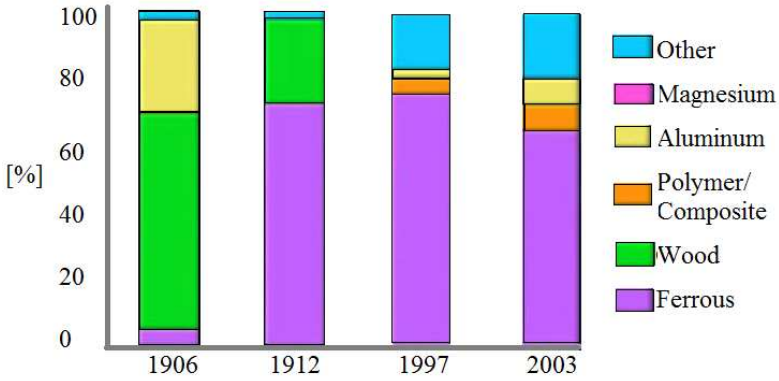

Figure 3.4: Automotive materials in a common vehicle (adapted from White (2006)).

On the contrary, Figure 3.5 shows the body mass reduction achievable by replacing steel with lightweight automotive materials.

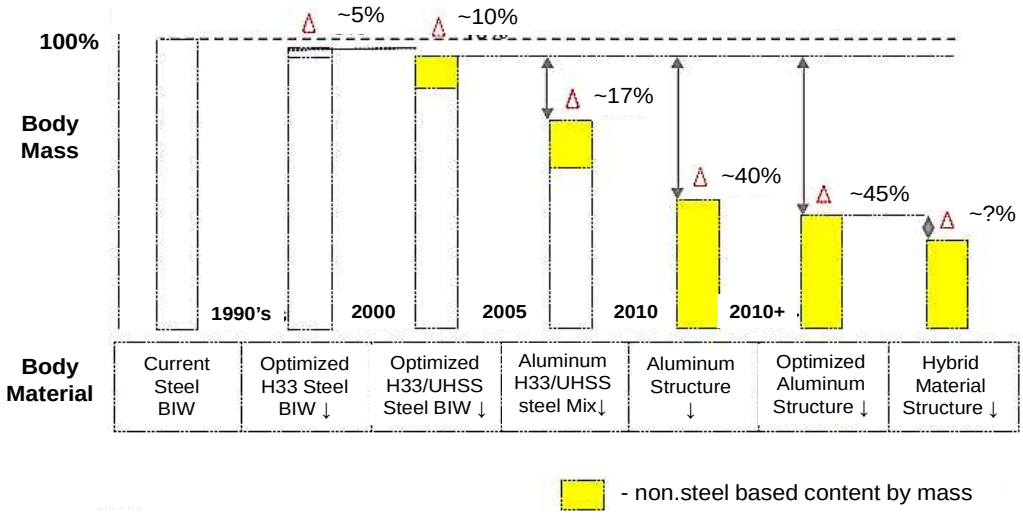

Figure 3.5: Body mass reduction by using non-steel based materials (adapted from White (2006)).

In terms of carbon emissions, it is worth pointing out that Light Weight Vehicles (LWVs) are even more efficient than other solutions for sustainability in the automotive sector like hybrid vehicle for instance, as it can be observed in Figure 3.6 below.

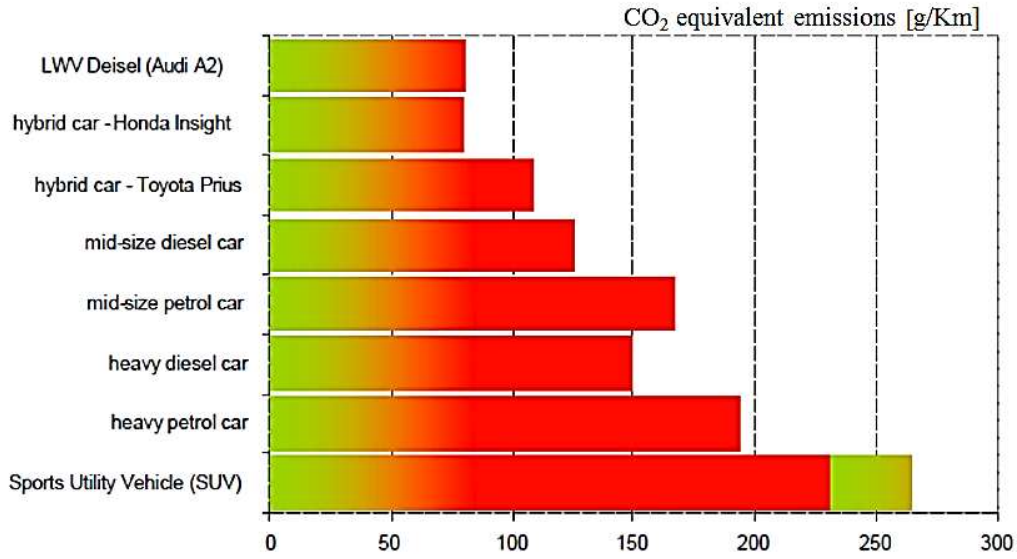

Figure 3.6: Carbon emissions by type of vehicle (White (2006)).

Many automakers have started using LWMs, like Audi for instance; in fact the model R8 in Figure 3.7 is an example of space frame totally made of aluminum and magnesium alloys, with a weight reduction of 40% (210kg less) over steel (www.audi-mediaservices.com).

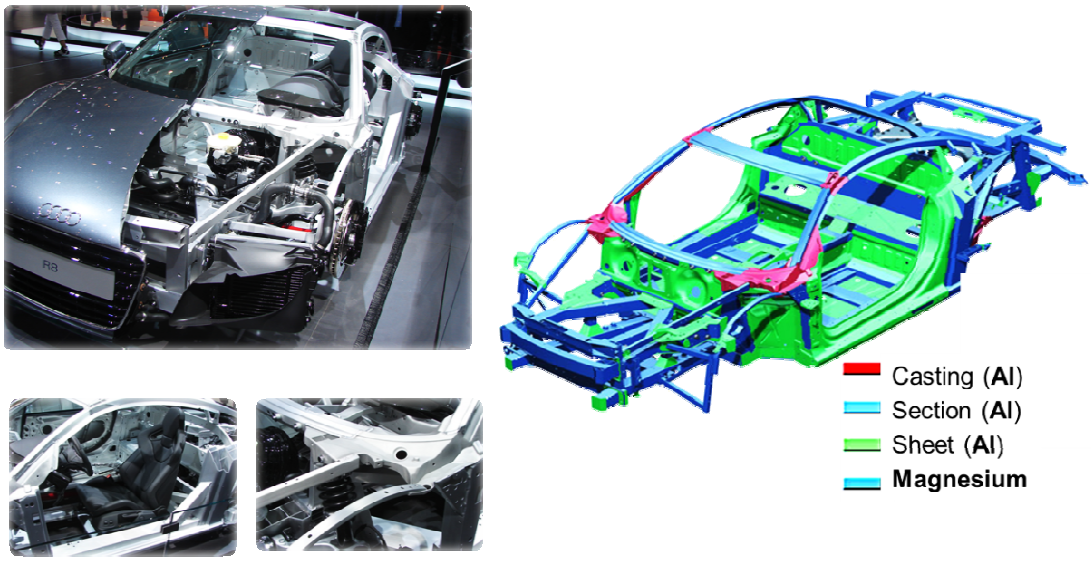

Figure 3.7: Space frame in aluminum and magnesium (www.autoblog.com, www.gwwsc.org).

The use of LWMs raises technical issues though: such materials feature in fact low formability at room temperature, possibly requiring hot or warm stamping operations. Therefore, beside LWMs, Light Weight Manufacturing (LWM) has been investigated in terms of technologies enabling the use of lightweight materials. For instance, hydro-forming and superplastic forming enable to draw magnesium alloys at lower temperature over conventional stamping processes (Neugebauer et al. (2006)). On the contrary, it is well know that aluminum and magnesium alloys have higher primary energy requirements, therefore the tradeoff in using those materials, still enabling significant fuel savings, should be evaluated.

Weight reduction comes from the application of TBs as well, together with lower scrap rates and higher efficiency in material use. In fact, beside weight reduction, another sustainable strategy is waste and scraps minimization as more efficient use of materials, for instance by carrying out net shape processes.

For such purpose, optimization techniques and nesting software are available in the technical literature as well (Azaouzi et al. (2010), Ghatrehnaby and Arezoo (2009)) to maximize the material use rate. Moreover, Di Lorenzo et al. (2009b) applied the RSM to optimize the initial blank shape in a rectangular deep drawing process taking into account both wrinkling and fracture risk.

Indeed, recycling is an effective strategy both to reduce primary energy requirements and resources use. Materials like steels and aluminum alloys have high recyclability rates, allowing potentially a massive use of low impact secondary material.

Deeper discussions on lightweight materials and manufacturing technologies are in the following section, as they represents really effective strategies to reduce the environmental impact of sheet stamping processes, with main focus on the automotive sector.

3.1 Strategies for sheet stamping process applications.

In order to make environmental conscious decisions for more sustainable sheet stamping applications, it is useful to first model a typical sheet stamping processes by input/output flows and factors to be accounted for. As it was earlier observed, sheet stamping processes still need proper modelling, even though it is particularly difficult as strongly process dependent. Gantar et al. (2005b) identified material efficiency and lubrication as main strategies to reduce the environmental impact of such processes. Some studies on

environmental friendly lubrication technology based on dry manufacturing or manufacturing with benign lubricants have been presented by Bay et al. (2005) and Wang (2004). Ingarao et al. (2011b) and (2011c) proposed a first attempt of modelling sheet forming processes. They proposed a comparison between incremental sheet forming (ISF) and deep drawing operations, accounting for the material use and the theoretical manufacturing energy. Nava et al. (2010) presented a model including also non-energy factors, such as lubrication. Petek et al. (2007) presented an approach involving the impact of material use, lubrication, and process energy as well.

A typical stamping process is sketched in Figure 3.8 by having toured GM's stamping plants at Lansing and Flint (MI, USA). In particular, input and output flows are all highlighted.

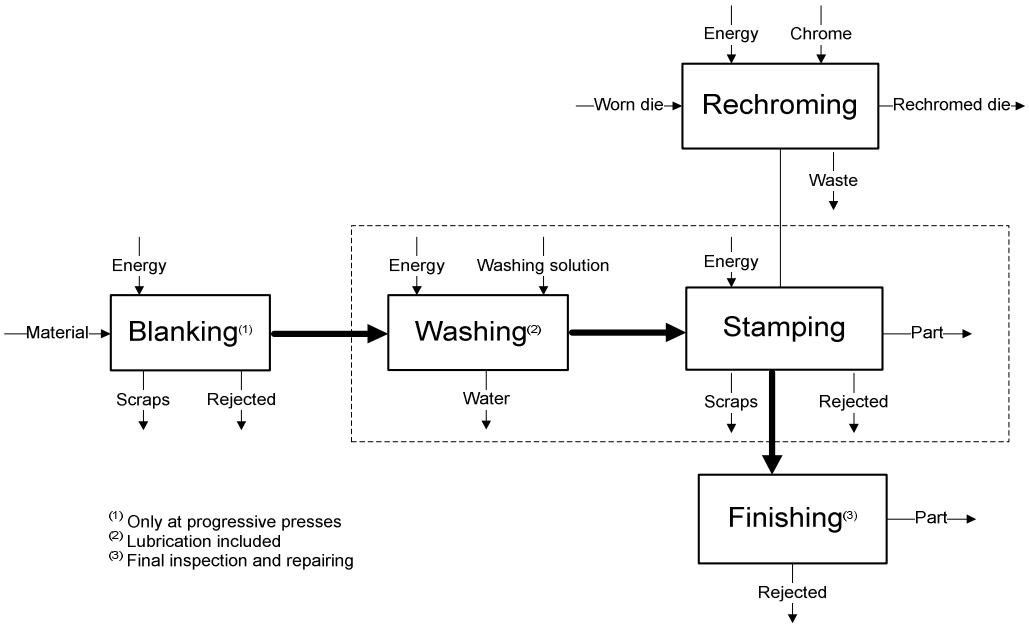

Figure 3.8: Sketch of a common stamping process with highlighted input and output flows.

The stamping routing is mostly housed in automated transfer presses (dashed line in Figure 3.8), except for blanking and finishing operations. Washing solutions for stamping are generally applied together with lubricants straight after blanking operations. Then, a sequence of deep drawing and trimming operations is carried out. The automated shift of the stamped parts according to the press slide eliminates material handling and inter-operation steps. Scraps are collected and separated by material. Moreover, re-chroming operations are periodically required because of the die wear.

Given the process baseline, three main aspects have to be focused on: material, both as

input and output, energy (not just deformation energy but also the one consumed during the press warm up, load, idle phase, die change, etc.) and lubricants/washing solutions.

But which strategy would be more effective and accordingly worth doing first?

According to Dornfeld (2010), "*manufacturing offers many opportunities for reducing environmental impact, utilizing resources more efficiently and, overall, greening the technology of production by process, machine or system improvements. But, there is more potential in manufacturing enhancements to have a larger impact on the life cycle impact of the product the manufactured item is used in*". Dornfeld (2010) defines this as "leveraging" referring to "*manufacturing-based efficiencies in the product that are due to improved manufacturing capability but which, in the long run, have their biggest effects on the lifetime consumption of energy or other resources or environmental impacts*".

Based on the considerations above, two are the main improvement directions that will be analyzed: improvements of the environmental performances of the sheet stamping processes themselves (i.e. without considering either the use phase or the end of life of any related stamped products) and solutions enabling to leverage the reduction of CO_2 emissions in the use phase of stamped components, in particular in the automotive sector.

The main strategies for sheet stamping applications will be discussed in the following section, together with two case studies.

3.1.1 Lightweight materials.

A crucial issue in material selection for automotive applications relates to the suitability of any automotive material on the basis of both strength and safety requirements. Therefore, even though some material choices might result more sustainable as lower impactful on the environment, the fulfillment of those specifications cannot be ignored or even neglected.

As far as the environmental performances, low density materials enable a significant weight reduction, leveraging lower consumptions in the use phase of a vehicle life cycle. Currently, magnesium alloys (International Aluminium Institute), titanium alloys (Froes et al. (2004)), and in particular advanced high strength steels (AHSS) and aluminum alloys are of interest for the transportation due to their high fuel saving potential (Bertram et al. (2005), Helms and Lambrecht (2006), International Aluminium Institute, Kim et al. (2008), Sujit (2000)), which make them very effective and directly impactful over the CO_2 emissions: a 6% to 8% fuel savings can be realized for every 10% reduction in weight

from substituting steel with aluminum and each kg of aluminum replacing 2 kg of steel will save 20 kg of CO_2 over the typical life time of a vehicle (Shaw and Coates (2008)). In other words, 9 g of carbon emissions might be saved per km by reducing the vehicle weight by 100 kg (Bertram et al. (2009)).

Despite these differing attributes, the eco-efficiency of any material or technology ought to be analyzed over an entire life cycle, as each phase is sometimes characterized by significantly different environmental impact: saving fuel in the use phase, and accordingly greenhouse gases emissions, may mean for instance to increase the environmental effect from manufacturing or material acquisition. While such materials enable a lower environmental impact in the use phase, their primary production and processing require much higher energy over traditional ferrous materials. For example, even though aluminum alloys provide significant benefits as fuel saving, its primary production involves large amounts of energy for raw material extraction and processing.

Additionally, as it was earlier observed, strength and safety requirements have to be accomplished as well. Moreover, formability issues have to be accounted for, as they strongly influence the feasibility of the process or just the number of steps to carry out.

Even from an environmental standpoint, higher number of manufacturing steps (e.g. due to lower formability or reworking) or higher rejection rates (connected to the compliance with the specifications) might imply higher manufacturing energy and material wasting.

Table 3.2 summarizes some material properties of such automotive materials that contribute to those (Ingarao et al. (2011a), Kleiner et al. (2006)).

Material Properties	**Al**	**Mg**	**Steel**	**Ti**
Density [$kgdm^{-3}$]	2.8	1.74	7.83	4.5
Young modulus [Gpa]	70	45	210	110
Tensile strength [Mpa]	150 - 680	100 - 380	300 - 1200	910 - 1190
Tensile strength/density [$10^6 Nmmkg^{-1}$]	52 - 243	57 - 218	38 - 153	202 - 264

Table 3.2: Main material properties of some automotive materials.

From Table 3.2 above, low density materials as aluminum and magnesium feature worse strength performances that steels have instead. That means that, if such LWMs are used in the automotive sector, in order to assure the same or at least suitable strength performances, it might be necessary to increase the initial blank thickness. For design

equivalence, the thickness ratio between aluminum and traditional steel blanks for structural applications may be approximately 1.5 (which means for instance that a thickness of 0.8 mm of a steel blank would be replaced by a 1.2 mm aluminum sheet), but the weight reduction would be still about 50% (http://aluminium.matter.org.uk). Figure 3.9 compares three materials by thickness and weight of a bonnet: by replacing conventional steel with aluminum and magnesium alloys, thicker blank have to be used (at least 1.5% ticker) but weight reductions respectively as high as 41% and 62% might be reached.

Mg	Al	St
S_0=1.3 mm	S_0=1.3 mm	S_0=0.75 mm
975g	1511g	2520g
-62%	-41%	100%

Weight reduction %

Figure 3.9: Comparison of three automotive materials by blank thickness and weight (adapted from Behrens et al. (2005)).

However, even though there are mechanical laws and equations to calculate the increase or decrease of the thickness by material, the relationship between the material properties and the structural and safety specifications is very complex to investigate as strongly influenced by geometry.

On the other hand, titanium alloys would provide with a quite good compromise of both strength and density as well. In fact, they features high tensile strength combined with low density value (i.e. highest specific strength). Titanium alloys exhibit a really low formability though, turning out to be extremely tough to draw for automotive applications.

An overview of the most common LWMs for sheet stamping applications is provided below according to (Ingarao et al. (2011a)).

Advanced High Strength Steels (AHSS): AHSS have been widely applied to the manufacturing of automotive components due to their attractive strength properties combined with good formability features. According to Geyer (2007) and www.wordautosteeel.com, even from an environmental standpoint the use of such advanced materials enables to reduce the mass of vehicles by 25% over traditional automotive steels, as it can be observed in Figure 3.10.

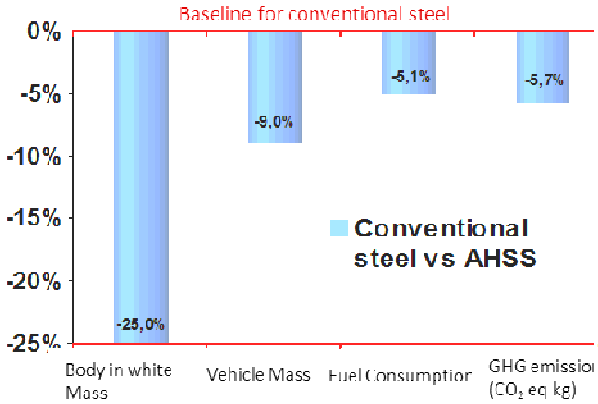

Figure 3.10: Comparisons (% reductions) between AHSS and conventional steels (Ingarao et al. (2011a) adapted from www.wordautosteeel.com).

Aluminium alloys: primary aluminum is produced by electrolysis where the Hall-Héroult process is generally utilized. To produce 1 ton of aluminum, 1.9 tons of alumina are required which means 4.2 tons of bauxite and 13,000-18,000 kWh/ton aluminum produced (Geyer (2007)). The process is carried out at 950°C by using carbon anodes under high intensity electrical current (www.eaa.net). Bauxite residues referred as ‘‘red mud’’ at the end of this process determine large amounts of solid waste. Additionally, there are high emissions of airborne and waterborne pollutants (like fluorides, polycyclic aromatic hydrocarbons, sulphur dioxides, carbon dioxides and per-fluorocarbons), cathode waste and high-energy requirements. In (Puri et al. (2009)), a Life Cycle Assessment of an Australian automotive component details higher aluminum energy consumption, global warming potential (GWP) and acidification potential (AP) in the production phase with respect to other automotive materials. Similar results are reported by Shaw and Coates (2009). Furthermore, higher manufacturing energy is consumed compared to traditional steels due to aluminum formability issues (Omar (2011)).

On the other hand, very effective results have been obtained over the years by replacing traditional steel with aluminum alloys for automotive applications (Du et al. (2010)). It has been analyzed that each kilo of aluminum replacing mild steel, cast iron or high strength steel saves 13kg to 20 kg of greenhouse gas (GHG) emissions. Moreover, aluminum results more effective than AHSS both as weight reduction, as it can be drawn from Figure 3.11 below, and fuel saving, as it can be observed instead in Figure 3.12.

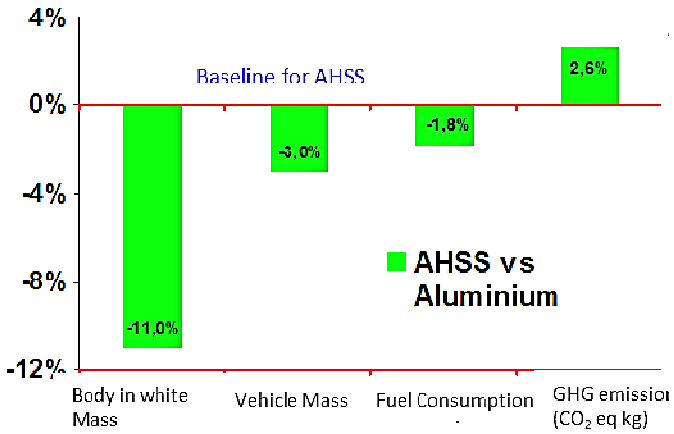

Figure 3.11: Comparisons (% reductions) between aluminum and AHSS (Ingarao et al. (2011a) adapted from www.wordautosteeel.com).

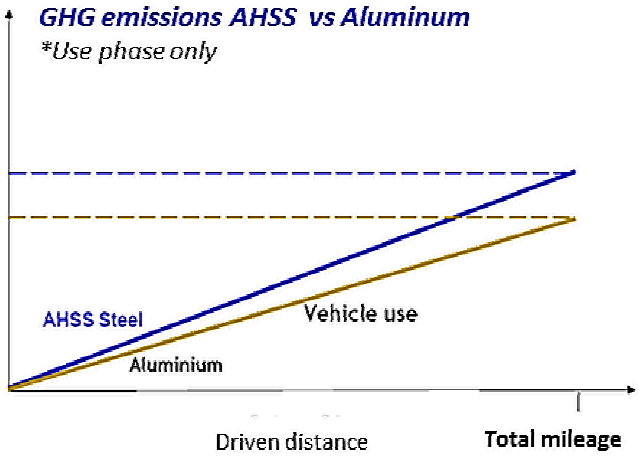

Figure 3.12: GHG emissions from aluminum in contrast with AHSS (Shaw and Coates (2008)).

In www.eaa.net, the trend of the aluminum usage is also reported: in 2020 about 20 million tons of aluminum is going to be used for transportation out of 60 million tons of total applications.

Magnesium alloys: the most of magnesium is produced in China by intensive energy processes, like Pidgeon, electrolytic, Carbothermic and solid oxygen-ion with membrane (SOM) ones, emitting a large amount of GHG (Cherubini et al. (2008)). Despite being very attractive because of lower production costs, carbothermic and SOM processes have not been commercially developed yet, while less Mg is produced by electrolysis over Pidgeon process due to high production costs (Cherubini et al. (2008), Ingarao et al. (2011a)).

11 tons of dolomite ore and 1.1 tons of ferrosilicon are used to get 1.0 ton of magnesium by Pidgeon process, while 11 to 13 MWh of electrical energy are consumed together with

4.5 to10 tons of coal per ton of magnesium (Ingarao et al. (2011a)). Thus, high energy requirements are involved in the primary production along with high GHG emissions. Figure 3.13 compares GHG emissions from primary production by material.

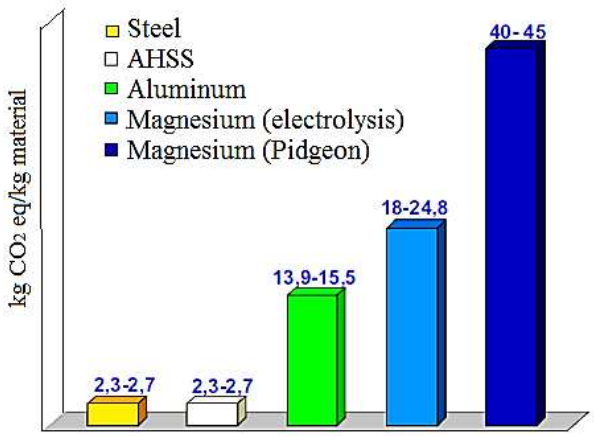

Figure 3.13: Average GHG emissions from primary production (Ingarao et al. (2011a) adapted from Shaw and Coates (2008)).

From Figure 3.13, magnesium produced by Pidgeon process is the most impactful over other LWMs. Despite having high energy requirements and GHG emissions from primary production, according to Du et al. (2010) magnesium alloys might enable a significant weight reduction together with fuel saving and GHG emissions in the use phase of vehicles life cycle. According to Das (2008), by replacing steel with magnesium for manufacturing of some automotive components (i.e. chassis, interior and body structure), the total weight of the vehicle would be reduced by 5.7% while the GHG emissions through the entire life cycle would decrease by 0.60 ton. Totally, 82 kg of Mg would be necessary over 165 kg of steel. Behrens et al. (2005) observed a weight reduction of 62% by using magnesium over steel and of about 41 % over aluminum for the same component.

Tailored Blanks (TBs): the possibility to use materials efficiently comes also from the applications of TBs. As it was earlier mentioned, TBs are sheets of variable thickness, material alloys or material grades: a smart location of both mechanical properties (like strength for automotive applications) and geometrical features (like different thicknesses) is possible, enabling material saving, weight reduction and even better performances for load-optimized components (Kleiner et al. (2003)). Figure 3.14 shows typical applications of TBs to the automotive manufacturing.

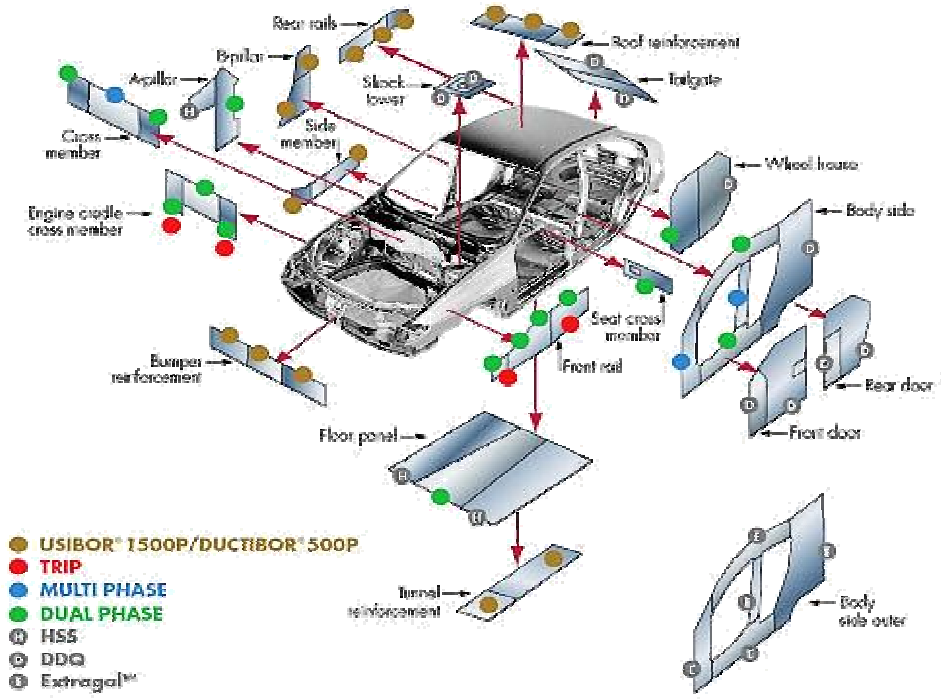

Figure 3.14: Applications of TBs to automotive manufacturing (www.arcelormittal.com/fce/repository/Tailored_Blanks/Catalogue-Chapter1.pdf).

Data related respectively to North American and European and Asian applications are also showed in Figure 3.15 and 3.16.

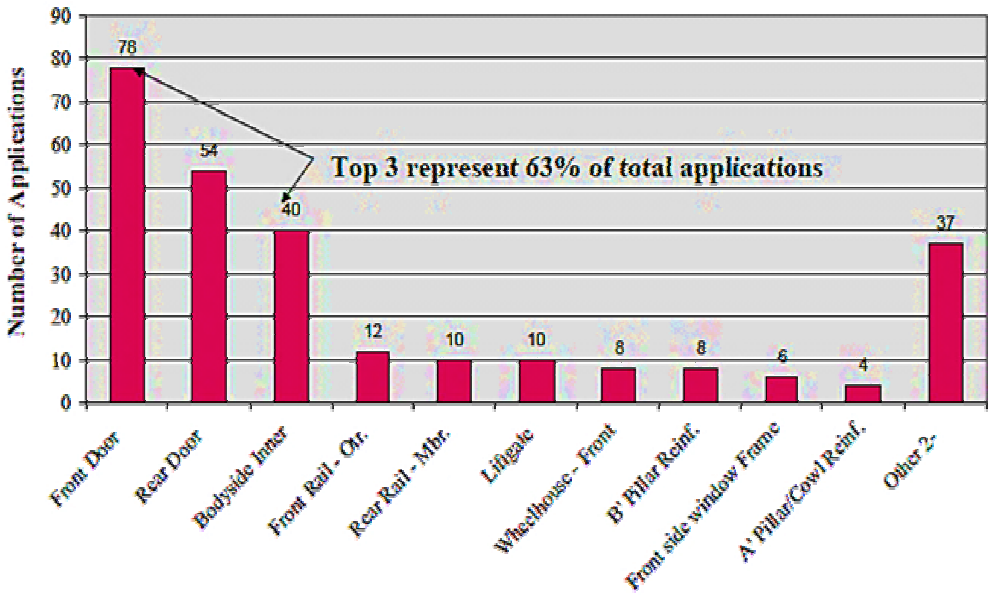

Figure 3.15: North American applications of TBs (Skilliter (2007)).

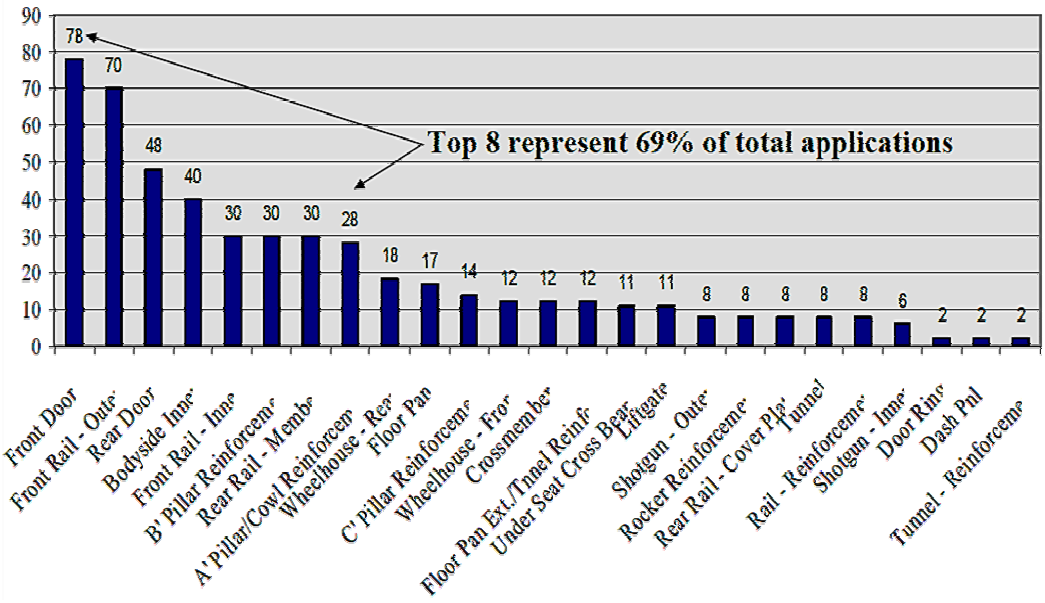

Figure 3.16: European and Asian applications of TBs (Skilliter (2007)).

TBs can be categorized as follows: Tailor Welded Blanks (TWBs), joined with a linear weld seam, or Tailor Engineered Blanks, if the weld seams is not linear; patchwork blanks, which are sheets, not necessarily of the same material, overlapped to get higher strength just where it is necessary; Tailor Rolled Blanks (TRBs) with uneven thickness through sheets of homogenous materials, provided by Flexible Rolling (FR) processes (Ryabkov et al. (2008)). Moreover, Strip Profile Rolling operations (SPR) can be carried out by a roll system inducing a continuous material flow to get defined thickness profiles. By combining FR and SPR, blanks with variable thickness both through the length and width directions can be produced (Ryabkov et al. (2008)): profiles with variable thickness are first obtained through by FR; then, a defined cross section is rolled by SPR. Figure 3.17 shows examples of TWBs and TRBs, while Figure 3.18 shows a sketch of Flexible Rolling combined with a Strip Profile Rolling process.

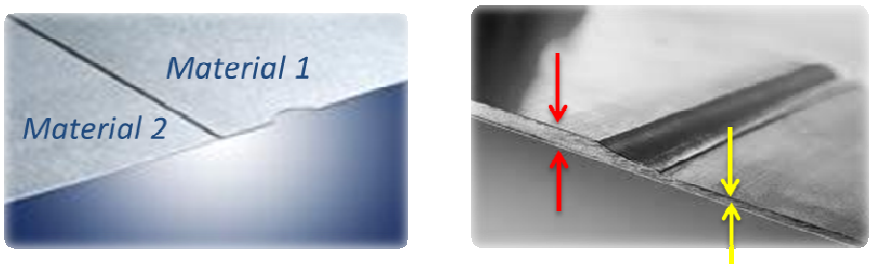

(a) (b)

Figure 3.17: Tailored Welded Blanks (a) and Tailored Rolled Blanks (b).

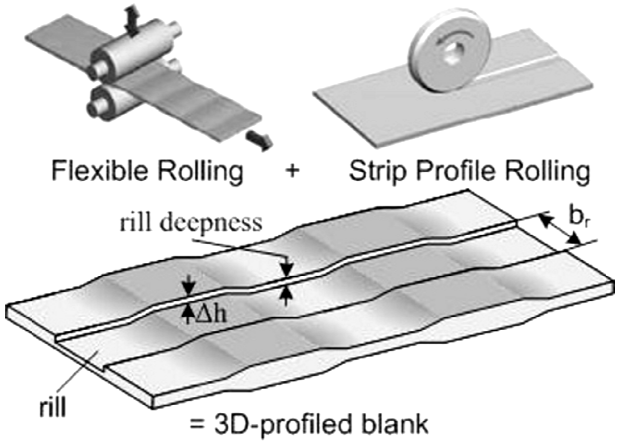

Figure 3.18: Combination of Flexible Rolling (FR) and Strip Profile Rolling (SPR) (Ryabkov et al. (2008)).

The smart combination of uneven thicknesses or different material alloys through the same blank is a key factor towards weight reductions and efficiency in material use: where lower loads will be applied, material can be locally saved, while a ticker material or a different material grade would be located where higher loads will be instead applied.

Moreover, the application of TBs in the automotive sector is a smart lightweight solution. Figure 3.19 sketches a front inner door manufactured by traditional blanks where usually hinge reinforcement is commonly welded to get locally a higher strength. Sealing is also needed in between of the two blanks to improve the corrosion resistance. On the contrary, Figure 3.20 shows how the application of tailored welded blanks for the manufacturing of same component would eliminate the reinforcement.

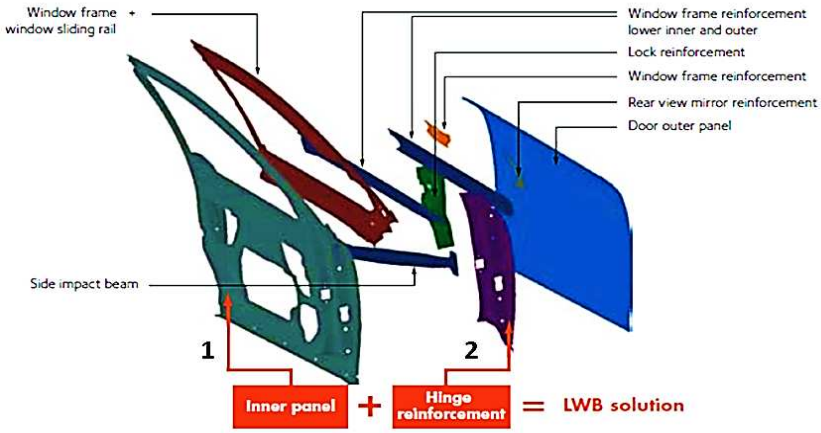

Figure 3.19: Front inner door from www.arcelormittal.com/fce/repository/Tailored_Blanks/Catalogue-Chapter1.pdf

Figure 3.20: Application of TB to the front inner door (adapted from Fenton and Mould).

In the application showed above, the use of TBs allows saving material by eliminating the reinforcement and by using thinner blanks as well. Scraps reduction by properly shaping the initial blank shape is also possible. Figure 3.21 provides the geometrical details of the initial blank comparing traditional blanks with TBs.

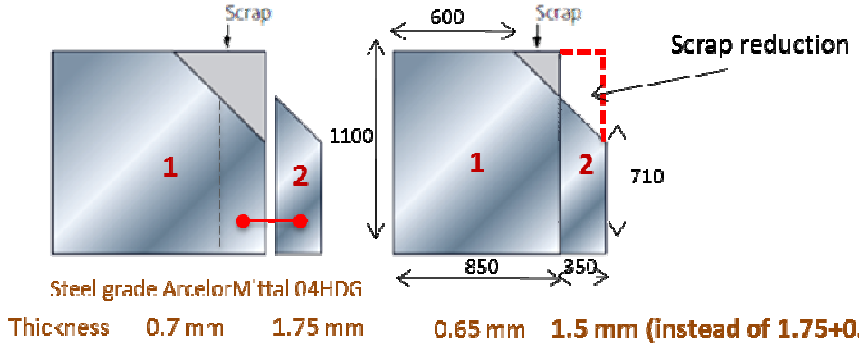

Figure 3.21: Scrap reduction and material saving by TBs over traditional blanks (adapted from www.arcelormittal.com/fce/repository/Tailored_Blanks/Catalogue-Chapter1.pdf).

As a matter of fact, tailored blanks generally provide with higher stiffness and maximum deep drawing depth over traditional blanks with even thickness (Meyer et al. (2008)). In fact, tailored blanks optimized by thickness distribution can enhance the maximum draw depth even by 19%, while reducing mass by 9% (Meyer et al. (2008)). Some researchers focused on forming and processing TRBs for lightweight crash structure (i.e. car cross member) (Kleiner et al. (2006)): tailor rolled crash structures for the automotive industry turned out to be as lighter as 13% than similar structures with homogeneous material, featuring at the same time an improved structural behaviour under static and dynamic load tests. Recently, integrated processes combining Tailor Rolled Blanks with advanced

manufacturing technologies like the high pressure sheet metal forming (HPSMF) were investigated (Kopp et al. (2005), Urban et al. (2006)): significantly higher stiffness has been observed for complex tailored rolled lightweight components manufactured by high-pressure sheet metal forming.

Patchwork blanks have become of interest as well: blanks reinforced in various areas with metal pieces of user-defined contours, so-called patches, are formed to add strength where it is needed (Geiger et al. (2005)). Welding constraints like edge conditions for butt welding are so eliminated with great flexibility and generally less costs than conventional TWBs.

3.1.1.1 Recycling strategies for automotive materials.

As it was earlier discussed, despite having a great potential as weight reduction and fuel saving, LWMs also feature high primary energy requirements, which might balance all the benefits from their application through the entire life cycle. Therefore, beside the use of lightweight materials, recycling such materials has become a crucial strategy as well, as it is discussed by Ingarao et al. (2011a).

Iron and steel are still the most recycled materials worldwide but other materials have high recyclability rate as well: magnesium is highly recyclable (Abu-Farha and Khraisheh, (2008)); aluminum alloys are 100% recyclable over uses and secondary aluminum alloys are like primary by properties (Gronostajski and Matuszak (1999)). From an environmental standpoint, just the 5% of the energy generally required to produce such materials is consumed for recycling. Figure 3.22 details the overall material flow within the automotive manufacturing chain. End of life is highlighted with indication of both recyclable parts and waste for final disposal, whose difference is better shown in Figure 3.23 for a typical passenger car.

As far as aluminum alloys, conventional recycling is carried out by melting with a high loss of material and energy consumptions (Gronostajski and Matuszak (1999), Gronostajski et al. (2000)). Recycling efficiency in fact is generally lower than 55%.

Novel recycling technologies are instead available in the technical literature for aluminum alloys: in particular, they are direct solid state techniques able to converts chips and scraps to a compact mixture by cutting chips to a granulated product that is then cold pressed and hot extruded or hot forged (Gronostajski and Matuszak (1999), Gronostajski et al. (2000)).

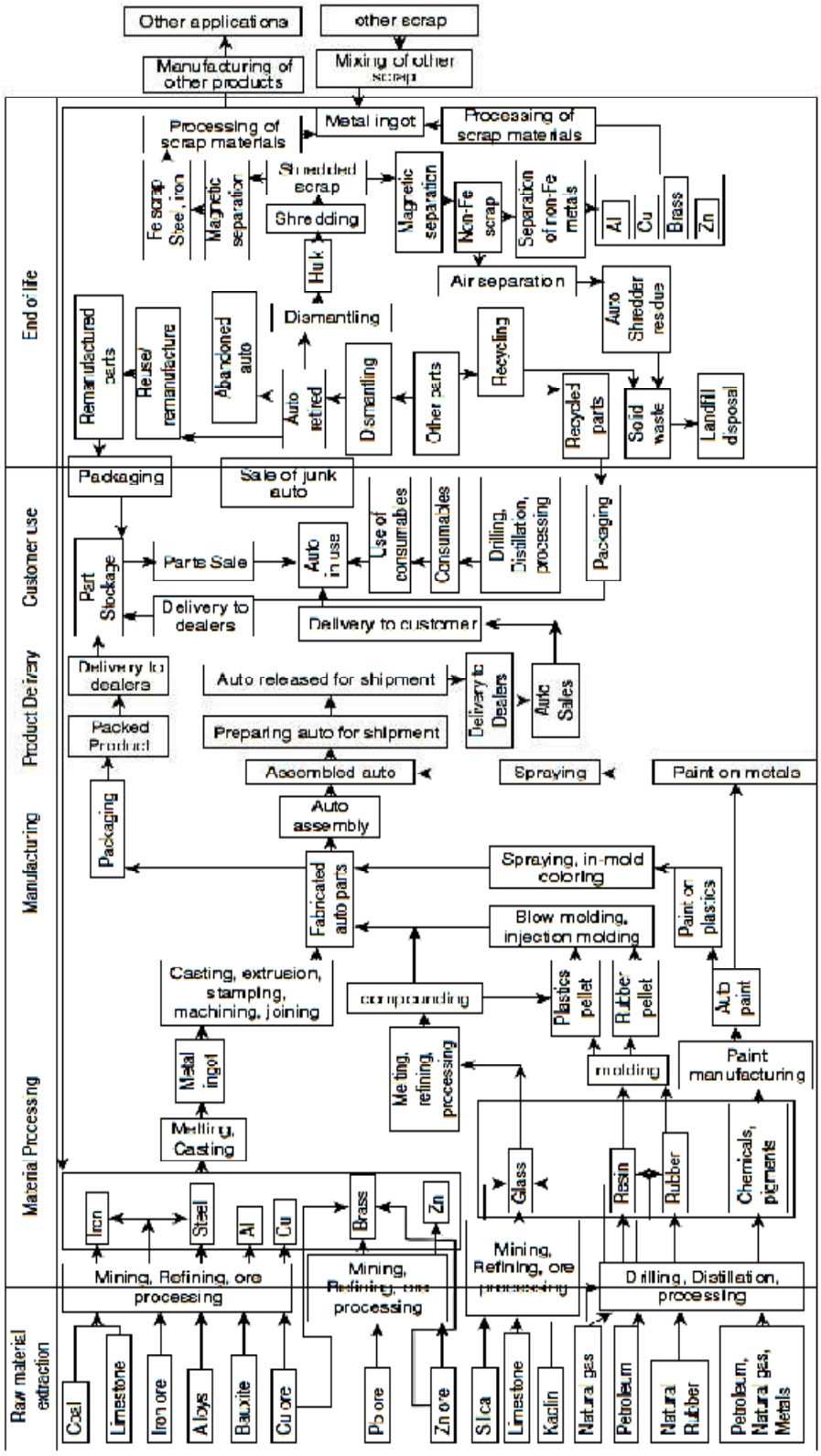

Figure 3.22: Overall material flow within the automotive manufacturing chain (Omar (2011)).

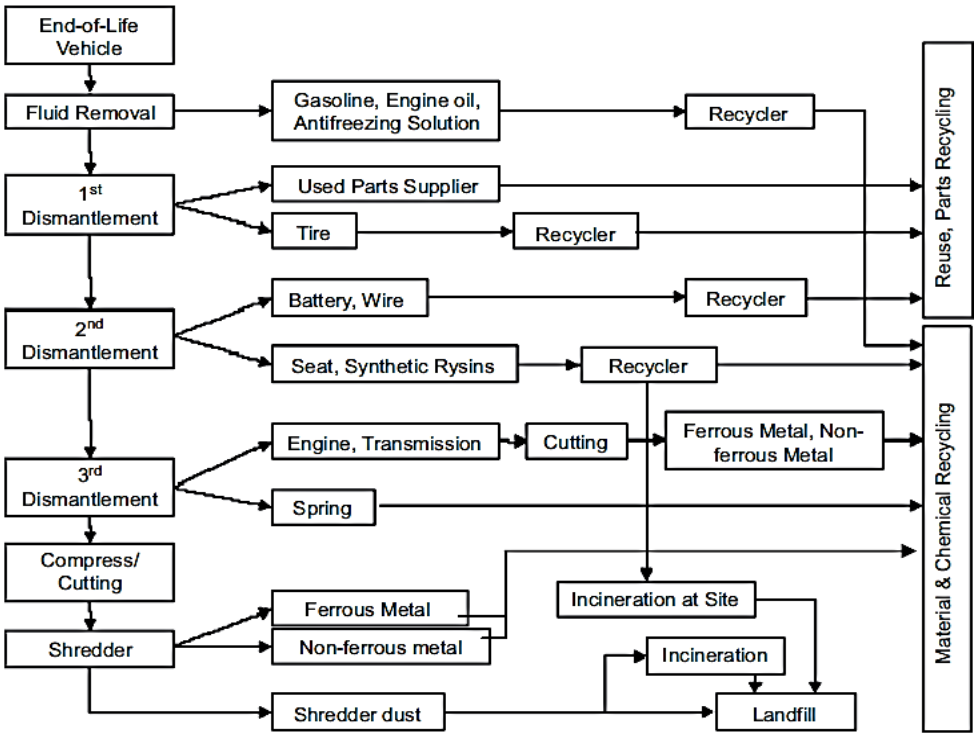

Figure 3.23: End of Life of automotive materials (Omar (2011)).

Higher recycling rate can be observed (just the 5% of material lost) and lower energy consumption (30% less). Solid state recycling can be applied also to iron, copper and it can be even extended to iron casting.

Samuel (2003) proposed a direct recycling method with intermediate milling, which allows low air emissions and high material saving over conventional methods.

An evolution of the direct recycling technique earlier discussed is reported by Fogagnolo et al. (2003): in particular they proposed to recycle chips directly by cold or hot pressing followed by hot extrusion, thus avoiding the milling step. They investigated an AA6061 aluminum alloy reinforced by Al2O3 and analyzed both cold and hot pressing steps by different extrusion ratios. Allwood et al. (2005) studied the possibility to substitute the hot extrusion process with a cold bonding method with the consideration that a considerable advantage could be obtained in terms of energy saving.

Tekkaya et al. (2009) proposed to reuse aluminum by direct hot extrusion in order to reduce the use of primary aluminum and to avoid melting processes for recycling. They came up with the conclusion that the yield strength of extruded chips is comparable with profiles extruded from solid billets.

A direct recycling of aluminum scraps was also presented by Güley et al. (2010): pins of

1050 aluminum alloy from extrusion were combined with AA-6060 aluminum chips from turning, obtaining the mixture in Figure 3.24 that it was cold compacted into billets and then hot extruded. Just the 10% of the energy required for conventional recycling by re-melting was required.

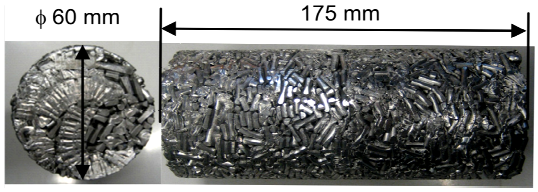

Figure 3.24: Compacted aluminum mixture of scrap and chips (Güley et al. (2010)).

As it is well discussed by Ingarao et al. (2011a), magnesium recycling has been investigated in the technical literature as well. Studies on recycling processes by re-melting showed that the recycled Mg alloys exhibit poorer service properties due to contaminations. Recycling by solid-state processes has been investigated for Mg alloys as well: machined chips are directly recycled by hot extrusion without re-melting, providing with a really efficient method avoiding oxidation loss and saving energy.

Studies were carried out on the extrusion of ZK60 magnesium alloy from machined chips in order to investigate the mechanical properties at microstructural level (Nakanishi et al. (1998)). On the other hand, Chino et al. (2006a) and (2006b) investigated the corrosion behaviors of pure Mg and AZ31 Mg alloy recycled by a solid-state process: the recycled specimen showed better corrosion resistance over pure magnesium along with better mechanical properties.

Wu et al. (2009) proved that AZ31B magnesium specimens recycled by hot extrusion feature higher strength because of the grain refinement strengthening. They observed that the grain size, the oxide amount and the density of billet influence the elongation of recycled materials. Thus, they came up with the result that the mechanical properties of recycled materials can be enhanced if the oxide dispersive distribution is reached.

In the end, a novel recycling method is investigated at the University of Palermo for aluminum alloys as reported by Ingarao et al. (2001a): the action of a rotating stirrer together with the plastic deformation by a plunger induce the material softening and allow mixing and homogenizing the material itself. Such a bonding process, which also allows oxide dispersion, is similar to the Friction Stir Welding technique.

In conclusion, the use of LWMs in manufacturing and especially in the automotive sector leads to several issues beside their remarkable potential as low density materials. A case

study is analyzed in the following section in order to breakdown all the advantages and disadvantages such materials might arise through their life cycle in term of environmental issues and performances for sheet stamping applications.

3.1.1.2 Case study: material substitution for automotive applications - a comparative life cycle analysis.

As it was earlier discussed, lightweight materials have become an important strategy in the automotive industry to enable vehicle weight reduction and reduce fuel consumption. However, it appears clear from the discussion above that when developing specific strategies the overall benefits of any material ought to be analyzed throughout its entire life cycle to comprehend energy/environmental differences that arise during its processing and its final use. As a matter of fact, each phase is characterized by significantly different environmental impact: saving fuel in the use phase, and accordingly greenhouse gases emissions may mean for instance increase the environmental effect from manufacturing or material acquisition. A key example is aluminum which despite having great potential in the use phase requires large amounts of energy to process: aluminum alloys provide lightweight benefits in the usage phase in automotive applications, but aluminum possesses requires relatively large amounts of energy for raw material extraction and processing.

Following, a comparison between aluminum and steel utilizing a life-cycle approach: in particular, the use of the AA5250 alloy and a draw quality (DQ) steel is contrasted for automotive applications by using GaBi4 (Gabi Education Handbook). A cradle-to-grave analysis was carried out as useful to map the eco-efficiency of using aluminum alloys over traditional automotive materials and the environmental impact was broken down by phase. The term “eco-efficiency” will be used as coined by the World Business Council for Sustainable Development (WBCSD) (Schmidheiny (1992)), which defines the idea of producing goods and services at a lower consumption of resources and correspondingly lower amounts of waste and pollution.

Mapping both material life cycles by environmental impact was then possible thereby, addressing improvement directions and highlighting possible strategies in the use of such light weight alloys: the importance of incorporating a recycling strategy came up as solution to leverage aluminum’s low-weight attributes.

Thus, as suggested by the first cradle-to-grave analysis, a recycling strategy was

considered as a possible scenario in the aluminum lifecycle. As it is known, aluminum is a highly recyclable with secondary and primary aluminum having the same properties. The content of recycled aluminum in body-in-white applications is still 0%-11% though while about 15% of secondary steel is used for automotive components (Geyer (2007)). An extensive recycling strategy could effectively leverage aluminum's low-weight attributes in the product use phase and improve its eco-efficiency and overcome its high initial processing energy requirements.

3.1.1.2.1 Comparative cradle-to-grave analysis.

The first important step of any life cycle assessment (LCA) is the identification of the goal of the study and the definition of the system boundaries that determine its scope. Based on the scope of the assessment, different classifications of life cycle assessment result such as cradle-to-gate, gate-to-gate, to name a couple. In this case study, a comparison between two different automotive materials throughout their life cycle is sought. In this manner, all phases of each component's life cycle are accounted for. In particular, raw material extraction, primary shaping processes, manufacturing processes, use phase and recycling are all included within a cradle-to-grave analysis of two different automotive components, namely a fender and a hood (Figure 3.15). A Draw Quality cold rolled carbon steel (DQ) and the AA5052 aluminum alloy (AA) were evaluated in this analysis.

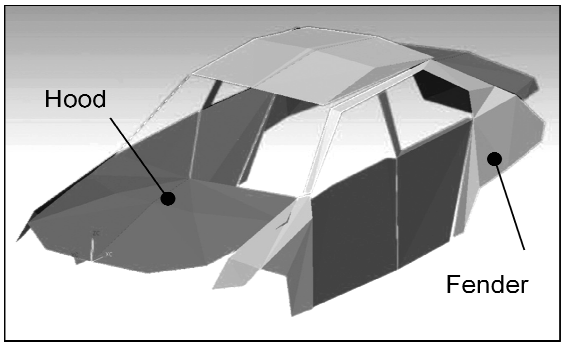

Figure 3.25: CAD model of the analyzed automotive parts (Omar (2011)).

Table 3.3 reports each component's weight and manufacturing energy by material (Omar (2011)). In particular, by using aluminum in lieu of traditional steel it is possible to save up to the 40% of weight (Δ%). Accordingly, a more efficient use of raw material is achievable as lower weight implies less input material. On the other hand, even though aluminum has lower yield strength than traditional steels, its lower strain hardening exponent often increases the number of shots required to get the same shape. In addition, higher spring-

back occurs in general, which increases its forming energy requirements.

	Hood			Fender		
	AA	DQ	Δ%	AA	DQ	Δ%
Weight [kg]	10.57	17.75	-40%	2.82	4.26	-35%
Mfg. energy [MJ]	126	72	+75%	82.8	46.8	+77%

Table 3.3: Input material and energy requirements (adapted from Omar (2011)).

When compared to traditional automotive materials, the design of the aluminum fender adds ∼+10 kWh/vehicle, while the aluminum hood adds ∼+15 kWh/vehicle. Namely, such energy accounts for all the steps required to manufacture the same final geometry.

The LCA software Gabi4 was used to evaluate the environmental impact of the life cycle of each component by the two different materials. In particular, Gabi4 is a LCA tool incorporating several databases for sustainability analyses of both products and processes. It is able to model material and energy flows through processes within life cycle of customized length and to calculate the environmental burden of each phase by a number of available LCA methodologies. Both global and intermediate evaluations are then possible, together with what if or parametric analyses. An example of the flows modeled by Gabi is shown in Figure 3.26, while Figure 3.27 shows an example of environmental balance by input and output flow categories.

In particular, as the environmental impact from energy is location dependent, the power grid location was specified to be in the US. Therefore, the average US power grid source mix was considered. Moreover, only the weight induced fuel consumption was accounted for in the use phase of the investigated components according to Koffler and Rohde-Brandenburger (2009). Gasoline was considered as fuel, for a commonly assumed life driving distance of 200,000 km (55% city / 45% highway).

Data were weighted and normalized in Gabi by using CML2001 as the LCIA (Life Cycle Impact Assessment) method. Thus, the following impact categories were considered individually and then aggregated to obtain a global environmental score referred as CML 2001 eco-score: Abiotic Depletion (ADP [kg Sb-eq]), Acidification Potential (AP [kg SO2-eq]), Eutrophication Potential (EP [kg Phosphate-eq]), Global Warming Potential (GWP 100 years [kg CO2-eq]), Ozone Layer Depletion Potential (ODP, steady state [kg R11-eq]), Photochemical Ozone Creation Potential (POCP [kg Ethene-eq]).

The environmental impact from dies and tooling systems was neglected here, as the same

manufacturing system was assumed to be used.

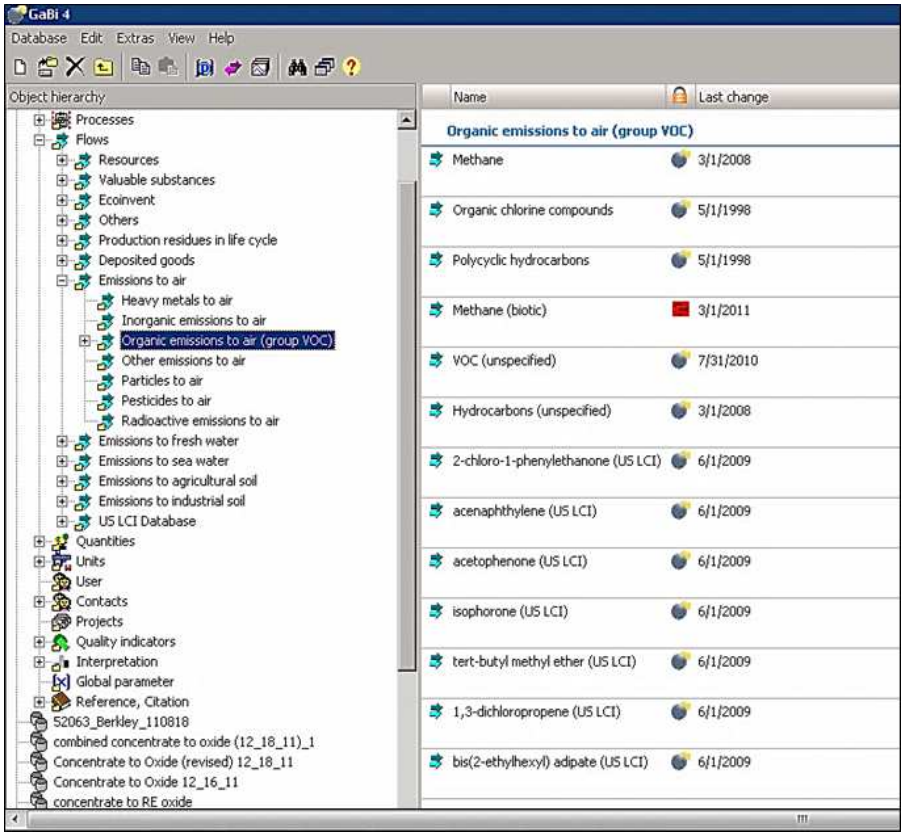

Figure 3.26: Flows modeled by GaBi.

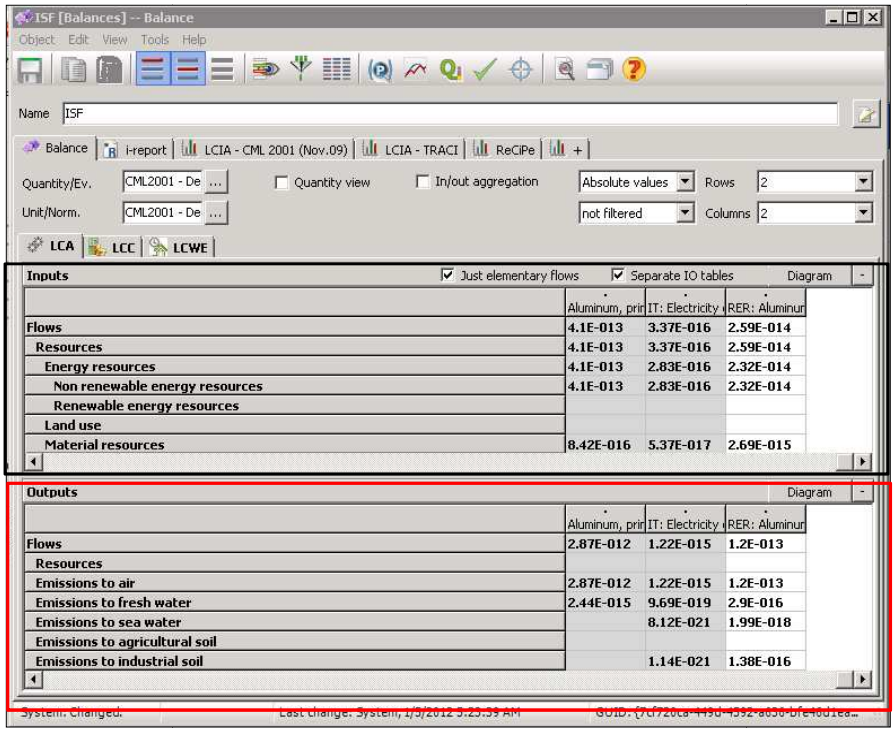

Figure 3.27: Example of environmental balance by GaBi.

AA5052 Aluminum Case Study.

A diagram of the Gabi model for the aluminum case study is shown in Figure 3.28, which is the same for both the hood and the fender case study. Since aluminum primary production is a long process chain, the entire life cycle inventory was therefore included in such cradle-to-grave analysis.

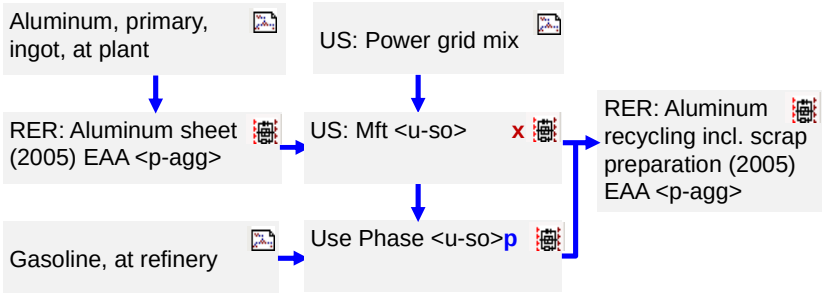

Figure 3.28: Gabi model of the aluminum case study.

The emissions analysis by impact category is shown in Figure 3.29 for the fender alone, but the same proportions on average were observed for the fender components as well.

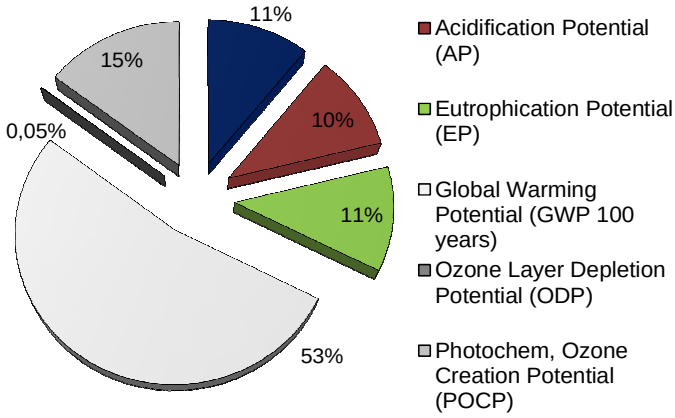

Figure 3.29: Emission breakdown from aluminum usage.

Global Warming Potential is noteworthy as 275 kgCO_2eq corresponds to 53% of the total weighted and normalized aluminum emissions, while, for instance, eutrophication potential is as high as 0.31 kg Phosphate-eq. The detailed emissions calculations by categories are reported in Table 3.4.

Impact Category (CML2001)	Hood	Fender
ADP [kg Sb-eq]	1.58	0.479
AP [kg SO2-eq]	1.47	0.46
EP [kg Phosphate-eq]	0.308	0.0849
GWP [kg CO2-eq]	275	83.8
ODP [kg R11-eq]	4.5E-006	2.35E-006
POCP [kg Ethene-eq]	0.304	0.0849

Table 3.4: Emissions of aluminum components by impact category.

To address strategies in material usage for automotive components, a breakdown by life cycle phases provides more insight: Figure 3.30 summarizes the environmental impact of the two vehicle parts allowing further discussion.

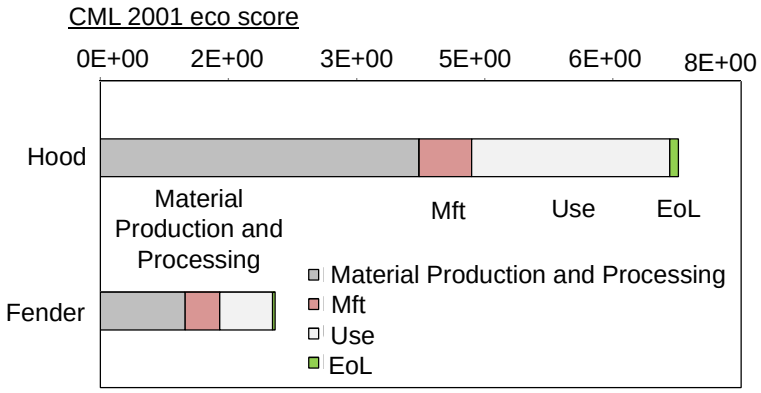

Figure 3.30: Aluminum's CML eco-score by life cycle phase.

The total impact from aluminum usage is about 7.5E-10 for the hood and 2.3E-10 for the fender case study, but in any case, the impact from the raw material extraction and processing is indeed the most critical one, followed by the use phase. It suggests that strategies aimed to improve the efficiency in material use should be addressed in order to reduce the consumption of input material. For such a purpose, non-conventional stamping technologies may increase formability of aluminum alloys while performing weight reduction at the same time (Ingarao et al. (2011a)). A more efficient use of material could be pursued by smoother mechanical deformations enabled by such technologies and allowing the use of thinner blanks for a given final geometry. For instance, incremental forming processes of aluminum components allow material savings of up to 10% when compared to traditional stamping technologies (Ingarao et al. (2011b)). Hydroforming (Novotny and Geyer (2003)) and superplastic forming processes (Fadi and Marwan (2008)) allow using thinner blanks when compared with traditional deep drawing operations. It bears consideration that the energy required by aluminum recycling is much lower than that used in primary production and processing and thus yields a promising energy saving scenario for aluminum usage. Finally, even though the fender is four times lighter than the hood, the difference in terms of environmental impact from manufacturing is not as remarkable.

Draw Quality (DQ) Cold Rolled Carbon Steel Case Study.

Figure 3.31 shows the Gabi model for the DQ steel case study. Similar proportions

amongst the emissions categories by impact were observed again between the steel hood and fender. Thus, Figure 3.32 simply shows the results of the hood case study. Emissions details are reported in Table 3.5.

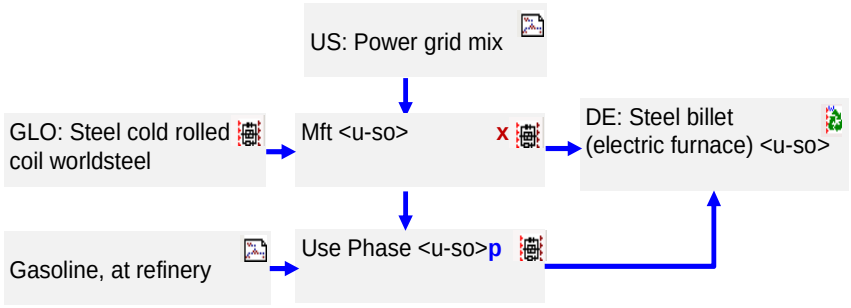

Figure 3.31: Gabi model of the steel case study.

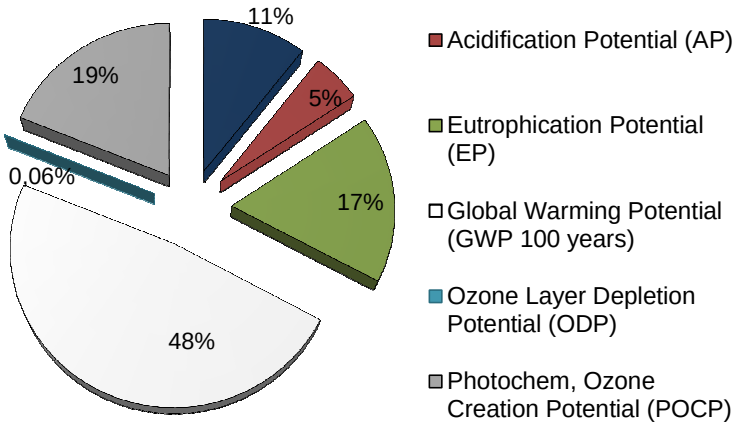

Figure 3.32: Emission breakdown of the steel case study by category of impact.

Impact Category (CML2001)	Hood	Fender
ADP [kg Sb-eq]	1.32	0.352
AP [kg SO2-eq]	0.513	0.164
EP [kg Phosphate-eq]	0.436	0.106
GWP [kg CO2-eq]	210	56.7
ODP [kg R11-eq]	2.86E-006	1.36E-006
POCP [kg Ethene-eq]	0.363	0.0894

Table 3.5: Emissions of steel components by impact category.

An overview of steel emissions by life cycle phases is shown in Figure 3.33. While the primary production of aluminum components result in the most significant source of emissions, the use phase of steel components heavily contributes to their cradle-to-grave environmental impact. Therefore, while efficiency in material use seems to be the best strategy towards a more sustainable use of aluminum for automotive applications, weight reduction seems to be the most promising action to carry out for steel components with

lower environmental impact life cycle. Moreover, impact from steel recycling is about 23% of its primary production.

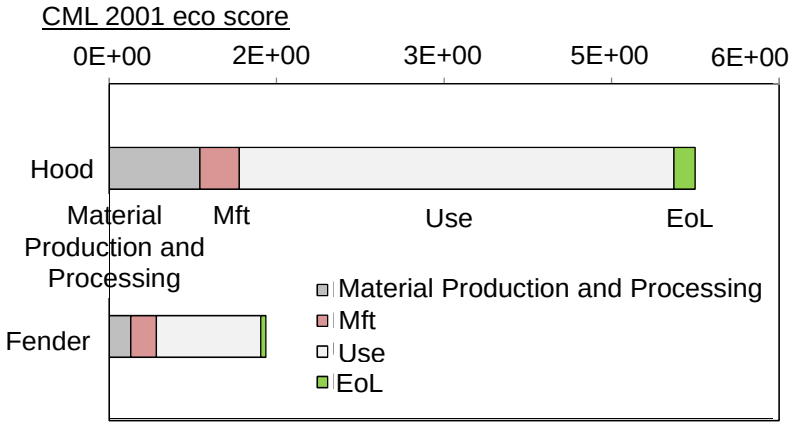

Figure 3.33: Steel's CML eco-score by life cycle phase.

It has been observed that the usage of advanced high strength steel (AHSS) in automotive applications allows production of even 25% lighter automotive steel components (Geyer (2007)). By combining good formability features with good mechanical properties, as with AHSS, it is possible to manufacture thinner blanks for a given final geometry while satisfying necessary performance requirements.

3.1.1.2.2 Comparison of the results.

The comparison of the CML eco-score between aluminum and steel components is reported by life cycle phase in Figures 3.34 and 3.35, respectively for the hood and the fender case studies.

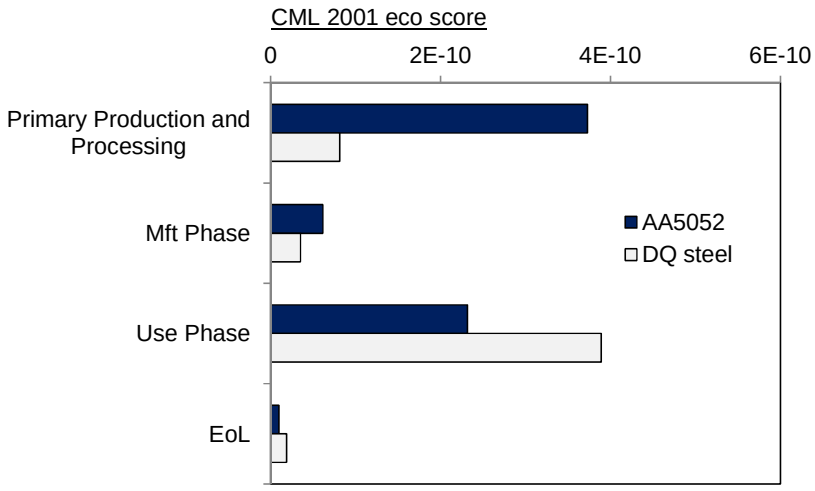

Figure 3.34: Comparison of the results (hood case study).

These results indicate that aluminum, either in the hood or the fender case study, is

globally more impactful than steel. While the total environmental impact from steel usage is respectively 6.5E-10 and 1.7E-10 for the hood and the fender case studies, aluminum's impact is 7.5E-10 for the hood and 2.3E-10 for the fender. Also, despite enabling a significant lowering of the environmental burden in the use phase, the impact from aluminum primary production and manufacturing phase negatively balances such advantages as fuel saving.

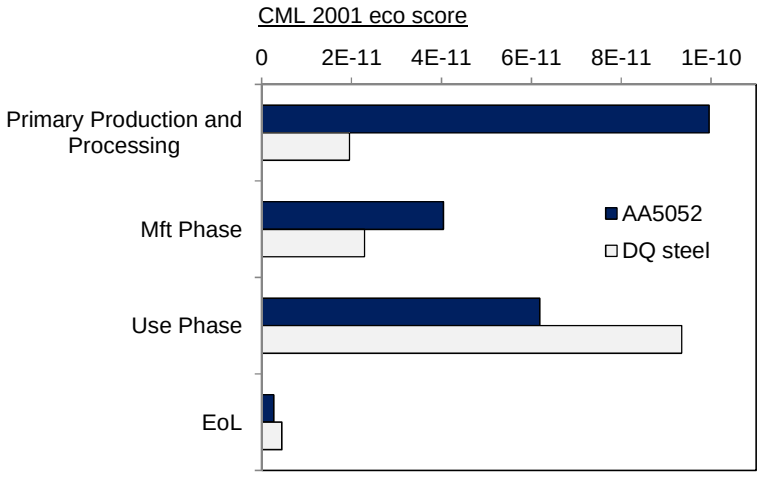

Figure 3.35: Comparison of the results (fender case study).

To better understand how significant the advantage or disadvantage of using aluminum might be, a leverage effect index (LE [%]) was formulated as follows:

$$LE = \frac{impact(DQ) - impact(AA)}{impact(AA)} * 100 \quad (3.1)$$

This LE index effectively quantifies the potential reduction (if positive) or increase (if negative) in the total emissions of each life cycle phase, which relates to the usage of aluminum alloy over traditional draw quality steel to the manufacture of a given automotive component. Figure 3.36 shows the leverage effect enabled by aluminum usage in both the automotive applications.

The analysis of the LE index reveals that even though the aluminum usage may globally increase the environmental burden, when contrasted with steel, a significant leverage effect may come from the recycling phase over the upstream life cycle phases. Importantly, by recycling aluminum, it may be possible to negate the disadvantage from aluminum primary production with respect to steel and perhaps even obtain a more sustainable life cycle.

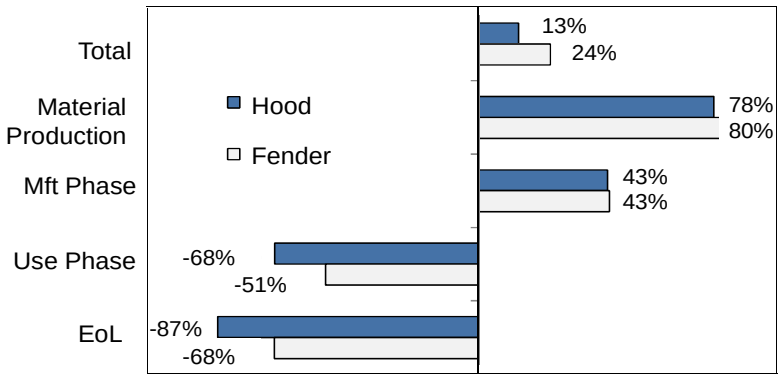

Figure 3.36: Leverage effect by aluminum usage.

3.1.1.2.3 Scenario analysis.

The results from the cradle-to-grave analysis identified efficiency in material use as the best strategy to lower the environmental impact from aluminum usage. Meanwhile, solutions solely aimed at reducing weight, as with advanced high strength steel or other lightweight non-ferrous materials, resulted in being the main contributing factor to improving the sustainability of the steel life cycle. A scenario analysis was then carried out to evaluate whether efficiently using aluminum could allow such lightweight alloys to be regarded as sustainable for automotive applications.

In particular, a recycling scenario was assumed within a cradle-to-cradle approach: the impact of the recycling phase at the end of the life cycle was incorporated in a closed loop as a credit in the material production and wholly recycled material was considered just in the aluminum life cycle. In contrast, mixed steel was assumed to be used by just considering credits from recycling at the end of life. Figure 3.37 illustrates the model of the aluminum cradle-to-cradle scenario.

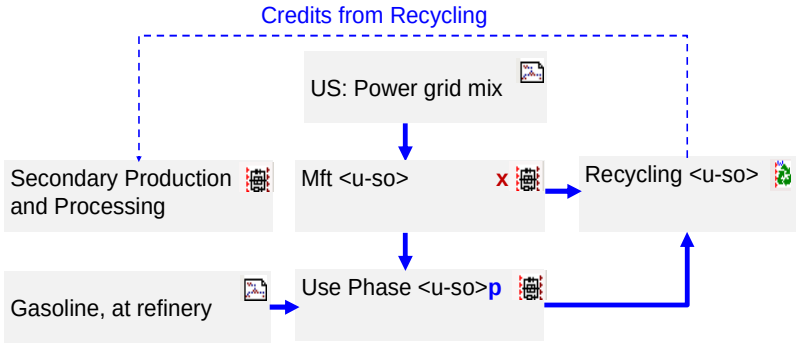

Figure 3.37: Cradle-to-cradle scenario.

If only recycled aluminum were to be used for automotive part production, it would be possible to drastically reduce the environmental score of the overall life cycle. For instance

for the hood case study, the CML eco-score of the cradle-to-grave aluminum life cycle would be about 4E-10 over 7.54E-10. Figure 3.38 details the scenario results for the hood case study. Analogous ratios resulted in the fender case study between the primary and recycled material per life cycle phase.

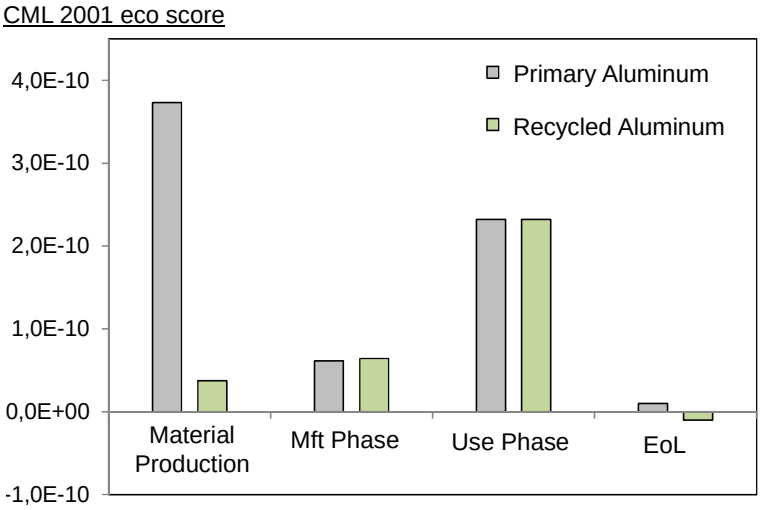

Figure 3.38: Balance of aluminum recycling scenario.

The secondary production of aluminum from recycled scrap requires just 5% of the total energy consumed in primary production and processing. Further, the environmental- score from producing 10.57 kg of primary aluminum would be as high as 3.73E-10, while the one related to secondary production of the same amount of aluminum would result in 1.7E-11. Of course, no changes occur in the manufacturing phase and in the use phase as well for a given aluminum weight. But, the energy saving achievable in the material production and processing would make aluminum strongly preferable to steel for automotive applications. Figure 3.39 shows the leverage effect, calculated by the LE index, enabled by a recycling strategy in comparison with steel, within a cradle-to-grave life cycle.

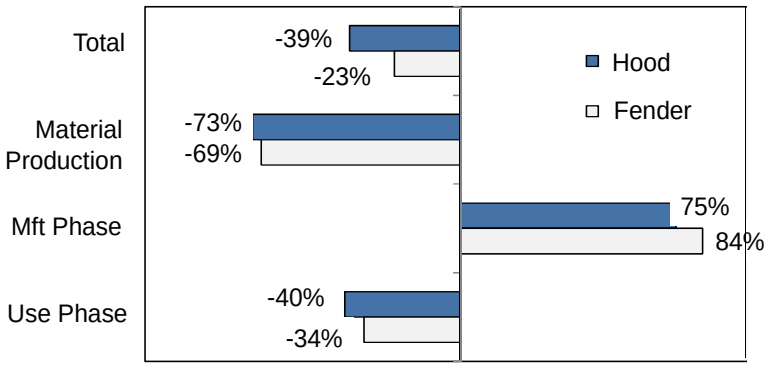

Figure 3.39: Leverage effect by recycled aluminum usage.

In this result, the eco-score alone of the manufacturing phase would be greater than the one corresponding to the same steel component, whereas over the other life cycle phases sizeable reductions in emissions would be possible.

Therefore, adoption of an aluminum recycling would provide a key strategy for emissions reduction by addressing the end use of these lightweight alloys in automotive part production. Today, recycling is the most effective solution to take advantage of the potential aluminum offers as a lightweighting solution in automotive applications. Otherwise, the prospective to save weight and accordingly fuel would be neutralized by its energy intensive primary production.

3.1.1.2.4 Summary and conclusions.

A cradle-to-grave analysis was first carried out in this paper to compare the use of aluminum alloys and traditional steel for automotive applications throughout their respective life cycles. Aluminum alloys, and more generally, other lightweight materials have grown in interest to the automotive sector for the significant weight reduction these materials potentially enable. Aluminum alloys also are characterized by the large energy requirements in their primary production and processing phase. Such large energy costs means that all the advantages from utilizing aluminum may be neutralized unless a comprehensive recycling strategy is adopted. Therefore, the life cycle in its entirety has to be accounted for to estimate how sustainable the use of lightweight materials is, when compared to traditional steels. A comparative cradle-to-grave analysis highlighted how sustainable steel usage would be in automotive part production if all the life cycle phases are fully taken into account. Moreover, different sustainable strategies from the life cycle analysis can guide an extensive recycling practice for aluminum components. A recycling scenario was investigated to evaluate the effect that aluminum recycling might leverage when compared with steel and a significant reduction of the environmental impact was observed. Also, only a widespread recyclable strategy could allow aluminum to be considered an environmental friendly material, otherwise its potential as fuel saving would be negatively affected by its primary energy requirements.

Nowadays, fuel saving by weight reduction is indeed one of the most promising strategies to reduce the environmental impact of the life cycle of automotive products, but the use of recycled materials offers additional opportunities towards environmental conscious

solutions for automotive applications.

3.1.2 Lightweight manufacturing technologies.

Beside the use of low density materials, lightweight manufacturing technologies may enable the capability to draw thinner blanks by smoother deformations, even while using low formability materials. In fact, one of the main issues related to the use of lightweight materials in particular in the automotive sector is their low formability, arising tough technical drawbacks limiting their applications. Therefore, enabling solutions and technologies are strongly required; otherwise all the benefits from lightweight would be neutralized. On the other hand, the capability of such techniques to smoothly induce plastic deformations over the material, allows weight reduction by using much thinner sheets.

In particular hot stamping has also been performed to enhance formability of automotive materials to get lighter components: titanium exhibits a better formability at temperatures higher than 500°C; the use of elevated temperatures below re-crystallisation induces lower yield point and strain hardening along with greater expansions in the case for instance of aluminium alloys. Additionally, higher processing forces and greater dimensional deviations arise in forming higher-strength, high-strength and ultra-high strength steels, involving high power machinery and great stresses on the forming tools and often requiring hot stamping (Neugebauer et al. (2006)).

Similarly, the hexagonal lattice structure with a low number of glide planes makes tough using magnesium for complex geometries, requiring forming processes at high temperatures. Investigations of the effect of temperature on deep drawing and stretch forming of several magnesium alloys are reported in the technical literature. The results showed a significant increase of the forming limits and higher limiting drawing ratios at temperatures between 200°C and 250°C (Neugebauer et al. (2006)). Results of hot hydraulic bulge tests were presented by Altan et al. (2005) for the Mg AZ31-O alloy: in particular, from room temperature to 225°C the bulge height increased from 12 mm to 38 mm at the strain rates of $0.025s^{-1}$. Behrens et al. (2005) developed a heated tool for deep drawing to investigate the formability of magnesium locally applying different temperature fields.

Research has been done also on the formability of commercially pure titanium sheets at room temperature up to 300 °C, whose results are synthesised in Figure 3.40 (Chen and

Chiu (2005)).

Figure 3.40: Ti cups drawn at different temperatures (Chen and Chiu (2005)).

Odenberger et al. (2008) analysed the thermo-mechanical properties of Ti-6242 by high temperature compression tests, observing good performances at high temperature against unsuccessful forming of the same alloy at room temperature.

Investigations were carried out also on the hot stamping of the quenchenable ultra high strength steels: Merklein et al. (2006) studied 22MnB5 for complex crash relevant components with a final strength over 1500 MPa. They observed that, despite having an initial ferritic-pearlitic microstructure with a tensile strength as high as 600 MPa, hot stamped 22MnB5 showed a martensitic structure with a strength 250 % higher (Hoffmann et al. (2007), Merklein et al. (2006)).

Besides hot stamping, non-conventional stamping technologies such as hydroforming, superplastic and incremental forming have been widely investigated over traditional deep drawing processes. Lately, besides the efforts produced on hydroforming operations at room temperature to increase the formability of lightweight materials (Geiger et al. (2005), Kang et al. (2004), Lang et al. (2004), Thiruvarudchelvan and Travis (2003)), investigations on thermal hydroforming have been done. Some researchers investigated formability, wall-thickness distribution, microstructure and strain distribution of aluminium alloys at enhanced temperatures for a tube hydroforming operation. Novotny and Geyer (2003) developed material tests to determine the behaviour of aluminium and magnesium alloys at elevated temperatures by proper hydroforming strategies. Interesting results on Mg alloys are reported by Neugebauer et al. (2005): the authors proved how crucial temperature is as process parameter in the design of a bonnet by tempered sheet metal hydroforming. As a matter of fact, no crack can be obtained by setting the process temperature from 200°C to 250°C, against wide crack areas at room temperature.

Hydro-mechanical deep drawing at high temperatures are even more effective than temperature-supported conventional deep drawing, in fact Neugebauer et al. (2006)

achieved higher limit drawing ratios for magnesium alloy at lower temperatures. Figure 3.41 compares the limiting drawing ratios for conventional and hydro-mechanical drawing of magnesium alloys, highlighting significant differences.

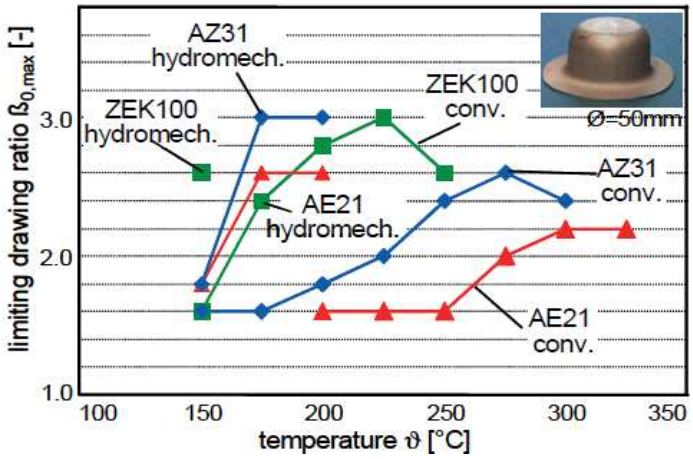

Figure 3.41: Limiting drawing ratios by hot hydro-forming and deep drawing of Magnesium alloys (Neugebauer et al. (2006)).

Additionally, superplastic forming processes (SPF) perform well with LWMs: studies confirmed a better formability by SPF over conventional sheet stamping processes, suggesting its potential applications to transportation (Abu-Farha and Khraisheh (2008)). SPF processes allow in fact a more uniform deformation of the material by the adaptive action of forming gas, replacing the punch action in conventional forming processes, under certain temperature conditions. Several lightweight alloys feature superplastic behaviour, like the Ti6Al4V titanium alloy, the 5083 aluminium alloy and the AZ31 magnesium alloy: to form such materials by any other technique would be unfeasible because of their strongly limited formability.

In particular, super plasticity is meant as the property of some materials to be deformed up to the 500% of the initial length, at temperature conditions usually higher than 50% of the material melting point. Figure 3.42 shows the achievable elongation of a superplastically formed specimen. This provides with the possibility to use blanks up to 40-50% thinner, and then to form materials usually hard to stamp at room temperature, like many lightweight alloys.

Studies prove that such alloys can be hydro-formed or super-plastically formed at lower temperatures than conventional stamping processes.

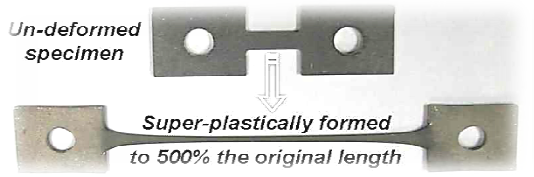

Figure 3.42: Super plastically formed specimen (Abu-Farha and Khraisheh (2008)).

As it is discussed by Ingarao et al. (2011a), studies on optimization approaches for superplastic forming of Mg AZ31 alloy were presented by Khraisheh et al. (2006) while investigations on post-superplastic forming (post-SPF) proposing a systematic approach for evaluating mechanical and microstructural properties of the AZ31 magnesium alloy post-superplastic forming are reported by Khraisheh et al. (2007).

Also Incremental Sheet Forming (ISF) has been focused on as it allows reaching higher strains level and formability over conventional stamping operations (Filice et al. (2002), Jeswiet et al. (2005)), resulting suitable for processing lightweight materials. High temperature incremental forming approaches have been developed to further increase the performances of incremental forming processes: Duflou et al. (2007) and (2008) carried out approaches to dynamic local heating in ISF of aluminium alloys and also laser assisted single point incremental forming of TiAl6V4 sheets, observing better formability of the investigated materials. Ji and Parkjournal (2008) investigated a warm incremental forming method for magnesium sheets to fully exploit the formability of the material: plane-strain and axi-symmetric stretching tests were performed at different temperatures to assess the influence of temperature on forming limits. Also Ambrogio et al. (2008) investigated a warm incremental forming of magnesium alloy AZ31: significant formability enhancement was possible and that maximum formability occurs at 250°C.

ISF of titanium alloys have been also proposed by Hussain et al. (2008a) and (2008b): in particular, they studied the influence of pitch, tool diameter, feed rate and friction at the interface between tool and blank on the formability of commercially-pure titanium, coming up with the result to obtain good formability performances even at room temperature.

A LCA case study comparing a traditional deep drawing process with the single point incremental forming of an aluminum part is discussed in the following: the two processes will be contrasted by accounting for their environmental performances on the basis of the deformation energy requirements, lubrication and efficiency in material use.

3.1.2.1 Case study: deep drawing versus single point incremental forming processes - a comparative cradle to gate analysis.

As it was widely discussed, as lightweight solutions have been sought for industrial applications, lightweight manufacturing technologies have emerged beside low density materials, as enabling to draw thinner blanks by inducing smoother plastic deformations over the thickness, even while using low formability materials. As it was earlier observed, the environmental efficiency of any material or technology ought to be analyzed by comprehensive approaches, as several factors contribute to determine their environmental impact. For example, while enabling lightweight manufacturing with good externalities for instance on weight reduction, incremental forming processes are high energy demanding in the manufacturing phase, besides being quite slow. Therefore, accurate evaluations of the environmental burden of processes themselves have to be carried out in order to assess their actual sustainability. In the following, a comparison between a traditional deep drawing (DD) and a single point incremental forming (SPIF) process is investigated for a truncated pyramid component in aluminum alloy. A comparative cradle-to-gate life cycle analysis from raw material extraction to the forming phase was here proposed to evaluate those processes by the environmental impact of energy consumptions, material use and lubrication. Experimental tests and numerical simulations were carried out and data analyzed by the LCA software Gabi4 was used. Additionally, results from Gabi were compared with the CES^{TM} method (Jeswiet and Kara (2008)) as far as the environmental impact from energy. A breakdown of the emissions by process input flows was possible, allowing highlighting the most remarkable sources of emissions. In particular, efficient material use strategies were pointed out by the cradle to gate approach as priority in sheet forming processes.

3.1.2.1.1 Problem modeling.

A simple shape, i.e. a frustum of pyramid, was chosen as specimen profile to compare the SPIF with the DD process. In particular, the truncated pyramid shown in Figure 3.43 has a base dimension of 120 mm, a final depth of 40 mm and a wall inclination angle of 45°. The AA5754 aluminium alloy, 1 mm thick, was considered as forming material.

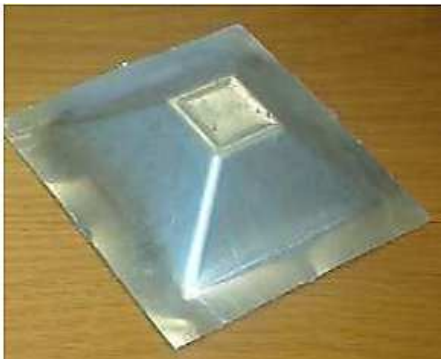

Figure 3.43: AA5754 truncated pyramid (Ingarao et al. (2011b)).

As far as the deep drawing (DD) process, FEM numerical simulations by LS-DYNA were run to get the necessary energy data for the analysis as earlier experimented by Ingarao et al. (2011b) and (2011c). Figure 3.44 shows a sketch of the process tools.

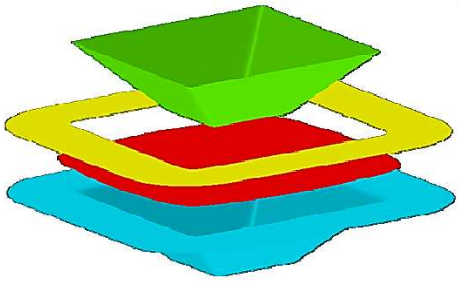

Figure 3.44: Sketch of the process tool.

The material behavior was modeled by Barlat- Lian's yield criterion with isotropic hardening law. Full integrated quadrilateral shell elements with 7 integration points along the thickness were used with three levels of geometric remeshing strategy was applied: over 1000 elements at the end of each run were thus obtained. Punch velocity was artificially increased to 1 m/s, while checking the kinetic energy below the 10% of the deformation work to avoid inertia effects. Coulomb's model was assumed for friction with a coefficient equal to 0.12. In particular, 0.079g of a mineral oil based lubricant was assumed on the basis of the process knowledge. Constant blank holder forces both in time and space were modeled by calibrating the maximum thinning as highest as 20%: Excessive thinning and wrinkling occurrence were both avoided. The initial blank shape has an area of 26336 mm^2 and it was designed minimizing wastes of material to trim out after forming by a trial and error approach. Figure 3.45 shows a map of the maximum thinning: as it can be observed the initial blank shape covers just the die fillet radii.

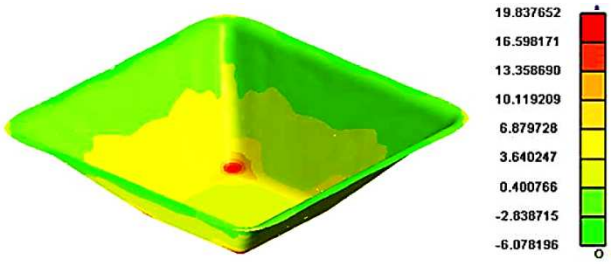

Figure 3.45: Map of the maximum thinning in LS-DYNA.

By the FEM simulations, the deformation energy required for the forming process can be calculated by computing the area below the punch load curve as function of the stroke, as it is showed in Figure 3.46.

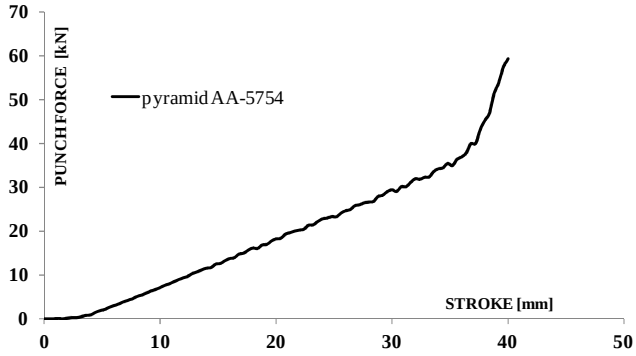

Figure 3.46: Load curve (punch load vs. punch stroke).

As far as the single point incremental forming process (SPIF), an experimental campaign was carried out in collaboration with the University of Calabria (Ingarao et al. (2011b)). In particular, they used a 4-axis CNC vertical machine and calculated the theoretical deformation energy by multiplying the force components arising during the SPIF operation, F_x, F_y, F_z, by the corresponding displacements. Figure 3.47 shows the force decomposition during the SPIF process from Ingarao et al. (2011b). Thus, the theoretical energy is the sum of those products. Moreover, they measured the vertical force, F_z (normal to the CNC frame), and the planar one, F_x (principal planar direction), by using a dynamometer, installed in between of the clamping system and the CNC machine frame.

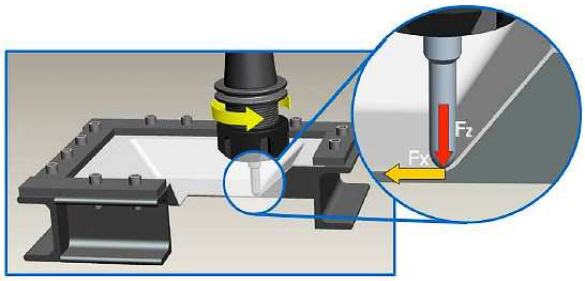

Figure 3.47: Force decomposition during the SPIF process (Ingarao et al. (2011b)).

Two charge amplifiers were connected to the dynamometer and a data acquisition system; given the process symmetry, they automatically derived F_y by F_x. Figure 3.48 displays the force distribution experimentally derived for the SPIF process.

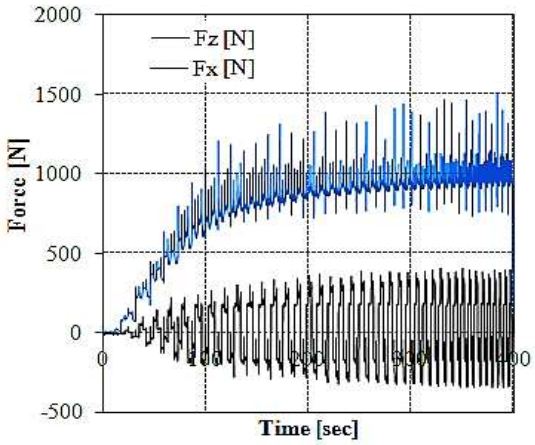

Figure 3.48: Load curves measured during a SPIF test.

The SPIF process is actually followed by a trimming operation to remove the exceeding material in the clamping area. Therefore, the theoretical energy for an entire SPIF process is actually split into two main components: the one required for the actual forming process and the one related to the trimming operation. As in (Anghinelli et al. (2011)), the trimming energy was calculated by considering a constant cutting force, given the mechanical properties of the used material and the blank geometry. Moreover, as lubrication is concerned, 0.64g of a conventional mineral oil was supplied at the beginning of the process.

The initial blank shape is different between the deep drawing and the single point incremental forming processes, due to different clamping features. As in (Ingarao et al. (2011b)), the clamping area in the SPIF process is assumed to be equal to 10 mm all around the sheet outline. The initial blank was in fact oversized (dimensions 155×155mm) to ensure a proper clamping. Thus, the initial blank shape for the SPIF process is a square with side as long as 155 mm. Given the thickness, the initial surface is of 24025 mm^2, while the clamping area that is cut off measures 9625 mm^2 and weighs about 0.026 Kg (i.e. the 40% of the initial shape).

Figure 3.49 compares the initial blank shape by process, while Table 3.6 in the following summarizes the differences between the two processes by material, energy and lubricant use.

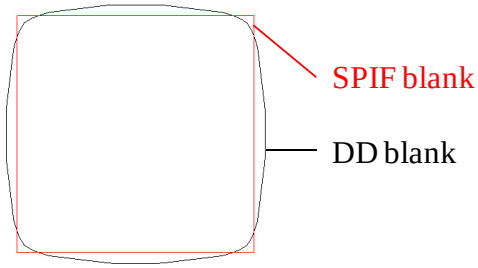

Figure 3.49: Initial blank shapes of the two processes.

	SPIF	DD	Δ [%] = 1-DD/SPIF
Deformation Energy [J]	2998.2	770.339	74%
Lubricant [g]	0.64	0.079	88%
Initial Shape [mm^2]	24025	26336	-10%

Table 3.6: Finale attributes of the investigated processes.

It has to be noticed how remarkable the difference is in terms of deformation energy (+74% by the SPIF), although material saving up to 10% could be leveraged due to different clamping features as earlier showed in Figure 3.49.

3.1.2.1.2 LCA model by using Gabi4.

The first important step of any life cycle assessment (LCA) is the definition of the system boundaries. In particular, raw material extraction, primary shaping processes and manufacturing processes are here included within a cradle-to-gate analysis of the two different forming technologies above described. Data were analyzed in Gabi by using CML2001 as the LCIA (Life Cycle Impact Assessment) method. Thus, the following impact categories were considered: Abiotic Depletion (ADP [kg Sb-eq]), Acidification Potential (AP [kg SO2-eq]), Eutrophication Potential (EP [kg Phosphate-eq]), Global Warming Potential (GWP 100 years [kg CO2-eq]), Ozone Layer Depletion Potential (ODP, steady state [kg R11-eq]), and Photochemical Ozone Creation Potential (POCP [kg Ethene-eq]. Then data were aggregated by normalization and weighting to obtain the global environmental score referred as CML 2001 eco-score. Gabi diagrams of the DD and the ISF processes are respectively shown in Figure 3.50 and 3.51: since aluminum primary production is a long process chain, the entire life cycle inventory was included in such cradle-to-gate analysis; besides accounting for the material impact both as material actually used and wasted, manufacturing energy and lubricant were also considered in the analysis. The environmental impact from dies and tooling systems was instead neglected.

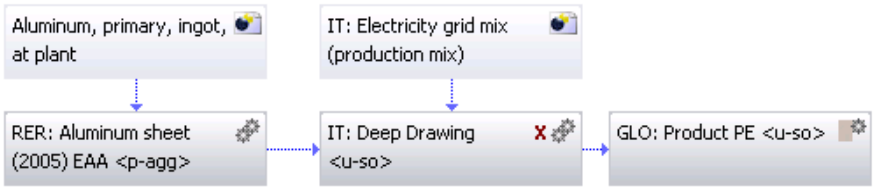

Figure 3.50: GaBi diagram of the DD process.

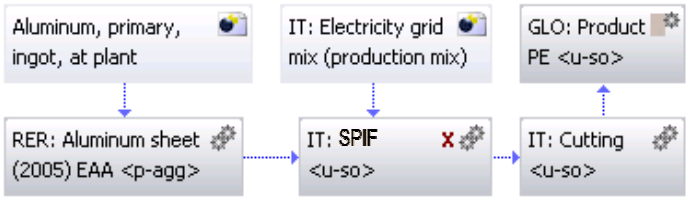

Figure 3.51: GaBi diagram of the SPIF process.

It is important to point out that, as the environmental impact from energy is location dependent, the power grid location was specified to be in Italy.

The environmental balance of the two processes showed in Figure 3.52 details the impact from the entire cradle-to-gate analysis by category.

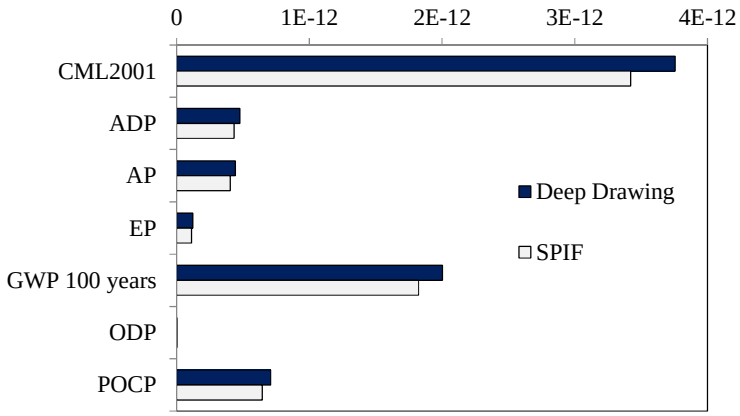

Figure 3.52: Comparative environmental balance.

DD has totally higher environmental impact than SPIF: despite being more energy demanding, SPIF allows in fact material saving, which causes actually the most significant impact on the environment. Figure 3.53 shows the environmental balance by life cycle phase: as a matter of fact, the forming phase has the lowest impact in comparison with both material primary production and shaping processes, where actually SPIF has a lower CML2001 score.

In the end, incremental forming processes result more eco-friendly over traditional deep drawing processes as enabling efficiency in material use and waste reduction. The

comparative cradle-to-gate analysis of such processes in fact pointed a material saving strategy as more effective for sustainability purposes in sheet forming applications.

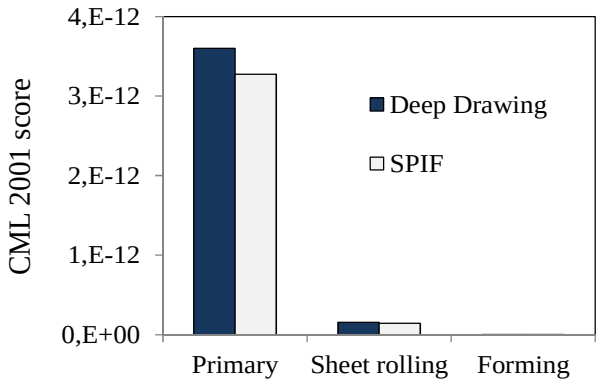

Figure 3.53: CML 2001 score by life cycle phase.

Table 3.7 reports just a focus on the carbon emissions from the two processes as kg of CO_2: data are not normalized neither weighted, as no comparison with other impact categories are in this case.

Process	kg CO_2			
	Total	**Primary production**	**Sheet Rolling**	**Forming Phase**
DD	1.04	0.99	0.045	0.00013
SPIF	0.94	0.91	0.04	0.000499

Table 3.7: Carbon emissions of the two forming processes.

3.1.2.1.3 Environmental evaluation by using the CES^{TM} method.

As it was discussed, there are several LCA methodologies whose application might lead to different or even contradictory results. In fact, each LCA technique uses different characterization factors to convert data from the inventory, such as water, air and soil emissions, to impact categories. Lately, another approach has been proposed by Jeswiet and Kara (2008), referred as Carbon Emission Signature (CES^{TM}) method: it accounts just for the carbon emissions from energy consumptions as function of the power grid primary sources (Jeswiet and Kara (2008), Nava et al. (2010)), which is location dependent. It means that 1 GJ produced in Italy might have a different environmental impact than anywhere else. Each primary energy source is expressed as a fraction: C (coal), NG (natural gas), P (petroleum), B (biofuel), H (hydro), S (solar), W (wind), G (geothermal), E (earth), Wa (waves) and T (tides). Each electrical power grid has then a specific Carbon Emission Signature (CES), as by (3.2) from (Jeswiet and Kara (2008)):

$$CES = \eta * (112 * \%C + 49 * \%NG + 66 * \%P) \quad (3.2)$$

The coefficients, 112, 66, and 49 are the kilograms of carbon emitted per GJ of heat released. A conversion efficiency of $\eta = 0.34$ is commonly used. Thus, as it is reported by Jeswiet and Kara (2008), the carbon emitted (CE) is given by multiplying the energy consumed (EC) by the Carbon Emission Signature (CES) as in equation (3.3):

$$CE = EC\ [GJ] * CES\ [kgCO_2/GJ] \quad (3.3)$$

Table 3.8 reports the primary source mix of the Italian power grid, whose CES results equal to 0.114 mg/J.

Energy resources	[%]
Coal	11.9
Natural gas	44.2
Petroleum and petroleum by-product	4.8
Other	4.8
Renewable	20.8
Balance from foreign countries	13.5

Table 3.8: Primary source mix of the power grid in Italy in 2009 (Anghinelli et al. (2011) from www.terna.it).

Electrical energy is mainly from thermal power stations, where CO_2 is emitted during the combustion of the fossil fuel, such as coal, natural gas, petroleum and petroleum by-product (Anghinelli et al. (2011), Jeswiet and Kara (2008)). On the basis of the data above, the carbon emissions both for the deep drawing and the incremental forming processes were calculated by the CES^{TM} method and then compared with the results obtained by the CML2001 LCIA method as far as the carbon emissions related to the energy consumptions. Such analysis was developed in collaboration with the Department of Mechanical Engineering at the University of Calabria. Results are showed in Table 3.9, highlighting a quite good matching.

Process	**Energy [J]**	**CO_2 [g] by CES**	**CO_2 [g] by CML2001**
Deep Drawing	2998.2	0.343	0.499
Incremental Forming	770.39	0.088	0.13

Table 3.9: Carbon emissions by the CES^{TM} and CML2001 methods.

3.1.2.1.4 Summary and conclusions.

A comparison between a conventional deep drawing process and a single point incremental forming has been proposed. Two approaches have been applied: an LCA cradle to gate analysis by GaBi4 and the CES^{TM} method by Jeswiet and Kara (2008). Despite having a

remarkably higher deformation energy requirement and accordingly environmental impact from the manufacturing phase, as highlighted by both the approaches, the SPIF process results globally more environmental friendly over the DD process as instead evidenced by the LCA cradle-to-gate analysis. In fact, the SPIF process enables a more efficient use of the input material, which represents the most significant cause of impact onto the environment. Therefore, it can be stated that a comprehensive cradle-to-gate approach would suggest efficient material use strategies as priority in sheet forming process design, over approaches just focused on the evaluation of the forming phase.

3.2 Decision making framework for sheet stamping applications.

As it has been discussed, since the 90% of a common passenger car is made by stamped components, an effective strategy to reduce the environmental impact through the life cycle of vehicles comes from the weight reduction. Therefore, many automakers, besides aiming at manufacturing hybrid electric vehicle, fuel cells to convert energy from fuel to electric energy, etc., have started manufacturing lightweight vehicles to reduce fuel consumptions and accordingly emissions to air. As it was earlier discussed, there are two main strategies for weight reduction: to use lightweight materials and to carry out non-conventional manufacturing technologies. The former provide direct mass reduction, while the latter enable efficient material use and saving, together with the possibility to manufacture lightweight materials featuring low formability.

It has to be observed though that besides remarkable benefits as fuel saving, there are also many shortcomings. LWM is in fact economically and technically challenging. The supply of lightweight materials is usually more expensive than conventional automotive materials as deep drawing steels.

Figure 3.54 shows the trend of the manufacturing costs by weight reduction scenarios obtained by replacing steel with aluminum (i.e. red line in the figure): despite lowering the carbon emissions in the use phase (i.e. blue line), a cost increase is observed (Kim et al. (2010)).

In particular, Figure 3.55 shows the additional manufacturing costs with focus on the mass reduction achievable by using different automotive materials (Fine (2010)).

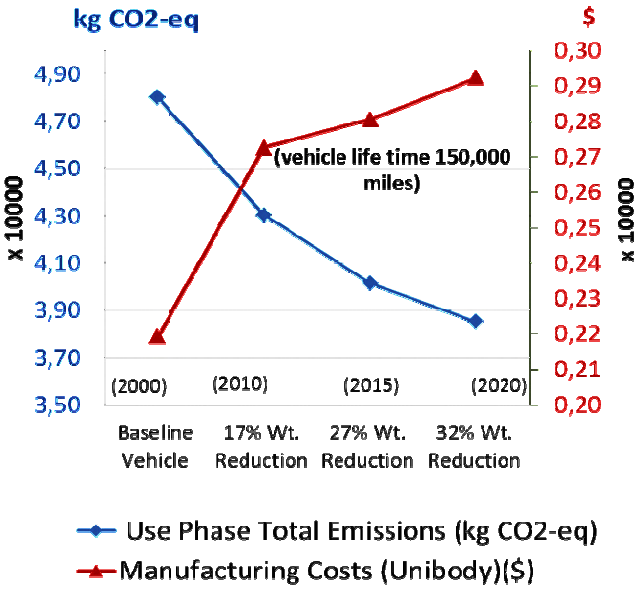

Figure 3.54: Manufacturing costs and GHG saving by weight reduction scenario (adapted from (Kim et al. (2010)).

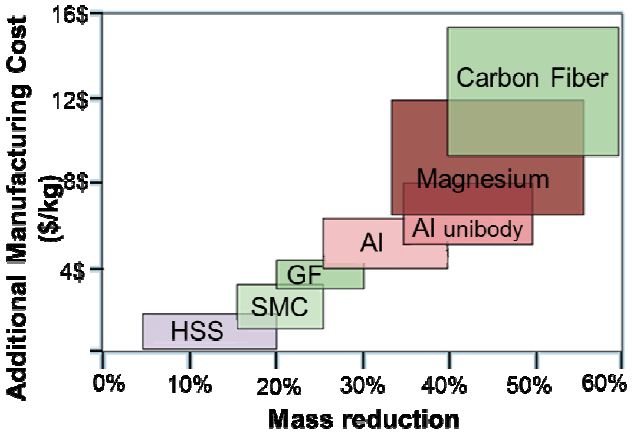

Figure 3.55: Additional manufacturing cost by mass reduction (Fine (2010)).

Usually lightweight alloys are technically challenging too, since they feature lower formability at room temperature over conventional steels. Therefore, reworking costs might arise, manufacturing costs might be higher if multi-steps processes are performed, and even hot stamping might be required involving of course higher energy consumptions. Moreover, as safety and crashworthiness are crucial specifications in the automotive sector, the suitability of such materials must to be assessed and further considerations have to be made to comply with those.

So the question becomes: is lightweight manufacturing affordable or even worth doing? What is the tradeoff among environmental, technical and economic performances?

A standalone application of any life cycle assessment model would not be able to account

for all of these considerations and a decision making framework addressing informed design choices is required. Thus, the objective of this section is the development of a comprehensive decision support tool allowing critically evaluating solutions to reduce the environmental impact throughout the vehicle life cycle, still concerning economical and technical issues.

In this context, Life Cycle Engineering (LCE) emerged to develop life cycles featuring the lowest possible environmental impacts, while offering economic and technical viability. LCE refers to ‘‘*Engineering activities which include: the application of technological and scientific principles to the design and manufacture of products, with the goal of protecting the environment and conserving resources, while encouraging economic progress, keeping in mind the need for sustainability, and at the same time optimizing the product life cycle and minimizing pollution and waste’’* (Jeswiet (2003)). Therefore, according to Wanyama et al. (2003) and Betz et al. (1998), LCE can be defined as a decision making methodology that considers performance, environmental and cost dimensions throughout the duration of a product, guiding design engineers towards informed decisions. Therefore, LCE differs from traditional life cycle assessment methodologies as more comprehensive view incorporating those three dimensions of analysis. Several authors have applied LCE to different case studies in automotive (Ribeiro et al. (2008), Saur et al. (2000)), construction (Banaitiene et al. (2006)) and computer industry (Ebert (2005), Penoyer et al. (2000)), among others. In particular, Ribeiro et al. (2008) proposed a LCE approach to support material selection, integrating the performance of the material for the specific application in technological, environmental and economic dimensions throughout the duration of an automobile fender currently made of mild steel. The methodology was applied to a case study aiming at the use of new metallic materials such as high strength steels and aluminum alloys. A quantitative method of material substitution was presented by Farag (2008): the author proposed a method to allow the designer developing different substitution scenarios based on the relative weights allocated to the different performance requirements for interior motorcar panels. A method to integrate mechanical and environmental performances in optimal choice is reported by Giudice et al. (2005): the authors proposed a selection procedure to relate data on material properties and process features to the required performances of product components, to finally calculate the values assumed by functions, which quantify the environmental impact over the whole life-

cycle and the cost resulting from the choice of materials. Multi-objective analysis techniques were used. Materials selection for an automotive structure by integrating structural optimization with environmental impact assessment was also reported by Ermolaeva et al. (2002) and (2004).

According to the LCE principles, an integrated decision making approach to evaluate products and processes and then to contrast two or more states of being is proposed in the following. The decision making framework below discussed is in particular referred as eco-efficiency analysis (Kicherer et al. (2007), Saling et al. (2000)) and it is adapted mainly from chemical and biotechnical applications (BASF website).

Eco-efficiency analysis applications aimed at increasing ecological performances while not disregarding economic or technical factors have been reviewed from the technical literature. Industrial examples in the automotive (Ribeiro et al. (2008)) and even in the bio-chemical sectors (Saling (2005), Adama et al. (2010)) bear out the use of such techniques in the decision making process. It should be pointed out that such methods provide comparative information and not just absolute values which are less useful in an improvement perspective.

The basic idea is to combine environmental, technical and economic performances and to develop a global eco-efficiency evaluation of all the investigated alternatives. In particular, the eco-efficiency of products and processes is meant as the weighted balance between environmental performances and any further parallel objective.

Therefore, Life Cycle Assessment, cost calculation and technical evaluation methods are first carried out separately; the results of each analysis are normalized and then aggregated by weighting. In fact, if the material to use has to be selected for automotive applications, crashworthiness might have higher weight over formability; similarly, if several sheet stamping technologies are compared, energy consumption would be more important than land use, among others. At the end, a final score is calculated for each objective, so getting an environmental score which measures the green performances, an economic and a technical score.

On the basis of such scores, tradeoffs can be evaluated and different alternatives easily compared by a comprehensive eco-efficiency indicator: this is the value added of such decision making methodology with respect to a standalone life cycle assessment.

The proposed methodology aims therefore to reach environmental goals while still offering

economic and technical viability and it can be better summarized in the following six steps:

1. **Life cycle analysis of the investigated products/processes according to the ISO 14040**: impact assessment will be arranged by categories (i.e. energy, materials consumptions, emissions, toxicity potential, land use, etc.) according to the LCA methodology used for the analysis. GaBi database and characterization methods can be used to aggregate data and to get metrics of sustainability;
2. **Environmental trade off analysis**: the obtained values can be optionally summarized in special plots depicting just the environmental pros and cons of the alternatives. A representation referred as environmental fingerprint may be effective in such a case as showed in Figure 3.56: it is a spider diagram that breaks down the environmental score by the impact categories of interest (depending on the LCA methodology that it was used for the analysis), each one represented on mutually independent axes.

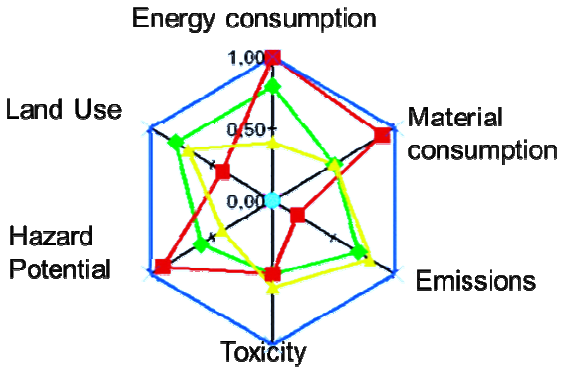

Figure 3.56: Environmental fingerprint (BASF website).

The colors in Figure 3.56 are different alternatives: the outer the alternative, the higher the environmental impact. The outermost alternative is thus least favorable in the environmental compartment in question.

3. **Other performances evaluation per product/process**: technical performances dictated by product requirements, production rate or costs can be considered. Thus, technical evaluations of the suitability of a material with respect to the specifications or, like in the automotive sector, to safety and crashworthiness requirements, will be carried out. Several methods for material choices are available in the technical literature (Ashby (2009)), as it will be better discussed later. Additionally, costs will be calculated accounting for material supply and energy consumptions among others, as showed in Figure 3.57 below.

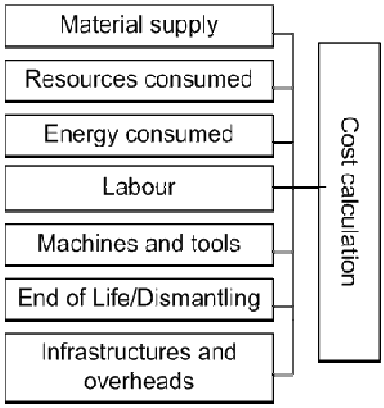

Figure 3.57: Cost calculation.

4. **Normalization**: data are normalized by relevance factors indicating how important each environmental compartment is. For example, when evaluating different manufacturing technologies, the throughput enabled by those might be more important than environmental aspects for the company. Thus, solutions providing improvements in such directions might be preferred. Targets and statistics per region/country can be used, together with traditional normalization methods;
5. **Weighting**: the scores are compressed to get a global indicator by weighing factors to be determined according to company priority, social and political aspects, etc. Surveys and expert interviews are generally used to properly derive weights;
6. **Global comparison (eco-efficiency analysis):** technical, economic and environmental performances are then aggregated. The eco-efficiency portfolio, as showed in Figure 3.58, eases comparisons among alternatives. Global environment impact, cost and technical performances are reported below on independent axes. The alternatives are placed on the basis of the earlier calculated scores and weighting is possible to place more importance on one or more performances: the most efficient solution would be on the right top, thus the yellow solution in Figure 3.58 is less efficient than the red one. Multi-criteria techniques can be effectively integrated to find the best alternative.

   The value added of the proposed assessment lies in the recognition of dominant influences and in the possibility of "what if…?" scenarios besides the description of the current state. Moreover, the impact of the designer choices can be tracked.

   Therefore, looking at all the objectives together, the eco-efficient portfolio provides with an effective decision support tool, quick visualizing the eco-efficiency of the

different alternatives and enabling simple scenario analyses.

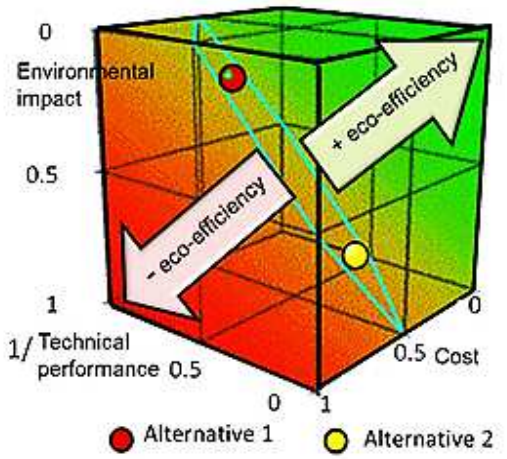

Figure 3.58: Eco-efficient portfolio with respect to environmental, economic and technical performances.

Beside the eco-efficient portfolio, an eco-efficiency score can be easily calculated as the inverse weighted sum of the intermediate scores according to the three dimensions of analysis: the higher such score, the better the alternative. For such purpose, the inverse of the technical score will be considered in calculation. A sketch of the decision making framework discussed above is provided in Figure 3.59.

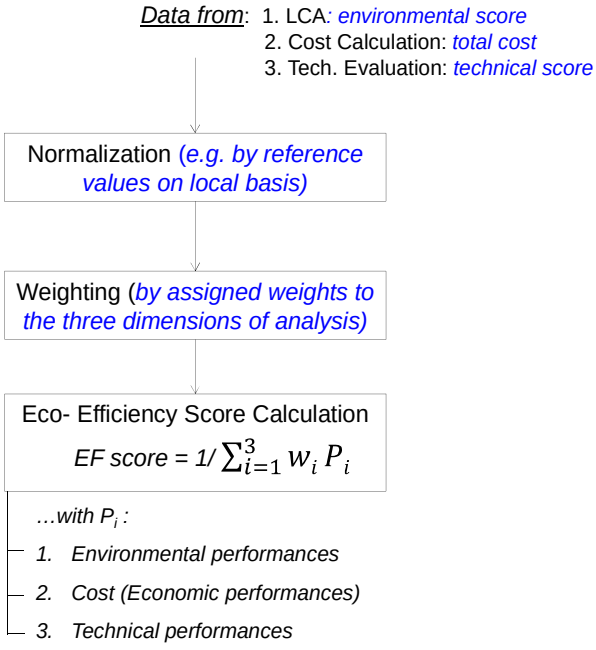

Figure 3.59: Sketch of the proposed decision making framework.

In the end, the light weight manufacturing provides the automakers with really effective strategies for more sustainable vehicles life cycle; further objectives besides sustainability

have to be accounted for though. The life cycle assessment methods are not able to handle environmental, economic and technical performances at the same time, raising the need of integration with further assessment methodologies.

The Eco-efficiency analysis within such a comprehensive decision framework allows on the other hand accomplishing all the objectives, tracking at the same time the impact of any design choices by fast scenario analyses: environmental conscious decisions could be made for sheet stamping applications, while concerning the technical feasibility and economic viability of any solution.

3.2.1 Technical evaluation for material substitution in automotive.

Materials selection is a multidisciplinary activity, which should account for environmental, economic and technical issues all along the product life cycle. In fact, according to Field et al. (2001) '*the four main factors upon which the designers rely when considering materials choice are the relationship between materials specifications and technical performance of the product, the economic performance of the product, the environmental performance of the product and the practice of industrial design embedded in the product and its functionality'*. Especially in automotive manufacturing, when selecting a material, all the relevant engineering properties have to be identified and correlated to all the design requirements and product specifications. In fact, strict safety and crashworthiness standards have to be fulfilled and assured to the customers, limiting the range of material choice for automotive applications. As it was discussed, the effort to reduce weight in order to improve fuel economy in the automotive industry and to comply with tighter governmental regulations on safety and emission has led to the introduction of higher strength steels and pre-finished sheets. Other low density alloys have emerged in response to lightweight performances, but technical issues cannot be neglected.

Therefore such competition among automotive materials make the evaluation whether the material used in making a given component should be substituted necessary. In particular, the decision on the substitution of currently used materials with new ones is more about the suitability of such materials with respect to all the requirements. For instance, as observed by Farag (2008), thinner high-strength low-alloy (HSLA) steel sheets are substituted for thicker steel sheets in motorcar bodies. Having overcome the processing problems, the substitution appears attractive as weight saving. However, while the strength of HSLA

steel is generally higher, corrosion resistance and elastic modulus are essentially the same as those for low carbon steel: thinner HSLA sheets would be damaged by corrosion in shorter time and undesirable vibrations can be a problem (Farag (1997)). Farag (2008) also highlights that in making a substitution, the new material should be mechanically, physically, and chemically compatible with the surrounding materials; replacing steel with plastic may cause for instance changes in deflection, thermal conduction, and thermal expansion due to differences in modulus of elasticity and thermal properties. Replacing steel with aluminum may cause galvanic corrosion with neighboring steel components.

Therefore, it appears clear that a preliminary technical evaluation ought to be done. Similarly, whenever new technologies and solution for sheet stamping processes are taken into account, a technical evaluation of the process viability have to be done to account for throughput, complexity and any other issue related to the suitability of such processes for the manufacturing of a given component. In fact, as it was earlier discussed, incremental forming processes feature a time cycle much longer than traditional deep drawing processes: it might be a critical issue if industrial applications are accounted for.

Farag (2002) described the different stages of design and the related activities of the material selection, which can be generalized for comparisons among manufacturing technologies too: initial screening, developing and comparing alternatives, and selecting the optimum solution. There are several methods of technical evaluations in the technical literature and a good review of material screening and selection methods is reported by Jahan et al. (2010).

According to Ashby et al. (2004) achieving the match with design requirements involves four fundamental steps: a way for translating design necessities into a requirement for material and process; a method for screening out those that cannot meet the specification, leaving a subset of the original menu; a method for ranking the remaining materials and process, identifying those that have the best potential; an approach of searching for supporting information about the top-ranked candidates. Ashby (2009) developed a material and process selection system based on specific charts, particularly useful for initial screening. The Cambridge Engineering Selector (CES), which is a powerful tool for material selection, is based on the Ashby's methodology.

There are two main chart types: bar charts and bubble charts. A bar chart is simply a plot of the value ranges of one property as showed in Figure 3.60, where a bar chart for

Young's modulus (E), which is the mechanical property that measures stiffness, is reported by Ashby (2009). The length of each bar shows the range of the property for each of the materials by family. The scales are logarithmic.

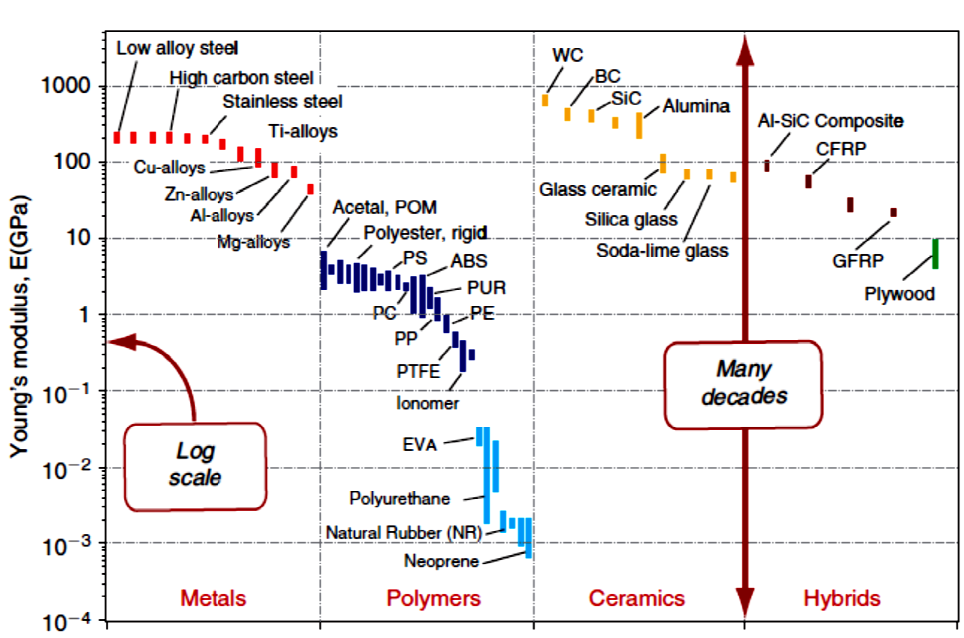

Figure 3.60: Bar chart of Young's modulus (Ashby (2009)) highlighting differences in stiffness by material.

If two properties are plotted, a bubble chart is given, as in Figure 3.61, where both Young's modulus and density (ρ) are reported by identifying distinct characteristic fields.

According to Ashby (2009), those charts become a tool for optimized selection of materials to meet given design requirements, and they help us understand the use of materials in existing products, since constraints and objectives can be plotted on them.

Material indices can be formulated to measure performance (e.g. the ratio between density and Young's modulus to measure the stiffness of a material), enabling ranking materials that meet the constraints of the design. An example is showed in Figure 3.62.

A multiobjective optimization method in material design and selection is described by Ashby (2000) on the basis of the considerations above.

Weaver et al. (1996) used the index-and-chart method for material selection of refrigerators, considering environmental impact indicators.

Sepe (1996) also illustrated some items which can be added or replaced in the current property chart. Chart method was extended by Holloway (1998) to take into account environmental factors.

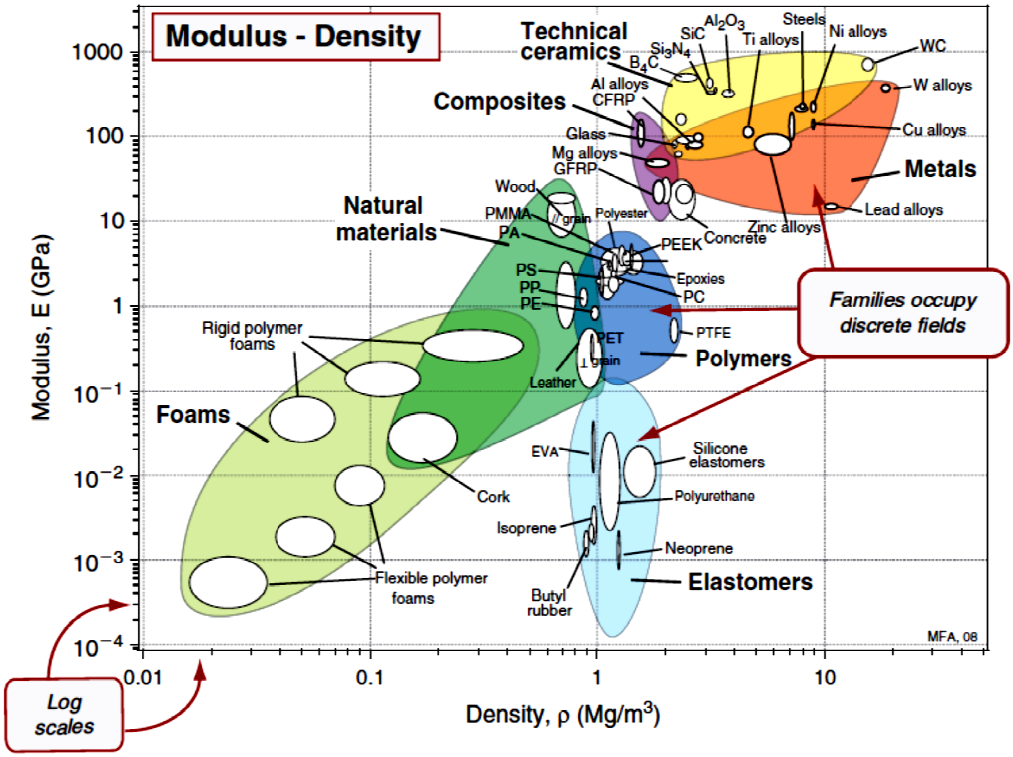

Figure 3.61: Bubble chart of Young's modulus and density by material (Ashby (2009)).

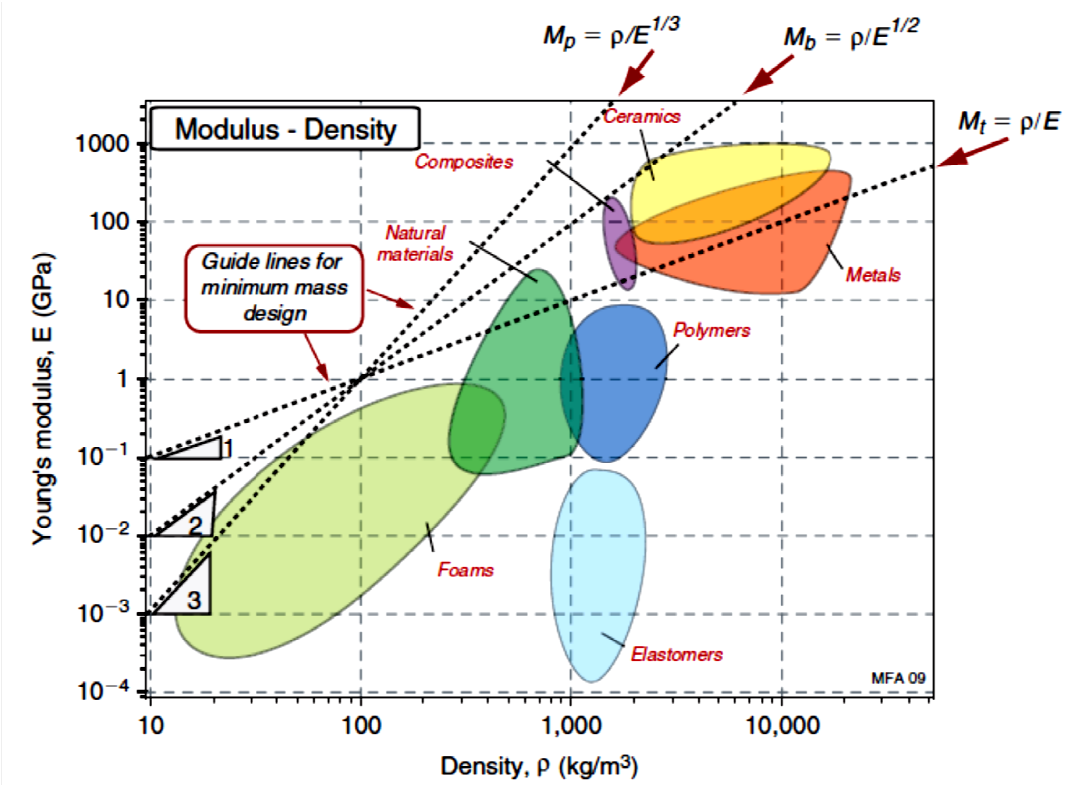

Figure 3.62: E-ρ chart with guidelines for three material indices for stiff and lightweight structures (Ashby (2009)).

As it is well discussed by Jahan et al. (2010), despite being systematic and unbiased in its focus on product/process objectives, such chart method is easy when a simple objective under a single constraint has to be accomplished. The chart limits the decisions in material selection to only solving two or three criteria though: multi-criteria decision making for material choice have to be implemented to address the problem. This is why technical evaluations should be just a step within a more comprehensive decision making framework for deeper eco-efficiency assessments.

For example, Maniya and Bhatt (2010) implemented a novel decision making tool for material selection based on the Preference Selection Index (PSI) method: PSI is a tool to select the best alternative among others without deciding relative importance between attributes. They also performed a validation and consistency test by comparisons with published results of graph theory and matrix approach (GTMA), and technique for order preference by similarity to ideal solution (TOPSIS) method, coming up with the conclusions that the PSI method is more appropriate for the material selection problems.

The technical evaluation method here proposed is adapted from (Ribeiro et al. (2008)) and it is illustrated in Table 3.10.

Technical Performance Evaluation of the Investigated Material

Material Properties	*Weights α (%)*	*Young's Modulus Gpa*	*Yield Stress MPa*	*Tensile Stress MPa*	*Anisotropy -*	*Strain hardening -*	*Poisson Modulus -*	*Corrosion resistance -*	*Density g/cm3*		
Strenght	15%	3	6	6						15	Weighted sum by requirement
Corrosion resistance	8%							15		15	
Stiffness	15%	5					5		5	15	
Allow forming process										-	
Formability	11%				7.5	7.5				15	
Springback		5	5	5						15	
Crashworthiness	14%		7.5	7.5						15	
Buckling	11%	7.5					7.5			15	
Oil canning	8%	7.5					7.5			15	
Dent Resistance	8%	7.5	7.5							15	
Lightness	11%								15	15	
Sum	100%	*Weighted Sum by property*								***Technical Score***	

Table 3.10: Technical evaluation for the selection of automotive materials.

The technical evaluation refers to material properties and their influence on technical requirements and specifications of the stamped part. For each candidate material, a score is assigned by property as relative contribution to the part requirements, whose importance is differentiated by assigned weights. Thus, the sum by property (i.e. by column) of the products between each score and the corresponding requirement weight is the global contribution of such material property to all the product requirements, while the total weighted sum through all the material properties represents the suitability of each material

for the technical performances of the product and it is referred as technical score. The best material will be the one with the highest technical score.

Therefore, both the criteria of assignment of the intermediate technical scores (i.e. by property) and the requirement weights have to be defined as preliminary steps.

As far as the intermediate technical scores, it is necessary to determine the relevant properties and correlate them with the requirements. As it is reported by Jahan et al. (2010), factors for material choice include mechanical properties (Young's Modulus, strength, yield stress, elasticity, fatigue, creep resistance, ductility, hardness and toughness), physical properties (crystal structure, density, melting point, vapor pressure, viscosity, porosity, permeability, reflectivity, transparency, optical properties, dimensional stability), magnetic properties, electrical (resistivity, permittivity, dielectric strength), thermal and radiation (specific heat, conductivity, expansively, diffusivity, transmissivity, reflectivity, emissivity), surface (texture, corrosivity, wear resist), manufacturing properties (machinability, formability, weld ability, cast ability, heat treatability, etc.), reliability, durability, performance characteristics, availability, fashion, market trends, cultural aspects, aesthetics, etc. In particular, there is a wide technical literature on the contribution of the material properties to the requirements of automotive products (Becque (2010), Jung (2002), Patton et al. (2004), Peixinho and Pinho (2006)), accounting for shape and thickness of the components. Automotive product requirements include rigidity and resistance to buckling, lightness, resistance to thermal distortion, and resistance to weather conditions and direct sunlight. For instance, according to Patton et al. (2004), the material performance for a stiff light structural member depends on the ratio between the Young's modulus and the material density, $E^{1/\lambda}/\rho$. λ is a number that varies between 1 and 3 depending on shape and thickness of the structural member. In particular, λ is equal to 1 for columns and beams when they are loaded in tension or 2 when loaded in bending and compression; to 3 for flat panels and plates under bending and buckling conditions (Farag (1997), Patton et al. (2004)). For the case of joints, an average value of $k = 1.44$ was calculated by Patton et al. (2004).

Moreover, it is well known that anisotropy has a strong influence on formability (Gabrielli et al. (2008)), as well as the strain hardening coefficient. On the other hand, the material density is the property that most influences lightness.

According to Ribeiro et al. (2008), such correlation of each requirement to one or more

technical properties of the candidate materials might not be easy, especially if the number of requirements is high; therefore, a pairwise comparison can be an effective and easy approach at the same time: to each material property different scores will be assigned from 0 to 15, meaning the correlation between the property and the requirement. A total of 15 points is then distributed among the material properties, considering their relevance to the requirement and the sum of scores by requirement must not exceed 15.

Additionally, all the requirements have to be weighted and a technique to properly calculate such weights has to be defined as well. A crucial aspect in weighting is indeed the arbitrariness of the weight definition process, which reduces the reliability of any evaluation, especially if the number of goals or part requirements is quite high. One of the most used methods in the technical literature on material selection is referred as Digital Logic Method (DLM) (Farag (2002)): evaluations are arranged such that only two properties are considered at a time. Every possible combination of the requirements or goals is compared and no shades of choice are required: just a yes or no decision has to be made for each evaluation, limiting arbitrariness in weighting. Table 3.11 from (Farag (2002)) shows details of the procedure: the part requirements or goals are listed in the left-hand column, and comparisons are made in the columns to the right. To the more important goal, 1 is given while 0 is assigned to the less important. The total number of possible decisions is equal to N = n (n - 1)/2, where n is the number of requirements or goals under consideration. A weighting factor α meaning the relative emphasis is thus easily obtained and it is the ratio between the number of positive decisions (i.e. 1) for given requirement and the total number of possible decisions.

	Number of Positive Decisions $N = n(n-1)/2$										Positive	Relative Emphasis Coefficient
Goals	1	2	3	4	5	6	7	8	9	10	Decisions	α
1	1	1	0	1							3	0.3
2	0				1	0	1				2	0.2
3		0			0			1	0		1	0.1
4			1			1		0		0	2	0.2
5				0			0		1	1	2	0.2
	Total number of positive decisions										10	$\Sigma\alpha = 1.0$

Table 3.11: Determination of relative importance by DLM (Farag (2002)).

There are some disadvantages in the digital logic method. In particular, the least important goal or property gets zero (0) in all comparisons and this implies that the positive decisions for it and its weighting factor would be zero (0) as well. Thus, this property would be

discarded from the material selection process and would not contribute in the selection process. Moreover, two properties with equal importance cannot have equal numerical values, as the original DLM assigns either zero (0) or one (1) to any pair of properties. In response to such disadvantages, Dehghan-Manshadi et al. (2007) suggested a modification of the DLM for materials selection in mechanical design: they assigned a value of 1 to the less important property and 3 to the more important one, when two properties are considered at a time. In this manner, the least important property still remains in the selection list and two properties with equal importance would have same score equal to 2.

Beside material selection and substitution applications, the technical evaluation procedure above discussed can be easily extended to comparisons among manufacturing technologies and processes. In fact, in such case, process requirements, such as throughput, complexity, etc., would be substituted for part requirements and the correlation between process requirements and technology features would be evaluated.

An example of technical evaluation is provided in the following section within an eco-efficiency analysis for both material and manufacturing technology selection.

3.2.2 Case study: eco-efficiency analysis of automotive components.

The decision making framework was applied to a case study on possible material substitution for automotive uses. Thus, the eco-efficiency analysis earlier discussed was developed in order to contrast the aluminum use with draw quality steel, traditionally used in deep drawing processes for automotive manufacturing. In particular, the material substitution case study analyzed in section 3.1.1.2 was deepened by extending the environmental evaluation to technical and economic considerations.

From the environmental analysis earlier developed for a hood and a fender component, the eco fingerprint in Figure 3.64 and 3.65 was easily obtained by plotting all the CML2011 categories of impact by material. As in the description of the eco-efficiency analysis, data were initially normalized and weighted by using such LCIA methodology.

As it can be observed, both for the hood and the fender, aluminum usage is more impactful than steel: the AA5250 spider diagrams are placed outer, highlighting a higher environmental impact through the cradle-to-grave life cycle of those automotive components.

As a matter of fact, it was observed in section 3.1.1.2 that only by massively recycling aluminum it would be possible to enhance its great potential as fuel saving.

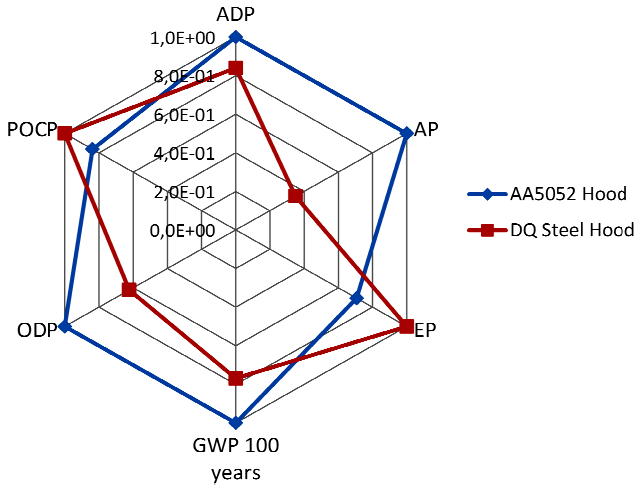

Figure 3.63: Eco fingerprint of the hood component by CML2001 impact categories.

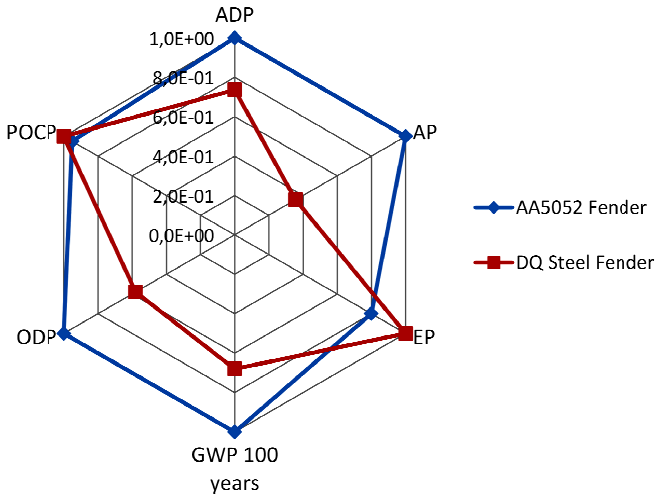

Figure 3.64: Eco fingerprint of the fender component by CML2001 impact categories.

Additionally, the technical and economic viability of aluminum usage over steel has to be evaluated for a more comprehensive analysis. The main part requirements commonly requested for automotive application were considered and then weighted by the novel Digital Logic Method (DLM) from (Dehghan-Manshadi et al. (2007)). Table 3.12 shows the weighting factor α so obtained.

In automotive applications, strength is mainly an anti-intrusion requirement and more in general any part must support the load without plastically failing. Stiffness is an anti-sag index either under the weight of the part itself or when pushed upon; stiffness is also considered an anti-fluttering index more specifically for large panels when moving. The most common mode of loading is in fact bending and not tension, so deflection must not exceed a critical value. Any part must support axial load as well without failing, then buckling is another issue.

Part requirements	Strenght	Corrosion resistance	Stiffness	Allow forming process	Crashworthiness	Buckling	Oil canning	Dent Resistance	Lightness	Positive Decisions	α
Strenght	-	3	2	3	2	3	3	3	2	21	15%
Corrosion resistance	1	-	1	1	1	1	2	2	2	11	8%
Stiffness	2	3	-	3	2	3	3	3	2	21	15%
Allow forming process	1	3	1	-	1	2	3	3	2	16	11%
Crashworthiness	2	3	2	3	-	2	3	3	2	20	14%
Buckling		3	1	2	2	-	3	3	2	16	11%
Oil canning	1	2	1	1	1	1	-	2	2	11	8%
Dent Resistance	1	2	1	1	1	1	2	-	2	11	8%
Lightness	2	2	2	2	2	2	2	2	-	16	11%
									N =	143	Σ 100%

Table 3.12: Weights definition for automotive part requirements by the modified DLM.

Crashworthiness is also strongly required in particular for safety component as pillars. On the other hand, other aesthetic requirements have to be fulfilled: oil canning, which is an elastic buckling problem at unsupported areas when loaded, would be perceived as waiweness avoidable by a suitable stretching and heavier thicknesses; dent resistance is instead a stretchability index, meant as a suitable level of strain, against hail, thrown stones, shopping carts out of control, etc. Even important, such aesthetic requirements got the lowest weighting factors, while strength, stiffness and crashworthiness the highest ones. Thus, according to the technical evaluation method earlier described, the properties of both the AA5052 alloy and the DQ steel were correlated to defined part requirements accounting for the type of contribution of each material property to a given requirement as in Table 3.13 and 3.14: for example, the higher the Young's modulus, the higher the stiffness but the lower the dent resistance; in this case, in fact, E would contribute by its inverse. Moreover, it has to be observed that the corrosion resistance was evaluated in a qualitative range: 1-good, 2-sufficient, 3-low.

In the end, besides having higher environmental impact, aluminum has a worse technical score as well. Additionally, in comparison with steel, aluminum has higher costs through the whole product life cycle: in fact, despite lowering costs from fuel consumption in the use phase, the cost of material and manufacturing are much higher. Unit costs by resource are reported in Table 3.15, while Tables 3.16 and 3.17 show the details of the cost calculation by component.

The fuel consumption through the life cycle was calculated given a life driving distance of 200,000 km (55% in the city and 45% on the highway) and a weight induced fuel consumption as high 0.15 l/(100km*100kg) (Koffler and Rohde-Brandenburger (2009)). Gasoline was assumed as fuel, being aware that a 1 l of gasoline corresponds to 0.735 kg.

Material Properties (DQ Steel)	α (%)	Young's Modulus Gpa	Yield Stress MPa	Tensile Stress MPa	Anisotropy -	Strain hardening -	Poisson Modulus -	Corrosion resistance -	Density g/cm3		
	Property	200	240	360	2.24	0.24	0.29	1	7.87		
Part requirements	Norm	1	1	1	1	1	0.88	1	1	**Sum**	**Weighted sum by requirement**
Strength	15%	3	6	6						15	2
Corrosion resistance	8%							15		15	1
Stiffness	15%	5					5		5	15	2
Allow forming process										-	2
Formability	11%				7.5	7.5				0	
Springback		5	5	5						15	
Crashworthiness	14%		7.5	7.5						0	2
Buckling	11%	7.5					7.5			0	2
Oil canning	8%	7.5					7.5			0	1
Dent Resistance	8%	7.5	7.5							0	1
Lightness	11%								15	15	0
Weighted Sum by Property	1	3.18	2.57	1.9	0.83	0.83	1.9	1.2	0.76	**Technical Score**	
	NormFacto	200	240	360	2,24	0,24	0.33	1	7.87	13.25	

*max or min between two alternatives

Table 3.13: Technical evaluation of the DQ Steel properties of interest.

Material Properties (AA5052)	α (%)	Young's Modulus Gpa	Yield Stress MPa	Tensile Stress MPa	Anisotropy -	Strain hardening -	Poisson Modulus -	Corrosion resistance -	Density g/cm3		
	Property	73.6	195	230	0.71	0.21	0.33	1	2.68		
Part requirements	Norm	0.37	0.81	0.64	1	1	1	1	1	**Sum**	**Weighted sum by requirement**
Strength	15%	3	6	6						15	1.47
Corrosion resistance	8%							15		15	1.20
Stiffness	15%	5					5		5	15	1.28
Allow forming process										-	
Formability	11%				7.5	7.5				0	1.22
Springback		5	5	5						15	
Crashworthiness	14%		7.5	7.5						0	1.52
Buckling	11%	7.5					7.5			0	1.13
Oil canning	8%	7.5					7.5			0	0.82
Dent Resistance	8%	7.5	7.5							0	0.49
Lightness	11%								15	15	0.002
Weighted Sum by Property	1	1.17	2.08	1.26	0.83	0.83	2.18	1.2	0.76	**Technical Score**	
	NormFacto	200	240	360	2,24	0,24	0.33	1	7.87	9.14	

*max or min between two alternatives

Table 3.14: Figure 57: Technical evaluation of the AA5250 properties of interest.

Gasoline cost [$/gallon]	Al cost [$/kg]	DQ cost [$/kg]	Energy cost [$/kWh]
3.28	8	3	0.12

* 1 gallon = 2.76 kg

Table 3.15: Unit Costs.

	Weight [kg]	Material Cost [$]	Mft Energy [KWh]	Mft Costs [$]	Total Cost (before use) [$]	Fuel [gallons]	Fuel Cost [$]	Total [$]
AA 5052	10.6	84.6	35.0	4.2	89	8.5	27.8	117
DQ Steel	17.8	53.3	20.0	2.4	56	14.2	46.5	102
Δ%	-40%		75%			-40%		14%

Table 3.16: Cost calculation of the hood part by material.

	Weight [kg]	Material Cost [$]	Mft Energy [KWh]	Mft Costs [$]	Total Cost (before use) [$]	Fuel [gallons]	Fuel Cost [$]	Total Costs
AA 5052	2.82	22.6	23	2.8	25	2.2	7.4	32.7
DQ Steel	4.26	12.8	13	1.6	14	3.4	11.2	25.2
Δ%	-34%		77%			-34%		28%

Table 3.17: Cost calculation of the fender part by material.

Thus, a comprehensive eco-efficiency analysis can be performed: by merging the results from the environmental, technical and economic evaluations, the eco-efficiency score can be calculated for both aluminum and steel, showing how viable the use of the two materials is, so suggesting possible material substitutions for automotive applications.

Additionally, the eco-portfolio can be plotted to fast visualize the two alternatives or to make scenario analysis. In particular, data were normalized by the maximum among the three intermediate scores and even weights were assigned. Figure 3.65 and 3.66 show the eco-portfolio of the two material candidates by component, highlighting a higher eco-efficiency for steel over aluminum. As a matter of fact, the eco-efficiency score of the DQ steel is higher over the AA5052 aluminum alloy in both cases.

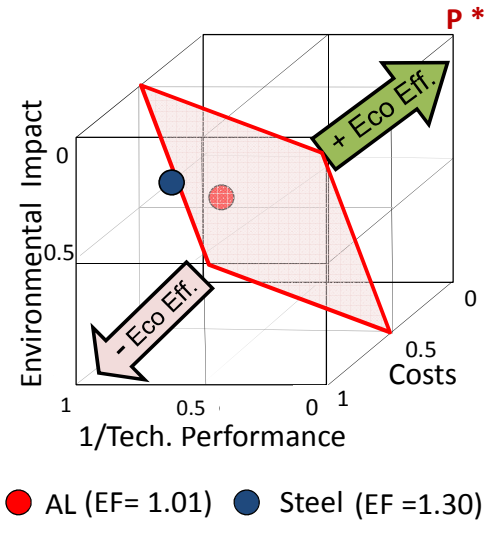

Figure 3.65: Eco-efficiency portfolio for the hood case study.

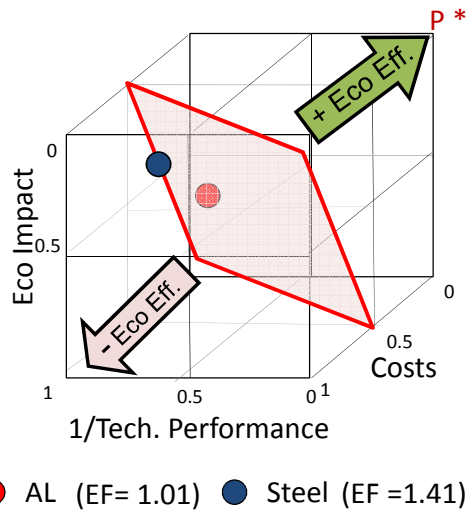

Figure 3.66: Eco-efficiency portfolio for the fender case study.

3.2.3 Case study: eco-efficiency analysis of sheet stamping processes.

The decision making framework earlier described can be easily adapted for process comparisons besides material substation and selection, as it will be discussed in the following. Therefore, the eco-efficiency analysis of both deep drawing and incremental forming processes of the AA5052 truncated pyramid discussed in section 3.1.2.1 was carried out as well. From the results of the environmental analysis performed by Gabi4, the eco-fingerprints showed in Figure 3.67 for the deep drawing and the incremental forming processes were obtained. Data were normalized by the maximum score for each impact category and, as it can be observed, the deep drawing process has higher environmental impact with respect to all them.

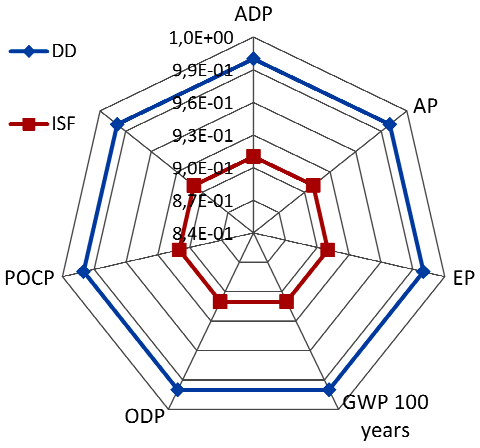

Figure 3.67: Eco-fingerprint of DD and ISF.

As far as the technical evaluation, Table 3.18 reports the weighting factors by the modified

Digital Logic Method.

Requirements	Throughtput	Equipment Acquisition	Allow formability	Rejection Rate	Concurrent Operations	Positive Decisions	α
Throughtput	-	3	3	3	3	12	30%
Equip. Acquis.	1	-	1	1	1	4	10%
Allow formability	2	2	-	2	2	8	20%
Rejection Rate	1	3	2	-	2	8	20%
Concurrent Op.	1	3	2	2	-	8	20%
					N=	40	Σ 100%

Table 3.18: Weight definition by the modified DLM of the process requirements.

As well known, throughput relates to the time cycle, thus the lower the process the lower the throughput. The ISF process of the truncate pyramid earlier discussed takes about 15 minutes, while deep drawing a few seconds. Equipment acquisition is meant as the accessibility of the tooling systems generally required (e.g. ISF can be carried out by using a milling machine), while formability refers to the material formability enhancement achievable by a given process technology (more remarkable differences might be observed between DD and ISF if more complex geometries are considered). Moreover, formability issues might result in some cases in higher rejection rate or even require sequential operations.

Table 3.19 summarizes the technical scores calculated for both the deep drawing and incremental forming processes, while Table 3.20 shows the results from cost calculations.

Due to the higher throughput allowed, the deep drawing process has a higher technical score as well, while its economic performances are worse because of the higher cost of the material, which is the most influent in comparison with energy.

Therefore, all environmental, technical and economic performances were accounted for and equally weighted in order to calculate the eco-efficiency score: no significant difference can be observed between the two processes as it is showed in Figure 3.68.

Process Requirements	*α (%)*	*DD*	*ISF*	*Weighted sum by requirement*	
				DD	*ISF*
Throughtput	33%	3	1	1.00	0
Equipment Acquisition	7%	1	3	0	0.20
Allow formability	20%	2	2	0	0.40
Rejection Rate	13%	2	2	0	0.27
Concurrent Operations	27%	2	2	0.53	1
Weights Sum	*100%*		*Tech. Score*	2.27	1.73

Table 3.19: Technical evaluation of DD and ISF.

	Material [kg]	Material Cost [€]	Energy [kWh]	Energy Cost [€]	Total Cost [€]
DD	0.071	0.43	2E-04	2.6E-05	0.43
ISF	0.064	0.38	8E-04	1.0E-4	0.38

Material Cost [€/kg]	Energy Cost [€/kWh]
6	0.12

Table 3.20: Cost evaluation of both DD and ISF.

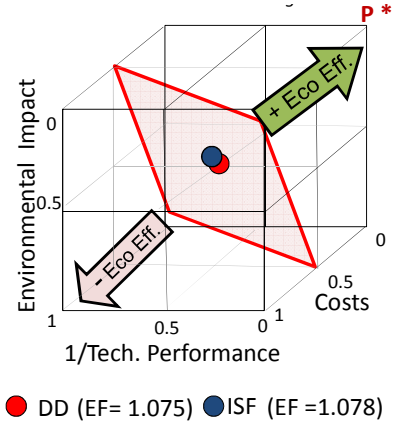

Figure 3.68: Eco-efficiency portfolio of DD and ISF.

It was also observed that one of the advantages of such decision making framework is actually the possibility to easily perform scenario analysis by changing the weights of each performance within the eco-efficiency calculation and portfolio. In fact, despite having a comparable eco-efficiency, if a higher importance is assigned for instance to the technical performances (e.g. 50%) while still evenly considering both the environmental and the economic ones, a different scenario would be observed. Figure 3.69 shows the corresponding eco-efficient portfolio highlighting higher efficiency for the deep drawing process.

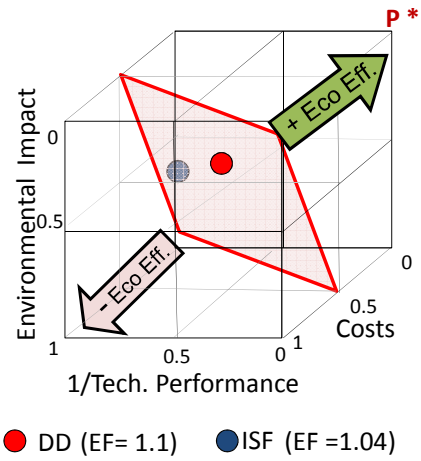

Figure 3.69: Eco-efficiency portfolio for the scenario analysis.

3.2.4 Summary and conclusions.

A decision making framework able to evaluate environmental performances of either products or processes, while accounting for technical and economic viability was proposed. In fact, life cycle assessment principles were combined with the evaluation of the technical feasibility alongside cost calculations. Moreover, such framework, referred as eco-efficiency analysis mainly from chemical and biotechnical applications, allows both to track the consequences of the designer's choices and to make scenario analyses in order to evaluate for instance material substitutions or alternative manufacturing technologies.

A standalone application of LCA, which might lead sometimes to even clashing conclusions depending on the specific LCIA methodology applied, cannot provide the designer with a comprehensive view of the crucial issues that might arise. On the contrary, such decision making framework allows highlighting weaknesses of any alternative strategy within more global evaluations.

CONCLUSIONS

As it has been extensively discussed, a wider concept of quality has been emerging in sheet stamping applications in response to both the needs of zero defect production and lower impact on the environment. The minimization of part faults as fractures alongside shape defects is a crucial issue in sheet forming even more if the unpredictability of the behavior of some variables is considered. In fact, beside process parameters controllable by the designer, other variables, uncontrollable instead but with a strong influence on the process results have to be handled as well. Such variables, referred as noises, among which coil to coil variations of the material properties are documented as some of the most remarkable ones, are generally assumed stochastic, introducing the necessity of a robust design for sheet stamping processes. The aim of robust tools for sheet stamping applications is to significantly reduce the effect of the noises on the final process results by properly identifying operative windows as insensitive as possible to the influence of such noise variability. The state of art on robust methodologies in particular for multiobjective problems was deepened and two main families of approaches were clustered: hybrid deterministic/stochastic approaches, which generally provide with an explicit analysis of the noise effects to finally calculate the Pareto front; stochastic approach, which determine the Pareto front while compensating somehow the effect of the noise variation.

In particular, as far as the former, the integration among Finite Element simulation, Response Surface Methodology and Monte Carlo simulations was proposed and investigated. The capability of such hybrid tool to enhance the awareness of the process designer about the possible effects of the noises over the process results, being at the same time a viable tool in terms of time and computational effort was proved. In particular, since metamodeling is a crucial step in the implementation of the abovementioned approach, a preliminary investigation on the commonly used techniques for sheet stamping application was done, by comparing Polynomial Regression, Kriging and Moving Least Square methods. A case study was also analyzed.

As far as the stochastic approaches, the Dual Response Surface Methodology was mainly investigated for multiobjective problems as well. Case studies were analyzed and comparisons done between the two kinds of approaches.

In particular, a better understanding of the effect of variability on the process results together with a more accurate investigation of the robustness of a generic solution turned out from the application of the integrated hybrid approach, earlier mentioned.

However, as it was previously introduced, it is not more possible to keep optimizing sheet stamping processes just accounting for the minimization of the product defects, since a increasing attention towards sustainability in manufacturing has been arising over the years, as from industry as from the scientific community. Therefore, wider considerations on the environmental impact from sheet stamping processes and applications have to be done towards progressively more environmental conscious decisions.

In particular, a strong interest in sustainable solutions in manufacturing is from the automotive sector, since the environmental impact of transportation, and particularly light duty vehicles, is significant all over the world. Sheet stamping processes have a great potential, even more in this sector, both in terms of sustainability improvement of the processes themselves and leveraging from manufacturing (as it was defined in Chapter 3). In fact, since sheet stamping represents the 90% of the manufacturing processes carried out for auto making, enhancements in such processes are definitely worth doing. In particular, lightweight materials and lightweight manufacturing technologies were identified from an analysis of the state of art as main strategies to reduce the environmental impact. In fact, while lightweight materials enable a remarkable reduction of the vehicle's weight, and accordingly fuel and CO_2 savings, lightweight manufacturing technologies enable both the use of thinner blanks (so reducing the weight of the individual components) and the forming of tough materials as magnesium, titanium or some aluminum alloys, which generally rise technical issues.

Life Cycle Assessment (LCA) methodologies were studied for environmental evaluations. In particular, a comparative cradle-to-grave analysis of some vehicle's components was carried out to evaluate the substitution of steel for aluminum. The analysis evidenced that the any material or solution ought to be investigated through its entire life cycle. In fact, despite having a great potential as fuel saving in the use phase of a common passenger car, aluminum resulted globally less environmental friendly over steel as higher energy demanding in the primary production phase. Recycling was then suggested as only strategy to exploit such potential and a scenario analysis was carried out.

Additionally, a comparison between a conventional sheet stamping process and a single

point incremental forming (SPIF) was developed in a cradle-to-gate life cycle perspective. In particular, despite requiring higher deformation energy, the SPIF process enables such a material saving to result globally more sustainable over conventional sheet stamping processes, confirming the necessity of analysis over the entire life cycle.

Life Cycle Assessment methodologies, whose generally requirements are standardized by the ISO 14000 standards, do not account for still important issues in manufacturing. In particular, a decision making framework able to provide the designer with tool to evaluate the environmental performances while considering technical and economic issues was discussed. Such framework, referred as eco-efficiency analysis, was adapted mainly from chemical and biotechnical applications, with the aim to provide a comprehensive tool for product or process design, even able to make scenario analyses and track the choices of the designer. Thus, the concept of eco-efficiency accounts for the sustainability of a product or a process, while evaluating also its viability. Therefore, life cycle assessment, technical evaluation and economic calculation were done both for the material substitution case study and the comparison between the two forming technologies.

In conclusion, the goal of the present PhD thesis was to investigate and to develop multiobjective methodologies for sheet stamping processes design and optimization, with respect to both zero defect quality, under the stochastic effect of some noise variables, and environmental conscious decisions, towards more sustainable sheet stamping processes and applications.

REFERENCES

Abu-Farha F.K. and Khraisheh M.K. (2008): An integrated approach to the superplastic forming of lightweight alloys: towards sustainable manufacturing; Int J Sustainable Manuf 1: 18-40.

Adama O., Azzaro-Pantel C., Pibouleau L., Domenech S., Baudet P,. Yao B. (2010): Eco-Efficiency Analysis for Chemical Process Design; 20th ESCAPE.

Allen T.T., Bernshteyn M.A., Kabiri-Bamoradian K. (2003): Constructing meta-models for computer experiments; J Quality Technol, 35:264-274.

Allwood J.M., Huang Y., Barlow C.Y. (2005): Recycling scrap aluminum by cold bonding; Proc ICTP Conf.

Altan T., Aue-u-lan Y., Palaniswamy H., Kaya S. (2005): State of the art, visions & priorities in research & development on metal forming; Proc ICTP Conf.

Ambrogio G., Filice L., Manco L. (2008): Warm incremental forming of magnesium alloy AZ31; CIRP Ann - Manuf Technol, 257-260.

Anghinelli O., Ambrogio G., Di Lorenzo R., Ingarao G. (2011): Environmental Costs of Single Point Incremental Forming; Steel Res Int., 525-530.

Arvidsson M. and Gremyr I. (2008): Principles of Robust Design Methodology; Qual Reliab Eng Int, 24:23–35.

Asgari S.A., Pereira M., Rolfe B.F., Dingle M., Hodgson P.D. (2008): Statistical analysis of finite element modeling in sheet metal forming and springback analysis; J Mater Proc Technol 203: 129–136.

Ashby M. F. (2009): Materials and the Environment: Eco-Informed Material Choice, Elsevier.

Ashby M.F. (2000): Multi-objective optimization in material design and selection; Acta Mat, 48: 359-369.

Ashby M.F., Brechet Y.J.M., Cebon D., Salvo L. (2004): Selection strategies for materials and processes; Mater Des, 25:51–67.

Auto/Steel Partnership Program, Body Systems Analysis Project Team (2000): Automotive Sheet Steel Stamping Process Variation: An Analysis of Stamping Process Capability and Implications for Design, Die Tryout and Process Control; www.a-sp.org.

Avram O.I. and Xirouchakis P. (2011): Evaluating the use phase energy requirements of a machine tool system; J Clean Prod, 19: 699-711.

Azaouzi M., Belouettar S., Rauchs G. (2010): A numerical method for the optimal blank shape design; Mat Des, 32: 756-765.

Bahloul R., Ben Ayed L., Potiron A., Batoz J.L. (2010): Comparison between three optimization methods for the minimization of maximum bending load and springback in wiping die bending obtained by an experimental approach; Int J Adv Manuf Techol, 48:1185–1203.

Banaitiene N., Banaitis A., Kaklauskas A., Zavadskas E.K. (2006): Evaluating the life cycle of a building: a multivariant and multiple criteria approach; Omega, 36:429-41.

Banu M., Takamura M., Hama T., Naidim O., Teodosiu C., Makinouchi A. (2006): Simulation of springback and wrinkling in stamping of dual phase steel rail- shaped part; J Mater Proc Techol, 173:178–84.

Barlat F., Cazacu O., Zyczkowski M., Banabic D., Yoon J.W. (2004): Yield surface plasticity and anisotropy; Raabe D, Chen L-Q, Barlat F, Roters F (eds), Continuum scale simulation of engineering materials fundamentals microstructures process applications, Wiley, Weinheim, 145–185.

Barlat F., Lian J. (1989): Plastic behaviour and stretchability of sheet metal, part 1. A yield function for orthotropic sheets under plane stress conditions; Int J Plast, 5:51–66.

BASF website, http://www.basf.com/group/corporate/en/sustainability/eco-efficiency-analysis/index.

Baumann H. (1996): LCA use in Swedish industry; Int. J. LCA 1: 122-126.

Bay N., Olsson D.D., Andreasen J.P. (2005): Testing environmentally friendly lubricants for sheet metal forming; Proc ICTP Conf.

Becque J. (2010): Inelastic Plate Buckling; J Eng Mech ASCE, 1123-1130.

Behrens B., Vogt O., Poelmeyer J. (2005): Forming of magnesium sheet metal; Proc ICTP Conf.

Belytschko T., Krongauz Y., Organ D., Fleming M., Krysl P. (1996): Meshless method: An overview and recent development; Comput Met Appl Mech Eng, 139: 3-47.

Beres D.L. and Hawkins D.M. (2001): Plackett–Burman technique for sensitivity analysis of many parametered models; Ecol Model, 141: 171-83.

Bertram M., Buxmann K., Furrer P. (2009): Analysis of greenhouse gas emissions related

to aluminum transport applications; Int. Journal of LCA, 62–69.

Betz M., Schuckert M., Herrmann C. (1998): Life cycle engineering as decision making support in the electronics industry; IEEE.

Bichon B.J., Eldred M.S., Swiler L.P., Mahadevan S., McFarland J.M. (2008): Efficient global reliability analysis for nonlinear implicit performance functions; AIAA J, 46:2459–68.

Bingham D., Sitter R.R., Tang B. (2009): Orthogonal and nearly orthogonal designs for computer experiments; Biometrika, 96: 51-65.

Breitkopf P., Naceur H., Rassineux A., Villon P. (2005): Moving least squares response surface approximation: Formulation and metal forming applications; Comput & Struct 83: 1411–1428.

Breitkopf P., Rassineux A., Savignat P.J.M. (2004): Integration constraint in diffuse element method; Comput Methods Appl Mech Eng, 193:1203–1220.

Browne M.T., Hillery M.T. (2003): Optimizing the variables when deep-drawing C.R.1 cups; J Mater Process Technol, 136: 64–71

Brundtland Commission (1987): The U.N. World Commission on environment and development: our common future; Oxford University press.

Buranathiti T., Cao J., Cedric Xia Z., Chen W. (2005): Probabilistic Design in a Sheet Metal Stamping Process under Failure Analysis; Numisheet, AIP Conf Proc ,778: 867-872.

Cao J. and Kinsey B.L. (2001): Next generation stamping dies - controllability and flexibility; Robotics Comput Integrated Manuf, 17:49–56.

Cao J., Kinsey B.L. (2001): Next generation stamping dies - controllability and flexibility; Robotics Comput Integrated Manufm,17:49–56.

Castro C., Antonio C., Sousa L. (2004): Optimisation of shape and process parameters in metal forging using genetic algorithms; J Mater Process Technol, 146: 356–364.

Chee W.P., Shi F.R., Zhiquan Y., Kenneth H.K.G., Ruisheng N., Bin S. (2011): Identifying Carbon Footprint Reduction Opportunities through Energy Measurements in Sheet Metal Part Manufacturing; Glocalized Solut Sustain Manuf, 389-394.

Chen F. and Chiu K (2005): Stamping formability of pure titanium sheets; J Mat Process Technol, 181–186.

Chen F.K., Liao Y.C. (2002): An Analysis of Draw-Wall Wrinkling in a Stamping Die

Design; Int J Adv Manuf Technol, 19: 253:259.

Chen P. and Koc M. (2007): Simulation of springback variation in forming of advanced high strength steels, J Mater Proc Technol, 190: 189–198.

Cherubini F., Raugei M., Ulgiati S. (2008): LCA of magnesium production technological overview and worldwide estimation of environmental burdens; Resour Conserv & Recy, 1093–1100.

Chino Y., Hoshika T., Lee J.S., Mabuchi M. (2006a): Mechanical properties of AZ31Mg alloy recycled by severe deformation; J Mater Res, 754-760.

Chino Y., Hoshika T., Mabuchi M. (2006b): Enhanced corrosion properties of pure Mg and AZ31Mg alloy recycled by solid-state process; Mater Sci Eng A, 435-437: 275-281.

Dahmus J. and Gutowski T. (2006): An environmental analysis of machining**;** IMECE2004-62600.

Das I., Dennis J.E. (1997): A closer look at drawbacks of minimizing weighted sums of objectives for Pareto set generation in multicriteria optimization problems; Struct Optim, 14:63–69.

Das S. (2008): Primary magnesium production costs for automotive applications; JOM J Miner Met Mater Soc, 60: 63-69.

de Souza T. and Rolfe B. (2008): Multivariate modeling of variability in sheet metal forming; J Mater Proc Technol, 203:1–12.

de Souza T. and Rolfe B. (2010): Characterising material and process variation effects on springback robustness for a semi-cylindrical sheet metal forming process; Int J Mech Sci, 52:1756–1766.

Deb K. (2001): Multiobjective optimization using evolutionary algorithms; Wiley, New York.

Dehghan-Manshadi B., Mahmudi H., Abedian A., Mahmudi R. (2007): A novel method for materials selection in mechanical design: Combination of non-linear normalization and a modified digital logic method; Mat Des, 28: 8–15.

Del Prete A., Manisi B., Strano M. (2008): Sheet Metal Hydromechanical Deep Drawing process optimization; Numisheet, 685-690.

Demir I, Kayabasi O., Ekici B. (2008): Probabilistic design of sheet-metal die by finite element method; Mat Des 29: 721–727.

Di Lorenzo R., Ingarao G., Chinesta F. (2009a): A gradient-based decomposition approach

to optimize pressure path and counterpunch action in Y-shaped tube hydroforming operations; Int J Adv Manuf Technol, 44:44–60.

Di Lorenzo, R., Ingarao, G., Marretta, L., Micari, F. (2009b): Deep drawing process parameter design: a multi objective optimization approach; Key Eng Mater, 410-411: 601-608.

Di Lorenzo R., Ingarao G., Chinesta F. (2010): Integration of gradient based and response surface methods to develop a cascade optimization strategy for y-shaped tube hydroforming process design; Adv Eng Softw, 41:336–348.

Diaz N., Choi S., Helu M., Chen Y., Jayanathan S., Yasui Y., Kong D., Pavanaskar S., Dornfeld D. (2010a): Machine Tool Design and Operation Strategies for Green Manufacturing; Proc 4th CIRP Int Conf High Perform Cutting.

Diaz N., Helu M., Jayanathan S., Chen Y., Horvath A., Dornfeld D. (2010b): Environmental Analysis of Milling Machine Tool Use in Various Manufacturing Environments; IEEE ISSST.

Dornfeld D. (2011): Leveraging Manufacturing for a Sustainable Future; 18th CIRP Int Conf LCE.

Du J., Han W., Peng Y. (2010): Life cycle greenhouse gases, energy and cost assessment of automobiles using magnesium from Chinese Pidgeon process; J Clean Prod, 18: 112-119.

Duflou J., Callebaut B., Verbert J., De Baerdemaeker H. (2007): Laser Assisted Incremental Forming: Formability and Accuracy Improvement; CIRP Ann - Manuf Technol, 273-276.

Duflou J., Callebaut B., Verbert J., De Baerdemaeker H. (2008): Improved SPIF performance through dynamic local heating; Intern J Machine Tools & Manuf, 543–549.

Ebert C. (2007): The impacts of software product management; J Syst Softw, 80:850-61.

Echard B., Gayton N., Lemaire M. (2011): AK-MCS: An active learning reliability method combining Kriging and Monte Carlo Simulation; Struct Saf, 33: 145–154.

EPA - U.S. Environmental Protection Agency (2011): Inventory of U.S. greenhouse gas emissions and sinks: 1990 – 2009; epa.gov.

Ermolaeva N.S., Kaveline K.G., Spoormaker J.L. (2002): Materials selection combined with optimal structural design: concept and some results; Mat Des, 23: 459–470.

Ermolaeva N.S., Castro M.B.G., Kandachar P.V. (2004): Materials selection for an automotive structure by integrating structural optimization with environmental impact assessment; Mat Des, 25: 689–698.

Fadi K. and Marwan K.K. (2008): Integrated approach to the superplastic forming of lightweight alloys: towards sustainable manufacturing; Int J Sust Manuf.

Fann K. and Hsiao P. (2003): Optimization of loading conditions for tube hydroforming; J Mater Process Technol, 140:520–524.

Farag M.M. (1997): Materials selection for engineering design; Prentice-Hall.

Farag MM. (2002): Quantitative methods of materials selection; Kutz M. editor, Handbook of materials.

Farag M.M. (2008): Quantitative methods of materials substitution: Application to automotive components; Mat Des, 29: 374–380.

Fenton F. and Mould P.R.: Tailored Steel Products - A Smart Investment for Future Vehicles; sponsored by ArcelorMittal, www.autosteel.org.

Field III R., Clark P., Ashby F. (2001): Market drives for materials and process development in the 21st century; MRS Bulletin, 716-25.

Filice L., Fratini L., Micari F. (2002): Analysis of Material Formability in Incremental Forming; CIRP Annals - Manuf Technol, 199-202.

Fine C. (2010): Lightweight Materials for Transport: Developing a Vehicle Technology Roadmap for the Use of Lightweight Materials; MIT Roundtable: The Future of Manufacturing Innovation – Advanced Technologies.

Fogagnolo J.B., Ruiz-Navas E.M., Simón M.A., Martinez M.A. (2003): Recycling of aluminum alloy and aluminum matrix composite chips by pressing and hot extrusion; J Mat Process Technol, 143-144: 792-795.

Ford (2009): Report on the business impact of climate change; media.ford.com.

Fratini L., Ingarao G., Micari F. (2008): On the springback prediction in 3D sheet metal forming processes; Steel Res Int, 79:77–83.

Friedman J. H. (1991): Multivariate adaptive regression splines, The Annals of Statistics, 19-1: 1–141.

Froes F.H.F., Kiese H., Bergoint D.J. (2004): Titanium in the family automobile: the cost challenge; JOM, 40-44.

Gabi Education Handbook; www.pe-international.com.

Gabrielli F. , Ippolito R., Micari F. (2008): Analisi e Tecnologia delle LavorazioniMeccaniche; McGraw-Hill.

Gantar G. and Kuzman K. (2002): Sensitivity and stability evaluation of the deep drawing process; J Mater Process Technol, 125-126:302–8.

Gantar G., Kuzman K., Filipic B. (2005a): Increasing the stability of the deep drawing process by simulation-based optimization; J Mat Proc Technol, 164–165:1343–1350.

Gantar G., Sehi E., Kuzman K. (2005b): Reduction of the environmental burden caused by household appliances; ICTP Conference.

Gantar G. and Kuzman K. (2005c): Optimization of stamping processes aiming at maximal process stability; J Mat Proc Technol, 167: 237–243.

Geffen C. and Rothenberg S. (2000): Suppliers and environmental innovation: the automotive paint process; Int J Oper & Prod Manag, 20:166-186.

Geiger M., Merklein M., Tolazzi M. (2005): Metal forming ensures innovation and future in Europe; Proc ICTP Conf.

Georgiou S.D. (2009): Orthogonal Latin hypercube designs from generalized orthogonal designs; J Stat Plan Inference, 139:1530 – 40.

Geyer R. (2007): Life cycle greenhouse gas emission assessments of automotive materials the example of mild steel, advanced high strength steel and aluminium in body in white applications methodology; Worldautosteel Report, www.worldautosteel.org.

Ghatrehnaby M. and Arezoo B. (2009): A fully automated nesting and piloting system for progressive dies; J Mat Proc Technol, 209: 525–535.

Giudice F., La Rosa G., Risitano A. (2005): Materials selection in the Life-Cycle Design process: a method to integrate mechanical and environmental performances in optimal choice; Mat Des, 26: 9–20.

Giunta A.A. (1997): Aircraft multidisciplinary design optimization using design of experiments theory and response surface modeling; PhD Dissertation and MAD center report.

Gomes C., Onipede O., Lovell M. (2005): Investigation of springback in high strength anisotropic steels; J Mater Proc Technol, 159:91–98.

Gronostajski J. and Matuszak A. (1999): The recycling of metals by plastic deformation: an example of recycling of aluminum and its alloys chips; J Mater Process Technol, 92-93: 35-41.

Gronostajski J., Marciniak H., Matuszak A. (2000): New methods of aluminium and aluminium-alloy chips recycling; J Mater Process Technol: 106, 34-39.

Güley V.N., Khalifa B., Tekkaya A.E. (2010): Direct recycling of 1050 aluminum alloy scrap material mixed with 6060 aluminum alloy chips by hot extrusion; Proc Esaform Conf.

Gutowski T. (2004): Design and Manufacturing for the Environment, Handbook of Mechanical Engineering, Springer-Verlag.

Gutowski T., Dahmus J., Thiriez A. (2006): Electrical Energy Requirements for Manufacturing Processes; 13th CIRP Int Conf LCE, Leuven, Belgium.

Haldar A. and Mahadevan S. (2000): Reliability assessment using stochastic finite element analysis; Wiley, New York.

Hauschild M., Jeswiet J., Alting L. (2005): From life cycle assessment to sustainable production: status and perspectives; CIRP Ann – Manuf Tech, 1-21.

Hazra S., Williams D., Roya R., Aylmore R., Smith A. (2011): Effect of material and process variability on the formability of aluminium alloys; J Mat Proc Tech 211: 1516–1526.

Helms H. and Lambrecht U. (2006): The Potential Contribution of Light-Weighting to Reduce Transport Energy Consumption; Int J LCA, 1-7.

Herrmann C. and Thiede S. (2009): Process chain simulation to foster energy efficiency in manufacturing; CIRP J Manuf Sci Technol, 1: 221-29.

Hoffmann H., So H., Steinbeiss H. (2007): Design of Hot Stamping Tools with Cooling System; CIRP Ann - Manuf Technol, 269-272.

Holloway L. (1998): Materials selection for optimal environmental impact in mechanical design; Mater Des, 19:133–43.

Hou B., Wang W., Li S., Lin Z., Cedric Xia Z. (2009): Stochastic analysis and robust optimization for a deck lid inner panel stamping; Mat Des, 31: 1191–1199.

http://aluminium.matter.org.uk/content/html/eng/default.asp?catid=7&pageid=230565674

http://ec.europa.eu

Hu W., Enying L., Li G.Y., Zhong Z.H. (2008): Development of metamodeling based optimization system for high nonlinear engineering problems; Adv Eng Softw, 39 629–645.

Hussain G., Gao Z.Y. (2008a): Formability evaluation of a pure titanium sheet in the cold

incremental forming process; Int J Adv Manuf Technol, 920–926.

Hussain G., Gao L., Hayatb N., Cuia Z., Pangc Y.C., Dard N.U. (2008b): Tool and lubrication for negative incremental forming of a commercially pure titanium sheet; J Mat Process Technol, 193–201.

Ingarao G., Di Lorenzo R., Micari F. (2009a): Internal pressure and counterpunch action design in Y shaped tube hydroforming processes: a multi-objective optimisation approach; Comput Struct, 87:591–602.

Ingarao G., Di Lorenzo R., Micari F. (2009b) Analysis of stamping performances of dual phase steels: a multi-objective approach to reduce springback and thinning failure; Mater Des, 30:4421–33.

Ingarao G., Di Lorenzo R. (2010): Optimization methods for complex sheet metal stamping computer aided engineering; Struct Multidisc Optim, 42: 459-480.

Ingarao G., Di Lorenzo R., Micari F. (2011a): Sustainability issues in sheet metal forming processes: an overview; J Clean Prod, 19: 337-347.

Ingarao G., Gagliardi F., Anghinelli O., Di.Lorenzo R. (2011b): A Sensitivity Analysis on Environmental Sustainability in Sheet Metal Forming; 10th ICTP.

Ingarao G., Ambrogio G., Di.Lorenzo R., Micari F. (2011c): On the sustainability evaluation in sheet metal forming processes; Key Eng Mat, 473: 824-829.

International Aluminium Institute: Improving Sustainability in the Transport Sector through Weight Reduction and the Application of Aluminium, www.world-aluminium.org.

International Energy Agency (2011): CO2 emissions from fuel combustion; www.iea.org.

International Standards Organization (ISO) (2006a): ISO 14040 Life cycle assessment – Principles and framework.

International Standards Organization (ISO) (2006b): ISO 14044 Life cycle assessment Requirements and guidelines.

Jahan A., Ismail M.Y., Sapuan S.M., Mustapha F. (2010): Material screening and choosing methods – A review; Mat Des, 31: 696–705.

Jaisingh A. and Narasimhan K. (2004): Sensitivity analysis of a deep drawing process for miniaturized products; J Mater Process Technol, 147:321–7.

Jakumeit J., Herdy M. and Nitsche M. (2005): Parameter optimization of the sheet metal forming process using an iterative parallel Kriging algorithm; Struct Multidisc Optim,

29, 498–507.

Jansson M., Nilsson L., Simonsson K. (2007): On process parameter estimation for the tube hydroforming process; J Mater Process Technol 190:1–11.

Jansson T., Nilsson L., Moshfegh R. (2008): Reliability analysis of a sheet metal forming process using Monte Carlo analysis and metamodels; J Mater Proc Tech, 202: 255-268.

Jeswiet JA. (2003): Definition of life cycle engineering; Bley H, editor. Proc 36th CIRP Int Seminar Manuf Systems; 17-20.

Jeswiet J., Micari F., Hirt G., Bramley A., Duflou J., Allwood J. (2005): Asymmetric Single Point Incremental Forming of Sheet Metal; CIRP Ann - Manuf Technol, 88-114.

Jeswiet J. and Kara S. (2008): Carbon Emissions and CES™ in Manufacturing; CIRP Ann – Manuf Technol, 57:17-20.

Ji Y.H. and Parkjournal J.J. (2008): Formability of magnesium AZ31 sheet in the incremental forming at warm temperature; J Mat Process Technol, 354–358.

Jin R., Chen W., Simpson T.W. (2000): Comparative studies of metamodeling techniques under multiple modeling criteria, American Institute of Aeronautics and Astronautics AIAA-2000-4801, 1- 11.

Joshi K., Venkatachalam A., Jaafar I.H., Jawahir I.S. (2006): A new methodology for transforming 3R concept into 6R concept for improved product sustainability; 4th Global Conf Sustainable Prod Dev & LCE.

Jovane F. ,Yoshikawa H., Alting L., Boer C.R., Westkamper E., Williams D.M. Tseng, Seliger G., Paci A.M. (2008): The incoming global technological and industrial revolution towards competitive sustainable manufacturing; CIRP Ann – Manuf Technol, 641–659.

Jung D.W. (2002): A Parametric Study of Sheet Metal Denting Using a Simplified Design Approach; KSME Int J, 16: 1673-1686.

Kaebernick H., Kara S., Sun M. (2003): Sustainable product development and manufacturing by considering environmental requirements; Robot Comput Integrated Manuf, 19: 461-468.

Kaebernick H., Kara S. (2006): Environmentally sustainable manufacturing: a survey on industry practices; 13th CIRP Int Conf LCE, 19-28.

Kang B., Son B., Kim J. (2004): A comparative study of stamping and hydroforming processes for an automobile fuel tank using FEM; Int J Machine Tools & Manuf, 87–

94.

Karthik V., Comstock Jr. R.J., Hershberger D.L., Wagoner R.H. (2002): Variability on sheet formability and formability testing; J Mater Proc Technol, 121:350–62.

Kaymaz I. (2005): Application of Kriging method to structural reliability problems; Struct Safety, 27:133–51.

Kazan R., Fırat M., Tiryaki A.E. (2009): Prediction of springback in wipe-bending process of sheet metal using neural network; Mater Des, 30:418–23.

Kellens K., Dewulf W., Duflou J.R. (2011): Environmental Analysis of the Air Bending Process; AIP Conf Proc 14th Esaform, 1353, 1650-1655.

Kellens K., Dewulf W., Overcash M., Hauschild M.Z., Duflou J.R. (2012a): Methodology for systematic analysis and improvement of manufacturing unit process life cycle inventory (UPLCI) CO_2PE! Initiative (cooperative effort on process emissions in manufacturing) - Part 1: Methodology Description; Int J LCA, 17: 69-78.

Kellens K., Dewulf W., Overcash M., Hauschild M.Z., Duflou J.R. (2012b): Methodology for systematic analysis and improvement of manufacturing unit process life cycle inventory (UPLCI) CO_2PE! Initiative (cooperative effort on process emissions in manufacturing) - Part 2: case studies; Int J LCA, DOI: 10.1007/s11367-011-0352-0.

Khraisheh M.K., Abu-Farha, F.K., Nazzal M.A., Weinmann K.J. (2006): Combined Mechanics-Materials Based Optimization of Superplastic Forming of Magnesium AZ31 Alloy; CIRP Ann – Manuf Technol, 233-236.

Khraisheh M.K., Abu-Farha, F.K., Weinmann K.J. (2007): Investigation of Post-Superplastic Forming Properties of AZ31 Magnesium Alloy; CIRP Ann - Manuf Technol, 289-292.

Kicherer A., Schaltegger S., Tschochohei H., Pozo B.F. (2007): Eco-Efficiency - Combining Life Cycle Assessment and Life Cycle Costs via Normalization; Int J LCA, 12: 537–543.

Kim H.J., McMillan C., Winebrake J.J., Keoleian G.A., Skerlos S.J. (2008): Evaluating Life Cycle Cost, Emissions and Materials Use for an Aluminum Intensive Vehicle: Preliminary Analysis; Proc NSF Eng Res Innov Conf.

Kleiber M., Rojek J., Stocki R. (2002): Reliability assessment for sheet metal forming operations; Comput Meth Appl Mech Eng, 191: 4511–4532.

Kleijnen J.P.C. (2009): Kriging metamodeling in simulation: A review; Europ J Oper Res,

192: 707-716.

Kleiner M., Geiger M., Klaus A. (2003): Manufacturing of Lightweight Components by Metal Forming; CIRP Ann - Manuf Technol, 521-542.

Kleiner M., Chatti S., Klaus A. (2006): Metal forming techniques for lightweight construction; J Mater Process Technol, 177: 2-7.

Kleinermann and Ponthot (2003): Parameter identification and shape/process optimization in metal forming simulation; J Mater Process Technol, 139:521–526.

Koehler J. R. and Owen A. B. (1996), Computer experiments; Handbook of Statistics,13, S. Ghosh and C.R.Rao, eds., Elsevier Science: Amsterdam, 261–308.

Koffler C. and Rohde-Brandenburger K. (2009): On the calculation of fuel savings through lightweight design in automotive life cycle assessments; Int J LCA, 15: 128-135.

Koplin J., Seuring S., Mesterharm M. (2007): Incorporating sustainability into supply management in the automotive industry - the case of the Volkswagen AG; J Cleaner Prod, 15: 1053–1062.

Kopp R., Wiedner C., Mayer A. (2005): Flexibly rolled sheet metal. Advanced material research; 81-92.

Lancaster P.and Salkauskas K. (1986): Curve and Surface Fitting: An Introduction; Academic Press, London.

Lang L., Danckert J., Nielsen K.B. (2004): Investigation into hydrodynamic deep drawing assisted by radial pressure Part I. Experimental observations of the forming process of aluminum alloy; J Mat Process Technol, 119–131.

Laurent H., Greze R., Manach P.Y., Thuillier S. (2009): Influence of constitutive model in springback prediction using the split-ring test. Int J Mech Sci, 51:233–45.

Lebaal N., Nouari M., Ginting A. (2011): A new optimization approach based on Kriging interpolation and sequential quadratic programming algorithm for end milling refractory titanium alloys; Applied Soft Computing, In Press.

Ledoux Y., Sébastian P., Samper S. (2010): Optimization method for stamping tools under reliability constraints using genetic algorithms and finite element simulations; J Mat Proc Technol, 210: 474–486.

Lee K.H., Park G.J., Joo W.S. (2005): A Global Robust Optimization Using the Kriging Based Approximation Model, 6th Congress of Struct Multidisc Optim.

Lee. K.H. (2010): A robust structural design method using the Kriging model to define the

probability of design success; J Mech Eng Sci, 224-379.

Lee S.W. and Yang D.Y. (1998): An assessment of numerical parameters influencing springback in explicit finite element analysis of sheet metal forming process; J Mater Proc Technol, 80–81:60–67.

Li B., Nye T.J., Metzger D.R. (2006): Multi-objective optimization of forming parameters for tube hydroforming process based on the Taguchi method; Int J Adv Manuf Technol, 28: 23–30.

Li K., Carden W.P., Wagoner R.H. (2002): Simulation of springback; Int J Mech Sci, 44:103–12.

Li Y.Q., Cui Z.S., Ruan X.Y., Zhang D.J. (2006): CAE-based six sigma robust optimization for deep-drawing sheet metal process; Int J Adv Manuf Technol, 30: 631–637.

Liew K.M., Tan H., Ray T. et al (2004) Optimal process design of sheet metal forming for minimum springback via an integrated neural network evolutionary algorithm; Struct Multidisc Optim, 26:284–294.

Lingbeek R., Huétink J., Ohnimus S., Petzoldt M.,Weiher J. (2005): The development of a finite elements based springback compensation tool for sheet metal products; J Mater Proc Technol 169:115-125.

Liu G., Lin Z., Bao Y. (2002): Improving dimensional accuracy of a u-shaped part through an orthogonal design experiment; Finite Elem Anal Des, 39:107–118.

Liu G.P., Han X., Jiang C. (2008): A novel multi-objective optimization method based on an approximation model management technique; Comput Methods Appl Mech Eng, 197: 2719-31.

Lophaven S.N., Bruun H.N., Søndergaard J. (2002): DACE - A MATLAB Kriging Toolbox; Technical Report IMM-TR-2002-12.

Lovell M., Higgs C.F., Deshmukha P., Mobley A. (2006): Increasing formability in sheet metal stamping operations using environmentally friendly lubricants; J Mat Proc Technol, 177: 87–90.

Magallanes J.F. and Olivieri A.C. (2010): The effect of factor interactions in Plackett-Burman experimental designs. Comparison of Bayesian-Gibbs analysis and genetic algorithms; Chemom Intell Lab Syst, 102: 8-14.

Majeske K.D. and Hammett P.C. (2002): Identifying sources of variation in sheet metal

stamping; Int J Flexible Manuf Syst.

Maniya K. and Bhatt M.G. (2010): A selection of material using a novel type decision-making method: Preference selection index method; Mat Des, 31: 1785–1789.

Martin J.D. and Simpson T.W. (2004): On the use of kriging models to approximate deterministic computer models, Proc DETC ASME.

Mazda Sustainability Report (2010): Management and Reduction of Substances with Environmental Impact; www.mazda.com.

McAuley J.W. (2003): Global Sustainability and Key Needs, in Future Automotive Design; Environ Sci Technol, 37: 5414-5416.

Meinders T., Burchitz I.A., Bonte M.H.A., Lingbeek R.A. (2008): Numerical product design: springback prediction, compensation and optimization; Int J Mach Tools Manuf, 48:499–514.

Merklein M., Lechler J., Geiger M. (2006): Characterisation of the Flow Properties of the Quenchenable Ultra High Strength Steel 22MnB5; CIRP Ann - Manuf Technol, 229-232.

Messac A., Mattson C.A. (2002): Generating well-distributed sets of Pareto points for engineering design using physical programming; Optim Engineering, 3:431–450.

Meyer A., Wietbrock B., Hirt G. (2008): Increasing of the drawing depth using tailor rolled blanks - Numerical and experimental analysis; Int J Machine Tools & Manuf, 522–531.

Morestin F. and Boivin M. (1996): On the necessity of taking into account the variation in the Young modulus with plastic strain in elastic-plastic software; Nucl Eng Des, 162:107–116.

Munoz A.A. and Sheng P. (1995): An analytical approach for determining the environmental impact of machining processes; J Mat Proc Technol, 53: 736-758.

Myers R.H., Montgomery D.C. (2002): Response surface methodology process and product optimization using designed experiments; 2nd ed. New York, USA: John Wiley and Sons, Inc.

Naceur H., Batoz J., Guo Y., Knopf-Lenoir C. (2004): Optimization of draw bead restraining forces and draw bead design in sheet metal forming process; J Mater Process Technol, 146:250–262.

Naceur H., Guo YQ, Ben-Elechi S. (2006): Response surface methodology for design of sheet forming parameters to control springback effects; Comput Struct, 84:1651–63.

Naceur H., Ben-Elechi S., Batoz J.L., Knopf-Lenoir C. (2008): Response surface methodology for the rapid design of aluminum sheet metal forming parameters; Mater Des, 29:781–90.

Nakanishi M., Mabuchi M., Saito N., Nakamura M., Higashi K. (1998): Tensile properties of the ZK60 magnesium alloy produced by hot extrusion of machined chip; J Mater Sci Lett, 17: 2003-2005.

Narasimhan N. and Lowell M. (1999): Predict springback in sheet metal forming: an explicit to implicit sequential solution procedure; J Mater Proc Technol 33:29–42.

Narita H., Kawamura H., Norihisa T., Jen L., Fujimoto H., Hasabe T. (2006): Development of a prediction system for environmental burden for machine toll operation; JSME, 49,1188-1195.

Nava P., Jeswiet J., Kim I.Y. (2010): Calculation of Carbon Emissions in Metal Forming Manufacturing Processes with Eco-Benign Lubrication; NAMRI/ SME, 38,751.

Neugebauer R., Sterzing A., Kurka P., Seifert M. (2005): The potential and application limits of temperature-supported hydroforming of magnesium alloys; Proc ICTP Conf.

Neugebauer, R.; Altan, T.; Geiger, M.; Kleiner, M.; Sterzing A. (2006): Sheet Metal Forming at Elevated Temperatures; CIRP Ann, 793-816.

Novotny S. and Geyer M. (2003): Process design for hydroforming of lightweight metal sheets at elevated temperatures; J Mater Process Tech, 594-599.

Odenberger E., Pederson R., Oldenburg M. (2008): Thermo-mechanical material response and hot sheet metal forming of Ti-6242; Mat Sci Eng A, 58–168.

Omar M.A. (2011): The automotive body manufacturing systems and processes; Wiley, New York.

Onur K., Yalcinoz T. (2008): Robust Design using Pareto type optimization: A genetic algorithm with arithmetic crossover; Computers & Industrial Engineering, 55: 208–218.

Oudjene M., Ben-Ayed L., Batoz J.L. (2007): Geometrical Optimization Of Clinch Forming Process Using The Response Surface Method; NUMIFORM, Proc AIP Conf 908: 531-536.

Oudjene M., Ben-Ayed L., Delameziere A., Batoz J.L. (2009): Shape optimisation of clinching tools using the response surface methodology with Moving Least-Square approximation; J Mat Proc Technol, 209:289-296.

Palaniswamy H., Thandapani A.K., Kulukuru S., Altan,T. (2004): Prediction of Blank

Holder Force in Stamping Using Finite Element Analysis; NUMIFORM.

Panthi S.K., Ramakrishnan N., Pathak K.K., Chouhan J.S. (2007): An analysis of springback in sheet metal bending using finite element method (FEM); J Mater Proc Technol 186:120–124.

Papeleux L. and Ponthot J.P. (2002): Finite element simulation of springback in sheet metal forming; J Mater Proc Technol, 125–126:785–791.

Patton R., Li F., Edwards K.L. (2004): Causes of weight reduction effects of material substitution on constant stiffness components; Thin-Walled Struct, 42: 613–37.

Peixinho N. and Pinho A.C.M. (2006): Dent resistance of aluminium and magnesium alloys; Proc. IMechE: J Automobile Eng, 220 D: 1191-1198.

Penoyer J.A., Burnett G., Fawcett D.J., Liou S.Y. (2000): Knowledge based product life cycle systems: principles of integration of KBE and C3P; Comput Aided Des, 32:311-20.

Petek A., Gantar G., Pepelnjak T., Kuzman K. (2007): Economical and Ecological Aspects of Single Point Incremental Forming versus Deep Drawing Technology; Key Eng Mat, 344, 931.

Piotr B., Hakim N., Alain R. et al (2005): Moving least squares response surface approximation: formulation and metal forming applications; Comput Struct, 83:1411–1428.

Post J., Klaseboer G., Stinstra E., van Amstel T., Huetink J. (2009): Multistage metal forming: Variation and transformation; J Mat Proc Technol 209: 2648–2661.

Powell M.J. D. (1987), Radial basis functions for multivariable interpolation: A review; Algorithms for Approximation, J. C. Mason and M. G. Cox, eds., Oxford University Press: London, 143–167.

Prescott P. (2009): Orthogonal-column Latin hypercube designs with small samples; Comp Stat Data Anal, 53: 1191-200.

Puri P., Compston P., Pantano V. (2009): Life cycle assessment of Australian automotive door skins; Int J LCA, 14: 420–428.

Pusavec F., Krajnik P., Kopac J. (2010a): Transitioning to sustainable production Part I: application on machining technologies; J Clean Prod, 18: 174-184.

Pusavec F., Krajnik P., Kopac J. (2010b): Transitioning to sustainable production Part II: evaluation of sustainable machining technologies; J Clean Prod, 18: 1211-1221.

Ragai I., Lazim D., Nemes J.A. (2005): Anisotropy and springback in draw-bending of stainless steel 410: experimental and numerical study; J Mater Proc Technol, 166:116–127.

Rahimifard S., Seow Y., Childs T. (2010): Minimising Embodied product energy to support energy efficient manufacturing. CIRP Ann- Manuf Technol, 59: 25-28.

Rajemi M.F., Mativenga P.T., Aramcharoen A. (2010): Sustainable machining: selection of optimum turning conditions based on minimum energy considerations; J Clean Prod, 18: 1059–1065.

Rao K.P. and Xie C.L. (2006): A comparative study on the performance of boric acid with several conventional lubricants in metal forming processes; Tribol Int, 39: 663–668.

Rassineux A., Breitkopf P., Villon P. (2003): Simultaneous surface and tetrahedron mesh adaptation using mesh free techniques; Int J Numer Methods Eng, 57:371–389.

Ribeiro I., Pec¸as P., Silva A., Henriques E. (2008): Life cycle engineering methodology applied to material selection, a fender case study; J Clean Prod, 16: 1887-1899.

Rijpkema J.J.M., Etman L.F.P., Schoofs A.J.G. (2001): Use of Design Sensitivity Information in Response Surface and Kriging Metamodels, Opt Eng, 2, 469–484, 2001.

Rojek J., Kleiber M., Piela A.,, Stocki R., Knabel J. (2004): Deterministic and stochastic analysis of failure in sheet metal forming operations; Suppl. Metal Forming, 29-34.

Romero V.J., Swiler L.P., Giunta A.A. (2004): Construction of response surfaces based on progressive-lattice-sampling experimental designs with application to uncertainty propagation; Struct Safety, 26:201–19.

Roshan J.V. and Hung Y. (2008): Orthogonal-maximin Latin Hypercube Designs; Stat Sinica, 18: 71-186.

Ryabkov N., Jackel F., van Putten K., Hirt G. (2008): Production of blanks with thickness transitions in longitudinal and lateral direction through 3D-Strip Profile Rolling; Int J Mater Form, 391–394.

Sacks J., Welch W.J., Mitchell T.J. and Wynn H.P. (1989): Design and analysis of computer experiments; Stat Sci, 4, 409–435.

Saling P. et al. (2002): Eco-efficiency Analysis by BASF: The Method; Int J LCA, 203-218.

Saling P. (2005): Eco-Efficiency Analysis of biotechnological processes; Appl Microbiol Biotechnol 68: 1–8.

Samuel M. (2003): A new technique for recycling aluminium scrap; J Mater Process Technol, 135: 117-124.

Santos A.D. and Teixeira P. (2008): A study on experimental benchmarks and simulation results in sheet metal forming; J Mater Proc Technol, 199:327–336.

Saur K., Fava J.A., Spatari S. (2000): Life cycle engineering case study automobile fender designs; Environmental Progress, 19:72-82.

Schenk O. and Hillmann M. (2004): Optimal design of metal forming die surfaces with evolution strategies; Comput & Struct, 82: 1695–1705.

Schmidheiny (1992): Changing course: a global business perspective on development and the environment; Cambridge, Mass, MIT Press.

Schweimer G. and Levin M. (2002): Life Cycle Inventory for the Golf A4; VW environmental report, www.volkswagenag.com.

Sepe MP. (1996): Proposed enhancements to the short-term property chart for improved material selection decisions; Proc Conf ANTEC, 3176–8.

Shaibu A.B. and Cho B.R. (2009): Another view of dual response surface modeling and optimization in robust parameter design; Int J Adv Manuf Tech, 41: 631-64.

Shaw J. and Coates G. (2008): Automotive Steel Performance Advantages for Mass Reduction and Climate Change; www.autosteel.org.

Sheng Z., Jirathearanat S., Altan T. (2004): Adaptive FEM simulation for prediction of variable blank holder force in conical cup drawing; Int J Mach Tools Manuf 44:487–494.

Sheng, Z. and Shivpuri R. (2004): Adaptive PI control strategy for prediction of variable blank holder force, 7th ESAFORM.

Shivpuri R. and Zhang W. (2008): Robust design of spatially distributed friction for reduced wrinkling and thinning failure in sheet drawing; Mater Des, 30: 2043–55.

Simões F., Ferreira Duarte J., Santos A., Barata da Rocha A. (2003): Tensile tests; INETFORSMEP Project Report.

Simpson T.W., Peplinski J.D., Koch P.N., Allen J.K. (2001): Meta-models for computer-based engineering design: survey and recommendations; Eng Comput, 17:129–150.

Simpson D., Power D., Samson D. (2007): Greening the automotive supply chain: a relationship perspective; Int J Oper & Prod Manag, 27: 28-48.

Skilliter M. (2007): Tailored Coils –A New Process to Further Expand Tailored

Applications; www.autosteel.org.

Smith C.B., Hinrichs J.F., Ruehl P.C.: Friction Stir and Friction Stir Spot Welding - Lean, Mean and Green; Friction Stir Link, Inc. W227 N546 Westmound Dr., Waukesha, WI 53186.

Sujit D. (2000): The Life-Cycle Impacts of Aluminum Body-in-White Automotive Material; JOM, 261: 20-24.

Sun G., Li G., Gong Z., Cui X., Yang X., Li Q. (2009): Multiobjective robust optimization method for drawbead design in sheet metal forming; Mat Des, 30: 3318–3324.

Sutherland J. and Gunter K. (2004): A global perspective on the environmental challenges facing the automotive industry: state-of-the-art and directions for the future; Int J Vehicle Design, 35: 86-110.

Taherizadeh A., Ghaei A., Green D.E., Altenhof W.J. (2009): Finite element simulation of springback for a channel draw process with drawbead using different hardening models; Int J Mech Sci, 51:314–25.

Tang Y. and Chen J. (2009): Robust design of sheet metal forming process based on adaptive importance sampling; Struct Multidisc Optim, 39:531–544.

Tekkaya A.E., Schikorra M., Becker D., Biermann D., Hammer N., Pantke K. (2009): Hot profile extrusion of AA-6060 aluminum chips; J Mater Process Technol, 209: 3343-3350.

Thiruvarudchelvan S. and Travis F.W. (2003): Hydraulic-pressure-enhanced cup-drawing processes—an appraisal; J Mat Proc Technol, 70–75.

Toyota Motor Corporation (2008): Sustainability report 2008 - A New Future for People, Society and the Plane; www.toyotainbusiness.com.

Toyota Motors Corporation (2008): Air Quality Report; www.toyota.com.

Urban M., Krahn M., Hirth G., Kopp R. (2006): Numerical research and optimisation of high pressure sheet metal forming of tailor rolled blanks M. Journal of materials processing technology; 360-363.

van Beers W.C.M., Kleijnen J.P.C. (2004): Kriging interpolation in simulation: a survey; Proc Winter Sim Conf, 113-121.

Vapnik V.N. (1995): The nature of statistical learning theory; Springer, Berlin.

Veleva V, Hart M., Greiner T., Crumbley C. (2001): Indicators of sustainable production; J Clean Prod, 447–452.

Verma R.K. and Haldar A. (2007): Effect of normal anisotropy on springback; J Mater Proc Technol, 190:300–304.

Vijayaraghavan A. and Dornfeld D. (2010): Automated energy monitoring of machine tools; CIRP Ann Manuf Technol, 59: 21-24.

Volkswagen AG and Florin H. (1995) from a presentation of A. Horvath, UC-Berkeley.

Wagoner R.H. (2002): Fundamental aspects of springback in sheet metal forming. Proc Numisheet Conf, 21-25.

Wagoner R.H. (2004): Role of plastic anisotropy and its evolution on springback. Int J Mech Sci, 44:123–48.

Wagoner R.H., Li M. (2007): Simulation of springback: through-thickness integration; Int J Plast, 23:345–50.

Wang Z.G. (2004): Tribological approaches for green metal forming; J Mater Process Technol, 151: 223-227.

Wanyama W., Ertas A., Zhang H.C., Ekwaro-Osire S. (2003): Life-cycle engineering: issues, tools and research; Int J Comput Integr Manuf; 16: 307-16.

Wang H., Li E., Li G.Y., Zhong Z.H (2008): Development of metamodeling based optimization system for high nonlinear engineering problems; Ad Eng Softw, 39: 629–645.

Weaver P.M., Ashby M.F., Burgess S., Shibaike N. (1996): Selection of materials to reduce environmental impact: a case study on refrigerator insulation. Mater Des; 17: 11–7.

Wei L. and Yuying Y. (2007): Multi-objective optimization of an auto panel drawing die face design by mesh morphing; Comput Aided Des; 39:863–79.

Wei L. and Yuying Y. (2008): Multi-objective optimization of sheet metal forming process using Pareto-based genetic algorithm; J Mater Proc Tech; 208: 499–506.

Wei L., Yuying Y., Zhongwen X., Lihong Z. (2009): Springback control of sheet metal forming based on the response-surface method and multi-objective genetic algorithm; Mater Sci Eng A; 499:325–338.

White M. (2006): Cans or Cars Aluminium & the Automotive Industry - JLR Light Weight Vehicle (LWV) Strategy; 21st Int Al Conf.

Wiebenga J.H., Klaseboer G., van den Boogaard A.H. (2011): Efficient Robust Optimization of Metal Forming Processes using a Sequential Metamodel Based

Strategy; Numisheet, 978-985.

Wu P.D., Graf A., MacEwen S.R, Lloyd D.J., Jain M., Neale K.W. (2005): On forming limit stress diagram analysis; Int J Solid Struct, 42:2225–41.

Wu S., Ji Z., Zhang T. (2009): Microstructure and mechanical properties of AZ31B magnesium alloy recycled by solid-state process from different size chips; J Mater Process Technol, 209: 5319-5324.

www.arcelormittal.com/fce/repository/Tailored_Blanks/Catalogue-Chapter1.pdf

www.audi-mediaservices.com

www.autoblog.com

www.eaa.net

www.gwwsc.org

www.terna.it

www.toyota-global.com

www.trade.gov/competitiveness/sustainablemanufacturing/how_doc_defines_SM.as.

www.wordautosteeel.com

www.worldautosteel.com.

Xu W.L., Ma C.H., Li C.H., Feng W.J. (2004): Sensitive factors in springback simulation for sheet metalforming; J Mater Proc Technol, 151:217–22.

Yeniay O., Unal R., Lepsch R.A. (2006): Using dual response surfaces to reduce variability in launch vehicle design: A case study; Reliab Eng Syst Saf, 91:407-412.

Yu H.Y. (2009): Variation of elastic modulus during plastic deformation and its influence on springback; Mater Des, 30:846–850.

Zhang Q. J. and Gupta K. C. (2000), Neural Networks for RF and Microwave Design, Artech House Publishers, Norwood, MA.

Zang SL et al. (2006): A new model to describe effect of plastic deformation on elastic modulus of aluminum alloy; Trans Nonferrous Met Soc China, 16s:1314–1318.

Zhang W. and Shivpuri R. (2009): Probabilistic design of aluminum sheet drawing for reduced risk of wrinkling and fracture; Reliab Eng Syst Safe, 94:152–61.

Zhao G., Ma X., Zhao X., Grandhi R. (2004): Studies on optimization of metal forming processes using sensitivity analysis methods; J Mater Process Technol, 147:217–228.

Zhu Q., Sarkis J., Lai K. (2007): Green supply chain management: pressures, practices and performance within the Chinese automobile industry; J Cleaner Prod, 15: 1041-1052.

PUBLICATIONS

Journal Publications

Marretta L., Ingarao G., Di Lorenzo R. (2010): Design of sheet stamping operations to control springback and thinning: a multi-objective stochastic optimization approach; Int J Mech Sci, 52: 914-927.

Marretta L. and Di Lorenzo R. (2010): Influence of material properties variability on springback and thinning in sheet stamping processes: a stochastic analysis; Int J Adv Manuf Technol; 51: 117-134.

Marretta L. and Di Lorenzo R.: An integrated stochastic framework to investigate sheet stamping process variability; submitted to Eng Opt.

Marretta L. and Di Lorenzo R.: Metamodel based design for robust sheet stamping processes; submitted to Opt Eng.

Conference Proceedings

Di Lorenzo R., Ingarao G., Marretta L., Micari F. (2009): Deep Drawing Process Design: A Multi Objective Optimization Approach, SheMet - Int Conf Sheet Metal, Birmingham, UK (also published in Key Engineering Materials, 410-411: 601-608).

Marretta L. and Di Lorenzo R. (2011): Robust design of a sheet stamping process: approaches to control the inner process variability; 10th AITeM Conf, Naples, Italy.

Marretta L. and Di Lorenzo R. (2011): A comparative analysis of different robust design approaches in sheet stamping operations; 14th ESAFORM Conf, Belfast, UK.

Marretta L., Ingarao G, Di Lorenzo R. (2012): A comparison between three meta-modeling optimization approaches to design a tube hydroforming process; accepted for 15th ESAFORM Conf, Erlangen, Germany.

Marretta L., Di Lorenzo R., Micari F., Arinez J., Dornfeld D. (2012): Material substitution for automotive applications: a comparative life cycle analysis; accepted for 19th CIRP LCE Conference, Berkeley, CA.

Marretta L., Di Lorenzo R., Ambrogio G., Anghinelli O., Dornfeld D. (2012): Deep Drawing versus Incremental Forming Processes: a comparative cradle to gate analysis; submitted to Metal Forming Conf, Cracovia, Poland.